

**PRODUCTION AND PERFORMANCE EVALUATION OF BIODIESELS FROM SOME
SEED OILS AND THEIR BLENDS WITH DIESEL**

BY

OGBU, IKECHUKWU MARTIN

2010547012P

**A DISSERTATION SUBMITTED TO THE DEPARTMENT OF PURE AND INDUSTRIAL
CHEMISTRY, FACULTY OF PHYSICAL SCIENCES, NNAMDI AZIKIWE UNIVERSITY,
AWKA**

**IN PARTIAL FULFILMENT OF THE REQUIREMENTS FOR THE AWARD OF DOCTOR
OF PHILOSOPHY DEGREE IN INDUSTRIAL CHEMISTRY**

AUGUST, 2017

CERTIFICATION

This is to certify that this thesis was written by OGBU, IKEECHUKWU MARTIN, a postgraduate student in the Department of Pure and Industrial Chemistry with Reg. No: 2010547012P.

The work embodied in the thesis is original and to the best of our knowledge has not been submitted in part or full for any other diploma or degree of this or any other University.

Prof. V.I.E Ajiwe
(Supervisor)

Date

Dr. J.K. Nduka
(Head of Department)

Date

External Examiner

Date

Prof. T.U. Onuegbu
(Faculty PG Sub-Dean)

Date

Prof. A.J. Ekpunobi
(Dean, Faculty of Physical Sciences)

Date

Prof. Harry Ike Odimegwu
(Dean, School of Postgraduate Studies)

Date

DEDICATION

This work is dedicated to my cherished wife, Ogbu Patience Nkemjika, my daughter, Ogbu Kamsiyochukwu Divine and my son, Ogbu Chinweotito Dominion.

ACKNOWLEDGEMENTS

I would like to specially thank my supervisor, Prof. V.I.E. Ajiwe for his guidance, friendship, financial and emotional supports throughout this work. I am grateful to Prof. T.U. Onuegbu, Prof. E. Ejike and Prof. P.K. Igbokwe for their wonderful contributions to this work. Thank you so much. I equally appreciate the goodwill of the entire lecturers of the Department.

My appreciation also goes to Dr. Peter Chukwunonso Okoli of Department of Chemistry, Vaal University of Technology, Vanderbijlpark, South Africa and Mrs. Clementina Chukwukanne of Advance Laboratory, Pure and Industrial Chemistry Department, Nnamdi Azikiwe University Awka, for their laboratory assistance. I also thank Dr. Obinna Oje of Federal University Ndufu-Alike Ikwo for his statistical assistance.

I am grateful to Dr. Chigozie Margaret Ejikeme, Dr. Uchechukwu Pauline Ofora, O. F. Obumselu and Moses Edeonovo for their wonderful words of encouragement. To my friends that helped me in sourcing the oil seeds, Chinedu of Oji River L.G.A, Joseph of Ugwuomu community Emene-Enugu, Friday of Ogburishi village Emene and Sunday Amechi, I extol your wonderful contributions to the success of this work.

I am highly indebted to my wife, Ogbu Patience, my parents, Mr. and Mrs. Ogbu Godwin and my siblings especially Sussan Chinyere Nechi, for their love, care, and emotional supports. To everyone not mentioned specifically here who directly or indirectly contributed to the success of this work, I deeply appreciate your supports.

ABSTRACT

Two types of biodiesels (methyl esters and butyl esters) were synthesized from *Cucurbita pepo*, *Azelia africana* and *Hura crepitans* seed oils using acid catalysis. Solid acid catalysts were prepared from biowastes (seed cake/shell) from the oil seeds via partial carbonization to aromatize the materials and subsequent sulfonation to introduce $-\text{SO}_3\text{H}$ group on them. Ten different solid acid catalysts (0HuSO₃H, 30HuSO₃H, 60HuSO₃H, 90HuSO₃H, 120HuSO₃H, 0ASO₃H, 30ASO₃H, 60ASO₃H, 90ASO₃H and 120ASO₃H) were obtained by varying the resident time of the carbonization before sulfonation. The catalysts were characterized using FTIR, TGA, SEM and XRD and were applied on the biodiesel synthesis alongside H₂SO₄. Various process parameters such as quantity of catalyst, stirring rate, temperature and time were investigated on the biodiesel production. Different esters/diesel blends were made from each biodiesel sample by diluting it with petrodiesel at various ratios and their fuel properties were tested in line with ASTM methods. From the results, the oil yields of the crops: 42.43 % (*C. pepo*), 21.80 % (*A. africana*) and 39.87 % (*H. crepitans*) were quite promising for commercial biodiesel production. Modified biowaste catalyst from the seed shell/cake exhibited high acid density up to 2.34 mmol/g and were effective for biodiesel synthesis; the most effective one gave 96 % biodiesel yields compared to 98 % of H₂SO₄ and showed advantage of easy separation after reaction and being recycled. The activities of the catalysts varied with the carbonization time; 30 to 60min. was optimal for acid site density, pore sizes and hydrolytic stability. SEM images of the catalysts showed that carbonization (at 500 °C) of the biowastes beyond 60 min. before sulfonation resulted in collapse of carbon framework and pores on the catalysts. TGA/DTG curves showed that the catalysts were thermally stable up to 230 °C after which $-\text{SO}_3\text{H}$ group started dissociating from the carbon structure. At alcohol/oil ratio of 6:1, optimal conditions for methyl ester synthesis from the oil samples were found to be 60 °C, 3 % catalyst (H₂SO₄), and 300 rpm stirring rate. Butyl esters required up to 80 °C and 400 rpm. The experimental data suggested that the esterification reaction followed second order model. The results of the fuel properties of the biodiesels and their blends indicated their suitability for biodiesel production. Methyl esters/diesel blends of 10:90 had viscosity that placed them in 2D grade diesel (2-4.3 mm²/s) suitable for fuelling mobile equipment while the higher blends fell within 4D grade diesel (5.0-34.0 mm²/s) suitable for powering stationary equipment. For the butyl esters, up to 50:50 blends fell within 2D grade. The cetane number, 64.25 (*H. crepitans*), 59.76 (*C. pepo*) and 43.44 (*A. africana*) were quite high for efficient combustion in diesel engine. The flash points, 102 °C (*C. pepo*), 88 °C (*A. africana*) and 150 °C (*H. crepitans*) signified low fire risk during transportation and storage. Other fuel properties including acid value (<0.6 mg KOH/g), pour point, ash content and density were within ASTM D6751 limits for biodiesels. *H. crepitans* exhibited the best fuel properties in terms of high cetane number, flash point and cold-flow properties. Most *C. pepo* and *A. africana* samples congealed below 5°C indicating that they might not be suitable for cold weather (below 5 °C). Butyl esters of the oil samples showed better fuel properties compared to the methyl esters in terms of viscosity and heating value. The FTIR results indicated that the bond structures of the vegetable oil esters were similar to those of petrodiesel and were stable up to 300 °C, signifying their thermal fitness as biodiesels.

TABLE OF CONTENTS

	Page
TITLE	I
CERTIFICATION	II
DEDICATION	III
ACKNOWLEDGEMENTS	IV
ABSTRACT	V
TABLE OF CONTENTS	VI
LIST OF TABLES	X
LIST OF FIGURES	XII
LIST OF PLATES	XIV
LISTS OF APPENDICES	XV
CHAPTER ONE: INTRODUCTION	1
1.1. Background of Study	1
1.2. Statement of Problem	3
1.3. Aim and Objectives	4
1.4. Scope of Study	4
1.5. Importance of Study	5
CHAPTER TWO: LITERATURE REVIEW	7
2.1. Progress in the Use of Vegetable Oil as Diesel Fuel	7
2.1.1. Engine Modification	8
2.1.2. Blending Straight Vegetable Oil with Petroleum Diesel	9
2.1.3. Micro-emulsification	9
2.1.4. Thermal Cracking (Pyrolysis) of Vegetable Oil	9

2.1.5. Hydrotreating (or hydrorefining)	10
2.1.6. Transesterification	10
2.2. Feedstock for Biodiesel Production	12
2.2.1. <i>Cucurbita pepo</i> as an Alternative Biodiesel Feedstock	13
2.2.2. <i>Africana africana</i> as an Alternative Biodiesel Feedstock	14
2.2.3. <i>Hura crepitans</i> as an Alternative Biodiesel Feedstock	15
2.3. Catalyst in Biodiesel Production	15
2.3.1. Base-catalyzed Transesterification	16
2.3.2. Acid-catalyzed Transesterification	18
2.3.3. Acid-catalyzed Esterification	19
2.3.4. Heterogeneous Catalysts for Biodiesel Production	20
2.3.5. Bio-based Solid Acid Catalyst for Biodiesel Production	21
2.4. General Applications of Biodiesel and its By-product	23
2.5. Fatty Acids in Vegetable Oil	24
2.5.1. Saturated and Unsaturated Fatty Acids	24
2.5.2. Iodine Value of Vegetable Oils	26
1.6. Effects of Fatty Acids Structures on Biodiesel Fuel Properties	27
2.7. Effects of Unique Fatty Acids on Biodiesel Properties	28
2.8. Methods for Lipid Analyses	29
2.9. Properties of Diesel Fuel	31
2.9.1. Cetane Number	31
2.9.2. Flash point (FP)	32
2.9.3. Specific Gravity	32
2.9.4. Cold-flow Properties	33
2.9.5. Kinematic Viscosity	34
2.9.6. Sulfated Ash	35
2.9.7. Acid Number	35
2.9.8. Copper Strip Corrosion	36
2.10. Engine Performance of Biodiesel	36

2.11. Biodiesel Engine Emissions	37
2.11.1. Unburned Hydrocarbon Emission	38
2.11.2. Carbon Monoxide (CO)	38
2.11.3. Nitrogen Oxides Emissions (NO _x)	38
2.11.4. Smoke and Particulate Emission	38
2.11.5. Exhaust Odour	39
2.12. Engine Compatibility	40
2.13. Biodegradability	41
2.14. Lubricity	41
2.15. Toxicity	41
2.16. Oxidation Stability	42
2.17. Specification for Biodiesel	42
2.18. The Nigeria's Biofuel Policy	44
CHAPTER THREE: MATERIALS AND METHOD	46
3.1. Equipment and Reagents	46
3.1.1. Collection and Preparation of Samples	47
3.1.2. Oil Extraction	47
3.2. Physicochemical Characterization of the Extracted	48
3.2.1. Determination of Moisture Content	49
3.2.2. Determination of Acid Value	49
3.2.3. Determination of Iodine Value	50
3.2.4. Determination of Saponification Value	51
3.2.5. Determination of Relative Density	51
3.2.6. Determination of Mineral Ash	52
3.2.7. Determination of Calorific Value	52
3.3. Preparation of Modified Biowaste Catalysts from the seed Cake/Shell	52
3.3.1 Catalyst Characterization	55

3.4. Biodiesel Synthesis	57
3.4.1. Effect of Kinetic Parameters on Biodiesel Synthesis	58
3.4.2. Bulk Biodiesel Preparation and Blending	59
3.5. Characterization of the Biodiesel Samples	61
3.5.1. Determination of Kinematic Viscosity	61
3.5.2. Determination of Flash Point	61
3.5.3. Determination of Pour Point	61
3.5.4. Estimation of Cetane Number	62
3.5.5. Gas Chromatography/Mass Spectroscopy (GC-MS) Analysis	62
3.5.6. Determination of Metallic Elements in the Samples	63
3.5.7. FTIR Bond Structure/Stability Relationship	64
CHAPTER FOUR: RESULTS AND DISCUSSION	66
4.1. Physicochemical Properties of the Extracted Oil	66
4.2. GC-MS Analysis of the Methyl esters and Fatty Acid Profile of the Oils	67
4.2.1. GC-MS Results of Butyl esters of the Oil Seeds	72
4.2.2. Properties of the Fatty Acids in the Oil Samples	76
4.3. Modified Biowaste Solid Acid Catalysts	77
4.3.1. FTIR Monitor of Changes in the Biowastes during Carbonization	77
4.3.2. Physicochemical Properties of the Modified Biowaste Catalysts	79
4.3.3. Hydrolytic Stability of the Catalysts	81
4.3.4. XRD Analysis of the Catalysts	82
4.3.5. Surface Morphology of the Solid Acid Catalysts	83
4.3.6. Thermogravimetric Analysis of the Catalysts	89

4.4. Effect of Process Parameters on the Biodiesel Synthesis	90
4.5. Fuel Properties of the Seed Oils and their Derivatives	100
4.5.1. Fuel Properties of the Seed Oils Derivatives (Butyl esters)	104
4.6. Biodiesel Property Changes as a Function of Intrinsic Structure	107
4.7. Correlations of Fuel Properties of the Methyl- and Butyl esters from the Various Seed Oils	117
4.8. Bond Structures/Stability Relationship of the Various Seed Oils and their Derivatives	121
4.9. Metal Composition Seed Oils and their Derivatives	146
CHAPTER FIVE: CONCLUSION AND RECOMMENDATION	147
5.1. Conclusion	147
5.2. Contribution to Knowledge	150
5.3. Recommendation	151
Reference	152
Appendices	172

LIST OF TABLES

	Page
2.1: Fuel Properties of Selected Vegetable Oils	8
2.2: Names of Some Fatty Acids	26
2.3: ASTM D6751 Specifications for Biodiesel (B100)	44
2.4: ASTM D7467 Specifications for Biodiesel Blends (B6–B20)	43
2.6: European Specifications (EN 14214) for Biodiesel	44
4.1: Physicochemical Properties of the Extracted Oil	66
4.2: Results of GC-MS Analysis of <i>C. pepo</i> Seed Oil Methyl esters	67
4.3: Fatty Acid Profile of the <i>C. pepo</i> Seed Oil	68
4.4: Results of GC-MS Analysis of <i>A. africana</i> Seed Oil Methyl esters	68
4.5: Fatty Acid Profile of the <i>A. africana</i> Seed Oil	69
4.6: Results of GC-MS Analysis of <i>H. crepitans</i> Seed Oil Methyl esters	69
4.7: Fatty Acid Profile of the <i>H. crepitans</i> Seed Oil	69
4.8: Results of GC-MS Analysis of <i>C. pepo</i> Butyl esters	72
4.9: Results of GC-MS Analysis of <i>A. africana</i> Butyl esters	73
4.10: Results of GC-MS Analysis of <i>H. crepitans</i> Butyl esters	74
4.11: Properties of Fatty Acids of the Oil Samples	76
4.12: FTIR Determination of Changes in the <i>H. crepitans</i> Seed Shell during Carbonization	78
4.13: FTIR Determination of Changes in the <i>A. africana</i> Seed Cake during Carbonization	78
4.14: Properties of Solid Acid Catalysts from <i>H. crepitans</i> Seed Shell	80
4.15: Properties of Solid Acid Catalysts from <i>A. africana</i> Seed Cake	80

4.16: Effect of Quantity of Catalyst (H ₂ SO ₄) on %Conversion of	90
4.17: Effect of Stirring Rate on Percentage Conversion of the Oil to Biodiesel	92
4.18: Effect of Temperature on %Conversion	93
4.19: Overall Rate Constants and the Correlation Coefficients (R ²) of Methylation of the base Oil Using H ₂ SO ₄	97
4.20: Overall Rate Constants and the Correlation Coefficients (R ²) of Butylation of the base Oil Using H ₂ SO ₄	97
4.21: Activation Energies of the Methyl- and Butyl esterification	99
4.22: Overall Rate Constants and the Correlation Coefficients (R ²) of Methylation and Butylation of <i>C. pepo</i> Oil Using 60Hu-SO ₃ H Catalyst	99
4.23: Fuel Properties of <i>C. pepo</i> Seed Oil and its Derivatives	101
4.24: Fuel Properties of <i>A. africana</i> Seed Oil and its Derivatives	102
4.25: Fuel Properties of <i>H. crepitans</i> Seed Oil and its Derivatives	103
4.26: Fuel Properties of <i>C. pepo</i> Seed Oil Butyl esters	104
4.27: Fuel Properties of <i>A. africana</i> Seed Oil Butyl esters	105
4.28: Fuel Properties of <i>H. crepitans</i> Seed Oil Butyl esters	106
4.29: Pearson Correlation Coefficients of the Fuel Properties of the Methyl esters and Butyl esters of <i>C. pepo</i> , <i>A. africana</i> and <i>H. crepitans</i> Oils	120
4.30-47: FTIR Bond Structure Comparison of the Samples at 28-300 °C	122
4.48: Heavy Metals Composition (mg/g) of the Fuel Samples	146

LIST OF FIGURES

Fig.	Page
2.1: The Structure of Some Fatty Acids	25
3.1: Flow Chart for Biodiesel Preparation and Characterization	60
4.1: GC-MA Spectrum of <i>C. pepo</i> methyl esters	70
4.2: GC-MA Spectrum of <i>A. africana</i> methyl esters	70
4.3: GC-MA Spectrum of <i>H. crepitans</i> Methyl esters	71
4.4: GC-MA Spectrum of <i>C. pepo</i> Butyl esters	74
4.5: GC-MA Spectrum of <i>A. africana</i> Butyl esters	75
4.6: GC-MA Spectrum of <i>H. crepitans</i> Butyl esters	75
4.7: XRD pattern of <i>H. crepitans</i> seed shell derived catalyst (60Hu-SO ₃ H)	82
4.8: XRD pattern of <i>A. africana</i> seed shell Derived catalyst (60A-SO ₃ H)	83
4.11: TGA Curves of <i>H. crepitans</i> Derived Solid Acid Catalysts	87
4.12: The Derivatives (DTG) Curves	88
4.13: TGA Curves comparing thermal stability of <i>H. crepitans</i> and <i>A. africana</i> catalysts	89
4.14: DTG Curves comparing thermal stability of <i>H. crepitans</i> and <i>A. Africana</i> catalysts	89
4.15: Effect of Quantity of Catalyst on Methyl esterification	91
4.16: Effect of Quantity of Catalyst on Butylation	91
4.17: Effect of Stirring Rate on Methylation of the Base Oil	92
4.18: Effect of Stirring Rate on Butylation of the Base Oil	92
4.19: Effect of Temperature on Methylation of the Base Oils	94

4.20: Effect of Temperature on Butylation of the Base Oils	94
4.21: Effect of Time on Methylation of the Oil at 70 °C	95
4.22: Effect of Time on Butylation of the Oils at 70 °C	95
4.94: Flash Points of the Various Seed Oils and their Derivatives	108
4.95: Kinematic Viscosity (at 40 °C) of the Various Seed Oils and their Derivatives	110
4.96: Effect of Temperature on Kinematic Viscosity of the Various Seed Oils and their Derivatives	111
4.97: Relative Density of the Various Seed Oils and their Derivatives	114
4.98: Calorific Value of the Various Seed Oils and their Derivatives	115
4.99: Pour Point of the Various Seed Oils and their Derivatives	117
4.100-108: Changes in C=O, C=C and OH peak intensities of the oils	143
4.30-56: Verification of order of the reaction for the methyl esterification using H ₂ SO ₄ catalyst	173
4.57-83: Verification of order of reaction for the butyl esterification using H ₂ SO ₄ catalyst	185
4.90-98: Verification of order of the reaction for the methyl esterification using Hu-SO ₃ H catalyst	196
4.99-107: Verification of order of reaction for the butyl esterification using Hu-SO ₃ H catalyst	200

LIST OF PLATES

Plate	Page
3.1: <i>C. pepo</i> seeds and the oil	49
3.2: <i>A. africana</i> seeds and the oil	49
3.3: <i>H. crepitans</i> seeds and oil	50
3.4: <i>H. crepitans</i> seed shell	55
3.5: <i>A. africana</i> seed cake	55
3.6: <i>H. crepitans</i> Seed shell carbonized at 500 °C at Varied Time	55
3.7: <i>A. africana</i> seed cake carbonized at 500 °C at Varied Time	56
3.8: Locally constructed carbonizer	56
3.9: Set up for biodiesel kinetic study	61
3.10: <i>C. pepo</i> methyl esters at different temperatures	67
3.11: <i>A. africana</i> methyl esters at different temperatures	67
3.12: <i>H. crepitans</i> methyl esters at different temperatures	67
4.9: SEM images of <i>H. crepitans</i> seed shell derived catalysts at ~870 magnification	84
4.10: SEM images of <i>A. africana</i> seed cake derived catalysts at ~870 magnification	86

LISTS OF APPENDICES

	Page
Appendix 1	172
Appendix 2	173

CHAPTER ONE

INTRODUCTION

1.1. Background of Study

Environment pollution concern associated with fossil fuel use and the fact that they are non-renewable and are being depleted have spurred much interest and researches on alternative energy sources. Studies have shown that combustion of fossil fuels has greatly increased anthropogenic carbon dioxide emission in the atmosphere with an attendant effect on the global temperature (US-EIA, 2005; Royal Society, 2008). Fossil fuels contain high percentage of carbon and their combustion releases into the atmosphere more carbon dioxide than plants can ordinarily absorb, leading to a net increase in carbon dioxide in the atmosphere annually. Carbon dioxide is a potent greenhouse gas and has been implicated as the major cause of global warming we are facing presently (US-EIA, 2005).

Fossil fuels are non-renewable; they take millions of years to form and the reserves are being depleted faster than the new ones are formed (Novaczek, 2000). Thus, they do not ensure energy security. Energy security can only be guaranteed by a shift to renewable energy sources. Renewable energies sources are replenish by nature and are not easily depleted.

Biodiesel is among the renewable alternative energy sources that can currently be implemented (Azil, 2007; Lee *et al.*, 2014). The fascinating things about biodiesel as alternative diesel fuel include its compatibility with existing diesel engines, simple production process, low in pollutants and greenhouse gas emissions (Ma and Hanna, 1999; Giakoumis, 2013; Wang *et al.*, 2014). Biodiesel is an oxygenated fuel; it contains a reduced amount of carbon and higher oxygen and hydrogen compared to fossil diesel. This favours its combustion in a diesel engine and reduces pollutants emission. High lubricity

which enhances engine longevity (Razon, 2009), biodegradability, reduced exhaust odour and smoke emissions (Murari, 2011) are other beneficial characteristics of biodiesel over petrodiesel.

Life-cycle analyses have shown that the source-to-wheel CO₂ emissions from neat biodiesel combustion account for at least 60 % savings with respect to petrodiesel, but with B20 blend, the savings is between 15 and 20 % (Agarwal, 2007; Giakoumis *et al.*, 2012). The use of biodiesel as alternative fuel has potential to ameliorate global warming and other environmental pollutions associated with fossil fuel use.

Biodiesel as alternative diesel fuel is increasing in popularity across the globe. In many European countries, a 5 % biodiesel blend is widely used and is available at thousands of gas stations where it serves basically as diesel additive (Good Energy, 2013). The current top world producers of biodiesel include Germany, United States, Brazil, France and Argentina with about 2.0 to 4.0 billion liters per annum, mainly from rapeseed, sunflower, soybean and cottonseed (Miguel Carriquiry, 2007; GAIN Report, 2005; Statista, 2016). However, the high demand of most of these crops for food makes their application for biodiesel production challenging. Thus, low cost feedstock which has less competition with food becomes desirable.

In addition, biodiesel production has relied mostly on the use of homogeneous catalysts such as H₂SO₄, NaOH and KOH. The catalysts are effective but have lots of downsides which include difficulty in separation after preparation, high wastes generation, corrosion of reaction chambers and they cannot be reused. All these lead to high cost of biodiesel production. Researches, however, have shown that the use of recyclable heterogeneous catalysts can significantly reduce biodiesel pump price and minimize waste generation (Zong *et al.*, 2007; Huang and Fu, 2013).

Bio-based heterogeneous catalyst for biodiesel conversion is gaining popularity (Hara *et al.*, 2004; Chen *et al.*, 2011; Liu *et al.*, 2013, Lee *et al.*, 2014). The catalysts are prepared by incomplete carbonization of carbonaceous material to form small polycyclic aromatic carbon rings and subsequent functionalization ($-\text{SO}_3\text{H}$) with sulphuric acid. Effectiveness of these catalysts for biodiesel conversion via transesterification/esterification reactions has been widely reported (Lee *et al.*, 2014) and they show advantage over many other heterogeneous catalysts in terms of hydrophobicity (which encourages active site retention), thermal stability and the fact that they can be prepared from a low cost material (Zong *et al.*, 2007; Huang and Fu, 2013, Liu *et al.*, 2013).

The focus of this work however is on the performance evaluation of selected underutilized Nigerian oil crops as biodiesel feedstock, and the potential of deriving efficient solid acid catalyst from seed cake/shell of the plants for biodiesel production.

1.2. Statement of Problem

Nigeria depends mainly on crude oil for her transportation fuel. Considering the environmental issues associated with the use of fossil fuel and the fact that they are being depleted, there is need to develop alternative energy sources for the country. Majority of non-edible and non-staple oil crops in Nigeria have remained underutilized despite their abundance. Utilization of these oils for biodiesel production can play an important role in providing eco-friendly alternative fuel for the country and diversification of the economy. However, information on the biodiesel properties of the individual oil is unavailable or limited. To facilitate their utilization for commercial biodiesel production, wide range information on their individual performance is necessary including chemical composition, fuel properties, thermal stability, as well as information on their optimal processing conditions.

Solid acid catalysts from carbonaceous materials have been reported as stable and efficient recyclable catalysts for biodiesel production but are often prepared from expensive materials such as glucose and starch (Hara *et al.*, 2004; Wang *et al.*, 2014). Biowaste such as seed cake/shell from oil extraction often constitutes environmental pollution due to their poor management. Utilization of these biowastes for solid acid catalyst preparation can provide cheaper catalysts for biodiesel conversion and as well act as waste disposal strategy.

1.3. Aim and Objectives

The aim of this study was to produce and evaluate performance of biodiesels from *Cucurbita pepo*, *Afzelia africana* and *Hura crepitans* seed oils.

The aim of the study would be achieved through the following objectives:

- i. To extract and characterize oils from *C. pepo*, *A. africana* and *H. crepitans* seeds.
- ii. To produce and characterize solid acid catalysts from seed cake/shell of the plants.
- iii. To synthesize two sets of biodiesels (methyl- and butyl esters) from each seed oil using the new catalysts in comparison with H₂SO₄.
- iv. To study the effect of process parameters on the biodiesel synthesis.
- v. To determine the fuel properties of the biodiesels and their diesel blends.
- vi. To compare the bond structure/stability of the vegetable oil esters with that of petrodiesel.

1.4. Scope of Study

The study covered:

- (1) Extraction and characterization of the seed oils.
 - i. Drying of the seed samples.
 - ii. Decortication and grinding of the dry seed samples.
 - iii. Extraction of oils from the ground samples using soxhlet extractor.

(2) Synthesis and characterization of biowaste-derived solid acid catalyst

- i. Drying, grinding and screening of the seed cake/shell.
- ii. Partial carbonization of the ground samples.
- iii. Sulfonation of the carbonized materials.
- iv. Characterization of the prepared catalysts using XRD, TGA, FTIR and SEM

(3) Biodiesel synthesis.

- i. Methyl esters synthesis from each oil using H_2SO_4 catalyst.
- ii. Butyl esters synthesis from each oil using H_2SO_4 catalyst.
- iii. Methyl esters synthesis from each oil using the solid acid catalyst.
- iv. Butyl esters synthesis from each oil using the solid acid catalyst.
- v. Verification of process parameters on the biodiesel synthesis- effect of quantity of catalyst, stirring rate, temperature and time, determination of order of reaction and activation energy.

(4) Formulation of esters/diesel blends from the prepared biodiesels.

(5) Biodiesel characterization

- i. Gas chromatography-mass spectroscopy (GC-MS) analysis.
- ii. Determination of fuel properties of the esters and the esters/diesel blends: flash point, pour point, cetane number, specific gravity, acid value, heating value, moisture content and ash content.
- iii. Fourier Transform Infrared spectroscopy (FTIR) analysis of the bond structures /stability biodiesel and petroleum diesel.
- iv. Determination of metal composition of the samples using AAS

1.5. Importance of Study

- i. This study has provided reliable information on fuel properties of the seed oils and would create an outlet for their commercial utilization.
- ii. Biofuel production from underutilized seed oils would play an important role in energy diversification and job creation in the country.

- iii. Utilization of seed cake/shell of the plants for catalyst production can provide effective catalysts from low cost materials for biodiesel production.
- iv. Utilization of the seed cake/shell for catalyst production can serve as a sustainable and effective waste management strategy.

CHAPTER TWO

LITERATURE REVIEW

2.1. Progress in the Use of Vegetable Oil as Diesel Fuel

The use of vegetable oil as diesel fuel is as old as diesel engine itself. Rudolf Diesel, the originator of diesel engine, in 1895 developed pioneer diesel engine which used vegetable oil (peanut oil) as the fuel (Knothe, 2001). However, following the discovery of petroleum based fuels, original diesel engines were adapted to use less viscous petrodiesel (Thiago, 2008). The fuel injection systems of most of these modern diesel engines are sensitive to viscosity, resulting that a lot of operational problems are encountered when they are run on straight vegetable oils (Tony, 2011).

High viscosity of vegetable oils compared to petroleum diesel fuel leads to poor atomization, resulting in carbon deposits formation in the engine due to incomplete combustion, oil ring sticking, thickening and gelling of the lubricating oils as a result of contamination (Srivastava and Prasad, 2000). The kinematic viscosity of vegetable oil varies in the range of 30-40 cSt at 38 °C which is about 20 times higher than that of petroleum diesel fuel (Jaichandar and Annamalia, 2011). Table 2.1 shows the fuel properties of some vegetable oils in comparison with petroleum diesel.

Over the years, efforts have been made to improve the suitability of vegetable oil as a fuel to diesel engine, the review of some of them is as follows.

Table 2.1: Fuel Properties of Selected Vegetable Oils

Vegetable Oil	Viscosity at 38 °C (cSt)	Cetane No.	Heating value (MJ/kg)	Cloud point (°C)	Flash point (°C)	Density (kg/L)
Diesel	3.06	50.0	43.8	–	76	0.8550
Corn	34.9	37.6	39.5	- 1.1	277	0.9095
Cottonseed	33.5	41.8	39.5	1.7	234	0.9148
Crambe	53.6	44.6	40.5	10.0	274	0.9048
Linseed	27.2	34.6	39.3	1.7	241	0.9236
Peanut	39.6	41.8	39.8	12.8	271	0.9026
Rapeseed	37.0	37.6	39.7	-3.9	246	0.9115
Safflower	31.3	41.3	39.5	18.3	260	0.9144
Sesame	35.5	40.2	39.3	-3.9	260	0.9133
Soya bean	32.6	37.9	39.6	-3.9	254	0.9138
Sunflower	33.9	37.1	39.6	7.2	274	0.9161
Palm	39.6	42.0	–	31.0	267	0.9180

Source: Jaichandar, S. and Annamalia, K., (2011): The Status of Biodiesel as an Alternative Fuel for Diesel Engine- An Overview, *Journal of Sustainable Energy & Environment*, (2), 71-75.

2.1.1. Engine Modification

Several engine modifications have been invented to allow the use of straight vegetable oil on diesel engines, they include:

- i. Incorporation of heater in the fuel tank to heat up the fuel prior to atomization. Pre-heating of the oil at temperature around 150 °C reduces viscosity and makes it compare very well with petrodiesel (ACREVO, 2000; Kopia, 2004).
- ii. The use of two-tank SVO kits. In this technology, one fuel tank is for petrodiesel diesel and one is for vegetable oil. The engine is started on petrodiesel and runs until it heats up, then the driver switches to the vegetable oil tank (Addison, 2013). When finish driving, the vehicle is

switched to diesel tank in order to get vegetable oil out of the fuel lines otherwise it will be difficult to start the engine next time.

2.1.2. Blending Straight Vegetable Oil with Petroleum Diesel

The possibility of blending straight vegetable oils (SVO) with conventional petroleum diesel to lower its viscosity has been tried. This technique gave a lot of improvement to physicochemical properties of the oil but the long term use of such blends in a modern diesel engine is reportedly compromised by the decrease in power output and thermal efficiency due to carbon deposits (Ma and Hanna, 1999).

2.1.3. Micro-emulsification

A micro-emulsion is technically defined as a stable dispersion of one liquid phase into another, which has a droplet diameter of approximately 100 nm or less (Kaewta, 2008). Micro-emulsification process has been studied to improve the viscosity of vegetable oils through blending with a simple alcohol such as methanol or ethanol. However, significant injector needle sticking, carbon deposits, incomplete combustion, and the increase in the viscosity of lubricating oils were major drawbacks reported in the technique for a long term use (Ziejewski *et al.*, 1984).

2.1.4. Thermal Cracking (Pyrolysis) of Vegetable Oil

Pyrolysis is defined as the conversion of one substance into another by means of heat in the absence of air or oxygen at temperatures range from 450 °C to 850°C or by heat with the aid of a Lewis acid catalyst (Kaewta, 2008). This method has been employed to produce more efficient fuel from vegetable oils. Removal of oxygen from the vegetable oil during the thermal cracking however eliminates the environmental benefits associated with using an oxygenated fuel (Ma and Hanna, 1999).

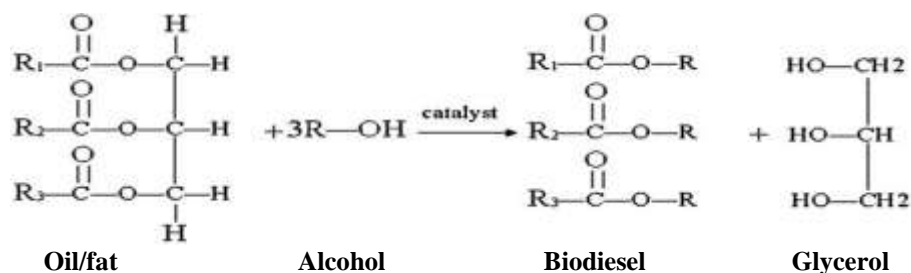
2.1.5. Hydrotreating (or hydrorefining)

Hydrotreating of vegetable oil converts it to fuel similar in chemical composition with petrodiesel and is referred to as ‘green diesel’. Green diesel just like petrodiesel comprises hydrocarbons and can be used in unmodified diesel engines (Immer *et al.*, 2009). During hydrotreating process, vegetable oil is converted to isoparaffin-rich diesel fuel via catalytic processes involving saturation, hydrodeoxygenation, decarboxylation and hydroisomerization (Boerrigter, 2002; Immer *et al.*, 2009). Though green diesels have many attractive characteristics such as high cetane number, lower specific gravity, good cold flow properties and excellent storage stability, the technology however is still at developmental stage and also eliminates the environmental benefits associated with using an oxygenated fuel.

2.1.6. Transesterification

Vegetable oils are composed of triglyceride molecules- esters of long chain fatty acids and glycerol (propan-1,2,3-triol). Transesterification of the oil using simple alcohol (methanol, ethanol, isopropanol or butanol) replaces glycerol component of the triglycerides, yielding monoesters known as biodiesel. Biodiesels have much closer fuel properties with petroleum diesel (Ajiwe *et al.*, 2001) and currently regarded as the best option for conversion of vegetable oils into alternative diesel fuel in terms of feasibility and environmental benefits (Royal Society, 2008; ECN, 2009). Most other methods are still at developmental stages.

During transesterification process, the oil or animal fats is mixed with a short chain alcohol such as methanol, isopropanol or butanol etc. in the presence of a catalyst and are heated to a temperature near the boiling point of the alcohol. The alcohol replaces glycerol component of the oil as represented Scheme 2.1.



Scheme 2.1: Transesterification Reaction

After production and separation from the glycerol, the biodiesel goes through a clean-up or purification process to remove the remaining residual alcohol, catalyst and soaps. Biodiesel purification consists of one or more washings with clean water and is then dried. Sometimes, biodiesel can go through an additional distillation step to produce a colorless, odorless, zero-sulfur biodiesel (ECN, 2009).

Biodiesel is an efficient diesel fuel in terms of engine performance and environmental friendliness. It requires only a simple method of preparation and the fuel is compatible with existing engines (Ajiwe and Obika, 2000).

Various literatures revealed that transesterification is an equilibrium process (Abigor *et al.*, 2000; Galadima and Garba, 2009). Elevated temperature (usually 40-70 °C) and high alcohol/oil ratio involved in the process contribute in shifting the equilibrium position sufficiently to the products side allowing very high reactants conversion. Monitored by chromatography studies, transesterification reaction was shown to involve sequential conversion (Galadima *et al.*, 2008; Anderson *et al.*, 2009):

Triglyceride \longrightarrow Diglyceride \longrightarrow Monoglyceride \longrightarrow Biodiesel and Glycerol

Freedman and co-workers studied both acid- and alkaline-catalyzed transesterification of soybean oil with methanol and at a molar ratio of 6:1 and proposed a second-order mechanism (Freedman *et al.*, 1984). Darnoko and

Cheryan, (2000) investigated the kinetics of palm oil transesterification and suggested pseudo-second-order model for the initial stages of the reaction which was followed by first-order or zero-order model. The chemical kinetics of transesterification of other feedstocks such as *Jatropha* (Kumar and Kumar, 2008), soybean (Noureddini and Zhu, 1997) and waste cooking oil (Dhanasekaran and Dharmendirakumar, 2012), have also been studied.

Apart from conventional transesterification method for biodiesel preparation, some other techniques have also been investigated with the aim of shortening the reaction time, they include (1) microwave assisted transesterification (Ramakrishnan *et al.*, 2010; Perreux and Loupy, 2001; Lidstrom *et al.*, 2001; Tierney and Lidstrom, 2005), (2) ultrasonic assisted transesterification reaction (Siriporn *et al.*, 2010) and (3) transesterification using supercritical method (Warabi *et al.*, 2004; Rathore and Madras, 2007; Ashley, 2011).

2.2. Feedstock for Biodiesel Production

Biodiesel can be prepared from varieties of fatty oils such as vegetable oils, animal fats, used cooking oils, soapstock, and algae. Vegetable oils however are currently the major source of commercial biodiesel due to their availability. Vegetable oils that have been extensively investigated as raw materials for biodiesel includes soybean oil, rapeseeds, sunflower, canola, *Jatropha curcas*, palm oil, castor oil, coconut oil, ground nut oil, Neem oil, pea nut oil and cotton seed oils. (Akintayo, 2004; Razon, 2009; Moser, 2009). Reports have shown that the most predominant feedstocks for biodiesel production worldwide include rapeseed oil (48 %), soybean (22 %), palm oil (11 %) and the rest (19 %) which include corn, sunflower, cottonseed, peanut, and coconut oils; the percentages are based on 2007 estimation (Moser, 2009). High demand of these oil crops for food, together with the increase in the global biodiesel demand has made search for alternative feedstocks a priority.

2.2.1. *Cucurbita pepo* as an Alternative Biodiesel Feedstock

Cucurbita pepo, L. (broad leaf pumpkin) is an annual climber belonging to *Cucurbitaceae* family that thrives in sandy, loamy and clay soils but prefers well-drained and moist soils. The plant is widely cultivated in temperate and tropical zones including Nigeria and is valued for its palatable fruit and leaf; its young leaf locally called “Ugbogulu” in Igbo is used as an indigenous leafy vegetable and has been shown to contain 43.8 % protein (Duke and Ayensu, 1985). *C. pepo* equally plays an important role in the traditional setting as a cover crop and weed control agent (Delahaut and Newenhouse, 2006).

Despite the abundance of *C. pepo* in Nigeria, the seeds have remained underutilized and have no commercial application yet in the country (Aruah *et al.*, 2011; Oloyede, 2012; Elinge *et al.*, 2012). Thus, in the search for alternative oils for biodiesel production, the *C. pepo* seed oil presents a promising choice. It was reported that the seeds not only contain nutritionally important bio-compounds but are also sources of other phyto-compounds which at certain critical levels have significant anti-nutritional effects (Elinge *et al.*, 2012).

Schinas *et al.*, (2008) reported that *C. pepo* seeds gave oil yield of about 45 %. The colour of the oil varies from light to dark green to brownish or reddish, depending on the thickness of the observed oil sample- an optical phenomenon known as dichromatism (Kreft and Kreft, 2007). Although the oil is edible, it is not commonly used (Schinas *et al.*, 2009). The oil seed has no commercial application yet in Nigeria and are regarded as wastes in some parts of the country.

Ajiwe *et al.*, (2006a) provided information on the flash point, relative density, carbon residue and viscosity of *C. pepo* seed oil and its methyl esters in regard to its potential to serve as biodiesel feedstock. However, more information on the fuel properties of the feedstock is still required for commercial biodiesel

production; there was no information on some vital fuel properties such as cetane number, cold-flow, heating value, thermal stability of the feedstock. Also fuel properties of diesel blends of the biodiesel was lacking. In addition to this, detailed information on the effect of different alcohols on fuel properties of the oil would provide wide range information on its fuel properties and facilitate optimal biodiesel blend formulation. Effect of process parameters on the production would equally facilitate commercial biodiesel production from the seed oil.

2.2.2. *Afzelia africana* as an Alternative Biodiesel Feedstock

Afzelia africana (African oak or African mahogany) belongs to the *Fabaceae* family. The plant is known as ‘akparata’ in Igbo. It is a large tree which when mature is between 10 and 20 meters in height and is valued for its quality wood; the wood has an excellent stability towards humidity, shrinkage during drying, insect attack and it has a good natural durability (Gérard and Louppe, 2011). The plant thrives very well in the Savannah, fringing forest and the drier parts of the forest regions of Africa including Nigeria. It was reported that the roots were efficacious for treatment of gonorrhoea, chest pains, kidney problems and snake bites (Hutchings *et al.*, 1996). The bark ash is applied externally to treat lumbago and bark powder to wounds and swellings. The bark is also used as fish poison (Gérard and Louppe, 2011).

A. africana plant bears dehiscent fruit containing about 6-10 hard, shiny, black bean-shaped seeds with yellow cap. Though the ground seed of *A. africana* is used as soup thickener in some part of Nigeria, its use is not very common, resulting in a huge quantity of the seed remaining unexploited annually. Thus, the oil could serve as biodiesel feedstock for Nigeria.

Ejikeme *et al.*, (2010) studied the physicochemical and toxicological properties of *A. africana* seed oil and reported that the oil was not toxic to human. The

potential of the seed oil to serve as biodiesel feedstock was reported by Igwenyi *et al.*, (2011). According to their reports, the oil was dominated by oleic acid and had high heating values. However, no information on many vital fuel properties such as cetane number, flash point, kinematic viscosity as well as fuel properties of the esters/diesel blends was reported. To facilitate commercial biodiesel production from the seed oil, detailed information on its fuel properties is necessary, including information on thermal stability and effect of process parameters on the production process.

2.2.3. *Hura crepitans* as an Alternative Biodiesel Feedstock

Hura crepitans commonly known as sandbox plant is an evergreen tree of family *Euphorbiaceae*; the trees can grow up to 60 metres (Swain and Tom, 1977) and it thrives well in wet soil. *H. crepitans* is mainly cultivated for shade; the tree is widely planted in Nigeria as shade tree in many households, roadsides and recreation parks. The fruit is a big capsule with explosive dehiscence. The seed is rich in oil and is non-edible (Abdulkadir *et al.*, (2013).

Despite the abundance of *H. crepitans* in Nigeria, its seed oil has remained underutilized (Oyeleke *et al.*, 2012; Abdulkadir *et al.*, 2013), hence seeds hold a promising future for biodiesel production in Nigeria. However, as at time of this study, no information on the biodiesel properties of the oil was available.

Oyeleke *et al.*, (2012) reported the proximate analysis of *H. crepitans* seeds; the seed was rich in crude protein, fat and carbohydrate. Abdulkadir *et al.*, (2013) equally evaluated the chemical composition of the oil and reported that the oil would have long shelf-life which is suitable for industrial applications.

2.3. Catalyst in Biodiesel Production

Catalyst is very important in biodiesel production via transesterification reaction. The reaction does not proceed to any substantial extent without catalyst unless it is carried out at supercritical condition (Ejikeme *et al.*, 2010).

Transesterification at supercritical condition requires sophisticated equipment and is still at developmental stage. Nevertheless, conventional biodiesel production is based on base catalyzed transesterification reaction as well as acid catalyzed esterification/transesterification reactions. Various catalyst systems for biodiesel production are hereby reviewed.

2.3.1. Base-catalyzed Transesterification

Alkali metal alkoxides such as CH_3ONa (for methanolysis) are the most active catalysts for base-catalyzed transesterification. They give high yields within a short reaction time of (about 30 min) and only little concentration (about 0.5 %) is required for a complete conversion (Ejikeme *et al.*, 2010). The use of this catalyst is however limited because it requires a complete absence of water in the feedstock to avoid deactivation. It is not appropriate for typical industrial process (Ulf *et al.*, 1998). Industrial biodiesel production is currently based on metal hydroxides such as KOH and NaOH as the catalysts. Although these catalysts are not as reactive as metal alkoxides, they equally give high conversion and are cheaper and easier to handle.

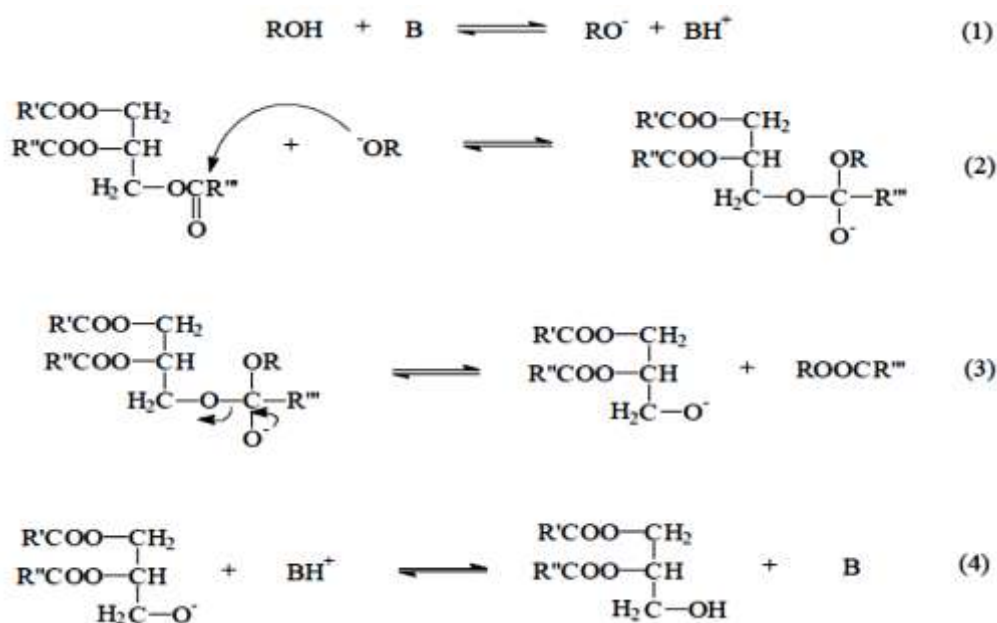
Several other base catalysts which have been reported to show activity towards transesterification reaction include potassium carbonate, sodium carbonate, lime, iron (III) oxide, sodium aluminate, zinc, copper, tin, lead and zinc oxides, ashes, clay, zeolites and metal complexes (Knothe *et al.*, 1997; Ejikeme *et al.*, 2010).

Usually, direct base catalyzed transesterification reaction is impaired when a feedstock contains high free fatty acids (FFAs) (>1 % or 2 mg KOH/g) (Freedman and Pryde, 1882) and moisture. Free fatty acid reacts with base catalyst, resulting in formation of undesired by-products (soap). This reduces catalyst activity, biodiesel yields and compromises easy separation of the product as well as by-product after production. Feedstock with high FFAs

content requires pretreatment before base catalyzed transesterification reaction can be applied. Many crude vegetable oils, animal fats and recycled greases are often high in FFAs. The pretreatment process usually involves acid catalyzed esterification reaction to remove the FFAs (Berrios *et al.*, 2007; Abiney *et al.*, 2008).

Mechanism of Base Catalyzed Transesterification Reaction

The base catalyzed transesterification can be shown to follow the steps illustrated in Scheme 2.2 (Ulf *et al.*, 1998).



Scheme 2.2: mechanism of base-catalyzed transesterification of vegetable oil

Step1: reaction between the catalyst (base) and the alcohol to form an alkoxide (equation 1).

Step2: nucleophilic attack of the alkoxide at the carbonyl group of the triglyceride generates a tetrahedral intermediate (equation 2)

Step3: intermediate dissociates to form the new ester (biodiesel) or goes back to the original ester (equation 3).

Step4: The resulted anion of diglyceride formed in equation (3) later deprotonates the catalyst, regenerating the active species (equation 4) which is now ready to start another catalytic cycle (Ulf *et al.*, 1998).

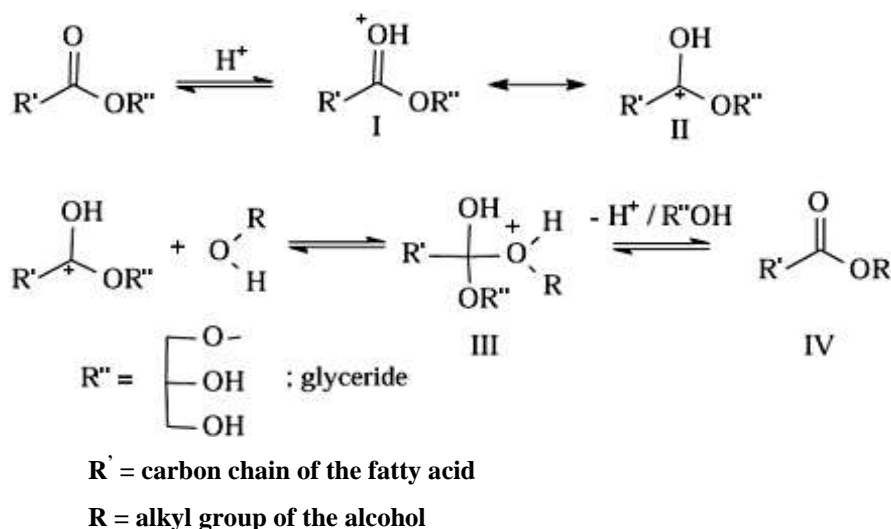
All the steps in the mechanism are reversible but with large excess alcohol the equilibrium is shifted until virtually the sole product is biodiesel.

2.3.2. Acid-catalyzed Transesterification

Acid-catalyzed transesterification reaction has been used successfully for biodiesel production from vegetable oils and animal fats (Lee *et al.*, 2014). Brønsted acids such as H_2SO_4 , HCl , BF_3 and H_3PO_4 can be used but H_2SO_4 is the most common. Acid-catalyzed process is particularly applied when the feedstock contains high FFAs and/or moisture and is common in most crude vegetable oils and other low grade feedstock (ECN, 2009). The catalyst is not deactivated by FFAs. Acid catalyzed transesterification reaction however takes a longer time (3-48h), higher temperatures and oil/alcohol ratio for a complete conversion (Ejikeme *et al.*, 2010). Ataya *et al.*, (2007) compared the rate of acid catalyzed and base catalyzed transesterification processes at ambient temperature and reported that, base (NaOH) catalyzed process was three times faster than acid (H_2SO_4) counterpart. They attributed this to the difference in concentration of the methoxy ions and the protonated triglyceride (TG) species.

Mechanism of acid catalyzed transesterification reaction

The acid-catalyzed transesterification can be shown to follow the steps illustrated in Scheme 2.3. (Christie, 1993; Ulf *et al.*, 1998).



Scheme 2.3: mechanism of acid-catalyzed transesterification of vegetable oil

Step 1: Protonation of the carbonyl group of the ester by the catalyst to form a carbocation (II).

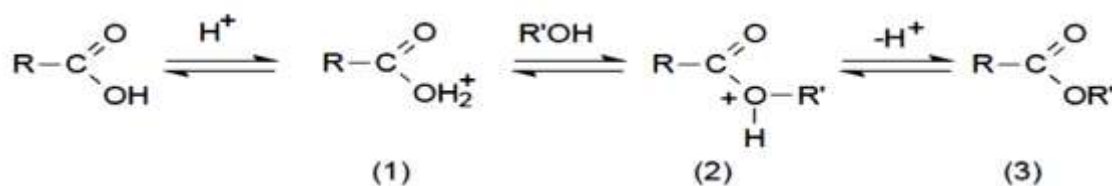
Step 2: Addition of the exchanging alcohol (nucleophilic attack) to the carbocation to give an intermediate (III)

Step 3: Intermediate dissociation via transition state to give the ester (IV).

2.3.3. Acid-catalyzed Esterification

Acid-catalyzed esterification reaction is a vital reaction in biodiesel industry especially for conversion of feedstock with high FFAs. Feedstocks containing high FFAs are often converted to biodiesel via two-step process involving esterification reaction (Ajiwe *et al.*, 2006a; Berrios *et al.*, 2007). Reported two-step methods include completely hydrolysis of the base oil to FFAs followed by acid catalyzed esterification to form biodiesel (Ajiwe *et al.*, 2006b) and pretreatment of the base oil via acid catalyzed esterification reaction to remove the FFAs followed by conventional base catalyzed transesterification reaction.

It has been shown that esterification reaction follows the steps illustrated in Scheme 2.4 (Christie, 1993).



Scheme 2.4: mechanism of acid-catalyzed esterification of FFA of vegetable oil

Step1: Protonation of the acid to give an oxonium ion (1).

Step2: The oxonium ion undergoes an exchange reaction with an alcohol to give the intermediate (2).

Step3: The intermediate in *step 2* can lose a proton to become an ester (3).

2.3.4. Heterogeneous Catalysts for Biodiesel Production

Biodiesel preparation has mostly relied on homogeneous base catalysts such as KOH, NaOH, and mineral acids such as H₂SO₄. These catalysts show faster conversion but have lots of downsides which include difficulty in separation after reaction, contamination of products, corrosion of reaction chamber and high waste generation (Aam, 2002; Alamu *et al.*, 2007). Research interest however has been on development of efficient heterogeneous catalysts for biodiesel production that can be separated easily after reaction with less waste generation and can be reused.

Several heterogeneous base and acid catalysts have been reported for biodiesel production. They include metals and metal oxides, cation-exchange resins, solid superacids acid zeolites, sulfonated polymers (Amberlyst-15 and Nafion-based composites), sulfonated mesostructured metal oxides such as silica, zirconia, zirconia-alumina, tungstated zirconia-alumina, tungsten oxide (Nakajima *et al.*, 2007; Yan *et al.*, 2008; Galadima *et al.*, 2008; Ejikeme *et al.*, 2010; Liu *et al.*, 2013; Lee *et al.*, 2014). However, metal oxides derived catalysts generally have been shown to exhibit high hydrophilicity, resulting in high leaching out of the active site and concomitant drop in catalytic activity (Liu *et al.*, 2013; Lee *et al.*,

2014). Polymer-based solid acid catalysts such as Amberlyst-15 and Nafion-based composites on the other hand, have been shown to be efficient heterogeneous acid catalysts for biodiesel production. However the catalysts are expensive (Liu *et al.*, 2013) and require only mild reaction temperature of about 60 °C to avoid denaturing (Ejikeme *et al.*, 2010); they are thermoplastic. Hence, development of efficient and cheaper catalysts for biodiesel production is one of the prime research targets in biodiesel development.

2.3.5. Bio-based Solid Acid Catalyst for Biodiesel Production

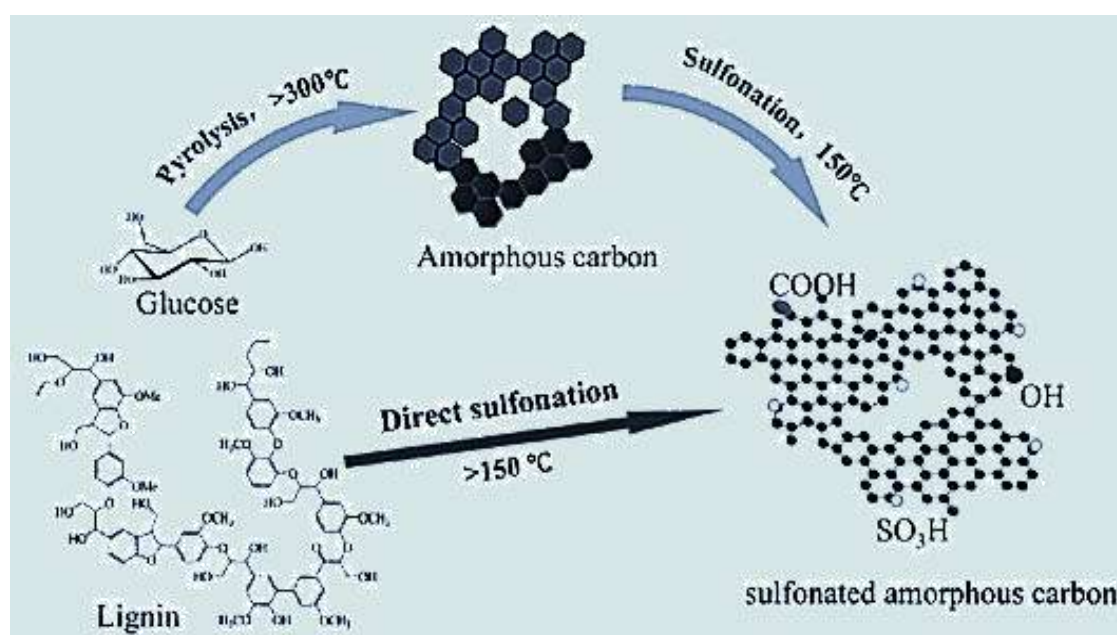
Most recently, carbon-based solid acid catalysts were reported. The catalyst can be prepared by the sulfonation of incompletely carbonized carbon precursor, such as natural organic material and biomass resources (Liu *et al.*, 2013, Arora *et al.*, 2014; Lee *et al.*, 2014; Wang *et al.*, 2014). The incomplete carbonization converts the biomass to a structure rich in small polycyclic aromatic carbon rings and then sulfonation of the material with sulphuric acid introduces sulfonic groups ($-\text{SO}_3\text{H}$) on it which acts as the active site for catalysing organic reactions. The schematic description of the preparation is shown in Scheme 2.5.

Thermal stability, hydrophobicity and the fact that they can be prepared from a low cost material offered bio-based solid acid catalyst advantage over other solid acid catalyst (Zong *et al.*, 2007; Huang and Fu, 2013). The use of carbon-based solid acid catalysts to catalyse biodiesel production via transesterification/esterification of vegetable oils and animal fats has been widely reported (Zong *et al.*, 2007).

Wang *et al.*, (2014) reported bio-based solid acid catalyst from cassava stillage residue prepared at varied carbonization temperature and concluded that 400 to 600 °C was optimal for formation of favourable aromatic structure for the attachment of $-\text{SO}_3\text{H}$ group. Lee (2013) studied the hydrolytic stability of bio-

based solid acid catalyst prepared from liginosulfonate (by-product of paper processing) and reported that about 20 % acid site leached out. Nature of carbon precursor and preparation method may have influence on the hydrolytic stability.

The efficiency of the catalyst in hydrolysis of cellulose to ethanol (Emrani and Shahbazi, 2012; Huang and Fu, 2013), and furanic ethers and levulinate esters (Russo *et al.*, 2014) has equally been reported.



Scheme 2.5: Preparation of bio-based solid acid catalyst

The major components of biomass are cellulose, hemicellulose and lignin, and each behaves differently during carbonisation (Mohammad *et al.*, 2012). During carbonization of biomass, the material undergoes a transformation through series of processes which include dehydration, decarboxylation, aromatization and recondensation (Judy *et al.*, 2011) resulting in a solid material rich in polycyclic aromatic compounds. The polycyclic aromatics form the frame for attachment of $-\text{SO}_3\text{H}$ group through sulfonation which gives the material its acidic properties.

Emrani and Shahbazi (2012) reported that bio-based solid acid catalyst was more active than other solid acid catalysts. Different types of biomass utilized in the preparation including cassava silage (Wang *et al.*, 2014), sugar (Zong *et al.*, 2007) and lignosulfonate (Lee, 2013).

A wide range of bio-wastes are generated from oil extraction in Nigeria most of which has no application yet and constitute environmental pollution. Solid acid catalysts production from these wastes can provide efficient catalyst for biodiesel production from low cost material and also, act as a sustainable waste management strategy.

2.4. General Applications of Biodiesel and its By-product

The use of biodiesel as alternative fuel to diesel engines has been certified by several studies (ASTM, 2009). Biodiesel can be used in pure form in some diesel engine but the common usage is in blend with petroleum diesel; the blends containing as much as 20 % biodiesel have proved satisfactory in all existing diesel engines without any modification (ASTM, 2009).

Apart from the use of biodiesel as alternative fuel for automobile diesel engines, it is a good solvent for non-automotive paints, spray paint and other adhesives. It can be used to dissolve deposits in fuel tanks, lines and delivery system from petrol diesel over a period of time. Other uses of biodiesel include, fuel for diesel heater, lanterns, and stoves. Biodiesel can also be used for machinery lubrication purposes and for cleaning up of petroleum oil spill on the land and in the water (ECN, 2009).

Glycerol is the main by-product of biodiesel. It is a colourless, odourless and non-toxic gel-like liquid. Glycerol has wide applications in oral care, food, tobacco, urethane foam production, pharmaceutical products manufacturing and animal feeds. Also, it can be fermented to bioethanol (ECN, 2009).

2.5. Fatty Acids in Vegetable Oil

Fatty acids present in lipids are in the range of C₁₄ to C₂₄. Table 2.2 presents fatty acid profile of vegetable oils and animal fats. The type of fatty acid is the major factor that determines their chemical and physical properties, and strongly influences their applications. Rapid developments in technologies have made the determination of the fatty acid profile within a biological material much easier, and such information is referred to as lipidome (Seppane-Laakso and Oresic, 2009).

2.5.1. Saturated and Unsaturated Fatty Acids

Saturated fatty acid does not contain carbon-carbon multiple bonds. Myristic acid (14:0), palmitic acid (16:0), and stearic acid (18:0), (Fig.2.6) are common and most abundant saturated fatty acids found in vegetable oils and animal tissues (Liping, 2010). Unsaturated fatty acids contain one or more carbon-carbon double bonds. When a fatty acid contains only one carbon-carbon double bond, it is known as monounsaturated fatty acids (MUFAs), e.g. oleic acid and erucic acid. If there are two or more carbon-carbon double bonds present in the fatty acid molecule, it is referred to as polyunsaturated fatty acids (PUFAs), e.g. linoleic acid and linolenic acid.

As the degree of unsaturation of lipids increases, the viscosity and melting point decreases (Addison, 2001). In general, oils contain more of unsaturated fatty acids and are liquid at room temperature while fats contain more of saturated fatty acids and are usually solid at room temperature. The absence of carbon-carbon double bonds in saturated lipids allows the chains of fatty acids to be straighter and more pliable so they harden at higher temperatures. On the contrary, as the number of double bonds increases, the ability of the chains to gain a conformation that would make them solid reduces so, they remain liquid at room temperature. This physical property which has long been used to distinguish between fats and oils, however, is not very precise since the

definition of room temperature varies, and natural oils and fats are mixtures and therefore have melting temperature range. Natural oils are mixture of compounds- varying blend of fatty acids, monoglycerides, diglycerides, triglycerides and unsaponifiable lipids.



(i) Palmitic acid (16:0)



(ii) Linoleic acid (18:2 n-6)



(iii) Arachidonic acid (20:4 n-6)



(iv) Oleic acid (18:1 n-9)



(v) α -linolenic acid (18:3 n-3)



(vi) eicosapentaenoic acid(EPA) (20:5 n-3)

Fig.2.1: The Structure of Some Fatty Acids

Table 2.2: Names of Some Fatty Acids

Shorthand name	Systematic name	Common name
4:0	Butanoic acid	Butyric acid
6:0	Hexanoic acid	Caproic acid
6:2	trans-3,4-hexadienoic acid	Sorbic acid
8:0	Octanoic acid	Caprylic acid
10:0	Decanoic acid	Capric acid
10:1	9-decenoic acid	Caproleic acid
12:0	Dodecanoic acid	Lauric acid
12:1	9-dodecenoic acid	Lauroleic acid
14:0	Tetradecanoic acid	Myristic acid
14:1	9-tetradecenoic acid	Myristoleic acid
16:0	Hexadecanoic acid	Palmitic acid
16:1	Hexadecenoic acid	Palmitoleic acid
18:0	Octadecanoic acid	Stearic acid
18:1 (n-9)	<i>cis</i> -9-octadecenoic acid	Oleic acid
18:1 (n-9)	trans-9-octadecenoic acid	Elaidic acid
18:2 (n-6)	<i>cis</i> -9,12-octadecadienoic acid	Linoleic acid
18:3 (n-3)	<i>cis</i> -9,12,15-octadecatrienoic acid	α -Linolenic acid
18:3 (n-3)	trans-9,12,13-octadecatrienoic acid	Eleostearic acid
18:3 (n-6)	<i>cis</i> -6,9,12-octadecatrienoic acid	γ -Linolenic acid
18:4 (n-3)	<i>cis</i> -6,9,12,15-octadecatetraenoic acid	Stearidonic acid
20:0	Eicosanoic acid	Arachidic acid
20:1	<i>cis</i> -9-eicosenoic acid	Gadoleic acid
20:1(n-9)	<i>cis</i> -11-eicosenoic acid	Gondoic acid
20:3 (n-9)	Eicosa-5,8,11-trienoic acid	Mead acid
20:4 (n-6)	<i>cis</i> -5,8,11,14-eicosatetraenoic acid	Arachidonic acid
20:5 (n-3)	<i>cis</i> -5,8,11,14,17-eicosapentaenoic acid	Timnodonic acid
22:0	Docosanoic acid	Behenic acid
22:1 (n-9)	13-docosenoic acid	Erucic acid
22:1	11-docosenoic acid	Cetoleic acid
22:4 (n-6)	<i>cis</i> -6,9,12-octadecatrienoic acid	Adrenic acid
22:6 (n-3)	<i>cis</i> -4,7,10,13,16,19-docosahexaenoic acid	Cervonic acid
24:0	Tetracosanoic	Lignoceic acid
24:1 (n-9)	<i>cis</i> -15-tetracosenoic acid	Nervonic acid

Source: Wikipedia (https://en.wikipedia.org/wiki/List_of_saturated_fatty_acids).

SELFNutrition: Fats and Fatty acids (<http://nutritiondata.self.com/topics/fatty-acids>).

Retrieved on 12th June, 2014.

2.5.2. Iodine Value of Vegetable Oils

Iodine value (IV) of oil is the amount of iodine required to iodize all carbon-carbon double bonds in the oil; it is the number of grams of iodine taken up by

100g of oil. IV is commonly used to measure the degree of unsaturation of oils and for the classification of oil into non-drying, semi-drying and drying oil (Addison, 2001). Oil with IV less than 120 is regarded as non-drying oil e.g. palm oil, groundnut oil, and melon seed oil. Oils with IV greater than 120 but less than 150 are classified as semidrying, an example is rubber seed oil. If the IV exceeds 150, the oils are classified as drying. Linseed oil, poppy seed oil and tung oil, are typical examples of drying oils. Drying oils tend to polymerize and harden when exposed to air. On exposure, oxidation at the double bond occurs gradually in air leading to rancidification in foodstuffs or drying in coatings.

For biodiesel production, the European Standard (EN14214) sets a maximum iodine value of 120 (Razon, 2009). This is because there is possibility of biodiesel with higher IV polymerizing and clogging the fuel injectors during use (Graboski and McCormick, 1998). Besides, fuels with a very high IV tend to have a poor oxidative stability (Knothe, 2007) and deteriorate more rapidly, but they have better cold-flow properties. On the other hand, oils with low IV make more efficient fuel in terms of higher cetane values but are less suitable in a very cold weather because of poorer cold-flow properties. Cold-flow properties include melting point (MP), cloud point (CP), cold filter plugging point (CFPP), and pour point (PP).

1.6. Effects of Fatty Acids Structures on Biodiesel Fuel Properties

Unlike other biofuels, properties of biodiesel depend greatly on the nature of the feedstock, i.e. the fatty acid profile of the oil or fats used in the production. Since the chemical composition of oils from different plant species varies, biodiesel from different feedstock are not exactly the same. The nature and the relative quantity of the alkyl groups (R' , R'' , R''') attached to the glycerin molecule determine the overall properties of the resultant biodiesel. While the detailed structure of each fatty acid has significant impact on the fuel

characteristics, the most frequently cited parameters are the average chain length and the degree of unsaturation of the fatty acids (Razon, 2009).

Consistent studies have shown that: cetane number, heat of combustion, melting point and viscosity tend to increase as the chain length increases and decrease as the number of double bonds increases (Knothe, 2005; Razon, 2009; Giakoumis, 2013). Lubricity decreases as the chain length increases (Knothe, 2005). The knowledge of the correlations between fatty acid structures and fuel properties will facilitate prediction of fuel properties from the fatty acid profile. For instance, a highly saturated feedstock is expected to be excellent in cetane number and oxidation stability but exhibits poorer cold flow properties, kinematic viscosity, flash point and heating value. This generalization however is more consistent using mixture of fatty acids methyl esters from pure fatty acids (Razon, 2009). The behavior of methyl esters from naturally occurring vegetable oil is rather more complex; the presence of minor components/contaminants contributes to the overall fuel properties of the biodiesel.

2.7. Effects of Unique Fatty Acids on Biodiesel Properties

Castor oil contains ricinoleic acid which gives the biodiesel from the oil exceptionally high lubricity; that is why castor oil is regarded as lubricity improver (Razon, 2009). The same fatty acid however gives biodiesel from the oil very high viscosity (Albuquerque *et al.*, 2009). The presence of eleostearic or conjugated linolenic acid in tung oil appreciably reduces its oxidative stability and increases its viscosity (Park *et al.*, 2008). Joboba oil is unique in that it does not contain triglycerides but instead contains long-chain esters formed by long chain fatty acids attached directly to fatty alcohols (Razon, 2009). This leads to a very high viscosity in the biodiesel from the oil (Canoira *et al.*, 2006). The oil of *sterculia foetida* (poon) is known to contain 72 % of sterculic acid (19-carbon cyclopropenyl fatty acid) which has been said to

undergo explosive polymerization when heated to 240 °C (Sonntag, 1979). The presence of cyclopropene and cyclopropane fatty acids in a lipid may be problematic during transesterification using acid catalysis. Both types of functional group may be destroyed by acidic conditions.

2.8. Methods for Lipid Analyses

Numerous methods have been developed to analyze lipids in biological materials. Some of these include separation and identification of the various components which make up the lipid. Lipid classification and fatty acid profile determination have been facilitated by the following techniques:

Gas chromatography: gas chromatography (GC) is the most common method for determination of fatty acid profile of vegetable oils, animal fats and their derivatives. In this method, fatty acid components of the lipids are first converted to fatty acid methyl ester (FAME) before the GC analyses. Capillary columns and a flame ionization detector (FID) are commonly employed in this method. Fused-silica capillary columns can easily achieve high resolution, their temperature can be programmed or the flow velocity of the carrier gas can be raised to optimize resolution and reduce the analysis time (Gutnikov, 1995). Fatty acid methylesters are identified by comparing the elution pattern and relative retention times of FAME with reference FAME mixture; most common fatty acids are available in commercial reference mixtures (Liping, 2010).

Gas chromatography-mass spectrometry (GC-MS) can be utilized in order to compare the mass spectrum with a reference spectrum stored in a computer database (Gutnikov, 1995). There are a number of software packages available which can be used to analyze data generated by MS lipids and other biological molecules.

High Performance Liquid Chromatography (HPLC): high performance liquid chromatography (HPLC) is extensively used in lipids analyses to separate

the lipids prior to mass analyses. It has higher separation capacity compared to Thin-layer-chromatography. Separation can be achieved by either normal-phase HPLC or reverse-phase HPLC. For instance, normal phase HPLC effectively separates glycerophospholipids on the basis of head group polarity (Malavolta *et al.*, 2004), whereas, reverse-phase HPLC effectively separates fatty acids on the basis of chain length, degree of unsaturation and substitution (Nakamura *et al.*, 1997). HPLC of lipids may either be performed offline or online where the eluent (carrier portion of the mobile phase) is integrated with the ionization source of a mass spectrometer. Fractions containing single lipid classes can easily be collected for further identification and analysis of molecular species. Mass sensitive detectors, such as evaporative light-scattering detectors (ELSDs) (Graeve and Janssen, 2009) and charged aerosol detectors (CADs) (Moreau *et al.*, 2006) have drastically made the development of HPLC methods for lipid class separations and identification quite simple. HPLC equipped with ELSD is valuable in determination of the triacylglyceride (TAGs) composition of oil sample (Emil *et al.*, 2009).

Solid-phase Extraction (SPE) Chromatography: solid-phase extraction (SPE) chromatography is useful for rapid, preparative separation of crude lipid mixtures into different lipid classes. This involves the use of prepacked columns containing silica or other stationary phases to separate glycerophospholipids, fatty acids, cholesteryl esters, glycerolipids, and sterols from crude lipid mixtures (Kaluzny, 1985).

Thin-layer chromatography (TLC): Just like HPLC and SPE, TLC is principally employed for separation of lipids into their various components. Although not as sensitive as the other methods, TLC offers a rapid and comprehensive screening tool prior to more sensitive and sophisticated techniques. Most studies of lipid classes are based on different TLC methods

(Volkman *et al.*, 1986; Nakagaki and Nakayama, 1997) and SPE procedures (Ruiz-Gutierrez and Perez-Camino, 2000).

2.9. Properties of Diesel Fuel

2.9.1. Cetane Number

Cetane number is one of the principal properties used to determine the quality of a particular diesel fuel (Hannu, 2007). By definition, cetane number is a measure of a fuel's ignition delay, the time between the start of injection and the start of combustion. In other words, cetane number measures the time between the start of injection and the first identifiable pressure increase. A diesel fuel with low cetane number will not ignite efficiently and this will bring about difficulty in starting the engine, cause noise and exhaust smoke emission. Increasing the cetane number of a fuel improves its combustion, reduces white smoke on startup, and tends to reduce NO_x and PM emissions (Chevron, 2007).

Cetane number scale was developed using the following standards: cetane (hexadecane) which ignites readily under compression was assigned a cetane number of 100 while alpha-methyl naphthalene which ignites less readily was assigned a cetane number of 0. These formed the scale for assigning cetane number to other fuels. Diesel engines run well with a CN ranging from 40 to 60 and beyond this range, the fuel's performance and emission advantage hits a plateau.

Cetane number of pure biodiesel (B₁₀₀) is usually higher than that of petroleum diesel and acts as a cetane improver in biodiesel/petroleum diesel blends. Biodiesel from highly saturated vegetable oils/fats tends to have higher cetane number than the one from unsaturated fats (Addison, 2001). Hence, blending feedstock of highly saturated fatty acids with that of highly unsaturated fatty acids will bring about synergic effect on cetane number and cold-flow properties.

ASTM D 613 specified the standard test method for cetane number of diesel fuel oil. The method involves running the fuel in a single-cylinder engine with a continuously variable compression ratio under a fixed set of conditions (Chevron, 2007). Measuring of cetane number is a difficult and expensive test and most often is estimated.

2.9.2. Flash point (FP)

Flash point of a fuel is the lowest temperature at which its vapour can be ignited (ASTM, 2009a). The test for flash point of a fuel is connected to the legal requirement and safety precautions involved in fuel handling and storage. It does not directly indicate the engine performance of a particular fuel. Flash point gives an indication of the most readily ignitable proportion of inflammable vapours at atmospheric pressure, and does not indicate the entire volatility or ignition properties of a fuel. Note that, flash point is different from auto-ignition temperature which is the temperature at which combustion will take place spontaneously without external source of ignition. This occurs under engine condition.

The flash point test is performed by passing a flame over the surface of a heated sample in an enclosed vessel, and observing the temperature at which it catches fire. This flash point is termed 'close flash point'. However, if the test is carried out with the vessel exposed to the atmosphere, it is known as 'open flash point'.

2.9.3. Specific Gravity

The energy content of the fuel brought into the engine at a given injector setting depends on the density of the fuel and it has effect on the emission characteristics of engine especially of older technology (Chevron, 2007). Specific gravity limit of 0.80-0.90 is specified for biodiesel to ensure sufficient air to fuel ratio and prevent incomplete combustion that could lead to particulate matter emission and coke deposition (Galadima and Garba, 2009).

2.9.4. Cold-flow Properties

Cold-flow properties include cloud point (CP), pour point (PP) and cold-filter plugging point (CFPP). In practice, these terms all mean about the same (Addison, 2001). Cold-flow properties of biodiesel depend on the fatty acid profile of the fuels and of course, presence of certain impurities. Biodiesels from unsaturated fats usually have better cold-flow properties than the ones from saturated fats. Most often, the presence of residual monoglycerides and diglycerides resulted from the incomplete transesterification of the triglycerides contribute immensely to poor cold-flow of biodiesel. Compared to petroleum diesel, biodiesel tends to have poorer cold-flow properties. This is a factor of great concern only for countries with very cold weather and not tropical countries like Nigeria where ambient temperature is always high. Blending biodiesel with petroleum diesel improves its cold-flow properties and makes them to compare very well with that of petroleum diesel (Razon, 2009).

If the temperature of a liquid fuel is decreased, a point will be reached when small solid crystals will begin to form at the bottom of the container. This point is referred to as the cloud point of the fuel. A fuel with a higher cloud point will freeze at higher temperature than the one with lower cloud point. Fuels with a high cloud point can also form crystals at a very cold weather which can cause filter plugging, clog filter and hinders the operation of the engine. Cloud point and pour point affect low-temperature operability and fuel handling (Chevron, 2007). It was reported that the addition of cloud point improver (additives) did not significantly reduce cloud point of biodiesel (Shresther *et al.*, 2008). This means that blending with petroleum diesel probably remains the best way to enhance cloud point of a biodiesel.

Cloud point test: a clean clear sample is cooled at a specified rate and examined at a time interval. The temperature at which a haze is first observed is the cloud point. Cloud point correlates very well with cold-filter plugging point

(Ajiwe *et al.*, 2001). Cold-filter plugging occurs when the fuel begins to clog filters and hinders the operation of the engine.

CFPP test: the sample is cooled by immersion in a constant temperature bath. The cooling rate is non-linear and fairly rapid – about 40 °C/hour. The CFPP is the temperature of the sample when 20 mL of the fuel fails to pass through a wire mesh in less than 60 seconds (Chevron, 2007).

2.9.5. Kinematic Viscosity

The resistance to flow of a fluid at a given temperature is referred to as viscosity. It is an internal friction which exists between the layers of a liquid or gas in motion. Kinematic viscosity, however, measures the ease with which a fluid can flow under force. It is different from dynamic viscosity and is obtained by dividing the dynamic viscosity by the density of the fluid. Kinematic viscosity is used to compare the flow properties of different fuels irrespective of their density. Two fuel samples with the same kinematic viscosity are expected to have similar flow property irrespective of their differences in density. Viscosity is an important property of a fuel. Too high or too low viscosity of a fuel can impair its engine performance. When viscosity is too high, there will be a problem of atomization, poor combustion and increased exhaust smoke emission (Schumacher and Tabitha, 1997). Conversely, when the fuel viscosity is too low, it may not reach precision fit of fuel injection pump, resulting into leakage.

The ASTM D445 limit for biodiesel kinematic viscosity at 40 °C is 1.9-6.0 mm²/sec. Nevertheless, when a biodiesel does not meet this specification, it can be corrected by appropriate blending (ASTM, 2009b).

In the test for kinematic viscosity, the sample is placed in a calibrated capillary glass viscometer tube and held at a closely controlled temperature. The time required for a specific volume of the sample to flow through the capillary under

gravity is measured. This time is proportional to the kinematic viscosity of the sample (Chevron, 2007).

2.9.6. Sulfated Ash

Sulphated ash is formed by the presence of inorganic metallic compounds in a fuel. Inorganic metallic compounds can be introduced into fuel through unremoved catalyst, soluble metallic soaps, abrasive solids, as well as metal-containing fuel additives. High amount of sulphated ash in a fuel can cause injection tip plugging, combustion deposits and injection wear, damage of piston ring and cylinder wall. Sulphated ash is abrasive and is different from carbon residue. It can cause more severe damage to engines. Carbon residue is formed by unburned hydrocarbon. The ash content of fuels is always in an inverse relationship with the heating value of a fuel. The higher the ash content the lower the heating value, and vice versa.

In determining sulphated ash in a fuel, the fuel ash is collected, treated with sulphuric acid and ignited gently at about 800 °C. This oxidizes and removes ash due to carbon residue as CO₂ gas, and transforms any metallic oxide into metallic sulphate. The remaining content is dried and recorded as the sulphated ash.

2.9.7. Acid Number

The level of the acidity of a fuel is referred to as acid number. It is determined by measuring the amount of milligram of KOH required to neutralize 1 gram of the fuel. Fuel with high acid number has great tendency to corrode the metallic parts of the fuel system (ECN, 2009). Chemically, biodiesel is not acidic but presence of free fatty acids in the fuel or unremoved acid catalyst in the fuel can make it acidic. Presence of free fatty acids in biodiesel fuel could be as a result of incomplete conversion during production, hydrolysis during washing after production or on a long storage.

2.9.8. Copper Strip Corrosion

Copper strip test is used to measure the corrosion effect of a fuel on the copper, brass or bronze parts of the fuel system. High copper strip corrosion value indicates a serious degradation of a fuel or acid contaminant in the fuel. The corrosion is caused by the presence of acid or sulphur-containing compounds. Copper strip test is carried out by immersing a polished strip of copper in about 30mL of the sample at 50 °C for three hours. After this, the copper strip is brought out and the corrosion evidence (tarnish) is observed. A value on the scale of 1-4 is assigned to the result based on a comparison with the ASTM copper strip corrosion standard (ASTM, 2009a).

2.10. Engine Performance of Biodiesel

Engine performance as well as emission test of a diesel is a very complex measurement and are often dependent on a number of considerable factors. There have been, to some extent, divergent results on the test so far conducted on some traditional feedstock (Razon, 2009). The differences in the results were due to some factors which include; the testing method and the condition under which it was conducted. Notwithstanding, several researchers reported that the use of biodiesel results in slightly higher brake specific fuel consumption, higher thermal efficiency and less power output compared to petroleum diesel (AltIparmak *et al.*, 2007; Lapuerta *et al.*, 2008).

Due to loss of heating values by volume bases of biodiesel, reduction in power of about 8 % is expected compared to that of petroleum diesel. Some researchers' findings were in agreement with this (Cetinkaya *et al.*, 2005; Kaplan *et al.*, 2006; Lin *et al.*, 2006) while some reported contrary observations (Jaichandar and Annamalia, 2011).

Many literatures have showed that there is no significant difference in the thermal efficiency between biodiesel and conventional diesel (Jaichandar and

Annamalia, 2011). In the other hand, few researchers reported a small improvement in the thermal efficiency for biodiesel blended with conventional diesel (Agarwal and Das, 2001), and suggested that the synergic blending effects could be because of reduction in friction associated with higher lubricity of biodiesel. Biodiesel has a better lubricity than conventional diesel.

Reports have also showed increase in Brake-specific fuel consumption (BSFC) of biodiesel (ranging from 2 % to 10 %) compared to petroleum diesel (Jaichandar and Annamalia, 2011). This was attributed to the loss of heating value due to higher oxygen content of biodiesel.

2.11. Biodiesel Engine Emissions

Ideal hydrocarbon fuel combustion produces predominately water vapour, carbon dioxide and nitrogen. But deviations from this ideal combustion leads to the emission of some volatile organic compounds (VOCs), carbon monoxide(CO), nitrogen oxides (NO_x), sulphur dioxide (SO₂), and particulate matter (PM). Diesel engines are substantial emitters of PM and NO_x, but only small emitters of CO and VOCs. Gasoline engines, in the other hand, are the greatest emitters of CO and substantial emitters of VOCs and NO_x, but only modest emitters of PM measured by mass (Chevron, 2007).

A common observation is that, there is always a significant reduction of pollutants emissions when biodiesel is used as diesel fuel compared to petroleum diesel. The exception is only NO_x emission which is often slightly higher (Graboski and McCormick, 1998). From comprehensive studies carried out by the U.S Environmental Protection Agency (EPA) comparing the emissions from biodiesel and diesel No.2, it was shown that B₂₀ (soybean) gave emission reduction of 10.1 %, 11.0 %, and 21.1 % of PM, CO, and HC respectively (EPA, 2002). They also confirmed a slight increase in NO_x emission by biodiesel.

2.11.1. Unburned Hydrocarbon Emission

Biodiesel emits less unburned carbon than petroleum diesel and this has been explained by many researchers to be as a result of more complete combustion of the fuel (Razon, 2009). Biodiesel is an oxygenated fuel and it burns more perfectly than petroleum diesel. However, some other researchers reported no much difference in the unburned carbon emissions between the two diesels (Serdari *et al.*, 1999; Labeckas and Slavinskas, 2006)

2.11.2. Carbon Monoxide

A better combustion in the engine has been attributed to the reduction in CO emission by biodiesel. The fuel burns more completely in the engine because of its oxygenated nature.

2.11.3. Nitrogen Oxides Emissions (NO_x)

Consistent investigations revealed a slight increase in emission of NO_x by biodiesel compared to petroleum diesel. Oxidation of some nitrogen in the air during combustion of the fuels is the principal cause of this. NO_x is formed by chain reactions involving nitrogen and oxygen in air (Jaichandar and Annamalia, 2011). This reaction highly depends on the gas temperature and residence time. Biodiesel emits higher NO_x because it has higher combustion temperature and longer combustion duration compared to petroleum diesel (US-EPA, 2002). Since diesel engines always operate with excess air, NO_x emissions are mainly a function of gas temperature and residence time. High NO_x emission by biodiesel can be reduced by certain strategies such as addition of cetane improvers, retardation of injection timing, exhaust gas recirculation, (Jaichandar and Annamalia, 2011).

2.11.4. Smoke and Particulate Emission

When fuel is injected into the hot compressed air in the combustion chamber, local regions develop that are fuel-rich and oxygen deficient. Due to the high

temperature and pressure in the combustion chamber, the fuel may start to break down before it has a chance to mix with air and burn normally. These high-temperature cracking reactions (pyrolysis) lead to the formation of carbonaceous soot particles (Chevron, 2007). Unburned or partially burned fuel can condense on the surfaces of these particles, increasing their size and mass. Eventually, these particles can agglomerate to form larger chains which can be seen as visible smoke.

Consistent reports showed that there is a significant reduction in particulate and smoke emission when biodiesel is used to fuel a diesel engine than when petroleum diesel is used (Jaichandar and Annamalia, 2011). This is due to complete combustion and the presence of oxygen in biodiesel. Particulate matter (PM) emission decreases with increase in biodiesel content in a biodiesel blend (US-EPA, 2002).

2.11.5. Exhaust Odour

Experience from the major cities of the world shows the level of air quality deterioration caused by emission from automobile engines fueled with fossil fuels. This odour remains as a problem in the minds of the general public. Oxides of nitrogen, aldehydes, sulfur oxides, organic acid and acrolein are among the major components of automobile exhaust which have been widely correlated with odour and eye irritation (Elliott *et al.*, 1955; Linnell and Scott, 1962). One of the most environmental benefits of biodiesel is that its use reduces exhaust odour compared to that of petroleum diesel.

In an effort to ascertain the intensity of odour emitted by various fuels, several techniques have been designed. They include; (i) odour instrument known as Olfactorium (Foster *et al.*, 1950), (ii) the use of odour panelists (Linnell and Scott, 1962) and (iii) the use of pH scale (Murari, 2007).

The Use of Odour Panel (Sensual Assessment): In this method, the nose is used as detector of odour intensity. A number of odour panelists perceive the exhausts and with a scale such as (a) no odour, (b) odour but not uncomfortable, (c) uncomfortable odour, (d) irritating odour and (e) very irritating odour, is used to evaluate the discomfort level of the exhaust gas by the panelists (Murari, 2011). The average value of the odour rating is evaluated.

The Use of pH Scale (Instrumental Assessment): this method uses pH scale measurement as indication of odour components of exhaust (Murari, 2007). The organic acid, aldehydes and other odourous components of the exhaust when condensed into an aqueous solution with distilled water will change the pH value. Therefore, the pH of exhaust gas solution is used as an indicator to evaluate the odour intensity of diesel exhaust. Bag sampling method was proposed for this technique (Tsunemoto *et al.*, 1996). In an experiment carried out by Murari, (2011), bags of about 1510mL volume were used to sample the exhaust from a diesel engine for 5 seconds. After the sampling, 250 mL of pure water was poured into the sample bag to create solution. The bag containing the sample solution was cooled to -10 °C for about 10 min. to condense the odour component and the pH was taken by a pH meter.

2.12. Engine Compatibility

Biodiesel blends up to B₂₀ are quite compatible with all kinds of diesel engine models. Some arguments about incompatibility of higher biodiesel blends (above B₂₀) with some modern diesel engines stems from the concern about the possibility of increasing engine oil dilution by the fuel. Also, since biodiesel is a natural solvent and will soften and degrade certain types of elastomers and natural rubber compounds, precautions are necessary to ensure that engines do not have seals made of these types of materials if higher biodiesel blends should be used on them. Original diesel engines manufactured from 1993 onwards are all equipped with fluorocarbon (viton) type seals and this material does not have

problem with biodiesel. For engine warranty, several engine manufacturers allow B₂₀. Caterpillar allows even B₁₀₀ in some of her engines (Caterpillar, 2001).

2.13. Biodegradability

It has been shown that biodiesel degrade four times faster than conventional diesel. B₂₀ blend of No.2 base diesel degrade twice as fast as No.2 base diesel alone (Tyson, 2001). Therefore, blending biodiesel with petroleum diesel will accelerate bioremediation in case of oil spill.

2.14. Lubricity

Some moving parts of diesel fuel pumps and injectors are protected from wear by the fuel. To avoid excessive wear, the fuel must have some minimum level of lubricity. Lubricity is the ability to reduce friction between solid surfaces in relative motion. Fuels with higher viscosities will provide better hydrodynamic lubrication. The use of fuels with poor lubricity can increase fuel pump and injector wear and at the extreme, cause engine failure. Biodiesel has better lubricity than petroleum diesel (Razon, 2009). Fuels with oxygen- and nitrogen-containing compounds and certain classes of aromatic compounds tend to have good boundary lubricity (Chevron, 2007). Mono acids, amides, and esters act as good lubricants.

Lubricity additives contain a polar group that is attracted to metal surfaces that causes the additive to form a thin surface film which acts as a boundary lubricant when two metal surfaces come in contact.

2.15. Toxicity

Toxicity is an important factor to be put into consideration in the choice of biodiesel feedstock. Generally, biodiesel from all commercial known feedstock is nontoxic. The use of toxic feedstock for biodiesel production can render the fuel toxic. However, there was a report that phorbol esters were detected in

jatropha biodiesel and its by-products (Makkar *et al.*, 2009). If this stands to be true, it means that detoxification of the feedstock becomes necessary for it to be safe. Great care should be taken in using toxic feedstock for biodiesel production; the seed processing facilities must be separated from those of edible oils to avoid any cross-contamination. *Ricinus communis* (castor), *Thevetia peruviana*, *Melia azederach*, *Teculia foetida*, *Balanites aegyptiaca*, *Orbignya speciosa*, *Sapium sebiferum*, and *Cerbera manghas*, were reported to have some toxic or anti-nutritive substances (Razon, 2009).

2.16. Oxidation Stability

Reports have shown a relative poor oxidative stability for biodiesel compared to petroleum diesel (Mariod *et al.*, 2006; Park *et al.*, 2008). The low stability is due to the presence of more polyunsaturated hydrocarbon in the fuel. The double bonds are the weak points of the fuel towards thermal, oxidative and microbial attack stability. Oxidative stability of biodiesel tends to worsen with increase in degree of unsaturation. Oxidative degradation of biodiesel can generate some polymeric materials which can cause deposits in the fuel line, leading to filter clogging and blockage of the system. Nevertheless, this problem can be solved by addition of antioxidant additive in the fuel.

2.17. Specifications for Biodiesel

ASTM has set standard to control the quality of biodiesel sold in the market. It specified that before a biodiesel should be sold in the market, it must meet the specifications, Table 2.3-2.4. This will provide more consistent fuel performance to the buyers. The standard can be met with a variety of feedstock and manufacturing processes. Currently, biodiesel market does not depend on the feedstock used but on meeting the specification.

Table 2.3: ASTM D6751 Specifications for Biodiesel (B100)

Property	Diesel	Biodiesel
Standard	ASTM D975	ASTM D6751
Composition	HC (C10-C21)	FAME (C12 –C22)
Kin. viscosity (mm ² /s) at 40°C	1.9-4.1	1.9-6.0
Boiling point (°C)	188-343	182-338
Flash point (°C)	60-80	100-170
Cloud point (°C)	-15 to 5	-3 to 12
Pour point (°C)	-35 to -15	-15 to 16
Water (vol%)	0.05	0.05
Carbon (wt%)	87	77
Hydrogen (wt%)	13	12
Oxygen (wt%)	0	11
Sulphur (wt%)	0.05	0.05
Cetane number	40-55	48-60

HC = hydrocarbon, FAME = fatty acids methylesters

Source: Lotero *et al.*, 2005; Kiss *et al.*, 2008.

Table 2.4: ASTM D7467 Specifications for Biodiesel Blends (B6–B20)

Property	Test method(s)	Limits	Units
Biodiesel content	ASTM D7371	6–20	% volume
Flash point (closed cup)	ASTM D93	52 min	°C
Cetane number	ASTM D976	40 min	
Water and sediment	ASTM D2709	0.050 max	% volume
Kinematic viscosity, 40°C	ASTM D445	1.9–4.1	mm ² /s
Acid value	ASTM D664	0.30 max	mg KOH/g
Ash content	ASTM D482	0.01 max	% mass

Source: Moser, 2009.

Table 2.5: European Specifications (EN 14214) for Biodiesel

Property	Test Method(s)	Limits	Units
Density, 15°C	EN ISO 3675, EN ISO 12185	0.860–0.900	g/cm ³
Kinematic viscosity, 40°C	EN ISO 3104, ISO 3105	3.5–5.0	mm ² /s
Flash point	EN ISO 3679	120 min	°C
Cetane number	EN ISO 5165	51 min	
Sulfated ash	ISO 3987	0.02 max	% (mol/mol)
Water content	EN ISO 12937	500 max	mg/kg
Acid value	EN 14104	0.50 max	mg KOH/g
Iodine value	EN 14111	120 max	g I ₂ /100 g
Linolenic acid content	EN 14103	12.0 max	% (mol/mol)
Methanol content	EN 14110	0.20 max	% (mol/mol)

Source: Moser, 2009.

2.18. The Nigeria's Biofuel Policy

On June 20th 2007 biofuel policy referred to as 'The Biofuels Policy and Incentives (2007)' was approved by the Federal Executive Council of Nigeria to facilitate the promotion of a national biofuels development programme in the country (NNPC, 2007). The framework of the policy and the incentives was meant to create an enabling environment that is expected to sensitize and catalyze the development of biofuels industry in the country. The policy was structured into two major components: The first phase defined as "seeding the market" involves the importation of commercial quantities of biofuel (ethanol) to seed the market base on 10 % ethanol blend (E-10) pending the time when the local production could be fully implemented; this was expected to take up to ten years from the initiation period.

The second stage would begin simultaneously with the seeding phase, with large scale plantations using the massive agricultural land distributed across the country which would eventually take over the importation. In line with this, the federal government of Nigeria approved the blending of biofuel as component of petroleum-based fuels in the country for all automotive uses with the expectation that, from the time of the take-off, full implementation could be achieved within 16years (Voice of America (VOA) News, 2007). To aid this, the government provided certain investment incentives under section 6.0 of the policy which include; funding of research and establishment of biofuels agency, waiver on customs and import duties, waiver on value-added tax, and withholding tax on interest, dividends, in respect of the interest on foreign loans, dividends and services rendered from outside Nigeria to biofuels companies by foreigners (VOA News, 2007; ECN, 2009). However, certain limitations have been identified in the biofuel policy which include; its dependence on importation, state-controlled monopoly, and lack of necessary legislative supports, (Oniemola and Sanusi, 2007).

CHAPTER THREE

MATERIALS AND METHOD

3.1. Equipment and Reagents:

Equipment

Atomic Absorption Spectrophotometer (Varian AA 280)

Density bottle (25mL)

Digital Magnetic Heater/Stirrer

Digital Weighing Balance (Adventurer™ Pro)

Emission Scanning Electron Microscope (JSM-6701F)

FTIR Spectrophotometer (8400S SHIMADZU)

GC-MS Apparatus (QP2010PLUS, SHIMADZU)

Locally Constructed Carbonizer

Muffle Furnace

Oven (XMTA)

Pensky Martens apparatus (K16200)

Ostwald viscometer

Rotary evaporator (TT-52)

UV/Visible Spectrophotometer (Pectrumlab 752s)

X-ray Powder Diffractometer (Rigaku D/Max 2500)

Thermogravimetric Equipment (TGA/DSTA851)

Reagents

KOH (Kermel)

Sodium thiosulphate (Kermel)

Starch (JHD)

Butanol (Sigma Aldrich)

Chloroform (JHD)

Glacial acetic acid (JHD)
Hydrochloric acid (JHD)
Iodine monochloride (JHD)
Methanol (Sigma Aldrich)

Methylene blue (JHD)
Nujol (JHD)
Phenolphthalein (Kem Light)
Potassium iodide (JHD)
Ammonium oxalate (JHD)
Sodium chloride (Kermel)
Sodium hydroxide (Kermel)
Tetraoxosulphate (VI) acid (Kermel)

3.1.1. Collection and Preparation of Samples

Hura crepitans, *Cucurbita pepo* and *Azelia africana* fruits were collected at Emene, Enugu State. The plants were identified by a taxonomist, Prof. J.C. Okafor, of Tree Crops and Tropical Ecology Centre, Independence Layout, Enugu State (16th September, 2011). The seeds were removed from the fruits and sun-dried for 7 days. The seed samples were ground and stored in air-tight plastic containers. Petroleum diesel (AGO) was sourced from NNPC Mega Station New-Haven, Enugu, Enugu State.

3.1.2. Oil Extraction

The oils from the ground samples were extracted with petroleum ether (60 – 80 °C) using a soxhlet extractor. The ground sample (50 g) was packed in the thimble of the soxhlet extractor and was extracted with 200 mL of the solvent for 6 h after which the oil was separated from the extracting solvent using rotary evaporator apparatus. The percentage oil yields were determined.



Plate 3.1: *Cucurbita pepo* seeds

Common name: Broad leaf pumpkin

Igbo name: Ugbogulu

Hausa Name: Kabewa

Yoruba Name: Elegede



Plate 3.2: *Afzelia africana* seeds

Common name: African oak

Igbo name: Akparata

Hausa Name: Kawo

Yoruba Name: Apa



Plate 3.3: *Hura crepitans* seeds
Common name: Monkey no-climb

3.2. Physicochemical Characterization of the Oil

3.2.1 Determination of Moisture Content

A clean porcelain crucible was dried in an oven at 100 °C for 30 min, cooled in desiccator and weighed. This was repeated until a constant weight was achieved. The sample (5.0 g) was weighed into the crucible and dried in the oven at 105 °C for about 2 h, cooled in the desiccator for 30 min and reweighed. The entire process was repeated until a constant weight was obtained (FSSAI, 2012).

$$\% \text{Moisture} = \frac{(W_1 - W_2) \times 100}{W_1} \quad (3.1)$$

Where,

W_1 = weight of sample when wet

W_2 = weight of sample when dried

3.2.2 Determination of Acid Value

The sample (0.5 g) was weighed into a 250 mL conical flask and 50 mL of absolute ethanol was added to dissolve the sample. Phenolphthalein indicator (0.5 mL) was added and the mixture was titrated with 0.05 M potassium

hydroxide solution while being stirred with magnetic stirrer. Blank titration was also performed using the same value of ethanol and indicator only (FSSAI, 2012).

$$\text{Acid value} = \frac{(a-b) \times \text{Molarity of KOH} \times \text{molar mass of KOH}}{m} \quad (3.2)$$

Where,

a = volume of KOH used for the sample

b = volume of KOH used for the blank

m = mass of oil used

3.2.3 Determination of Iodine Value

The sample (0.3 g) was weighed into a 500 mL conical flask and dissolved with 25 mL of chloroform. Iodine monochloride (25 mL) was added. The flask was tightly covered, vigorously shaken and placed in a dark cupboard for two hours with vigorous shaking at interval of 30 min. The same procedure was repeated for the blank test (the same type of solution prepared using the same procedure but without the oil sample). After standing, 15 mL of 10 % aqueous potassium iodide and 100 mL of recently boiled and cooled water were added. This was to convert the un-reacted reagent (iodine monochloride) to iodine. The mixture was titrated against a standard solution of 0.1 M sodium thiosulphate until the yellow colour almost disappeared. Few drops of 1 % starch indicator was added and the titration continued by adding the sodium thiosulphate drop wise until the blue coloration disappeared. The blank solution was also titrated in the same way (FSSAI, 2012).

$$IV = \frac{12.69 \times M \times (V_1 - V_2)}{m} \quad (3.3)$$

Where;

IV – Iodine value

M = Molarity of sodium thiosulphate used

V_2 = Volume of sodium thiosulphate used for the titration

V_1 = Volume of sodium thiosulphate used for the blank

m = Mass of the sample.

3.2.4 Determination of Saponification Value

The sample (1.0 g) was weighed into a round bottom flask and 50 mL of 1 M alcoholic potassium hydroxide was added. The flask was fitted with a reflux condenser and left to boil under magnetic heater for 45min. Exactly 10 mL of hot ethanol was used to wash down the inside of the condenser into the flask. The solution was then titrated against 1 M of hydrochloric acid while hot using few drops of phenolphthalein indicator. The same procedure was equally used for the blank titration (FSSAI, 2012).

$$\text{Saponification value} = \frac{(V_1 - V_2) \times M \times \text{molar mass of KOH}}{m} \quad (3.4)$$

Where,

V_2 = volume of HCl used for the sample

V_1 = volume of HCl used for the blank

M = molarity of HCl

m = mass of the sample used

3.2.5 Determination of Relative Density

The relative density was determined at room temperature (28 °C) using relative density bottle. A clean and dry density bottle of 25 mL capacity was weighed (W_0) and then filled with distilled water, stopper inserted and weighed to obtain (W_1). The bottle was emptied, dried, refilled with the oil sample and weighed to get (W_2) (FSSAI, 2012).

$$\text{Relative Density} = \frac{(W_2 - W_0)}{(W_1 - W_0)} \quad (3.5)$$

3.2.6. Determination of Mineral Ash

Crucible was ignited with a Bunsen burner, cooled in a desiccator and weighed until a constant weight was obtained (W_1). The sample (2.0 g) was added into the crucible and weighed (W_2). The crucible was charred over a Bunsen flame until no more soot was given off. The crucible was transferred by the help of a tong to a muffle furnace and heated at 600 °C for 1 h, after which it was fully ashed.

The crucible was removed, cooled in a desiccator and reweighed; the weighing was repeated at interval of time until a constant weight was obtained (W_3) (FSSAI, 2012).

$$\% \text{Mineral ash} = \frac{(W_3 - W_1) \times 100}{(W_2 - W_1)} \quad (3.6)$$

3.2.7. Determination of Calorific Value

The calorific value of the samples was estimated using the API Table (Appendix 1) which relates the relative density and the gross calorific value.

3.3. Preparation of Modified Biowaste Catalysts from the Seed Cake/Shell

Solid wastes generated from the oil extraction process: *H. crepitans* seed shells (Plate 3.4) and *A. africana* seed cake (Plate 3.5) was utilized to prepare bio-based solid acid catalysts. Method described by Liu *et al.*, (2013) and Wang *et al.*, (2014) was used with some modifications. The biomass was partially carbonized to convert them to polyaromatic-rich structure and then sulphonated to introduce sulphonic group ($-\text{SO}_3\text{H}$) on them.

The seed shell/cake was ground and screened to particle sizes not more than 0.841 mm (Mesh No. 20). The prepared biomass (10 g) was partially carbonised in limited supply of oxygen at 500 °C, with varied residence time of: 0, 30, 60, 90 and 120 min. The carbonization was done using a locally prepared

carbonizer. 1g of the carbonized material was mixed with 10 mL of concentrated H_2SO_4 in a 250 mL flask and heated in an oil bath at 150 °C for 4 h. The mixture was allowed to cool at room temperature and carefully transferred into a beaker containing 150 mL distilled water. The catalyst was separated by filtration and washed repeatedly using hot distilled water until no sulphate ions was detected in the wash water by testing with barium chloride. The washing removed all the residual sulphuric acid from the material, leaving only $-\text{SO}_3\text{H}$ strongly attached to the polyaromatic structure. The solid catalysts were dried at 105 °C for 6 h in an oven and stored in an air-tight container.



Plate 3.4: *H. crepitans* Seed shell



Plate 3.5: *A. africana* seed cake



Plate 3.6: *H. crepitans* Seed shell carbonized at 500 °C at Varied Time

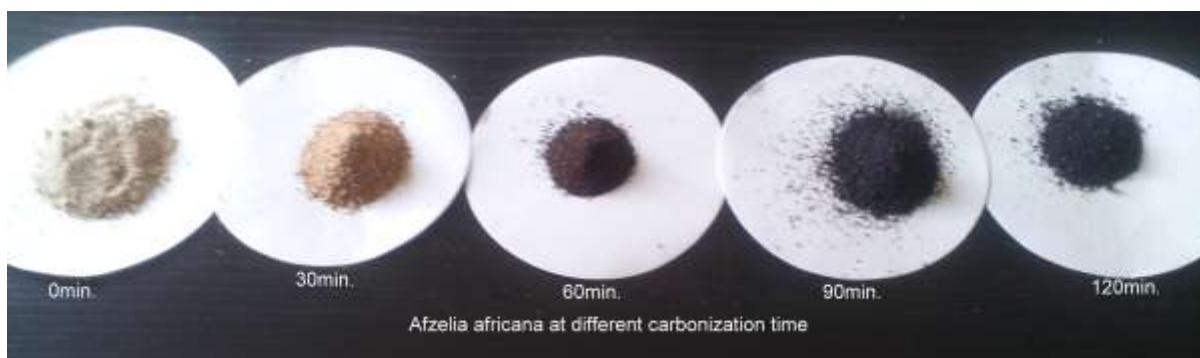


Plate 3.7: *A. africana* seed cake carbonized at 500 °C at Varied Time



Plate 3.8: Locally constructed carbonizer

The locally constructed carbonizer comprised two-layered stainless cylindrical container. Two metallic pipes connected the inner chamber of the container to two sealed conical flasks containing 2 M NaOH. The alkali was to absorb gaseous pyrolysate such as $\text{CO}_2(\text{g})$, $\text{H}_2\text{O}(\text{g})$ and other acidic gases from the inner

chamber, thereby reducing pressure in the inner chamber of the reactor to avoid explosion. The inner chamber was packed with copper turnings which was to remove oxygen from the chamber when heated. The biomass was packed in a crucible, covered and then placed in the reactor. The reactor was heated to a desired temperature using infrared heater with temperature regulator.

3.3.1 Catalyst Characterization

(a) X-ray diffraction (XRD) analysis was carried out using a Rigaku D/Max 2500 X-ray powder diffractometer. The surface morphology of the catalysts were obtained using a field emission scanning electron microscope (JSM-6701F/JEOL). The bond structures of the samples were characterized using FTIR spectrophotometer. Thermogravimetric analysis (TGA) was carried out using TGA/DSTA851 equipment. The samples were heated from room temperature to 900 °C at a heating rate of 10 °C/min. in an N₂ stream.

(b) Determination of specific surface area of the catalyst: The specific surface area of the catalyst was determined using methylene blue adsorption test method (Santamarina *et al.*, 2002; Dawodu *et al.*, 2012; Okeola *et al.*, 2012). The sample (0.05 g) was added in 10 mL of 5 ppm of methylene blue solution and agitated in a shaker for 2 h. It was then kept for 12 h for equilibrium to be attained. The solution was centrifuged, decanted and the absorbance taken at 645 nm using UV/visible spectrophotometer (Spectrumlab 752s). The same procedure was repeated for 10, 15, 20 and 25 ppm solutions of methylene blue. The amount of methylene blue adsorbed on the catalysts from each solution was calculated by the Equation (3.7) (Itodo *et al.*, 2010).

$$q_e = \frac{(C_o - C_e)V}{M} \quad (3.7)$$

Where C_o (mg L⁻¹) is the initial concentration of the methylene blue solution, C_e (mg L⁻¹) is the concentration of the methylene blue solution at equilibrium, V

(L) is the volume of the methylene blue solution used and M (g) is the mass of the catalyst used. According to Langmuir equation: $1/q_e = (1/K_a q_m)1/C_e + 1/q_m$ (Itodo *et al.*, 2010), a plot of $1/q_e$ versus $1/C_e$ would give a straight line with slope $(1/K_a q_m)$ and intercept $(1/q_m)$.

The specific surface area (SSA) was calculated from the amount of methylene blue absorbed at the optimum point of cation replacement using equation 3.8.

$$SSA = \frac{q_m \times AMB \times N_A \times 10^{-20}}{319.98} \quad (3.8)$$

Where, q_m is the maximum amount of methylene blue per unit weight of catalyst to form a complete adsorbed methylene blue monolayer, N_A is the Avogadro's number (6.02×10^{23}), AMB is the area covered by one methylene molecule (assumed to be 197.2 \AA^2) and 373.9 is the molar mass of methylene blue (Itodo *et al.*, 2010).

(c) Determination of acid site density of the catalyst: Acid site density of the catalyst measures the amount of sulphonic group ($-\text{SO}_3\text{H}$) present per unit mass of the catalyst (Bennett *et al.*, 2016).

The sample (0.1 g) was dispersed in 20 g of saturated aqueous solution of NaCl (2 M) and stirred at room temperature for 4 h. The Na^+ was expected to displace protons belonging to the sulphonic group in the catalyst according to equation 3.9.



The mixture was filtered and the filtrate titrated with 0.1 M NaOH solution. Acid density was calculated using equation 3.10 (Lee, 2013; Liu *et al.*, 2013).

$$N_{\text{SO}_3\text{H}} (\text{mmole/g}) = \frac{V \times N}{m} \quad (3.10)$$

Where, NSO_3H = acid density, V = volume of NaOH used (mL), N = the normality of the NaOH solution, m = mass of the catalyst.

(d) Determination of hydrolytic stability: the stability of the acid sites of the catalyst towards leaching into reaction medium was determined by the method described in Lee, (2013) with some modifications. Exactly 0.1 g of the prepared solid acid catalyst was dispersed in 25 mL of deionized water and the solution was stirred at 95 °C for 5 h. The catalyst was separated by filtration and the filtrate was titrated with 0.1 M sodium hydroxide solution. The concentration of the sulphonic group leached into the water was calculated and expressed as percentage of the initial acid density of the catalyst.

3.4. Biodiesel Synthesis

Methyl esters and butyl esters were synthesized from each oil sample using two-step transesterification process. This method was necessitated due to high free fatty acid content of the crude vegetable oils (between 36 to 58 mg KOH/g) and the need to ensure complete conversion. The oil was completely hydrolysed to free fatty acids (FFAs) by the method described by Ajiwe *et al.*, (2001). The resultant FFAs were esterified with methanol and butanol via acid catalysed esterification reaction. H_2SO_4 and the modified biowaste catalysts were applied in the esterification reaction.

The oil sample (300 mL) was measured into a 1000 mL beaker and saponified with sodium hydroxide solution prepared by dissolving 47.5 g of NaOH granules in 150 mL of distilled water. The product formed was salted out using saturated NaCl solution, separated and washed with warm distilled water. It was re-dissolved in warm distilled water and 1:3 H_2SO_4 solution was gradually added to make the mixture neutral. This released the FFAs in the mixture. The FFAs were separated with separating funnel, washed with warm distilled water

and was used as the base oil for synthesis of biodiesels via acid catalysed esterification reaction.

3.4.1. Effect of Process Parameters on the Biodiesel Synthesis

250 mL conical flask equipped with a reflux condenser was used as a reactor. Various process parameters such as quantity of catalyst, stirring rate, reaction temperature and time were studied on the biodiesel synthesis. The process variables were aimed at achieving optimum biodiesel yields.

(a) Effect of quantity of catalyst – 5 mL of the base oil and 30 mL of methanol were added into the reactor. 1 % catalyst (by weight of the base oil) was added and temperature was set at 70 °C. The reaction was allowed to run for 60 min at stirring rate of 200 rpm. At the end, the reaction was immediately quenched by adding excess distilled water. The product was separated using separating funnel and washed five times with distilled water to remove the remaining residual methanol and catalyst and then dried in an oven (105 °C) for 2 h. The acid value of the dried product was determined using standard procedure described earlier.

As the base oils (comprising FFAs) were being converted to methyl esters, the acid value of the sample was expected to drop. The acid value at each point gave indication of the extent to which the base oil has been converted to methyl esters (Pasias *et al.*, 2006; Berrios *et al.*, 2007; Abiney *et al.*, 2008; Thiruvengadaravi *et al.*, 2009; Alípio *et al.*, 2009; Muhammad and Satriana, 2009).

$$\%conversion = \frac{(A_i - A_f)}{A_i} \quad (3.11)$$

Where A_i = initial acid value of the base oil

A_f = final acid value

The above procedure was repeated using 2, 3, 5 and 10 % catalyst.

(b) Effect of Stirring Rate - stirring rate was varied: 0, 200, 400, 600 and 800 rpm, the optimum catalyst for each oil sample were used while maintaining oil/alcohol ratio and temperature at 1:6 and 70 °C respectively.

(c) Effect of Temperature and Time: Effect of temperature and reaction time was studied on the esterification reaction. Temperature was varied: room temperature (28 °C), 40, 50, 60, 70 and 80 °C. For each run, optimum catalyst and stirring rate were used and oil/alcohol ratio was maintained at 1:6. At each temperature, some sample was withdrawn from the reaction mixture at interval of time and the %conversion determined.

The entire procedure was repeated using butanol.



Plate 3.9: Set up for biodiesel kinetic study

3.4.2. Bulk Biodiesel Preparation and Blending

For the bulk biodiesel preparation, 1000 mL conical flask equipped with a reflux condenser was used as a reactor. At oil/alcohol ratio of 1:6, the optimal catalyst, temperature, stirring rate and time for each oil were used to prepare methyl esters and butyl esters from each oil sample. The product was separated using separating funnel and washed severally with warm distilled water. Separating the residual butanol after the esterification reaction required several

washing to remove the unreacted butanol which was miscible with the oil phase during the reaction unlike methanol which was immiscible and was simply separated using separating funnel. The biodiesel samples were dried in oven at 105 °C for 2 h.

Using measuring cylinder, each biodiesel sample was blended with the petroleum diesel in the ratio of 0:100, 10:90, 20:80, 30:70, 40:60, 50:50, 60:40, 70:30, 80:20, 90:10 and 100:0. The blends were labelled appropriately.

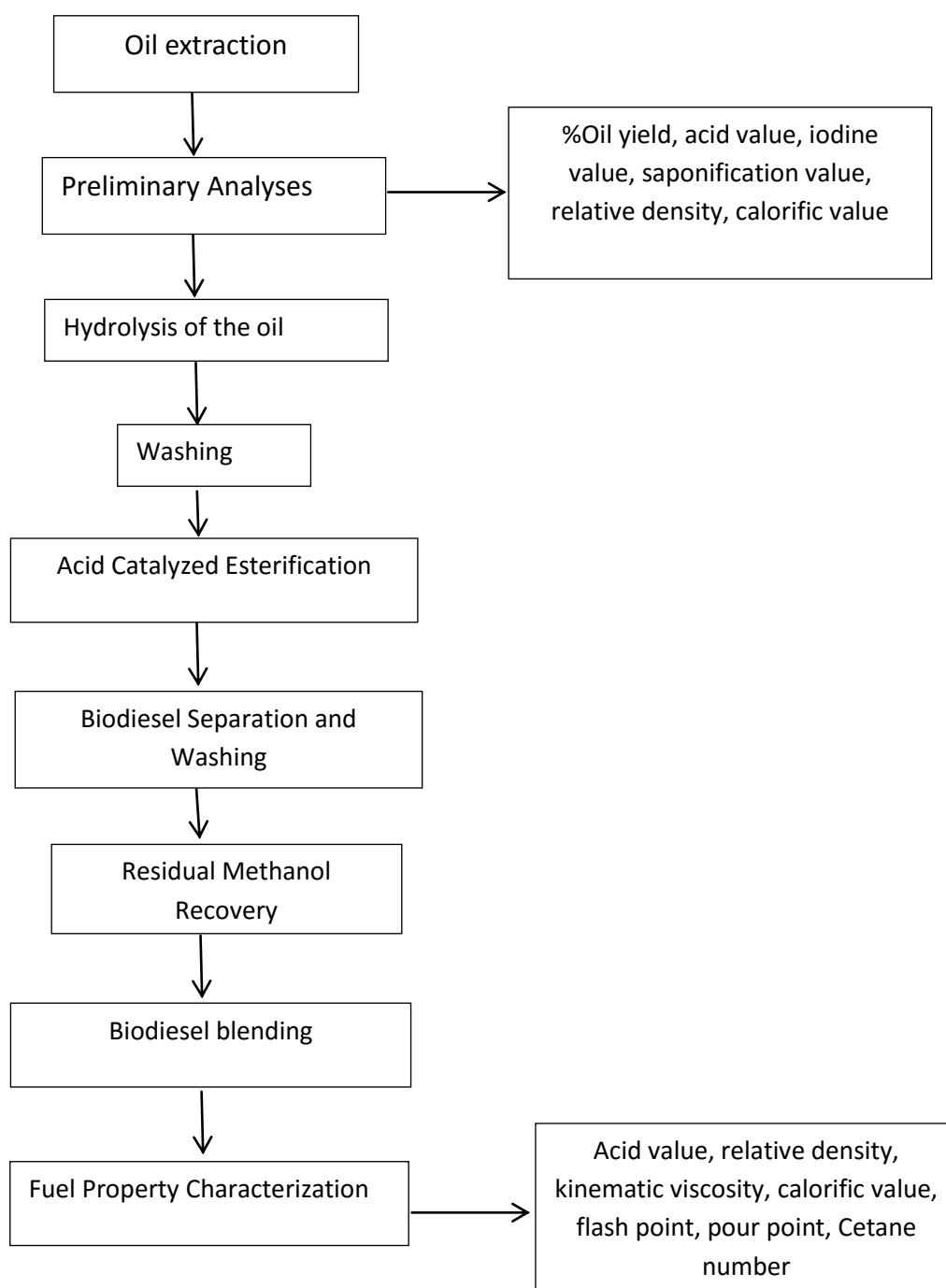


Fig.3.1: Flow Chart for Biodiesel Preparation and Characterization

3.5. Characterization of the Biodiesel Samples

3.5.1. Determination of Kinematic Viscosity

Kinematic viscosity was determined using Ostwald Viscometer. The sample was filled into the viscometer up to the mark “A”, corked and allowed to stand and attain the temperature of the water bath (40 °C). The cork was removed to allow the sample to flow down the viscometer arm gently. Using a stopwatch, the time taken for the sample to flow from the mark “D” to “B” of the equipment was recorded. The sample was pumped back with pipette filler and the experiment was repeated. The average time of flow was evaluated. The kinematic viscosity is the product of the measured flow time and calibration constant (C) of the viscometer in centistokes (cSt). The process was repeated at water bath temperature of 70 °C and 100 °C for each sample.

$$\text{Viscometer in centistokes} = C \times t \quad (3.12)$$

Where; C is a constant.

3.5.2. Determination of Flash Point

Each sample was shaken and filled into a flash point cup up to the level inscribed in the cup. The cup was placed in the Pensky Martens tester, and the power was switched on to heat and stir the sample. The pilot flame was then ignited and with the help of the shutter operating knob, the cup was lowered at intervals to check when it has flashed. The flash point was recorded as the temperature when the flame flashed inside the cup.

3.5.3 Determination of Pour Point

The sample (50 mL) was first warmed in a beaker and then refrigerated at a specified rate. It was observed at interval of 5 min by tilting it for 5 s. The point at which the sample movement was observed to stop when the container was tilted was noted; pour point was 3 °C higher than the temperature of the sample at that point (ASTM D97).

3.5.4 Estimation of Cetane Number

The cetane number of the samples were estimated using equation (3.13) developed by Tong *et al.*, (2011). Cetane number test is very expensive to carryout and for this reason several equations have been developed to predict cetane number of biodiesel from fatty acid profile. It has been shown that predicted cetane number agrees very well with cetane number obtained from engine test (Knothe *et al.*, 2005).

$$\text{Cetane number (CN)} = 1.068 (\sum \text{CN}_i w_i) - 6.747 \quad (3.13)$$

Where CN_i is the cetane number of each pure fatty acid methyl esters obtained from literature data (Knothe *et al.*, 2005; Ramos *et al.*, 2009; Tong *et al.*, 2011) and w_i is the weight fraction of the fatty acid methyl esters present in each sample.

Other fuel properties of the biodiesel including acid value, mineral ash and calorific value were determined using the same procedure as discussed earlier in the analyses of the oil samples.

3.5.5 Gas Chromatography/Mass Spectroscopy (GC-MS) Analysis

GC-MS apparatus (QP2010PLUS, SHIMADZU) with auto sampler and auto analyser- fused silica capillary column (60x60mm i.d) and helium as the carrier gas (flow rate=1.61 mL/min) was used. The injection temperature was 250 °C and oven temperature was kept at 60 °C for 5 min, and then ramped to 140 °C for another 5min. This was followed by adjusting it to 280 °C at a rate of 20 °C/min. and then kept at 280 °C for 15 min. The end of capillary column was inserted directly into the ion source of MS and interface temperature was maintained at 250 °C. The mass spectrometric data were acquired and processed with SHIDMAZU MAT 330 data system. The run button was switched on to generate the peaks which started appearing on the computer screen at different times. This profile was later printed out.

The set up had an accompanying library coupled to it. The esters were identified using the National Institute of Standard and Technology (NIST) mass spectral library based on their similarity indices.

From the GC-MS results, the fatty acid profiles of the vegetable oils were determined. Degree of unsaturation and average chain length of the fatty acids in each oil sample were evaluated using equation 3.14 and 3.15 respectively. Percentage carbon, oxygen and hydrogen in each vegetable oil esters were also calculated from the molecular formula of the compounds as indicated by the GC-MS results.

$$\text{Degree of unsaturation} = \sum n_i w_i \quad (3.14)$$

Where n_i is the number of carbon-carbon double bonds in each fatty acid (xx:n) and w_i is its weight fraction in each sample.

$$\text{Average chain length} = \sum C_i w_i \quad (3.15)$$

Where C_i is the number of carbon atoms (xx) in each fatty acid.

3.5.6. Determination of Metallic Elements in the Samples

Digestion of the sample: The oil sample (0.5 g) was weighed into a conical flask. Exactly 10 ml of concentrated nitric acid was added and heated until the brown fumes subsided. Concentrated sulphuric acid (10 mL) was added and heated for more 20 min until the liquid turned nearly colourless. Saturated solution of ammonium oxalate (5 mL) was added to facilitate the removal of coloured nitro-compounds. The liquid was heated till no brown fumes were observed (Uoro *et al.*, 1982). The clear solution was made up to 100 mL in a volumetric flask and filtered with a filter paper and stored in a 100 mL sample bottle for analysis.

The metals present in the digested samples were analysed using atomic absorption spectrophotometer model Varian AA 280.

3.5.7. FTIR Bond Structure/Stability Relationship

The bond structures/stability of the fuel samples were analysed at varied temperatures: room temperature (28 °C), 50, 100, 150, 200, 250 and 300 °C using FTIR spectrophotometer (FTIR-8400S SHIMADZU). Thermal stability of a fuel sample is usually examined at a short exposure time without appreciable deterioration of the fuel (Batts and Fathoni, 1991). The sample was heated at each temperature for 10 min and allowed to cool before the FTIR analyses. Plate 3.10-3.12 show the pictures of methyl esters of the oil samples heated at the various temperatures before the analysis.

A drop of the sample was placed in between two sodium chloride plates with groove by the help of a dropper. The sodium chloride Plate was then attached to a Fourier transform infrared spectrometer coupled to a computer with a print out system. The sample in the plate was irradiated by infrared source lamp at one end of the spectrometer and the absorption frequencies (cm^{-1}) recorded

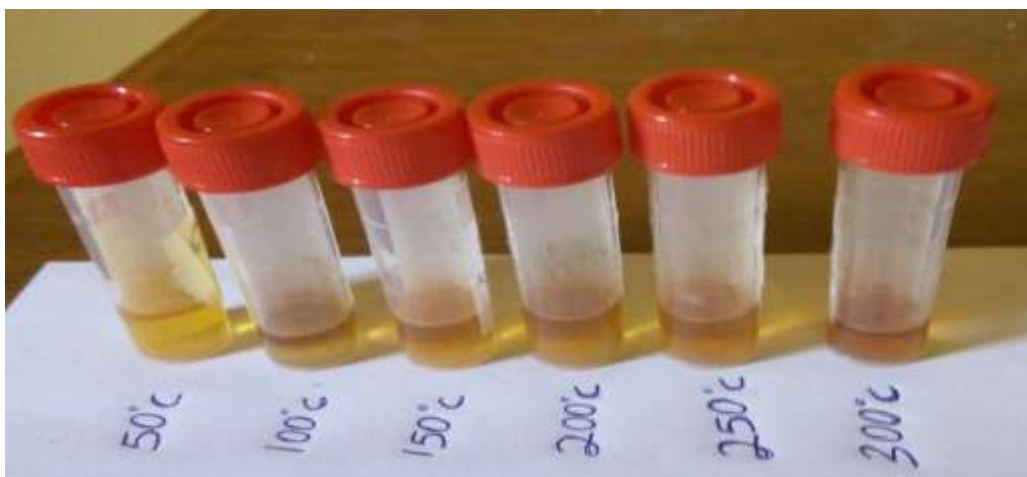


Plate 3.10: *Cucurbita pepo* methyl esters at different temperatures

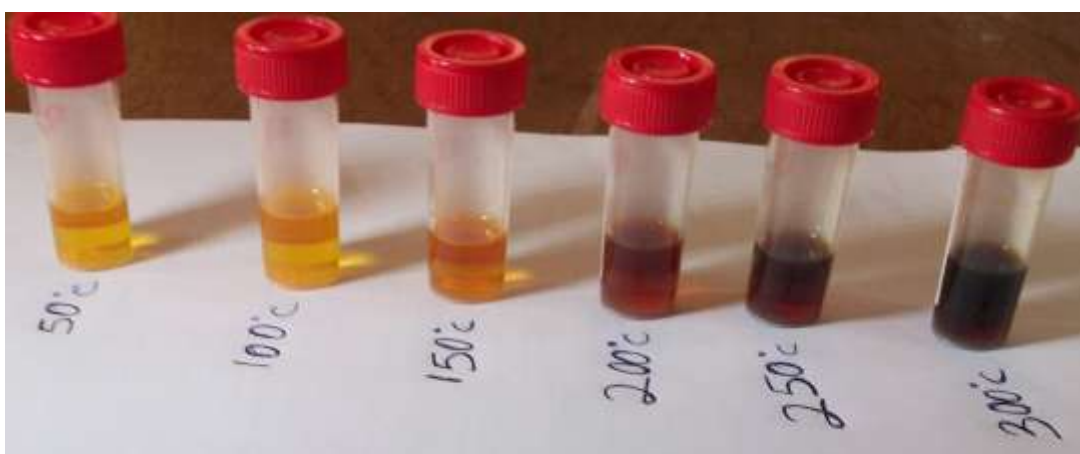


Plate 3.11: *Afzelia africana* methyl esters at different temperatures

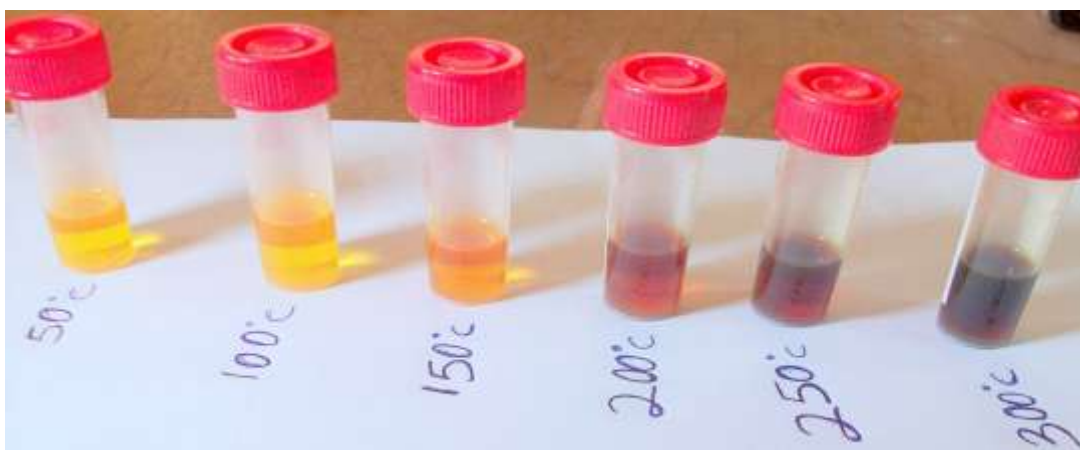


Plate 3.12: *Hura crepitans* methyl esters at different temperatures

CHAPTER FOUR

RESULTS AND DISCUSSION

4.1. Physicochemical Properties of the Extracted Oils

The results of physicochemical properties of the extracted seed oil samples are presented in Table 4.1. The oil obtained from *C. pepo* was light brown and that of *A. africana* and *H. crepitans* were golden yellow and pale yellow respectively. The percentage oil yields of the oil crops: 42.43 % (*C. pepo*), 21.80 % (*A. africana*) and 39.87 % (*H crepitans*) were quite promising for commercial biodiesel production.

Table 4.1: Physicochemical Properties of the Extracted Oils

Properties	<i>C. pepo</i>	<i>A. africana</i>	<i>H. crepitans</i>
Yield (%)	42.43	21.90	38.87
Colour	Light brown	Golden yellow	Pale yellow
Acid value (mg KOH/g)	26.32	23.52	52.08
Kinematic viscosity (40 °C, mm ² /s)	21.92	23.84	18.97
Relative density (at 28 °C)	0.9038	0.8971	0.8962
Ash content (%)	0.005	0.006	0.004
Moisture content (%)	1.70	2.10	1.90
Saponification value (mg KOH/g)	188.21	128.07	149.59
Iodine value (g/100 g of oil)	115.00	120.09	109.00
Calorific value (kJ/g)	44170	44190	44234

* = Average of three replicate determinations

The acid values, 26.32, 23.52 and 52.08 mg KOH/g for *C. pepo*, *A. africana* and *H. crepitans* respectively were very high indicating that the oils could not be processed directly into biodiesel using base-catalysed transesterification method

(Sivanesan, 2009). High FFAs in oil deactivates base catalyst and leads to soap formation with attendant decrease in biodiesel yield.

The results of iodine value showed that *C. pepo* and *H. crepitans* seed oils have iodine value of 115 and 109 respectively indicating that they were non-drying oils (< 120) while *A. africana* had iodine value of 120.09 and fell within semidrying oil (> 120).

4.2. GC-MS Analysis of the Methyl esters/Fatty Acid Profile of the Oils

The results of the GC-MS analysis of methyl esters of the oil samples and their fatty acid profiles are presented in Tables 4.2-4.7.

Table 4.2: GC-MS Analysis of *C. pepo* Seed Oil Methyl esters

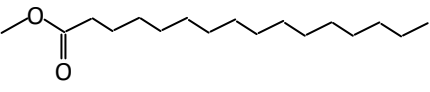
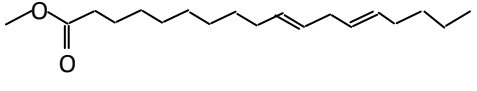
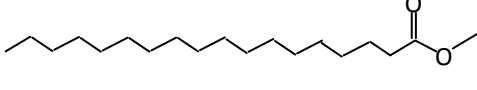
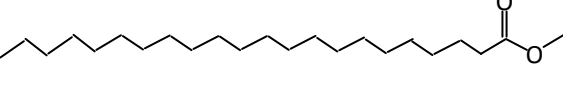
Peak No.	R.A (%)	Molecular formula	M. wt	Name	Structure
1	32.42	C ₁₇ H ₃₄ O ₂	270	Hexadecanoic acid methylester (methyl palmitate)	
2	37.56	C ₁₉ H ₃₄ O ₂	294	10,13-octadecadienoic acid methylester	
3	27.42	C ₁₉ H ₃₈ O ₂	298	Octadecanoic acid methylester (methyl stearate)	
4	2.60	C ₂₃ H ₄₆ O ₂	354	docosanoic acid methylester (methyl behenate)	

Table 4.3: Fatty Acid Profile of the *C. pepo* Seed Oil

	Common name	Systematic name	Shorthand name	R.A (%)
1	Palmitic acid	Hexadecanoic acid	16:0	32.42
2	-	10,13-Octadecadienoic acid	18:2	37.56
3	Stearic acid	Octadecanoic acid	18:0	27.42
4	Behenic acid	Docosanoic acid	22:0	2.60

Table 4.4: GC-MS Analysis of *A. africana* Seed Oil Methyl esters

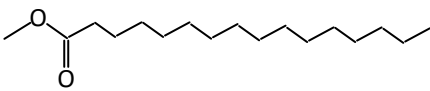
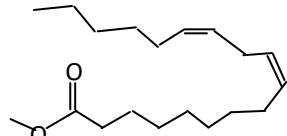
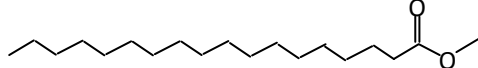
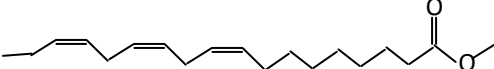
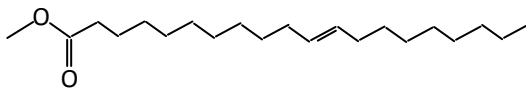
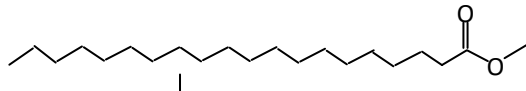
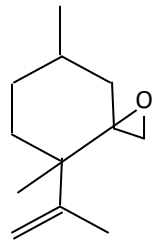
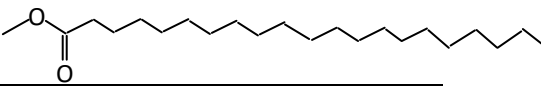
Peak No.	R.A (%)	Molecular formula	M. wt.	Name	Structure
1	12.24	C ₁₇ H ₃₄ O ₂	270	Hexadecanoic acid methylester (methyl palmitate)	
2	26.23	C ₁₉ H ₃₄ O ₂	294	cis-9,12-octadecadienoic acid methylester (methyl linoleate)	
3	8.76	C ₁₉ H ₃₈ O ₂	298	Octadecanoic acid methylester (methyl stearate)	
4	36.32	C ₁₉ H ₃₂ O ₂	292	cis-9,12,15-otadecatrienoic acid methylester (methyl linolanate)	
5	1.71	C ₂₁ H ₄₀ O ₂	324	11-eicosenoic acid methyl ester	
6	2.27	C ₂₁ H ₄₂ O ₂	326	Eicosanoic acid methylester (methyl arachidate)	
7	2.61	C ₁₂ H ₂₀ O	180	4-isopropenyl-4,7-dimethyl-1-oxaspiro[2,5]octane	
8	9.86	C ₂₂ H ₄₄ O ₂	340	Heneicosanoic acid methylester	

Table 4.5: Fatty Acid Profile of the *A. africana* Seed Oil

	Common name	Systematic name	Shorthand name	R.A (%)
1	Palmitic acid	Hexadecanoic acid	16:0	12.24
2	Linoleic acid	<i>cis</i> -9,12-octadecadienoic acid	18:2(n-6)	26.23
3	Stearic acid	Octadecanoic acid	18:0	8.76
4	linolenic acid	<i>cis</i> -9,12,15-otadecatrienoic acid	18:3 (<i>n</i> -3)	36.32
5	Gandoic acid	<i>cis</i> -11-eicosenoic acid	20:1	1.71
6	Arachidic acid	Eicosanoic acid	20:0	2.27
7	Heneicosanoic acid	Heneicosanoic acid	21:0	9.86

Table 4.6: GC-MS Analysis of *H. crepitans* Seed Oil Methyl esters

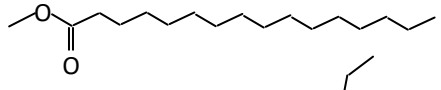
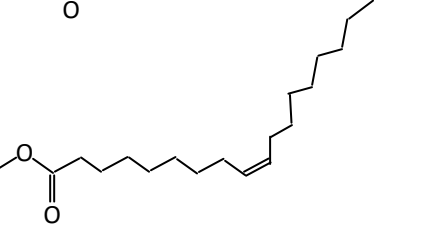
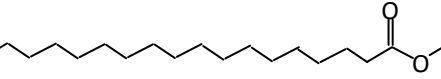
Peak No.	R.A (%)	Molecular formula	M. wt.	Name	Structure
1	30.69	C ₁₇ H ₃₄ O ₂	270	Hexadecanoic acid methylester (methyl palmitate)	
2	45.67	C ₁₉ H ₃₆ O ₂	296	<i>cis</i> -9-octadecenoic acid methylester (methyl oleate)	
3	23.64	C ₁₉ H ₃₈ O ₂	298	Octadecanoic acid methylester (methyl stearate)	

Table 4.7: Fatty Acid Profile of the *H. crepitans* Seed Oil

	Common name	Systematic name	Shorthand name	R.A (%)
1	Palmitic acid	Hexadecanoic acid	16:0	30.69
2	oleic acid	<i>cis</i> -9-octadecenoic acid	18:1	45.67
3	Stearic acid	Octadecanoic acid	18:0	23.64

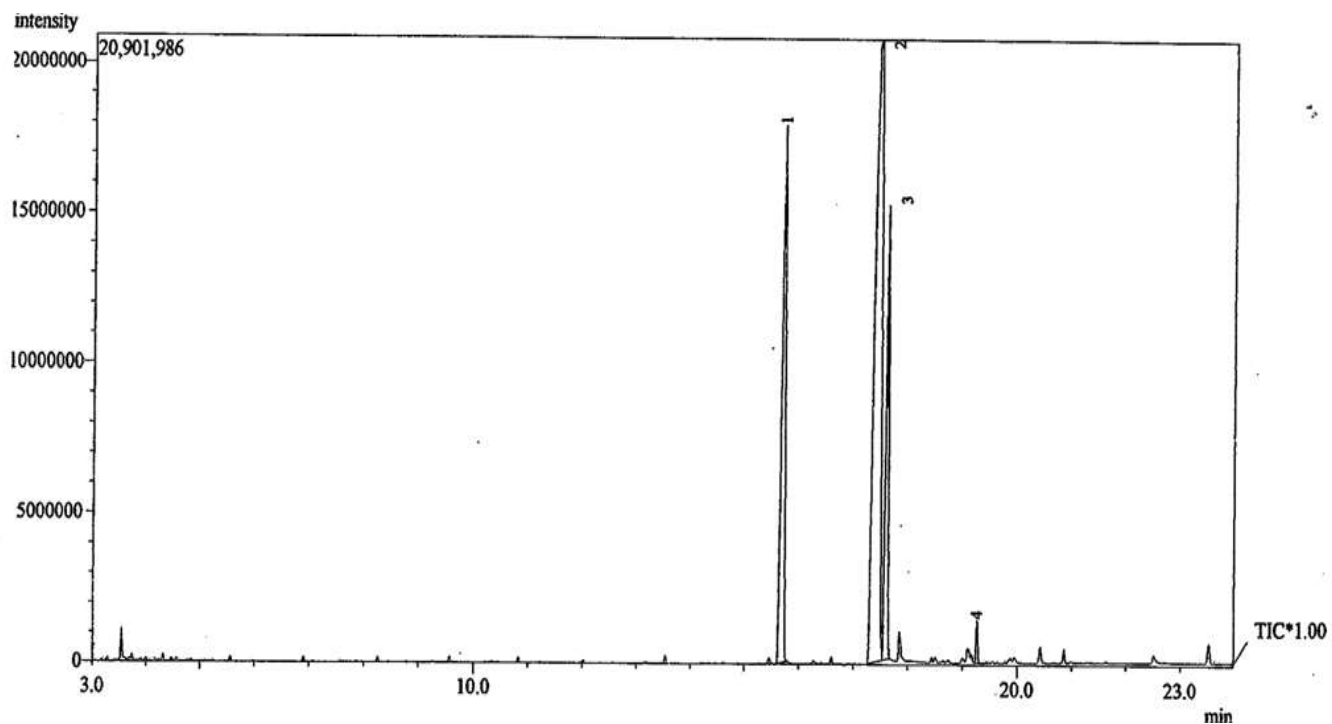


Fig. 4.1: GC-MS spectrum of *C. pepo* methyl esters

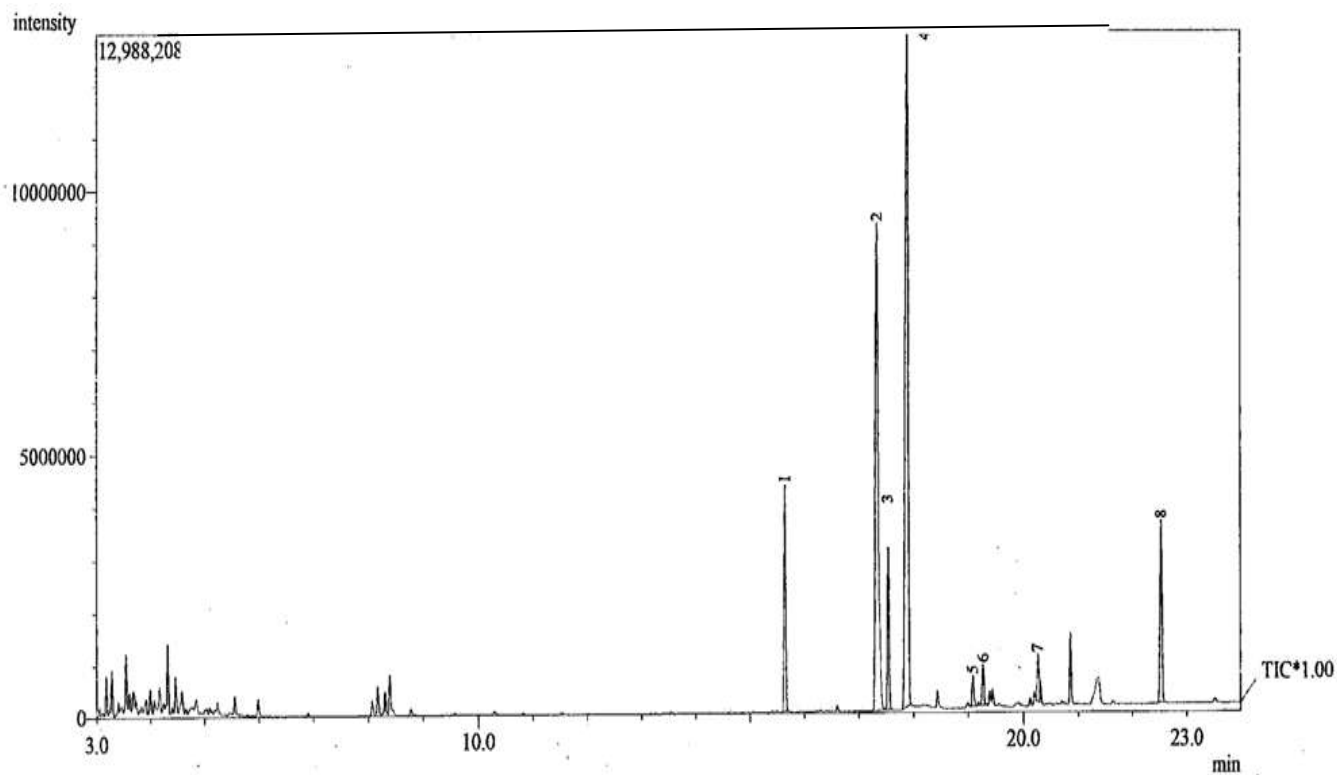


Fig. 4.2: GC-MS spectrum of *A. africana* methyl esters

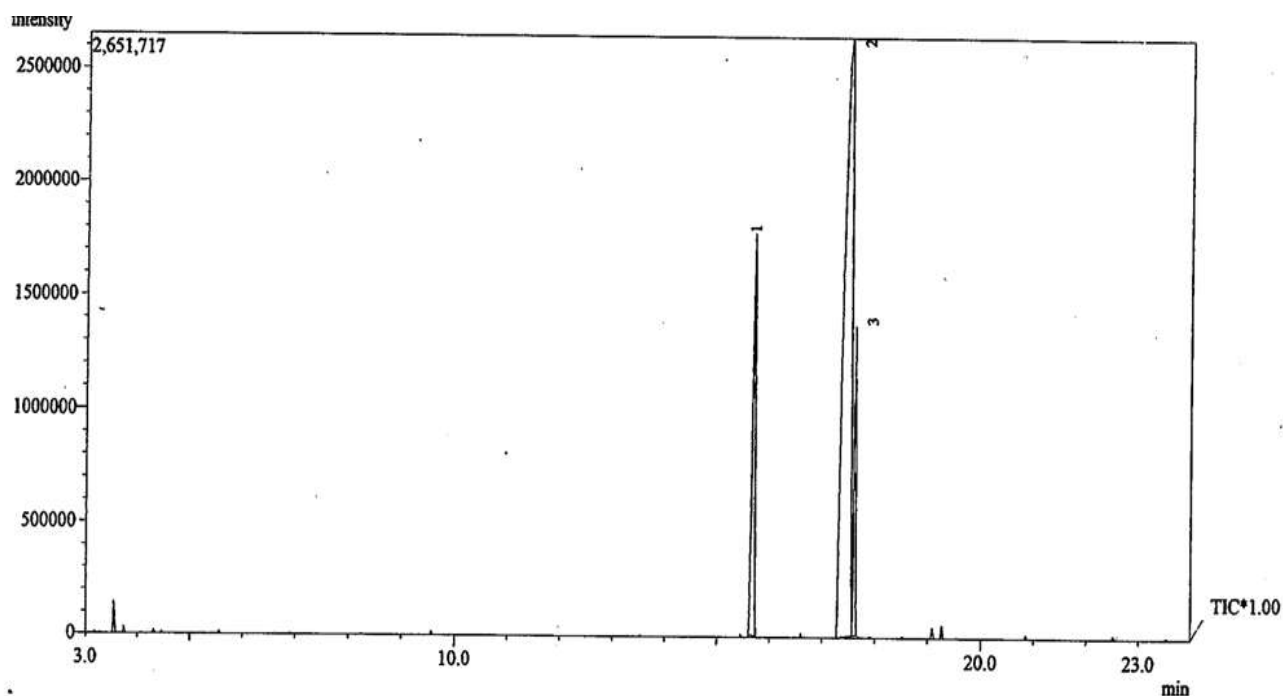


Fig. 4.3: GC-MS spectrum of *H. crepitans* methyl esters

From the results of the fatty acid composition, *C. pepo* oil contained palmitic acid (32.42 %), 10,13-Octadecadienoic acid (37.56 %), stearic acid (27.41 %) and Behenic acid (2.60 %). The total percentage of SFAs was 62.43 % while that of PUFAs was 37.56 %. The sample did not contain MUFAs. *A. africana* contained linolenic acid (36.32 %), linoleic acid (26.23 %), palmitic acid (12.24 %), stearic acid (8.76 %), eicosanoic acid (2.27 %), eicosenoic acid (1.71 %) and heneicosanoic acid (9.86 %). The oil contained a total of 33.13 % SFAs, 1.71 % MUFAs and 62.55 % PUFAs. *H. crepitans* contained only three major fatty acids: oleic acid (45.67 %), palmitic acid (30.69 %) and stearic acid (23.64 %). It contained a total of 45.67 % SFAs and 54.33 % MUFAs. It did not contain PUFAs.

High PUFAs content of *A. africana* indicated that the feedstock might have poor oxidative stability and would need antioxidant additive to prevent it from rapid deterioration during a long storage. Nevertheless, high PUFAs in biodiesel favours cold-flow properties and lubricity (Razon, 2009). High %SFA in *C.*

pepo was an indication that the feedstock would have good oxidative stability, high heat of combustion and cetane number. *H. crepitans* contained high percentage of oleic acid (45.675 %) which has been identified as an ideal fatty acid for biodiesel feedstock (Gunstone, 2004).

4.2.1. GC-MS Results of Butyl esters of the Oil Seeds

The results of GC-MS analysis for butyl esters of the three seed oils are shown in Table 4.8-4.10. It was shown that the fatty oils were appreciably converted to butyl esters by the transesterification process. Ester contents of 98.21, 88.24 and 100 % for *C. pepo*, *A. africana* and *H. crepitans* respectively were achieved. *C. pepo* and *A. africana* contained 1.79 % and 5.96 % unconverted FFAs and this could be attributed to de-esterification of some butyl esters during washing after preparation.

Table 4.8: Results of GC-MS Analysis of *C. pepo* Butyl esters

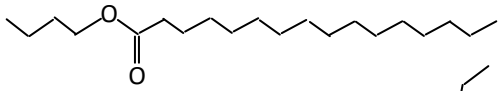
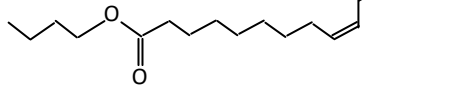
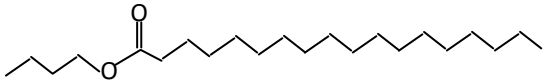
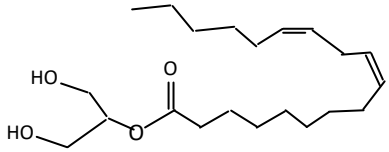
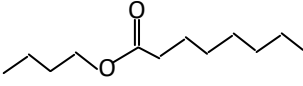
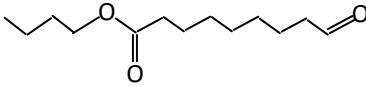
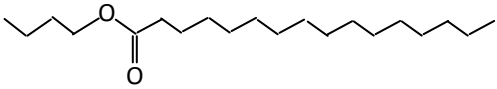
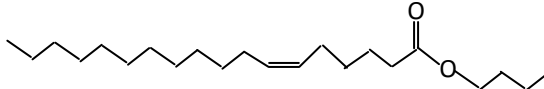
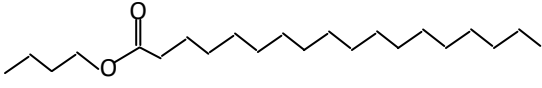
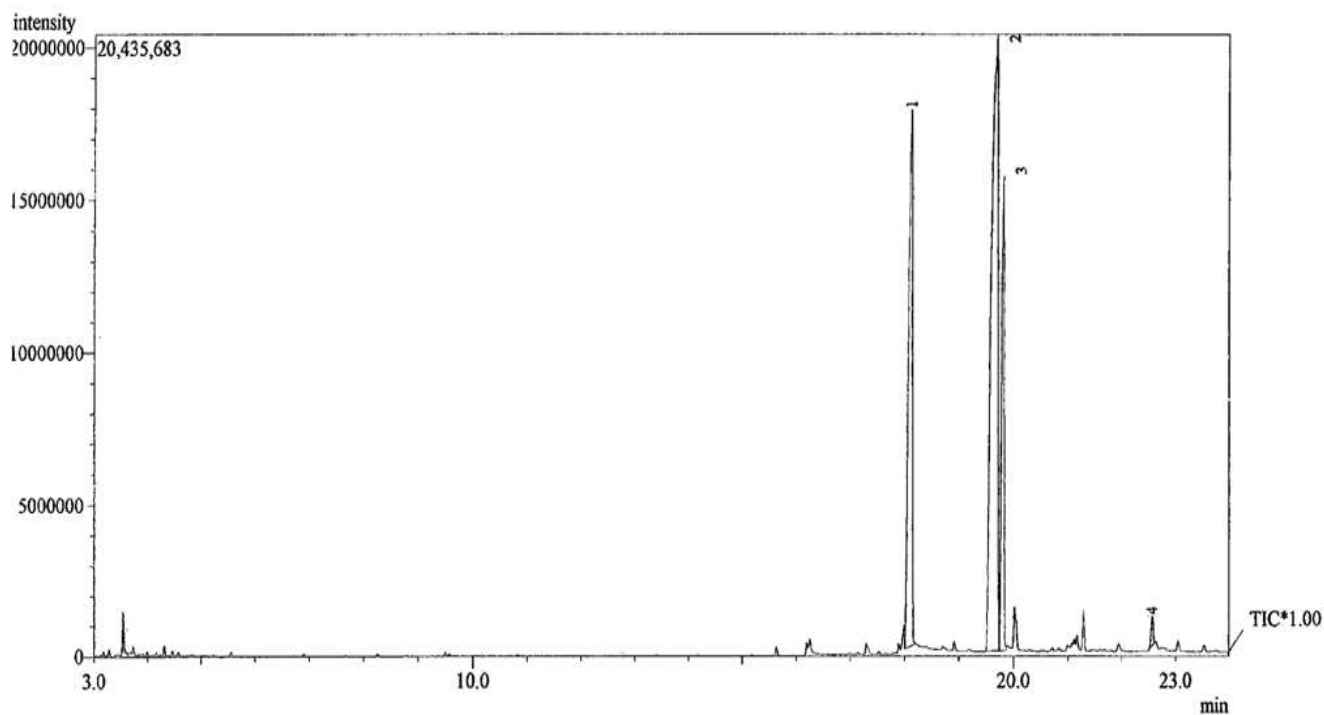
Peak No.	R.A (%)	Molecular formula	M. wt	Name	Structure
1	32.36	C ₂₀ H ₄₀ O ₂	312	Hexadecanoic acid butylester (butyl palmitate)	
2	37.18	C ₂₂ H ₄₂ O ₂	338	9-octadecenoic acid butyl ester (butyl oleate)	
3	28.67	C ₂₂ H ₄₄ O ₂	340	Octadecanoic acid butylester (butyl stearate)	
4	1.79	C ₂₁ H ₃₈ O ₄	354	9,12-octadecadienoic acid,(z,z)-,2-hydroxy-1-(hydroxymethyl) ethyl ester	

Table 4.9: GC-MS Analysis of *A. africana* Butyl esters

Peak No.	R.A (%)	Molecular Formula	M. wt.	Name	Structure
1	5.05	C ₁₂ H ₂₄ O ₂	200	Octanoic acid butylester (butyl caprylate)	
2	2.01	C ₁₃ H ₂₄ O ₃	228	Butyl-9-oxonanoate (Azelaaldehydic acid butylester)	
3	14.76	C ₂₀ H ₄₀ O ₂	312	Hexadecanoic acid butylester (butyl palmitate)	
4	23.03	C ₂₂ H ₄₂ O ₂	338	9-octadecenoic acid butyl ester (butyl oleate)	
5	14.58	C ₂₂ H ₄₄ O ₂	340	Octadecanoic acid butylester (butylester stearate)	
6	25.54	C ₂₄ H ₄₀ O ₂	361	5,11,14,17-eicosatetraenoic acid methylester	
7	2.59	C ₁₈ H ₂₈ O ₂	276	10,12-octadecadiynoic acid	
8	3.37	C ₁₈ H ₃₄ O ₂	282	<i>cis</i> -9-octadecenoic acid (oleic acid)	
9	3.78	C ₁₂ H ₂₀ O	180	4-Isopropenyl-4,7-dimethyl-1-oxaspiro[2,5]octane	
10	5.28	C ₂₀ H ₄₀ O ₂	312	Hexadecanoic acid, 1,1-dimethylethyl ester (tert-Butyl palmitate)	

Table 4.10: GC-MS Analysis of *H. crepitans* Butyl esters

Peak No.	R.A (%)	Molecular Formula	M. wt.	Name	Structure
1	4.47	C ₁₂ H ₂₄ O ₂	200	Octanoic acid butyl ester (butyl caprylate)	
2	3.54	C ₁₃ H ₂₄ O ₃	228	Butyl-9-oxonanoate (Azelaaldehydic acid butylester)	
3	29.94	C ₂₀ H ₄₀ O ₂	312	Hexadecanoic acid butylester (n-Butyl palmitate)	
4	35.20	C ₂₂ H ₄₂ O ₂	338	6-Octadecenoic acid butylester	
5	26.85	C ₂₂ H ₄₄ O ₂	340	Octadecanoic acid butyl ester (n-butyl stearate)	

**Fig. 4.4: GC-MS spectrum of *C. pepo* butyl esters**

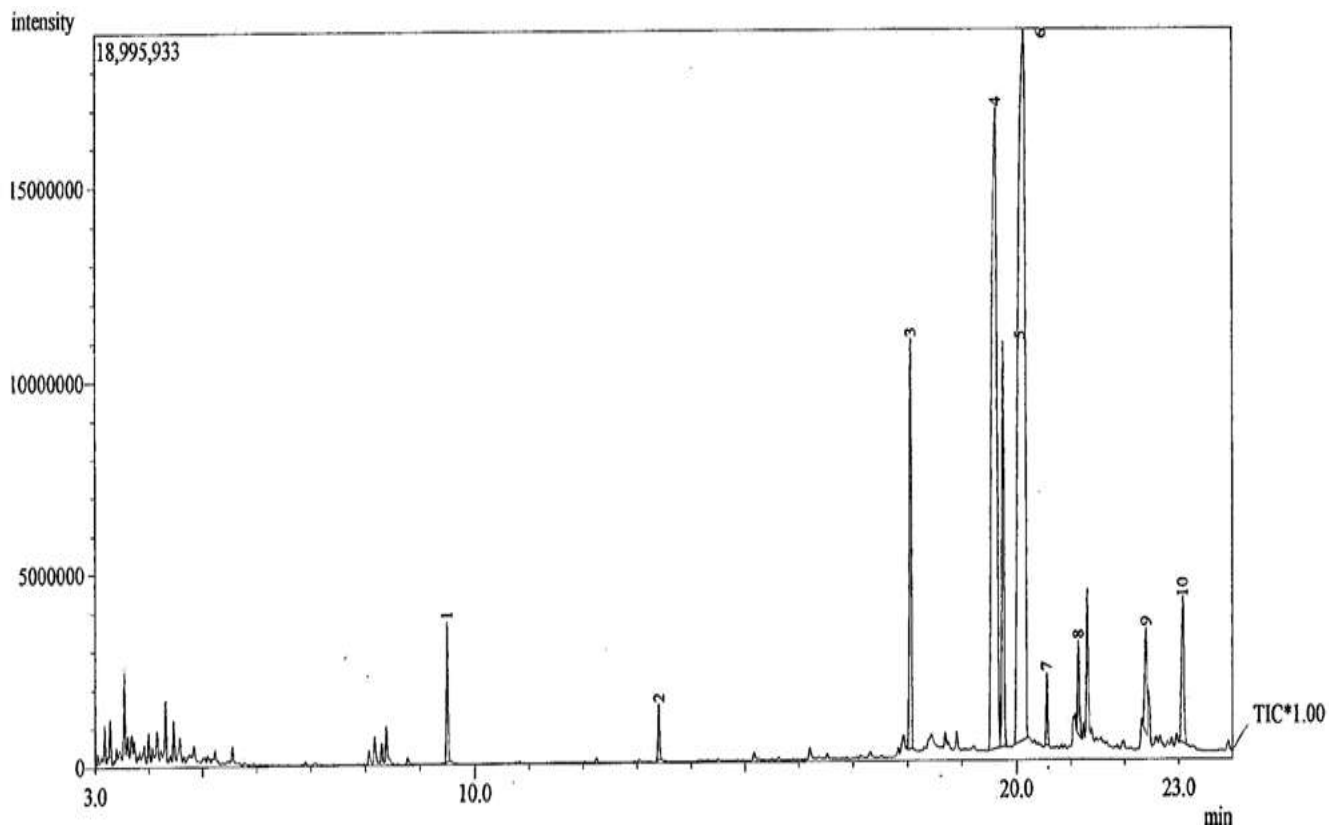


Fig. 4.5: GC-MS spectrum of *A. africana* butyl esters

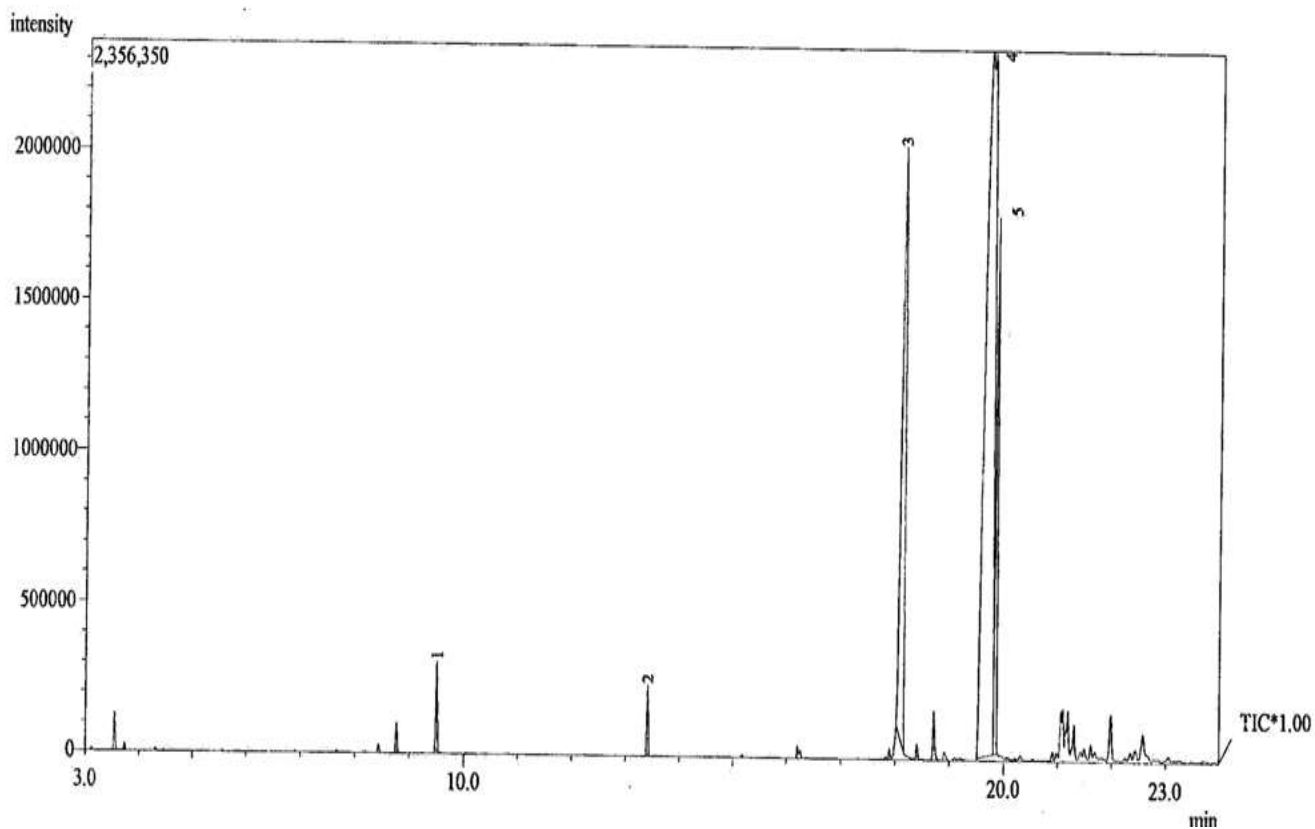


Fig. 4.6: GC-MS spectrum of *H. crepitans* Butyl esters

4.2.2. Properties of the Fatty Acids in the Oil Samples

The properties of fatty acids in the oil samples as revealed by the GC-MS analysis are presented in Table 4.11. The results showed that *A. africana* had the highest degree of unsaturation (1.63) and average chain length (17.66) followed by *C. pepo*. The degree of unsaturation was calculated based on “fully weighted” degree of unsaturation which corresponds to the average number of double bonds per molecule in a sample (Ramos *et al.*, 2009; Giakoumis, 2013).

Table 4.11: Properties of Fatty Acids of the Oil Samples

Samples	%SFA	%MUFA	%PUFA	Degree of Unsaturation	Average Chain Length	% C	% O	% H	Cetane Number*
<i>Cucurbita</i>	62.43	0.00	37.56	0.75	17.45	76.08	11.62	12.13	59.76
<i>Afzelia</i>	33.13	1.71	62.55	1.63	17.66	76.99	11.27	11.63	43.44
<i>Hura</i>	54.33	45.67	0.00	0.46	17.39	75.88	11.64	12.31	64.25

SFA = saturated fatty acid, MUFA = monounsaturated fatty acid, PUFA = polyunsaturated fatty acid.

* Estimated from the fatty acids structures.

The results also show that *H. crepitans* is the most oxygenated among the three oil samples analysed with 11.64 % oxygen content while *A. africana* (11.27 %) had the least. High oxygen content will encourage complete combustion of the fuel which has a lot of environmental benefits.

Chain length and degree of unsaturation of biodiesel feedstock have strong influence on the fuel properties- Cetane number, heat of combustion, melting point, viscosity and oxidative stability increase with increase in chain length but decrease with increases in degree of unsaturation (Knothe, 2005; Razon, 2009). Following these standards, *H. crepitans* appeared to have more advantage for biodiesel production among the three oil crops analysed followed by *C. pepo*. Aside biodiesel production, *A. africana* can be useful in making quick drying oil due to its richness in linoleic and linolenic acids. Palmitic acid is an antioxidant

and a good source of vitamin A, *C. pepo* (32.42 %) and *H. crepitans* (30.69 %) were rich in palmitic acids. High oleic acid in *H. crepitans* (45.57 %) as well may be used as excipient in pharmaceuticals and as an emulsifying or solubilising agent in aerosol products.

4.3. Modified Biowaste Solid Acid Catalysts

4.3.1. FTIR Analysis of the Changes in the Biowastes during Carbonization

FTIR was used to monitor changes in the chemistry of the *H. crepitans* seed shell and *A. africana* seed cake during carbonization and the results are presented in Table 4.12- 4.13. As the carbonization time was increased, the aliphatic C-H stretching (2941 cm^{-1}) peaks shifted to a higher wavenumber and eventually disappeared at 90 min in *H. crepitans* meanwhile C=C stretching vibrations of aromatic rings ($1487 - 1500\text{ cm}^{-1}$) appeared. Band around 1242 cm^{-1} was due to -C-O- stretching. The band disappeared after 60min indicating cleavage of oxygen in the molecules. FTIR results also revealed that resident time of 60 min was most favourable for formation of polyaromatic-rich structure needed for attachment of -SO₃H group.

Table 4.12: FTIR Determination of Changes in the *H. crepitans* Seed Shell during Carbonization

Hu-00	Hu-30	Hu-60	Hu-90	Hu-120	Description
3892.48	3874.16	3774.82	3761.32	3764.21	O-H unbounded
3755.53	3752.64				
3406.40	3408.33	3410.26	3419.90	3409.30	O-H stretch of cellulose, hemicelluloses (Rutherford <i>et al.</i> , 2004)
2941.54	2941.54	2951.19	absent	absent	C-H stretching of methyl and methylene groups
2359.02	2951.19	2394.70	2271.26	2398.56	
	2386.99			2278.97	
1640.51	absent	1640.51	1642.44	1644.37	Conjugated C=O (Pandey, 2003)
absent	absent	1487.17	1500.64	1497.78	C=C stretching vibrations in aromatic rings
1437.98	1425.44	absent	absent	absent	C-H deformation in lignin and carbohydrates (Pandey, 2003)
1243.16	1243.16	absent	absent	absent	O-H phenolic (Colom, 2003; Pandey, 2003)
1054.13	1051.24	1133.22	1127.43	1138.04	C-O vibration in cellulose and hemicelluloses (Rutherford <i>et al.</i> , 2004)
			1050.28		
657.75	595.06	669.63	596.02	872.82	C-H deformation in cellulose
		606.63		679.93	
403.14	438.82	481.26	437.86	412.78	C-H deformation for alkyl groups.
		408.92			

Hu-00, Hu-30, Hu-60, Hu-90 and Hu-120 are *Hura crepitans* seed shells carbonized at 0, 30, 60, 90, and 120min. respectively.

* = carbonization temperature of 500°C

Table 4.13: FTIR Determination of Changes in the *A. africana* Seed Cake during Carbonization

A-0	A-30	A-60	A-90	A-120	Description
3763.24	3912.73 3757.46	3760.35	3768.07	3765.17	O-H unbounded
3404.47	3397.72	3409.30	3425.69	3413.15	O-H stretch of cellulose, hemicelluloses (Rutherford <i>et al.</i> , 2004)
2935.76 2395.67	2935.76 2951.19	2945.40 2357.09	2951.19	2949.26 2368.66	C-H stretching of methyl and methylene groups
1646.30 absent	absent absent	1643.41 1502.6	1643.41 absent	1644.37 absent	Conjugated C=O (Pandey, 2003) C=C stretching vibrations in aromatic rings
1545.03	1539.25	absent	absent	absent	N–O asymmetric stretch
1422.55 absent	1422.55 1257.63	absent absent	1425.44 absent	1415.80 absent	C-H deformation in lignin and carbohydrates (Pandey, 2003) O–H phenolic (Colom, 2003; Pandey, 2003)
1053.17	1047.38	1136.11	1134.18 1055.100	1139.00	C-O vibration in cellulose and hemicelluloses (Rutherford <i>et al.</i> , 2004)
654.85 609.53	590.24	658.71 592.17	586.38	583.49	C-H deformation in cellulose
409.89	410.85	479.33 411.82	429.18	424.35	C-H deformation for alkyl groups.

A-0, A-30, A-60, A-90 and A-120 are *Afzelia africana* seed cakes carbonized at 0, 30, 60, 90, and 120min. respectively.

4.3.2. Physicochemical Properties of the Modified Biowaste Catalysts

The properties of modified biowaste catalysts prepared from *H. crepitans* seed shell and *A. africana* seed cake are presented in Table 4.14-4.15. The results show that the catalysts are effective for biodiesel synthesis. The activity of the catalysts varied with carbonization time; 60 min carbonization before sulfonation (60Hu-SO₃H) gave the highest activity (96.58 %) for *H. crepitans* samples. This activity compared very well with that of H₂SO₄ (98.80 %).

However, longer reaction time (3 h) and higher temperature (80 °C) were required compared to that of H₂SO₄, 1 h and 60 °C.

Table 4.14: Properties of Solid Acid Catalysts from *H. crepitans* Seed Shell

Sample	Specific surface area (m ² /g) x10 ³	-SO ₃ H density (mmol/g)	%Acid Site Leached out	%Conversion ^c		
				<i>Hura</i>	<i>Afzelia</i>	<i>Cucurbita</i>
0Hu-SO ₃ H	4.85	1.36	26.03	83.07	82.17	79.33
30Hu-SO ₃ H	7.47	1.46	5.34	77.18	83.44	83.78
60Hu-SO ₃ H	44.84	2.00	17.22	96.58	95.54	89.43
90Hu-SO ₃ H	41.31	1.38	17.03	84.82	91.87	86.04
120Hu-SO ₃ H	20.60	1.66	16.50	91.42	84.14	94.45
H ₂ SO ₄				98.80	98.40	98.10

0Hu-SO₃H, 30Hu-SO₃H, 60Hu-SO₃H, 90Hu-SO₃H and 120Hu-SO₃H are catalysts prepared by carbonizing *H. crepitans* seed shell for 0, 30, 60, 90 and 120min. respectively before sulfonation.

c = % conversion of the base oil to methyl esters.

Table 4.15: Properties of Solid Acid Catalysts from *A. africana* Seed cake

Sample	Specific surface area (m ² /g) x10 ³	-SO ₃ H density (mmol/g)	%Acid Site Leached out	%Conversion ^c		
				<i>Hura</i>	<i>Afzelia</i>	<i>Cucurbita</i>
0A-SO ₃ H	9.66	1.42	87.36	84.97	82.47	90.13
30A-SO ₃ H	45.49	1.19	56.63	90.44	84.14	88.84
60A-SO ₃ H	6.21	2.34	11.92	87.54	91.50	89.13
90A-SO ₃ H	3.66	1.20	5.00	86.14	91.07	87.05
120A-SO ₃ H	29.91	1.20	13.37	89.87	90.34	89.42
H ₂ SO ₄				98.80	98.40	98.10

0A-SO₃H, 30A-SO₃H, 60A-SO₃H, 90A-SO₃H and 120A-SO₃H are catalysts prepared by carbonizing *A. africana* seed cake at 0, 30, 60, 90 and 120min. respectively before sulfonation.

Activity of bio-based solid acid catalyst is strongly influenced by the acid site density and also other properties such as adsorption ability or accessibility to substrates (Wang *et al.*, 2014). The results (Table 4.15) show that the acid density was optimal at carbonization time of 60 min for both biomass samples; 60Hu-SO₃H had the highest acid density (2.00 mmol/g) for *H. crepitans* samples while 60A-SO₃H (2.34 mmol/g) was the highest for *A. africana*

samples. Acid density measures the amount of $-\text{SO}_3\text{H}$ group on the catalyst and it is directly proportional to the catalytic strength of the catalysts. A drop in the acid density after 60 min could be due to collapse of some of the aromatic carbon framework in the samples leading to inhibition of the attachment of $-\text{SO}_3\text{H}$ group onto the surface of the material.

Increase in specific surface area enhances accessibility of substrates to the surface of the catalyst and hence, favours reactivity. Catalysts from *H. crepitans* seed shell showed higher specific surface area compared to those of *A. africana* seed cake. This possibly contributed to the observed differences in the activities of catalysts derived from both materials. It was equally indicated that carbonization time had a pronounced effect on the specific surface area of the catalysts. Specific surface area increased with increase in carbonization time and reached optimum at 30 and 60 min for *A. africana* and *H. crepitans* samples respectively.

4.3.3. Hydrolytic Stability of the Catalysts

Hydrolytic stability of solid catalysts determines the stability of the acid site towards leaching out in an aqueous medium; it is the acid site retention capacity of a solid catalyst in aqueous reaction medium. The hydrolytic stability which was studied by exposing the catalysts to hot water (95 °C) for 5h under constant stirring indicated that catalyst prepared from uncarbonized biomass samples had the weakest hydrolytic stability; 26.03 % (0Hu- SO_3H) and 87.36 % (0A- SO_3H) of the acid site leached out during the test. This can be attributed to insufficient aromatic framework for the firm attachment of $-\text{SO}_3\text{H}$ group. However, carbonization of the biomass before sulphonation enhanced the acid site retention capacity. 30min carbonization for *H. crepitans* seed shell (30Hu- SO_3H) and 90min for *A. africana* seed cake (90A- SO_3H) showed highest hydrolytic stability; only 5.34 and 5.0 % respectively of the acid site leached

out. Nevertheless, 60 min carbonization might be mostly considered in terms of a balance between acid site retention and catalytic activity.

Generally, the solid acid catalysts from both biowastes showed superior catalytic activity and acid site retention capacity compared to some reported bio-based solid acid catalysts (Bennett *et al.*, 2016; Lee, 2013). This can be attributed to the differences in the nature of the carbon precursors and the methods used in the preparation.

4.3.4. XRD Analysis of the Catalysts

Fig. 4.7-4.8 show the XRD patterns of the *H. crepitans* seed shell derived solid acid catalyst (60Hu-SO₃H) and that of *A. africana* seed cake (60Hu-SO₃H) respectively. Catalysts prepared from both biomass materials had diffraction peaks (broad range) at the 2θ angle of 10–30 and 40–50, which are attributed to the (002) and (101) faces of amorphous carbon (Wang *et al.*, 2014). This conformed to the XRD patterns of bio-based solid acid catalysts reported by other researchers (Liu *et al.*, 2010; Liu *et al.*, 2013; Wang *et al.*, 2014). *H. crepitans* derived catalyst however appeared to have more orderly microstructure compared to that of *A. africana*.

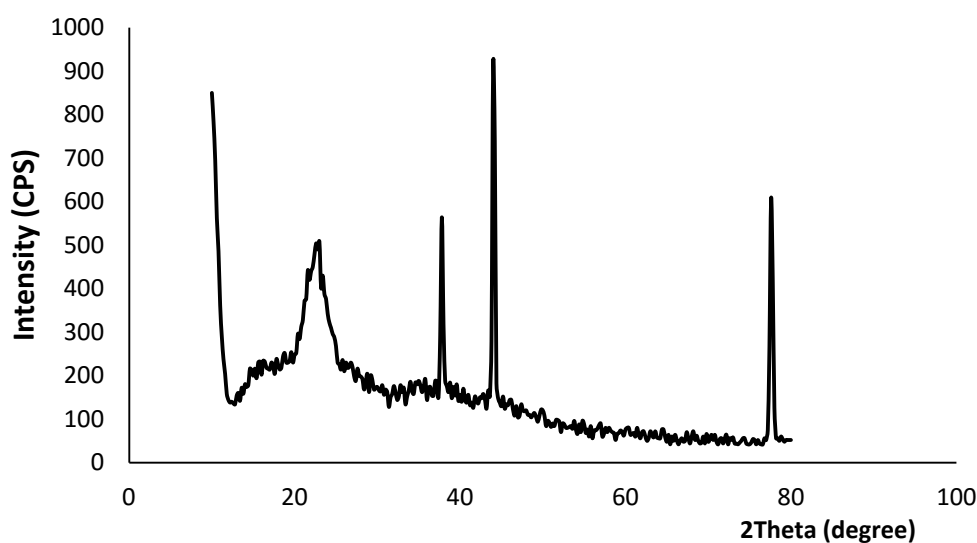


Fig.4.7: XRD pattern of *H. crepitans* seed shell derived catalyst (60Hu-SO₃H)

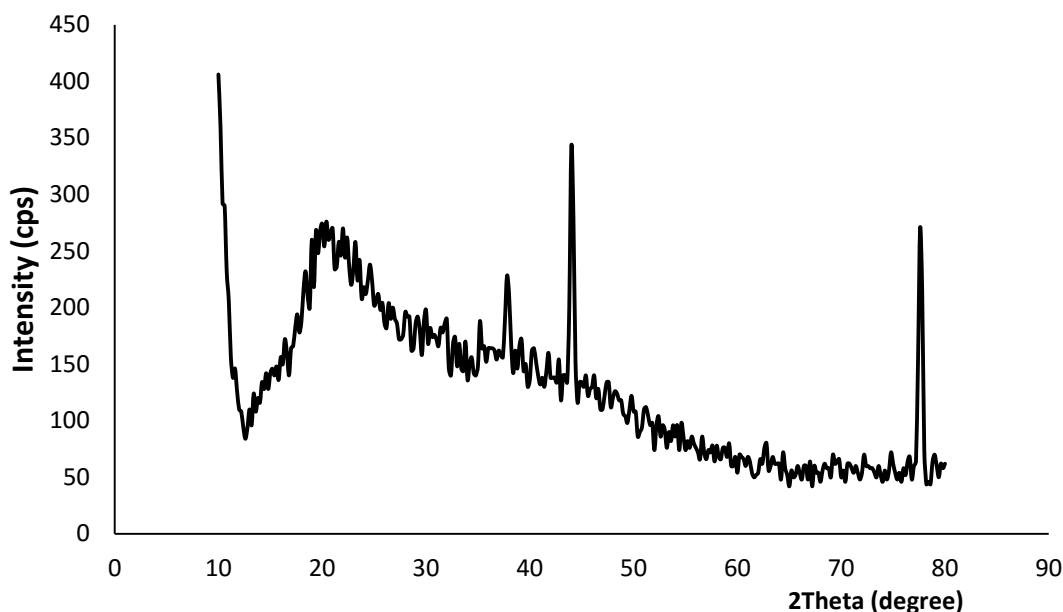


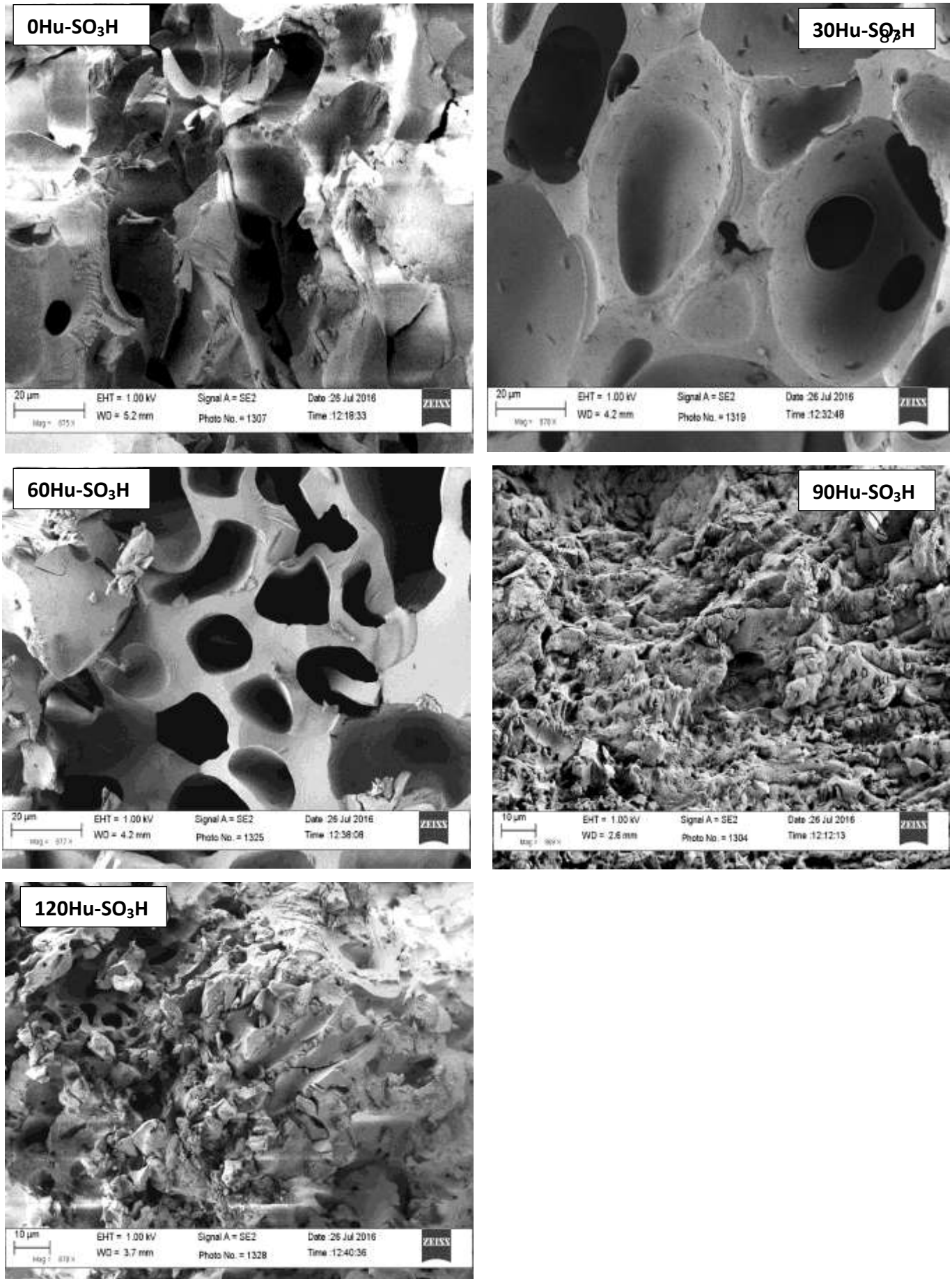
Fig.4.8: XRD pattern of *A. africana* seed shell Derived catalyst (60A-SO₃H)

4.3.5. Surface Morphology of the Solid Acid Catalysts

The surface morphology of the catalysts obtained using scanning electron microscope (SEM) are presented in Fig. 4.9-4.10. The SEM images reveal that the biowaste-derived solid acid catalysts were morphologically heterogeneous, showing the presence of carbon structure covered with pores. Carbonization of the materials before sulfonation showed varying effects on the pore sizes of the catalysts.

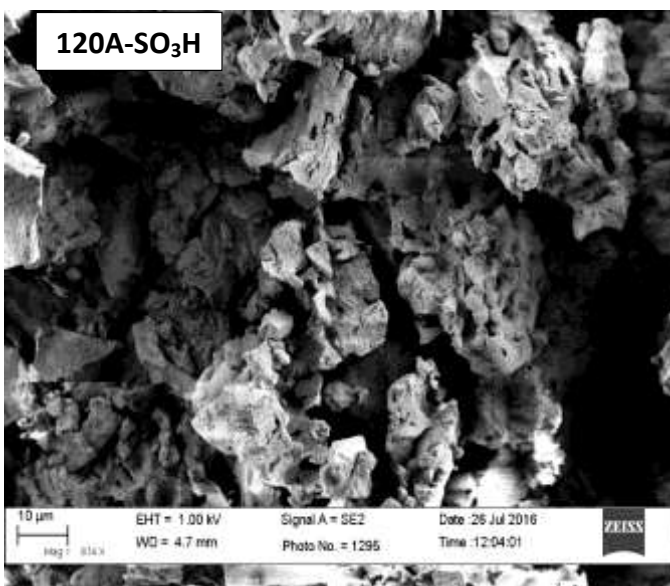
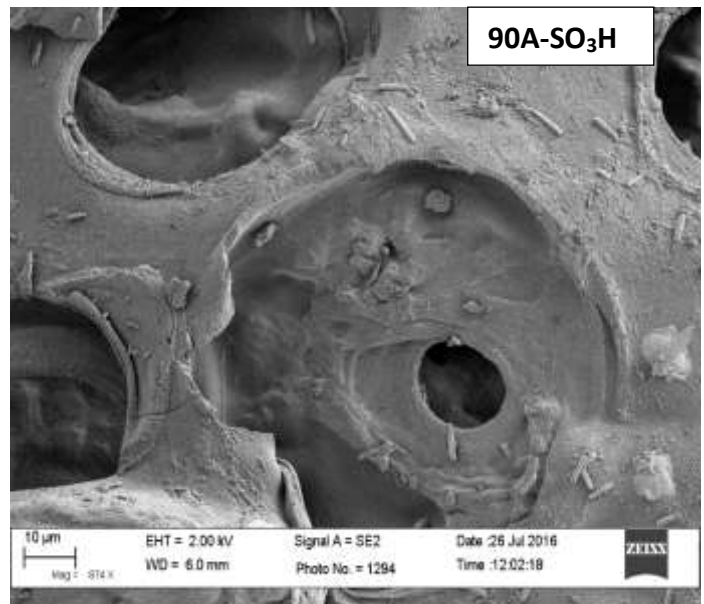
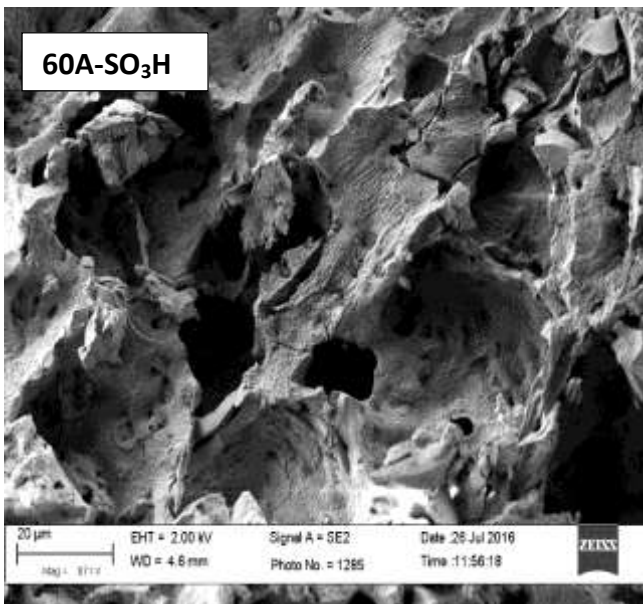
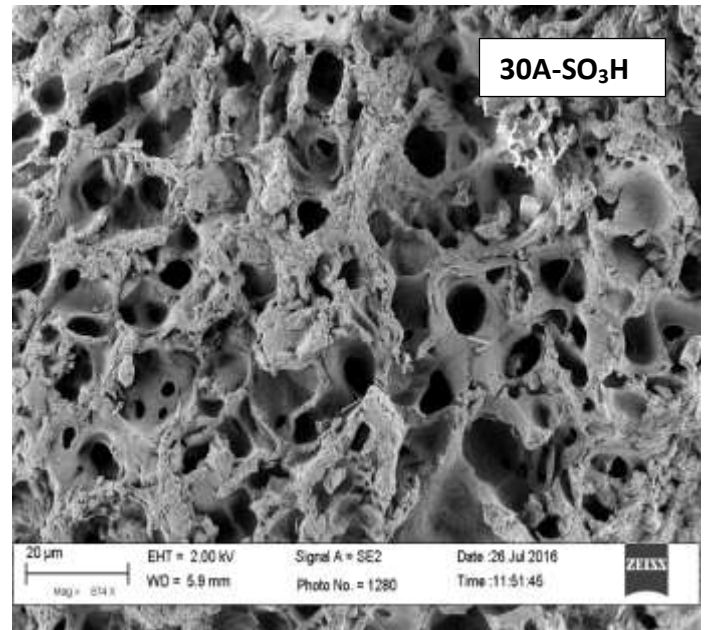
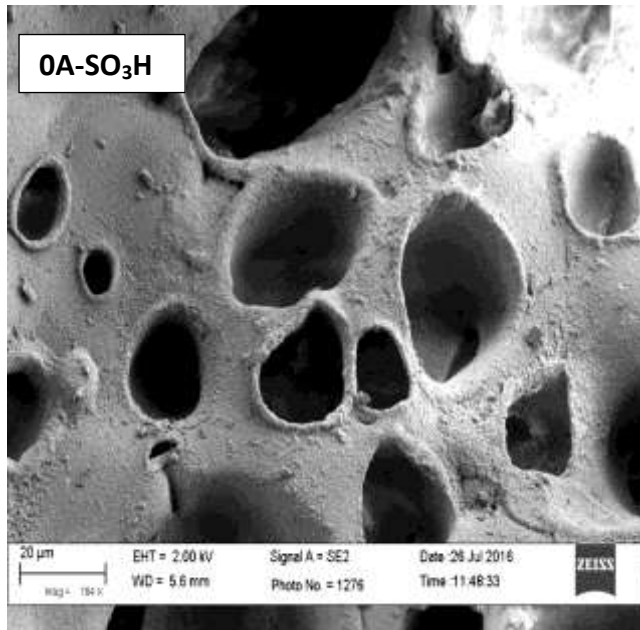
The SEM images of *H. crepitans* shell derived catalysts show that the pore sizes of the carbon structures appreciated as the carbonization time increased and reached optimal at 60 min (60Hu-SO₃H) after which the pores collapsed (90Hu-SO₃H and 120Hu-SO₃H), Fig. 4.9. Catalysts prepared by carbonizing the material between 30 and 60 min (30Hu-SO₃H and 60Hu-SO₃H) had the largest and well-ordered pores. Large pore sizes would increase the surface area of the catalyst and favour transformation of bulky molecules such as bio-oils. This implies that, for catalyst preparation from *H. crepitans* seed shell, partial carbonization at 500 °C might not exceed 60min to achieve large pore sizes. The

collapse of the carbon framework beyond 60 min of carbonization could be as a result of transformation of the biomass into graphite (Wang *et al.*, 2014).



Plates 4.9: SEM images of *H. crepitans* seed shell derived catalysts at ~870 magnification

Fig.4.10 show surface images of catalysts derived from *A. africana* seed cake. Catalyst prepared by direct sulfonation of the seed cake without carbonization (0A-SO₃H) had fewer large pore sizes. However, carbonization of the material for 30min. before sulfonation resulted in a carbon structure full of numerous smaller pores (30A-SO₃H). As the carbonization progressed to 60 min, the carbon framework started collapsing (60A-SO₃H) and at 90min., the pores in the carbon framework were almost covered with structures resulting from the flow of molten material (90A-SO₃H). Then at 120 min, a total collapse of the carbon structure with formation of irregular pores was observed (120A-SO₃H). This results suggested that 30min carbonization of *A. africana* seed cake (at 500 °C) before sulfonation was most favourable for increasing the pores in the catalyst. Nevertheless, catalyst of small pores would be more suitable for transformation of small molecules.



Plates 4.10: SEM images of *A. africana* seed cake derived catalysts

4.3.6. Thermogravimetric Analysis of the Catalysts

The thermogravimetric analysis (TGA) curves and their derivative thermogravimetric (DTG) curves of the solid acid catalysts are presented in Figs. 4.11-4.12. TGA curve is a plot of weight versus temperature while DTG curve is a plot of the rate of change in weight with respect to temperature. Thermogravimetric data are often presented in both TGA and DTG curves for easy interpretation (Dunn, 2012). Certain features that are not clearly seen in the TGA curves are more clearly detected in the DTG curves.

From the DTG curves, three stages of weight loss were shown. The first stage (1) below 100 °C was due to desorption of absorbed water (Liu *et al.*, 2013). The level of water released varied with duration of carbonization of the biomass during preparation. Water adsorption capacity of the catalysts decreased with increase in carbonization time. This indicated that carbonization enhanced hydrophobicity of the biomass materials. Hydrophobicity reportedly favours acid site retention of biomass derived solid catalysts (Lee *et al.*, 2014).

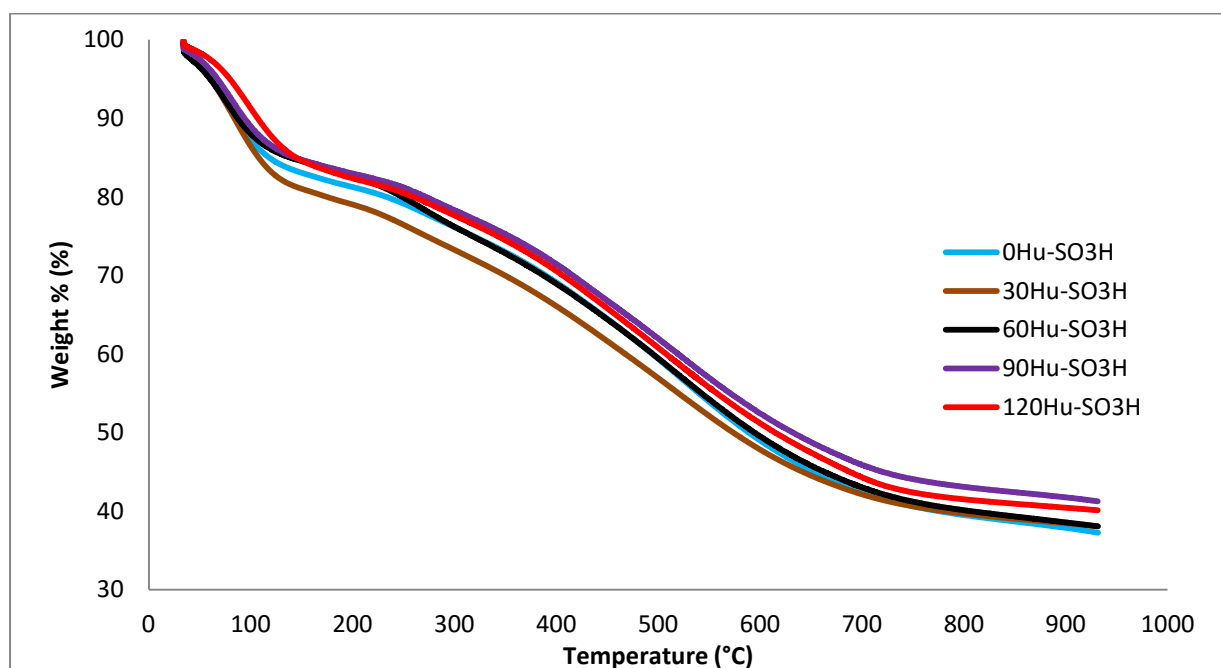


Fig. 4.11: TGA Curves of *H. crepitans* Derived Solid Acid Catalysts

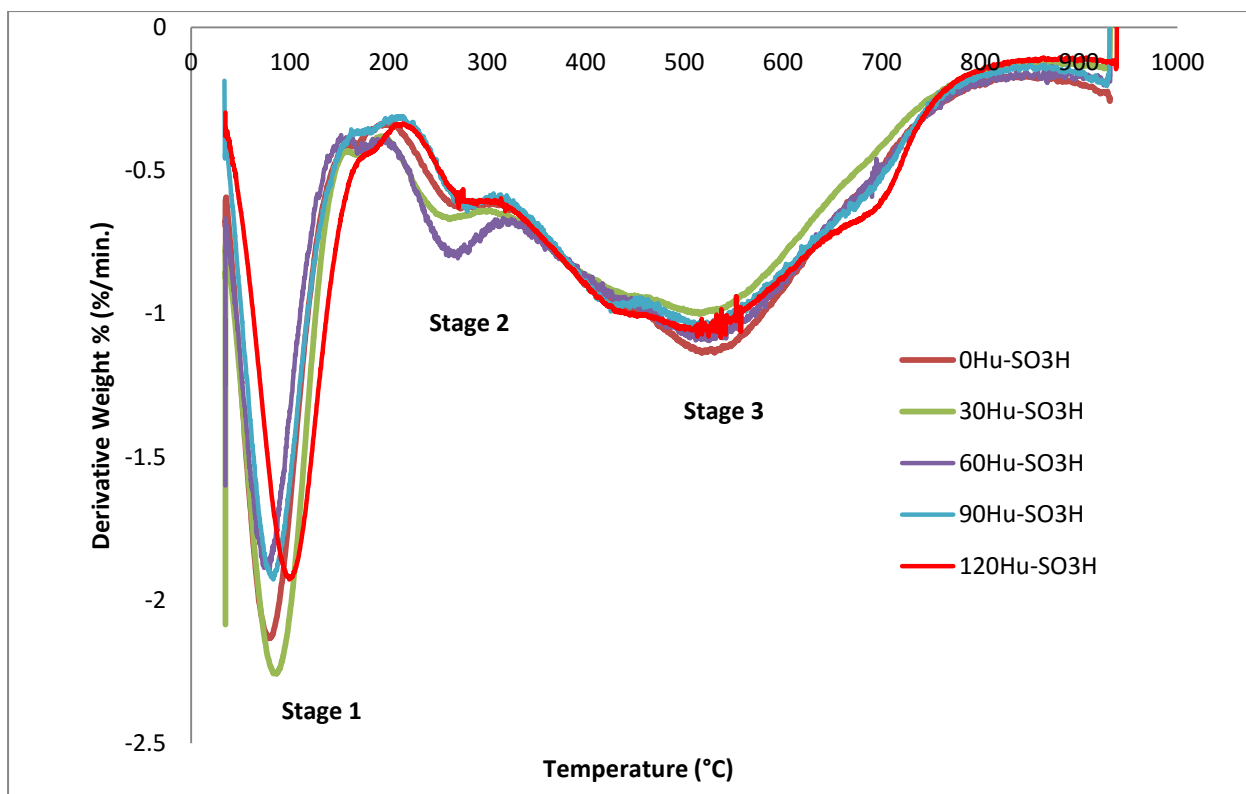


Fig. 4.12: The Derivatives (DTG) Curves

The second stage (2) between 230 and 270 °C can be attributed to decomposition of -SO₃H (Lee, 2013; Liu *et al.*, 2013). This was buttressed by the fact that derivative weight at this stage correlated with the -SO₃H contents of the catalysts. For instance, 60HuSO₃H had the highest -SO₃H content (Table 4.14) and the DTG curves showed that it had the highest weight loss at this stage (0.8 %/min). This result implied that the solid acid catalysts would be thermally stable until about 230 °C after which sulfonic acid groups would start dissociating from the carbon structures.

The third stage (3) of weight loss was between 360 and 780 °C could be due to pyrolysis of the carbon framework. Residual mass between 37 to 41 % weight of the material still left at 950 °C.

Figs. 4.13-4.14 compared the thermal stability of *H. crepitans* derived solid acid catalyst to that of *A. africana*. The carbon structure of *A. africana* sample

appeared to be more firm than that of *H. crepitans*. However, $-\text{SO}_3\text{H}$ on both materials had similar stability; they started decomposing at about 230 °C. This suggested that both catalysts had similar thermal stability. From the DTG curve also, it was observed that the derivative weight % between 230 and 270 °C was higher in *A. africana* (stage II) and this correlated with the $-\text{SO}_3\text{H}$ contents of the catalysts, Tables 4.14-4.15.

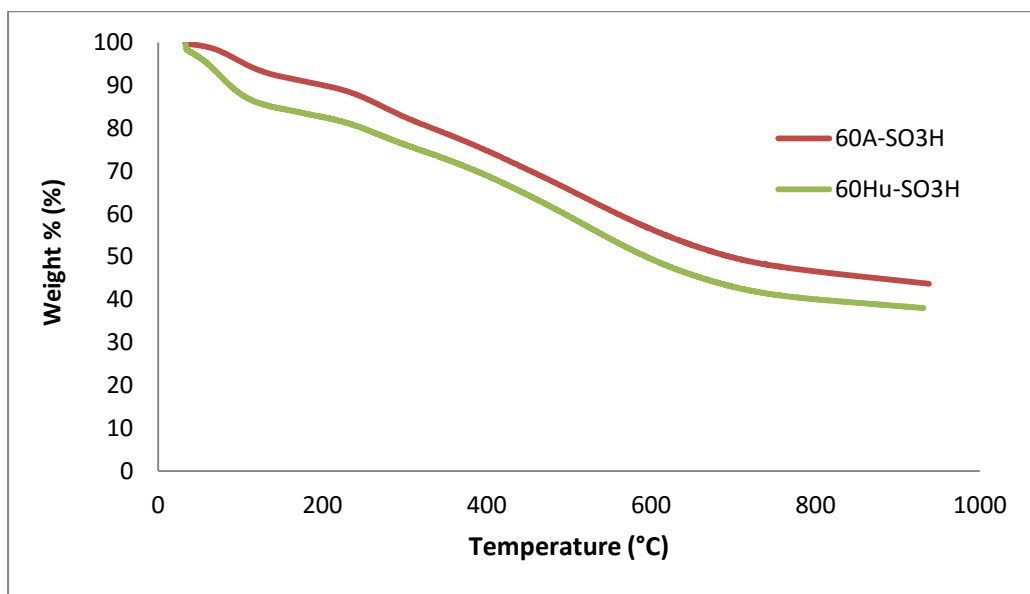


Fig. 4.13: TGA Curves comparing thermal stability of *H. crepitans* and *A. africana* catalysts

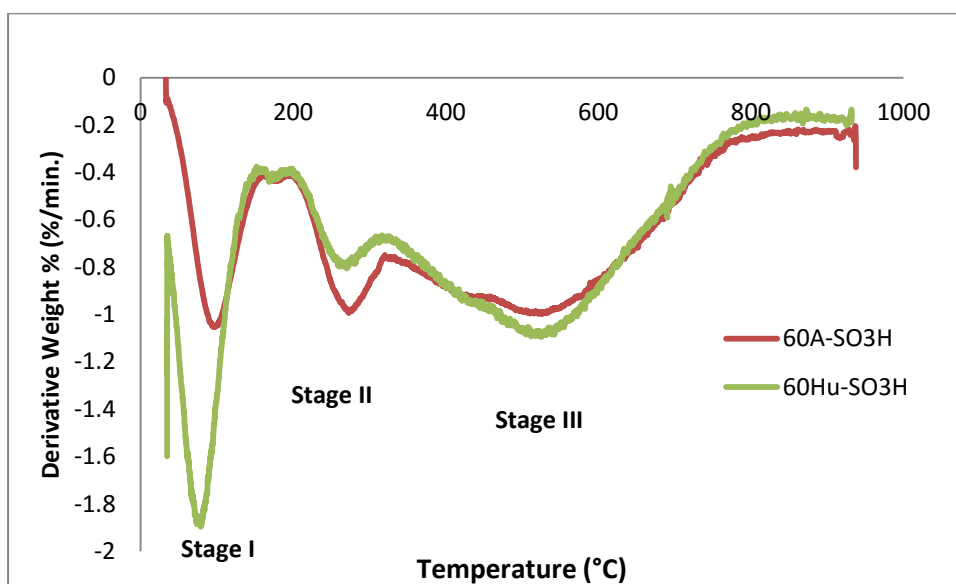


Fig. 4.14: DTG Curves comparing thermal stability of *H. crepitans* and *A. Africana* catalysts

The reusability of the solid acid catalysts was evaluated; the catalyst was filtered from the reaction mixture after each catalytic run, washed with methanol to remove the residual reactants off the catalyst surface, dried in an oven at 80 °C for 2 h and reused in subsequent runs. Only about 15 % drop in catalytic activity was recorded after four cycles, showing that the catalyst could be reused effectively for up to five times.

4.4. Effect of Process Parameters on the Biodiesel Synthesis

4.4.1. Effect of Quantity of Catalyst

The effect of quantity of catalyst on %conversion of the base oil to biodiesel are presented in Tables 4.16, Fig. 4.15-4.16. It was shown that %conversion increased with increase in quantity of catalyst and reached plateau at 3 % for both methylation and butylation except *H. crepitans* butylation which was 2 %.

Table 4.16: Effect of Quantity of Catalyst (H₂SO₄) on %Conversion of the base Oils to Biodiesel

Quantity of Catalyst (wt.%)	%Conversion on Methylation			%Conversion on Butylation		
	<i>Cucurbita</i>	<i>Afzelia</i>	<i>Hura</i>	<i>Cucurbita</i>	<i>Afzelia</i>	<i>Hura</i>
1	90.00	87.30	89.00	87.30	89.20	89.90
2	89.50	97.30	96.50	97.33	96.50	94.50
3	98.10	98.40	98.20	98.40	98.20	98.10
4	98.10	98.70	98.80	98.70	98.70	98.10
5	98.04	99.00	98.40	99.50	98.40	98.04
10	98.10	98.80	98.40	98.80	98.40	98.10

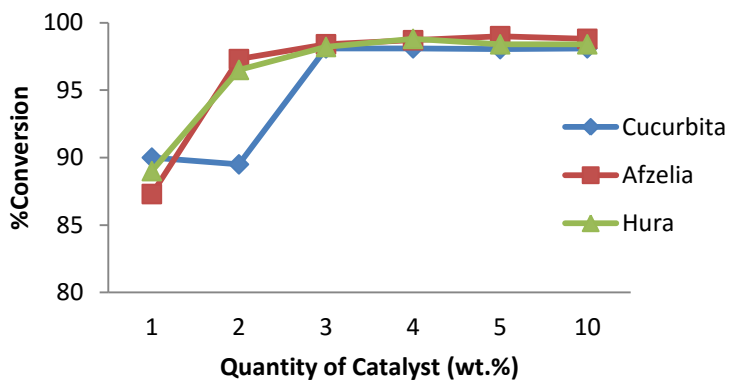


Fig. 4.15: Effect of Quantity of Catalyst on Methylation

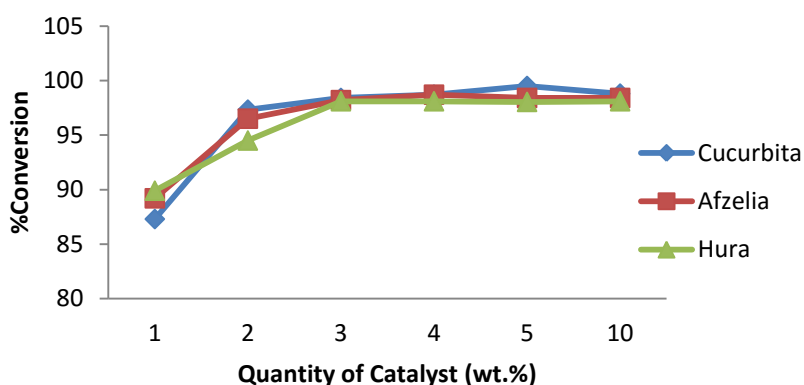


Fig. 4.16: Effect of Quantity of Catalyst on Butylation

4.4.2. Effect of Stirring Rate

Tables 4.17, Fig.4.17-4.18 show the effect of stirring rate on methylation and butylation of the base oil to biodiesel at 70 °C, alcohol/oil ratio of 6:1 and optimum amount of catalyst. It was evident that stirring had great influence on the conversion rate. The %conversion increased with increase in stirring rate and reached saturation at: 200 rpm for *H. crepitans* and *C. pepo* methylation, 300rpm for *A. africana* methylation and 400 rpm for butylation of the oil samples. The results indicate that greater agitation was required for butylation than methylation. This might be attributed to higher molecular weight of butanol compared to methanol. Also, *H. crepitans* oil appeared to require the least agitation compared to other feedstock. This could be related to differences in the viscosities of the oil samples. *H. crepitans* had the least viscosity than other oil samples (Table 4.1). The higher the viscosity the more agitation

required to provide an excellent mixing between the two liquid phases (oil and catalyst phases).

Table 4.17: Effect of Stirring Rate on Percentage Conversion of the Oil to Biodiesel

Stirring rate (rpm)	%conversion on methylation			%conversion on butylation		
	<i>Cucurbita</i>	<i>Afzelia</i>	<i>Hura</i>	<i>Cucurbita</i>	<i>Afzelia</i>	<i>Hura</i>
0	85.37	84.37	87.23	57.50	64.00	75.61
200	98.99	97.40	99.50	97.93	79.20	75.62
400	98.39	98.98	99.00	98.87	98.50	98.86
600	98.80	98.89	98.90	98.98	98.23	98.57
800	98.19	98.98	99.00	98.58	98.09	98.89

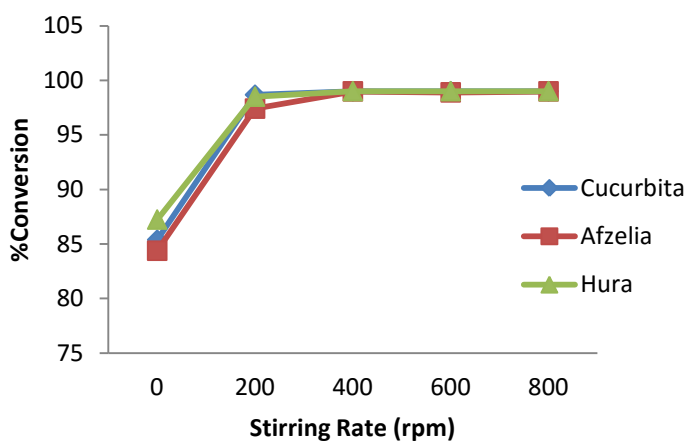


Fig. 4.17: Effect of Stirring Rate on Methylation of the Base Oil

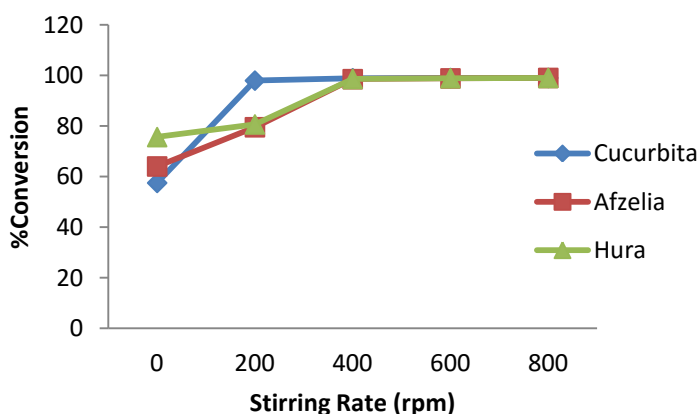


Fig. 4.18: Effect of Stirring Rate on Butylation of the Base Oil

4.4.3. Effect of Temperature on the Conversion of the Oils to Biodiesel

The effect of temperature on the reaction was studied at room temperature (28 °C), 40, 50, 60, 70 and 80 °C using the optimum catalyst and stirring rate for each oil sample. Expectedly, temperature had a pronounced effect on the rate of reaction. Rate of the reaction increased with increase in temperature and reached optimum between 50 and 70 °C for methylation (Tables 4.18, Fig.4.19-4.20). For butylation, 70 °C was found optimal for *A. africana* but reaction rate increased up to 80 °C for *H. crepitans* and *C. pepo*.

Mittelbach and Trathnig, (1990) reported that the rate of transesterification is temperature dependent, but the per cent conversion is not a strong function of temperature provided that the reaction has progressed up to 10 min. At room temperature, there was up to 61 to 78 % conversion on methylation and between 30 to 52.94 % conversion for butylation. This show that the reaction could proceed at ambient temperature but would require a long period of time for appreciable conversion. Freedman *et al.*, (1986) reported similar observation. Secondly, the results indicat that butylation required higher temperature than methylation and this can be attributed to higher molecular size of butanol compare to methanol.

Table 4.18: Effect of Temperature on %Conversion

Temperature (°C)	%conversion on methylation			%conversion on butylation		
	<i>Cucurbita</i>	<i>Afzelia</i>	<i>Hura</i>	<i>Cucurbita</i>	<i>Afzelia</i>	<i>Hura</i>
28	78.08	77.78	61.04	52.94	40.00	30.19
40	95.22	85.56	92.40	53.47	60.34	60.30
50	97.77	96.67	97.92	53.47	88.33	78.89
60	97.88	97.78	99.57	55.29	98.88	66.14
70	98.00	97.82	99.50	89.84	98.88	76.62
80	98.20	97.78	99.50	92.46	98.67	96.75

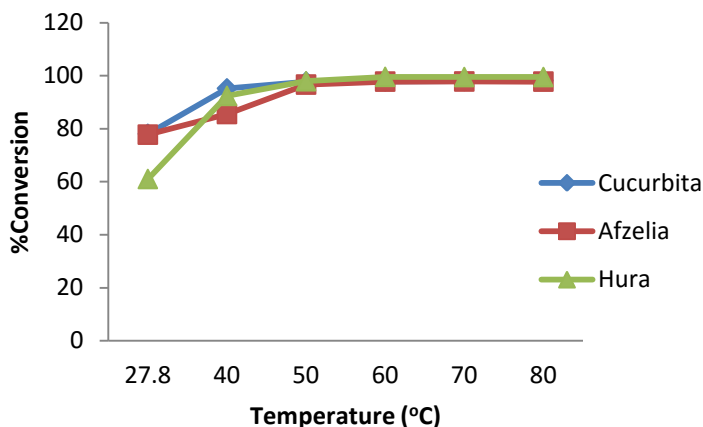


Fig. 4.19: Effect of Temperature on Methylation of the Base Oils

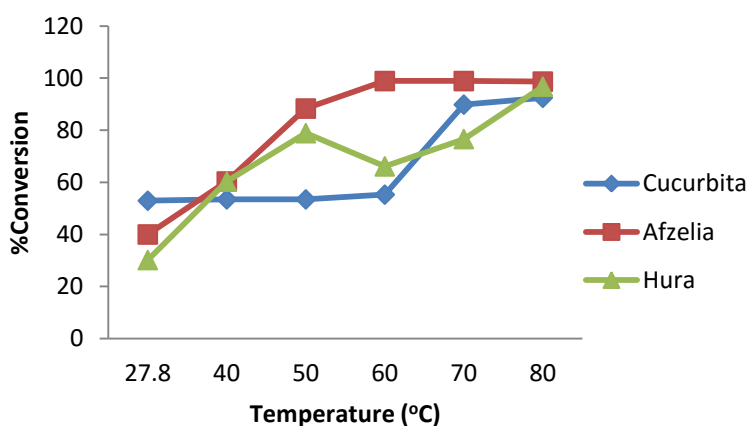


Fig. 4.20: Effect of Temperature on Butylation of the Base Oils

4.4.4. Effect of Time on Conversion of the Oils to Biodiesel

The time of the reaction was varied to obtain kinetic curve at each temperature. Figs. 4.21 - 4.22 showed the kinetic curves at 70 °C while the rest (Figs. 4.23-4.93) are in Appendix 2. From the curves, rate of the reaction was more rapid at the initial stages and retarded as the reaction progressed; within 10 min there was up to 97 to 98 % conversion for methylation of *C. pepo* and *H. crepitans*, and the rate later diminished and attained equilibrium at about 30 min. The rate of butylation, however, was shown to be slower; 90 % conversion was attained after about 60 min. The variation in the rate of methylation and butylation can be attributed to differences in their activation energy according to collision theory of reaction rate. Bigger molecules have higher activation energy and tend

to react more slowly than smaller ones. Secondly, lower rate of butylation compared to methylation can also be attributed to the fact that butanol was completely miscible with the oil phase during butylation unlike in methylation. This monophasic nature of butylation influence the extent of reaction; in the case of methylation, glycerol separation from methyl esters sufficiently curtails the unwanted reverse reactions (Moser, 2009).

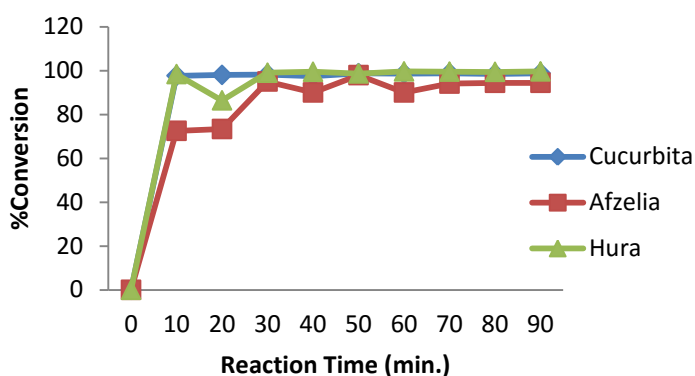


Fig. 4.21: Effect of Time on Methylation of the Oil at 70 °C

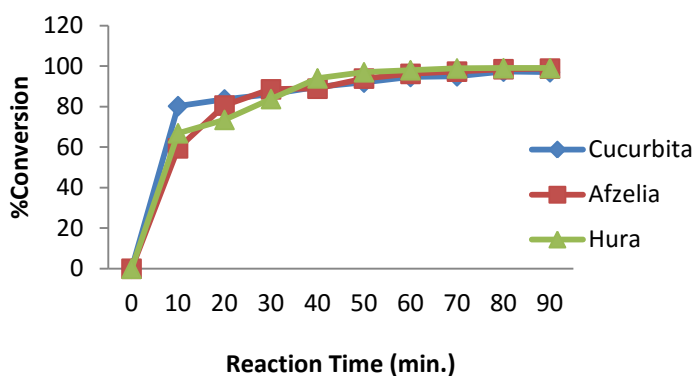


Fig. 4.22: Effect of Time on Butylation of the Oils at 70 °C

4.4.5. Verification of Rate Constant and Order of Reaction

Esterification reaction is a reversible reaction which follows equation (4.1)



According to literature, the reaction may follow pseudo first order kinetics, a situation where the rate is controlled by the concentration of the FFAs alone, and may likely occur when the concentration of alcohol is in excess such that it

remains approximately constant throughout the reaction (Thiruvengadaravi *et al.*, 2009). In that case the rate can be expressed in terms of disappearance of FFAs (A) as represented in equation (4.2).

$$-d[A]/dt = k[A] \quad (4.2)$$

Integrating equation (4.2) will yield equation (4.3) and the equation can be used to describe the substrate concentration variation in relation to time (Abiney *et al.*, 2008).

$$\ln [A]_t = -kt + \ln [A]_0 \quad (4.3)$$

Where $[A]_0$ and $[A]_t$ represent the initial and final concentrations of FFAs (mg KOH/g) after a time, t.

Conversely, esterification reaction can obey a second order kinetics, a situation where the rate is controlled by the concentrations of the two reactants (alcohol and FFAs) according to equation (4.4) and this will likely occur when the ratio of alcohol to FFAs is not too high.

$$-d[A]/dt = k_2 [A][ROH] \quad (4.4)$$

The purpose of this study however was to verify the possible order of reaction which fits esterification reactions at alcohol/oil ratio of 6:1, a ratio widely used for commercial biodiesel production (ECN, 2009). Therefore, our experimental data were fitted into first and second order kinetic models and the best fit was identified. A plot of $\ln[A]$ versus reaction time was made to verify pseudo first order, the slope equals to $-k_1$. For second order verification, a plot of reaction time versus $1/[A]$ was made and the slope is equal to k_2 (Davis, 2010). The plots for verification of first and second order are shown in Appendix 2 (Fig. 4.23-4.93). Table 4.19- 4.20 showed the results of overall rate constants and the correlation coefficients.

Table 4.19: Overall Rate Constants and the Correlation Coefficients (R^2) of Methylation of the base Oil Using H_2SO_4

Sample	Temp. ($^{\circ}C$)	1st Order		2nd Order	
		K_1 ($min.^{-1}$)	R^2	K_2 ($g/(mgKOH.min)$)	R^2
<i>A. africana</i>	40	0.064	0.974	0.003	0.866
	50	0.102	0.867	0.042	0.870
	60	0.106	0.780	0.075	0.886
	70	0.112	0.732	0.089	0.913
<i>C. pepo</i>	40	0.080	0.939	0.005	0.876
	50	0.107	0.859	0.044	0.969
	60	0.111	0.767	0.087	0.830
	70	0.103	0.687	0.090	0.925
<i>H. crepitans</i>	40	0.062	0.834	0.0057	0.524
	50	0.110	0.951	0.0290	0.937
	60	0.100	0.772	0.0599	0.964
	70	0.092	0.684	0.0621	0.950

K_1 and K_2 are overall rate constants for first and second order respectively

Table 4.20: Overall Rate Constants and the Correlation Coefficients (R^2) of Butylation of the base Oil Using H_2SO_4

Sample	Temp. ($^{\circ}C$)	1st Order		2nd Order	
		K_1 ($min.^{-1}$)	R^2	K_2 ($g/(mgKOH.min)$)	R^2
<i>A. africana</i>	40	0.0062	0.841	0.000129	0.821
	50	0.0326	0.949	0.0007	0.968
	60	0.0317	0.921	0.0007	0.885
	70	0.0565	0.952	0.0031	0.876
<i>C. pepo</i>	40	0.0133	0.987	0.0002	0.983
	50	0.0276	0.954	0.0007	0.941
	60	0.0439	0.965	0.0019	0.934
	70	0.0460	0.957	0.0022	0.934
<i>H. crepitans</i>	40	0.0129	0.897	0.0002	0.818
	50	0.0331	0.982	0.0009	0.959
	60	0.0341	0.957	0.0010	0.916
	70	0.1076	0.952	0.0424	0.748

Considering the correlation coefficients (R^2), the best kinetic model for our data appeared to be a second order model for methylation while butylation showed more of pseudo first order behaviour. Pseudo-first order behaviour in esterification reaction is normally encountered when the concentration of alcohol is in great excess (Thiruvengadaravi *et al.*, 2009). Pseudo-first order behaviour exhibited by butylation could be due to monophasic nature of the reaction mixture; butanol was miscible with oil phase, forming a homogeneous mixture unlike methanol in methylation. This homogeneous mixing possibly increased the concentration of butanol in contact with oil molecules during the reaction, resulting in a condition that favoured pseudo first order kinetic at oil/alcohol ratio of 1:6.

Furthermore, the overall rate constants of both methylation and butylation increased with increase in temperature. The results presented here are in line with literature (Atkins, 1992).

Information on the order of reaction is very useful because it tells us the functional relationship between concentration and rate. It determines how the concentration of a reactant speeds up or retards a reaction.

Finally, the values of rate constants obtained were used to determine the activation energy (E_a) through a plot of $\ln k$ versus the reciprocal of absolute temperature, according to the Arrhenius equation (4.5).

$$\ln k = (-E_a / R) / T + C \quad (4.5)$$

Where E_a is the activation energy, R is the gas constant, k is rate constant and C is a constant. The plots are shown in Appendix 2 (Fig. 4.23- 4.93) while the activation energies are listed on Table 4.21. Activation energy can be defined as the minimum amount of energy reacting molecules must possess before a reaction can take place. The activation energies of methyl esterification of the base oil samples were 99.25 kJ/mol, 85.31 kJ/mol and 74.12 kJ/mol for A.

africana, *C. pepo* and *H. crepitans* respectively. While that of butyl esterification were 77.24 kJ/mol, 39.24 kJ/mol and 55.69 kJ/mol for *A. africana*, *C. pepo* and *H. crepitans* respectively.

Table 4.21: Activation Energies of the Methylation and Butylation

Methylation	E_a (KJ/mol)	R²
<i>A. africana</i>	99.25	0.809
<i>C. pepo</i>	85.31	0.832
<i>H. crepitans</i>	74.12	0.867
Butylation		
<i>A. africana</i>	77.24	0.843
<i>C. pepo</i>	39.19	0.923
<i>H. crepitans</i>	55.69	0.912

Table 4.22: Overall Rate Constants and the Correlation Coefficients (R²) of Methylation and Butylation of *C. pepo* Oil Using 60Hu-SO₃H Catalyst

Sample	Temp. (°C)	1st Order		2nd Order	
		K₁ (min.⁻¹)	R²	K₂ (g/mgKOH.min)	R²
<i>Methylation</i>	50	0.0492	0.8998	0.0019	0.9526
	60	0.0480	0.9318	0.0021	0.9626
	70	0.0458	0.7720	0.0020	0.8952
	80	0.0518	0.8505	0.0033	0.9663
<i>Butylation</i>	50	0.0335	0.6898	0.0008	0.7752
	60	0.0319	0.6830	0.0009	0.7556
	70	0.0448	0.8094	0.0021	0.9132
	80	0.0772	0.9194	0.0032	0.9608

The overall rate constants of the methyl- and butyl esterification of the base oil using the solid acid catalyst (60Hu-SO₃H) are presented in Table 4.22, Figs. 4.76- 4.93. Though the biowaste derived solid acid catalyst showed advantage

over H_2SO_4 in terms of easy separation after reaction and reusability, it required a longer reaction time for appreciable conversion. The reactions obeyed second order kinetic model and had activation energies of 18.23 kJ/mol ($R^2 = 0.969$) and 48.09 kJ/mol ($R^2 = 0.922$) for methylation and butylation respectively.

4.5. Fuel Properties of the Seed Oils and their Derivatives

The results of fuel properties of the seed oils, methyl esters and esters/diesel blends of *C. pepo*, *A. africana* and *H. crepitans* are presented in Tables 4.23 - 4.25. The results confirm that transesterification of vegetable oils using methanol greatly improves their fuel properties. The viscosity dropped as the oils were converted to methyl esters, from 21.92 to 14.99 mm^2/s (*C. pepo*), 23.84 to 14.27 mm^2/s (*A. africana*), and 18.97 to 14.38 mm^2/s (*H. crepitans*). This was due to replacement of more bulky alcohol (glycerol) in the oil with a simpler alcohol (methanol). High viscosity is one of the major drawbacks in the use of vegetable oil directly as alternative fuel in diesel engine (Ajiwe *et al.*, 2006b; Jaichandar and Annamalia, 2011). One of the fundamental objectives of transesterification of vegetable oils and animal fats for fuel purposes is to reduce the viscosity.

Blending the methyl esters with petroleum diesel further improved their viscosity. Methyl esters/diesel blend (10:90) of the feedstocks had viscosity that placed them in 2D grade diesel (2-4.3 mm^2/s) and therefore could be recommended for fuelling of mobile equipment while the higher blends fell within 4D grade diesel (5.0-34.0 mm^2/s) and could be used for powering stationary equipment (Diesel Power Products, 2011).

The flash points of the feedstocks appreciated as they were converted to methyl esters, from 70 to 108 °C (*C. pepo*), 60 to 108 °C (*A. africana*) and 80 to 150 °C (*H. crepitans*). Flash point is the lowest temperature at which a fuel will start to vaporize to form ignitable mixture when it comes in contact with air. It is a

safety indicator of a fuel. During the transesterification process, volatile components of the parent oils were reduced and thus improved the flash point of the fuels. The fact that the flash points of the biodiesels were higher than that of the parent oils is equally an indication that volatile compound inherent in the oils as well as residual alcohols used in the transesterification process was thoroughly removed from the products. The flash points of the fuel samples were quite high for safe handling. Though ASTM specified minimum of 130 °C flash point for sole biodiesel, European specifications require at least 101 °C, whereas in the US as low as about 93 °C is allowed (Giakoumis, 2013).

Table 4.23: Fuel Properties of *C. pepo* Seed Oil and its Derivatives

Sample	Flash Point (°C)	Pour Point (°C)	Relative Density at 28 °C	Calorific Value (kJ/Kg)	Viscosity at 40 °C (mm ² /s)	Viscosity at 70 °C (mm ² /s)	Viscosity at 100 °C (mm ² /s)	Ash Content (%wt)	Acid Value (mg KOH/g)
Diesel (D)	76	-8	0.8529	45,179	3.93	2.03	1.43	0.002	0.45
<i>C. pepo</i> Oil	70	5	0.9038	44,170	21.92	10.25	5.81	0.004	26.32
CME	108	2	0.8913	44,478	14.99	4.33	2.76	0.003	0.50
10CME: 90D	98	-3	0.8625	44,993	3.93	2.22	1.70	0.006	0.49
20CME: 80D	64	4	0.8658	44,821	4.34	2.48	1.73	0.003	0.48
30CME: 70D	80	9	0.8686	44,677	4.63	2.51	1.77	0.005	0.46
40CME: 60D	82	4	0.8720	44,834	5.10	3.32	1.84	0.003	0.50
50CME: 50D	96	-5	0.8701	44,932	5.28	2.88	1.90	0.004	0.49
60CME: 40D	86	3	0.8780	44,528	5.96	3.00	2.00	0.002	0.50
70CME: 30D	84	6	0.8796	44,447	6.39	3.56	2.29	0.003	0.45
80CME: 20D	82	5	0.8819	44,655	7.35	3.78	2.41	0.006	0.49
90CME: 10D	90	5	0.8900	44,543	6.44	3.80	2.40	0.007	0.50
ASTM Limit	100min	16max	0.80-0.90	NA	1.9-6.0	NA	NA	0.02max.	0.80max.

C. pepo = *Cucurbita pepo*, CME = *Cucurbita pepo* methyl esters,

NA: not available, min. = minimum, max. = maximum

Table 4.24: Fuel Properties of *A. africana* Seed Oil and its Derivatives

Sample	Flash Point (°C)	Pour Point (°C)	Relative Density at 28 °C	Calorific Value (kJ/Kg)	Viscosity at 40 °C (mm ² /s)	Viscosity at 70 °C (mm ² /s)	Viscosity at 100°C (mm ² /s)	Ash Content (%wt)	Acid Value (mg KOH/g)
Diesel (D)	76	-8	0.8529	45179	3.93	2.03	1.43	0.002	0.45
<i>A. africana</i> Oil	60	4	0.8971	44190	23.84	6.99	4.24	0.006	23.52
AME	108	10	0.9212	43880	14.27	10.30	5.96	0.006	0.56
10AME: 90D	70	8	0.8658	44821	5.07	2.65	1.63	0.004	0.45
20AME: 80D	80	-1	0.8677	44723	5.31	2.83	1.80	0.005	0.49
30AME: 70D	76	-9	0.8819	44655	6.76	3.30	2.28	0.003	0.50
40AME: 60D	78	3	0.8911	44488	6.76	4.00	2.70	0.004	0.53
50AME: 50D	80	6	0.8913	44478	9.51	4.76	3.00	0.002	0.56
60AME: 40D	84	-2	0.8982	44136	9.51	5.00	3.70	0.002	0.54
70AME: 30D	82	-6	0.9055	44087	13.33	6.49	3.94	0.003	0.56
80AME: 20D	78	4	0.9110	44098	13.98	7.90	4.50	0.004	0.54
90AME: 10D	84	6	0.9101	44142	12.90	7.94	4.71	0.002	0.55
ASTM Limit	100min	16max	0.80-0.90	NA	1.9-6.0	NA	NA	0.02max	0.80max.

AME: *Afzelia africana* methyl esters

Table 4.25: Fuel Properties of *H. crepitans* Seed Oil and its Derivatives

Sample	Flash Point (°C)	Pour Point (°C)	Relative Density at 28 °C	Calorific Value (kJ/Kg)	Viscosity at 40 °C (mm ² /s)	Viscosity at 70 °C (mm ² /s)	Viscosity at 100°C (mm ² /s)	Ash Content (%wt)	Acid Value (mg KOH/g)
Diesel (D)	76	-8	0.8529	45,179	3.93	2.03	1.43	0.002	0.45
<i>H. crepitans</i> Oil	80	-8	0.8962	44234	18.97	8.77	5.02	0.004	52.08
HME	150	-2	0.9102	44137	14.34	6.56	4.13	0.004	0.89
10HME: 90D	78	-8	0.8696	44625	4.27	2.23	1.56	0.004	0.11
20HME: 80D	82	0	0.8752	44671	4.87	2.63	1.83	0.003	0.17
30HME: 70D	98	-4	0.8762	44620	5.70	3.04	1.94	0.005	0.56
40HME: 60D	90	0	0.8791	44472	6.10	3.30	2.20	0.004	0.49
50HME: 50D	94	2	0.8875	44373	7.78	3.74	3.68	0.002	0.56
60HME: 40D	88	2	0.8800	44752	8.50	4.10	3.70	0.003	0.60
70HME: 30D	94	-2	0.8901	44537	9.30	4.80	3.90	0.003	0.58
80HME: 20D	82	-1	0.8921	44438	9.30	5.80	4.00	0.004	0.68
90HME: 10D	90	2	0.9011	44702	9.41	5.95	4.21	0.003	0.72
ASTM Limit	130min	NA	0.80-0.90	NA	1.9-6.0	NA	NA	0.02max	0.80max.

HME: *Hura Crepitans* methyl esters

The cetane numbers of the feedstocks were quite high for efficient combustion. Table 4.11 shows that *H. crepitans* had the highest cetane number (64.25), followed by *C. pepo* (59.76) and *A. africana* (43.44). Cetane number is used to characterize ignition quality of a diesel fuel. It measures how quickly a fuel starts to burn (auto-ignites) under diesel fuel conditions. Increase in cetane number improves combustion quality of the fuel and reduces smoke, NO_x and PM emissions (Chevron, 2007). ASTM-D6750 specified minimum of 40 for cetane number of biodiesel.

Low ash contents of the fuel samples indicated low non-combustible materials in the fuel samples and the fuels would not cause injector, fuel pump, piston and ring wear (Ajiwe *et al.*, 2006b). The pour point showed that the fuel would not have operational problem during cold weather (as low as 11 °C). Other fuel properties of the methyl esters and esters/diesel blends including acid values and density were within ASTM D6751 limits. Therefore, the samples could be used as alternative diesel fuels.

4.5.1. Fuel Properties of the Seed Oils Derivatives (Butyl esters)

The results of fuel properties of butyl esters and butyl esters/diesel blends of the oil samples are presented in Tables 4.26 - 4.28.

Table 4.26: Fuel Properties of *C. pepo* Seed Oil Butyl esters

Sample	Flash Point (°C)	Pour Point (°C)	Relative Density at 28 °C	Calorific Value (kJ/Kg)	Viscosity at 40 °C (mm ² /s)	Viscosity at 70 °C (mm ² /s)	Viscosity at 100°C (mm ² /s)	Ash Content (%wt)	Acid Value (mg KOH/g)
CBE	102	5	0.8771	44574	6.91	3.37	2.33	0.005	5.58
10CBE:10D	80	1	0.8611	45066	3.83	2.10	1.47	0.003	1.00
20CBE:80D	84	8	0.8629	44972	4.14	2.55	1.58	0.004	1.01
30CBE:70D	86	-2	0.8650	44863	4.32	2.79	1.70	0.003	1.98
40CBE:60D	90	0	0.8686	44677	4.87	2.61	1.79	0.002	2.52
50CBE:50D	82	4	0.8658	44821	5.12	2.81	1.83	0.004	1.20
60CBE:40D	90	3	0.8660	44811	5.30	3.00	2.00	0.005	2.37
70CBE:30D	76	4	0.8762	44620	5.62	3.10	2.03	0.003	3.29
80CBE:20D	100	4	0.8801	44746	5.88	3.21	2.20	0.004	4.87
90CBE:10D	86	4	0.8856	44469	5.91	3.36	2.22	0.003	5.02
ASTM Limit	130min	16max	0.80-0.90	NA	1.9-6.0	NA	NA	0.02max	0.80max.

CBE: *Cucurbita pepo* butyl esters

Table 4.27: Fuel Properties of *A. africana* Seed Oil Butyl esters

Sample	Flash Point (°C)	Pour Point (°C)	Relative Density at 28 °C	Calorific Value (kJ/Kg)	Viscosity at 40 °C (mm ² /s)	Viscosity at 70 °C (mm ² /s)	Viscosity at 100°C (mm ² /s)	Ash Content (%wt)	Acid Value (mg KOH/g)
ABE	88	5	0.8799	44432	6.39	3.79	2.19	0.004	5.12
10ABE:90D	76	2	0.8629	44972	4.11	2.36	1.45	0.003	0.56
20ABE:80D	80	2	0.8629	44972	4.31	2.31	1.52	0.002	0.74
30ABE:70D	86	-11	0.8611	45066	4.58	2.43	1.59	0.005	1.08
40ABE:60D	72	4	0.8629	44972	4.73	2.48	1.70	0.004	1.32
50ABE:50D	75	2	0.8629	44972	4.76	2.64	1.72	0.003	0.91
60ABE:40D	74	-1	0.8701	44574	5.00	2.70	1.18	0.006	0.95
70ABE:30D	70	9	0.8771	44218	5.29	2.87	1.93	0.002	2.58
80ABE:20D	79	5	0.8781	44168	5.80	3.01	2.00	0.003	3.64
90ABE:10D	74	10	0.8801	44746	6.16	3.28	2.16	0.004	3.95
ASTM Limit	130min	16max	0.80-0.90	NA	1.9-6.0	NA	NA	0.02max	0.80max.

ABE: *Afzelia africana* butyl esters

Test results show that butylation of the oil samples improved their fuel properties greatly just as for methylation. The viscosity dropped from 21.92 to 6.91mm²/s (*C. pepo*), 14.27 to 6.39 mm²/s (*A. africana*) and 18.97 to 6.87 mm²/s (*H. crepitans*) as the oils were converted to butyl esters. The flash point increased from 70 to 102 °C (*C. pepo*), 60 to 88 °C (*A. africana*) and 80 to 158 °C (*H. crepitans*). Calorific value, ash contents as well as acid value also showed remarkable improvement.

Table 4.28: Fuel Properties of *H. crepitans* Seed Oil Butyl esters

Sample	Flash Point (°C)	Pour Point (°C)	Relative Density at 28 °C	Calorific Value (kJ/Kg)	Viscosity at 40 °C (mm ² /s)	Viscosity at 70 °C (mm ² /s)	Viscosity at 100°C (mm ² /s)	Ash Content (%wt)	Acid Value (mg KOH/g)
HBE	158	2	0.8771	44574	6.87	3.55	2.37	0.005	4.72
10HBE: 90D	80	-8	0.8629	44972	4.08	2.23	1.47	0.002	0.280
20HBE: 80D	78	-6	0.8535	45148	4.29	2.25	1.59	0.005	0.960
30HBE: 70D	84	-10	0.8573	44947	4.45	2.78	1.65	0.004	0.801
40HBE: 60D	92	-9	0.8601	45118	5.04	2.51	1.68	0.002	0.98
50HBE: 50D	88	-9	0.8705	44912	5.15	2.73	1.85	0.003	4.01
60HBE: 40D	90	2	0.8711	44881	5.50	2.84	1.89	0.002	4.97
70HBE: 30D	120	-2	0.8720	44834	6.02	2.99	1.90	0.004	5.62
80HBE: 20D	99	-1	0.8740	44732	6.50	3.10	2.05	0.003	4.70
90HBE: 10D	109	2	0.8761	44625	6.40	3.00	2.01	0.005	4.81
ASTM Limit	130min	16max	0.80-0.90	NA	1.9-6.0	NA	NA	0.02max	0.80max.

HBE: *Hura crepitans* butyl esters

Blends containing 10:90 to 20:80 butyl esters/diesel feedstocks had viscosity that placed them in 2D grade diesel (2-4.3 mm²/s) while the higher blends fell within 4D grade diesel (5.0-34.0 mm²/s). The flash points of the samples were quite high, higher than that of petroleum diesel. It signified that the fuel samples would be safe to handle and not constitute fire risk.

The ash contents, pour point, density and viscosity of the fuel samples were within the ASTM specifications. However, the acid value of butyl esters were above the ASTM limit and this could be attributed to de-esterification of some

of the butyl esters during separation after preparation. Butanol was miscible with the oil phase of the reaction medium. Separation of residual butanol after transesterification reaction required washing the product repeatedly with distilled water (about seven to ten times). During this process, some de-esterification might have occurred, releasing some FFAs into the products.

4.6. Biodiesel Property Changes as a Function of Intrinsic Structure

4.4.1. Flash point

Variation of flash points of the methyl esters, butyl esters and esters/diesel blends of the oil samples are presented in Fig. 4.94. *H. crepitans* had the highest flash point; 150 °C and 158 °C for the pure methyl esters and butyl esters respectively, followed by *C. pepo* 108 °C and 102 °C. The variation was due to relative amount of volatile components inherent in the feedstocks. The results suggested that *A. africana* had the highest volatile components among the three oil crops. The presence of essential oil: 4-isopropenyl-4,7-dimethyl-1-oxaspiro[2,5]octane identified in its GC-MS results might have contributed to this.

The nature of alcohol used for the transesterification had negligible influence on the flash point of the samples. There was not much difference between the flash point of the methyl esters and butyl esters.

Petroleum diesel had lower flash point compared to the biodiesel samples. Expectedly, increase in percentage composition of the biodiesels samples in the esters/diesel blends increased the flash points of the blends. This agreed with already established fact that blending biodiesel with petroleum diesel improves the flash point of the fuel (Razon, 2009). Flash point is a safety indicator during the storage, transportation and operation of fuel. It has no direct influence on the engine performance. ASTM D93 specified 52 °C for the biodiesel blends (B6-B20) and all the biodiesel blends met this limit.

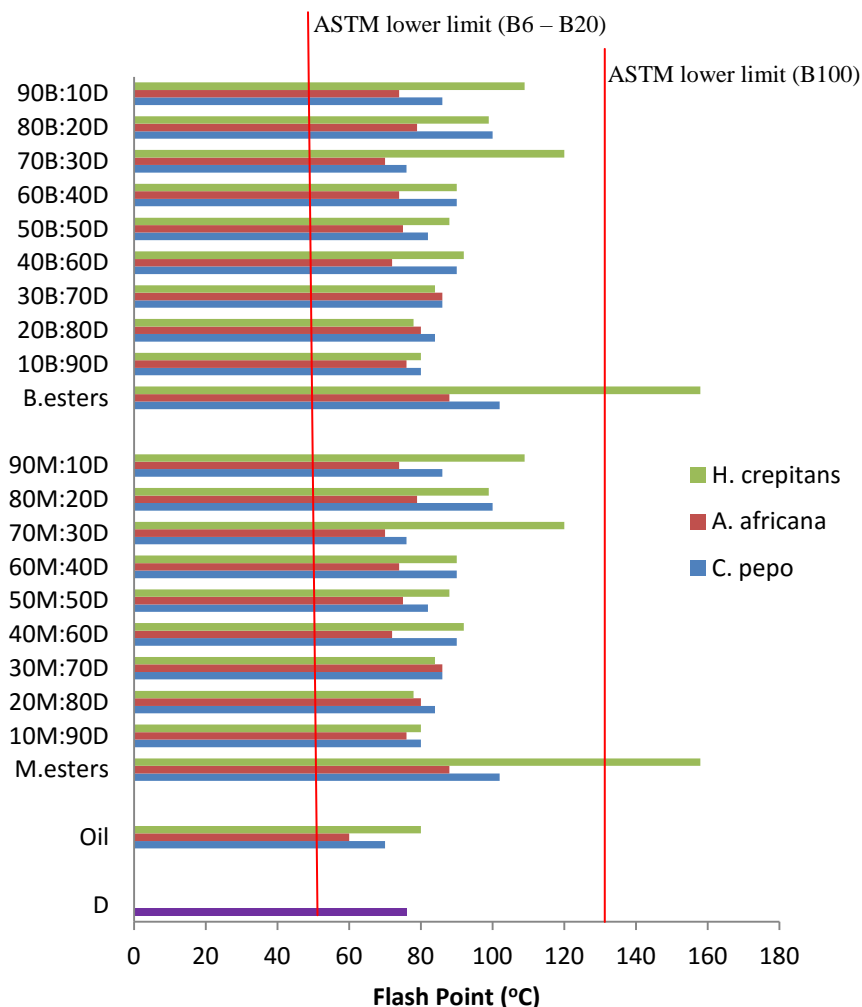


Fig.4.94: Flash Points of the Various Seed Oils and their Derivatives

D = petroleum diesel

M. esters = methyl esters, 10D:90M = 10 % by vol. methyl ester + 90 % by vol. petroleum diesel, etc.

B. esters = butyl esters, 10D:90B = 10 % by vol. butyl esters + 90 % by vol. petroleum diesel, etc.

4.4.2. Kinematic Viscosity

Kinematic viscosity is a very important property of biodiesel. It plays a dominant role in fuel spray, fuel-air mixture formation and the combustion process (Jahirul *et al.*, 2013). In a diesel engine, high viscosity leads to less accurate operation of the fuel injectors, and poorer atomization of the fuel spray. Likewise, very low viscosity does not provide sufficient lubrication for the precision fit of fuel injection pumps thereby resulting in leakage. Fig. 4.95 showed the kinematic viscosities of the biodiesel samples at 40 °C.

A. africana samples appeared to have the highest viscosity followed by *C. pepo* and lastly *H. crepitans*. Several literatures have reported that viscosity strongly correlates with degree of unsaturation and chain length; viscosity decreases with increase in the degree of unsaturation and increases with increase in chain length (Knothe, 2005; Knothe and Steidley, (2005); Ramos *et al.*, 2009; Refaat, 2009; Giakoumis, 2013). The results indicate that chain length however, played a leading role in the viscosities of the fuel samples. *A. africana* had the highest average chain length (17.66) followed by *C. pepo* (17.45) and lastly *H. crepitans* (17.39). The kinematic viscosity increased in the same order notwithstanding the degree of unsaturation.

Butyl esters had lower viscosity than methyl esters and this was due to higher polarity of the latter. A similar observation has been made by Knothe and Steidley, (2005) that longer alcohol gives lesser polar esters. The lower the polarity the lower the intermolecular forces between the fuel molecules and the more freely they flow.

ASTM specified $6\text{mm}^2/\text{s}$ maximum for B100 and 4.1 for the blends (B6 – B20). Butyl ester blends of all the feedstock met the limit for biodiesel blends. For methyl esters, *A. fricana* and *C. pepo* did not meet the limit and only 10:90 blend can be recommended for vehicles. Higher blends fell within 4D grade suitable for powering stationary equipment.

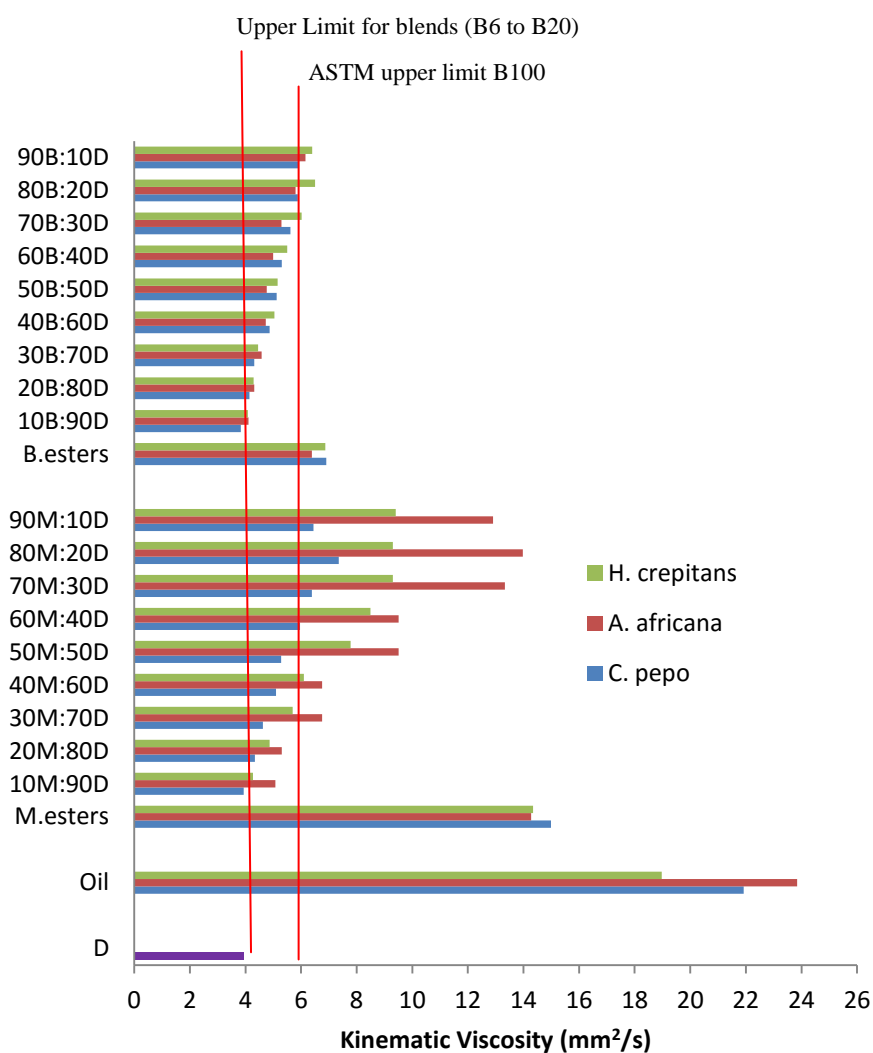


Fig.4.95: Kinematic Viscosity (at 40 °C) of the Various Seed Oils and their Derivatives

Effect of temperature on the viscosities of the various fuel samples was studied at 40 °C, 70 °C and 100 °C. The results are shown in Fig. 4.96. Unsurprisingly, increase in temperature decreased viscosity of the samples due to weakening of intermolecular forces within them, allowing the molecules to flow more freely. Presence of strong or weak interactions at the molecular level can greatly affect the way the molecules of an oil or fat interact, thereby affecting their resistance to flow (Giakoumis, 2013). From the results, it was observed that response of viscosity to temperature increase varied with the feedstock. Increase in temperature had the highest effect on the viscosity of *C. pepo* seed oil followed by *H. crepitans* oil and lastly *A. africana* oil. Viscosity of *C. pepo* mostly decreased with increase in temperature followed by *H. crepitans*. This was clearly noticed in the pure methyl- and butyl esters and could be attributed to

the differences in the strength of the intermolecular forces operating in the different oil samples. It appears that the intermolecular forces in *C. pepo* oil samples were easily weakened by temperature compared to other samples, possibly due to its high degree of saturation.

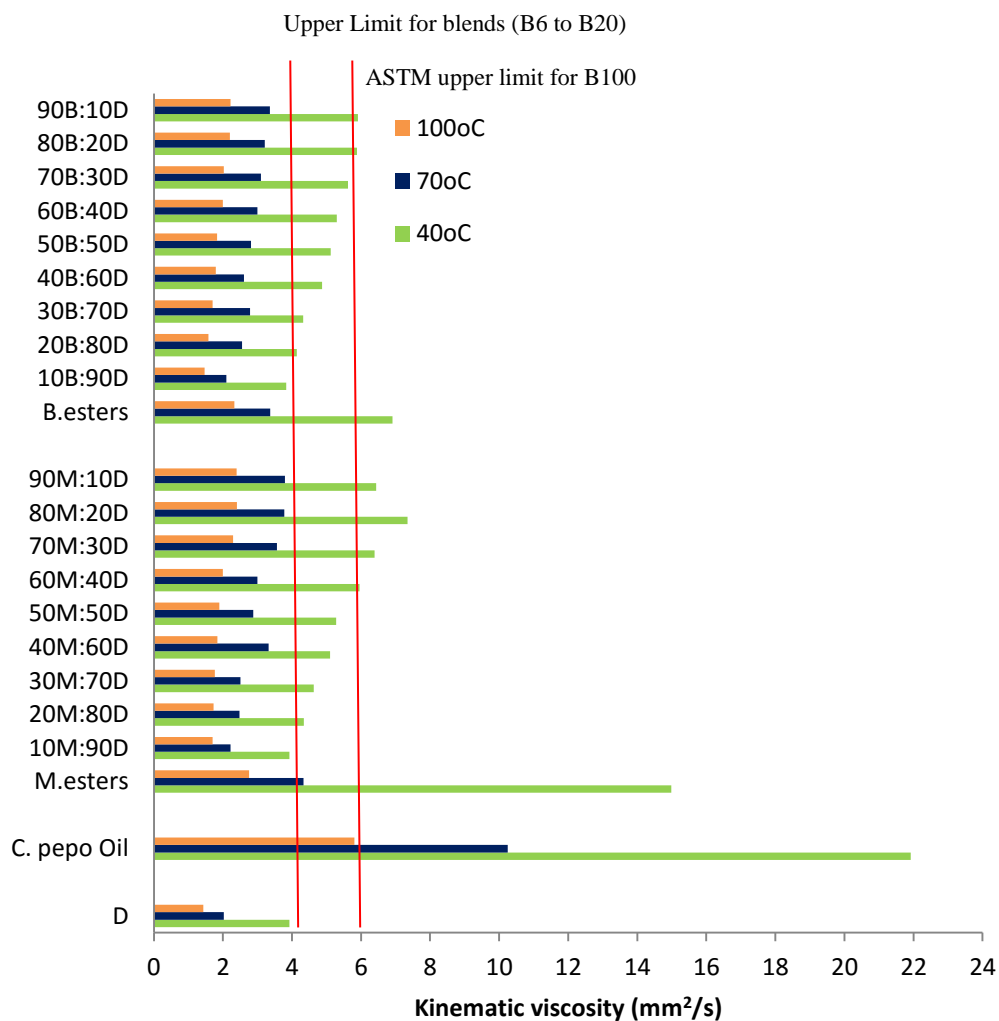


Fig.4.96a: Effect of Temperature on Kinematic Viscosity of the Oil and its Derivatives from *C. pepo* Seed

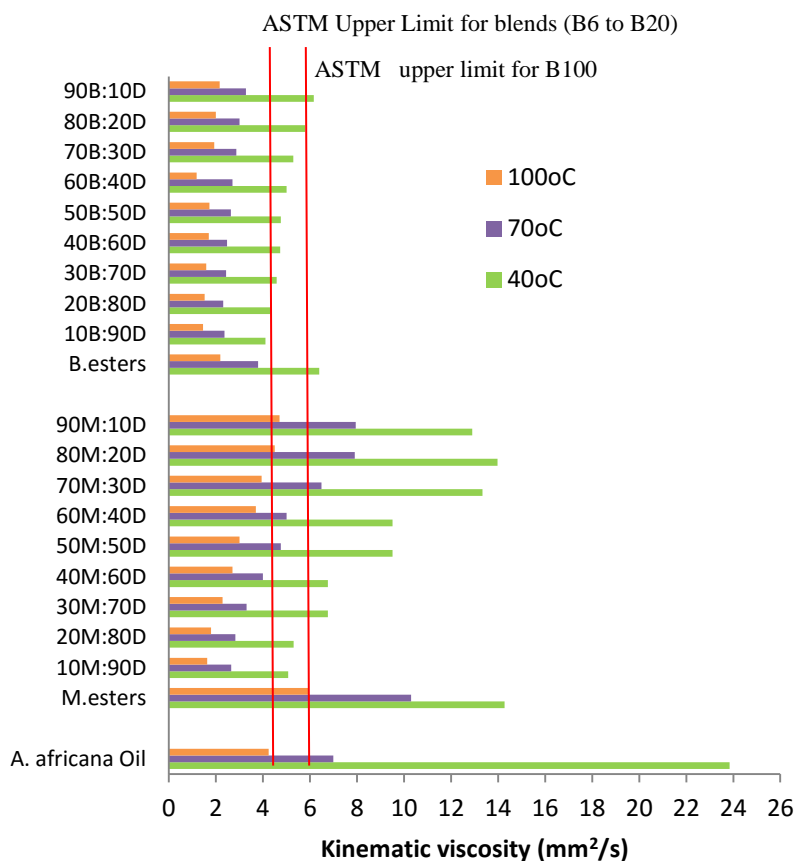


Fig.4.96b: Effect of Temperature on Kinematic Viscosity of the Oil and its Derivatives from *A. africana* Seed

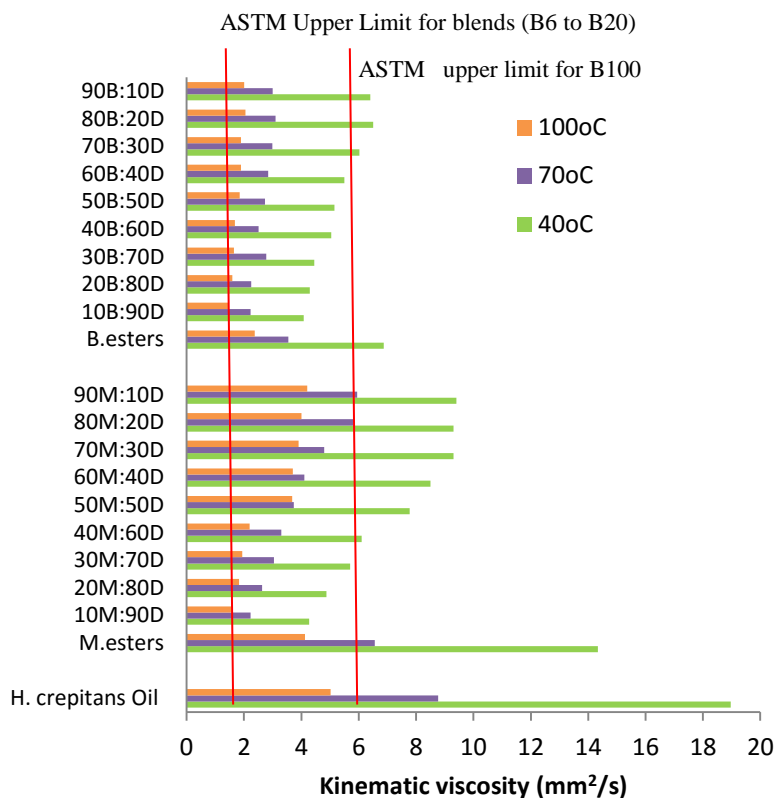


Fig.4.96c: Effect of Temperature on Kinematic Viscosity of the Oil and its Derivatives from *H. crepitans* Seed

4.4.3. Variation of Density

The variations in the relative densities of the biodiesel samples are presented in Fig.4.97. The results showed that the relative densities of the samples were within ASTM specification (0.90) B100 methyl esters of *A. africana* and *H. crepitans* and *A. africana* and blends higher than B60. Density is mass per unit volume of a sample. Specification on density is necessary because with fuels above upper limit, the fuel pump will inject greater mass of biodiesel compared to that of petroleum diesel which may affect the air-fuel ratio and the general burning characteristics of the fuel (Galadima and Garba, 2009). The densities of the feedstock varied in the following order: *A. africana* > *H. crepitans* > *C. pepo* and the variations were majorly due to differences in chain lengths and degree of unsaturation of the samples. It has been shown that increase in both parameters increased density due to corresponding increase in %carbon (Blangino *et al.*, 2008; Giakoumis, 2013). *A. africana* had the highest chain length and degree of unsaturation followed by *C. pepo* and the density increased in that order in both methyl- and butyl esters.

Comparing the results of butyl esters and methyl esters showed that methyl esters had higher density than butyl esters and this can be related to the polarity of the molecules. Butyl esters are less polar than methyl esters as we have mentioned earlier. High polarity increases intermolecular forces between the fuel molecules with attendant decrease in mass per unit volume.

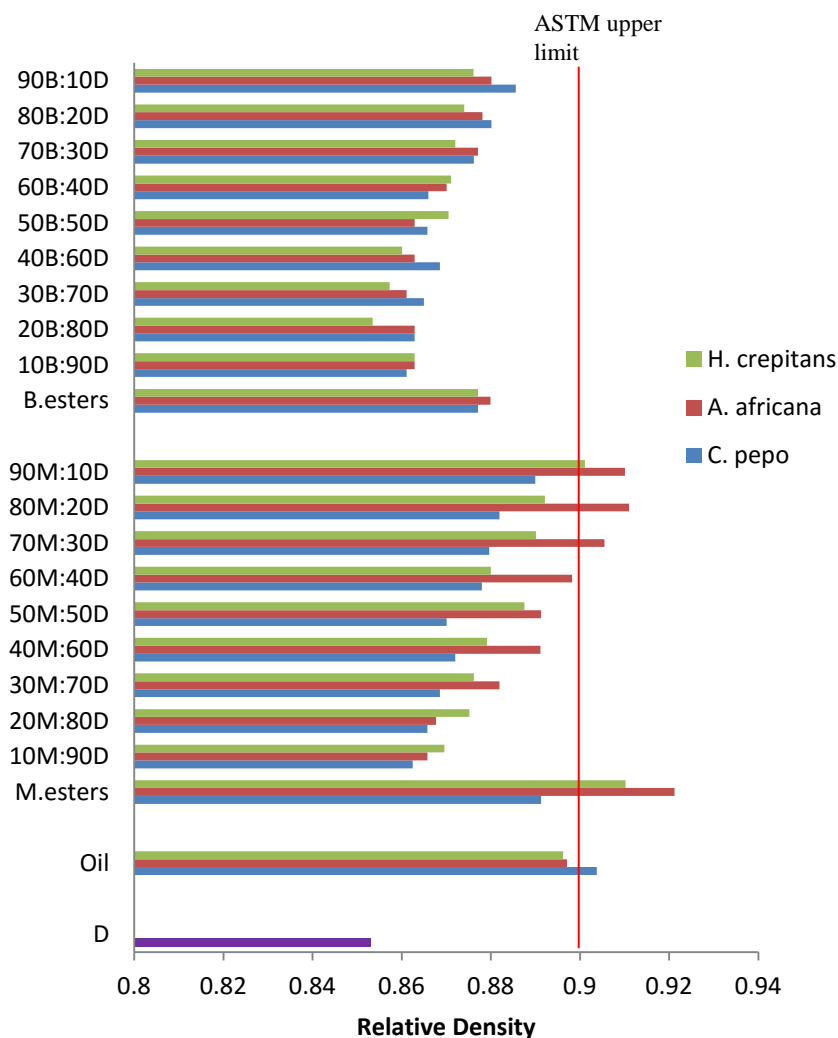


Fig.4.97: Relative Density of the Various Seed Oils and their Derivatives

4.4.4 Variation of Calorific Value

Calorific value indicates the amount of heat a fuel can release on combustion. The calorific values of the three feedstocks are presented in Fig. 4.98. Petroleum diesel expectedly had higher calorific value than the biodiesel samples and the calorific value of the blends slightly decreased with increase in the amount of biodiesel in them. Biodiesel contains about 10–12 % w/w oxygen, which leads to proportional decrease of energy density and heating value (Kaplan *et al.*, 2006). Nevertheless, better combustion of biodiesel compensates for its loss in calorific value. ASTM has no specification for calorific value for biodiesel.

Literature revealed that heating value increases with increase in the degree of saturation (Razon, 2009). The results obtained are in accord with literature; *C. pepo* samples containing the highest saturated fatty acids (62.43 %) had the highest calorific value. This was followed by *H. crepitans* containing 54.33 % saturated fatty acids and lastly *A. africana* containing 33.13 % saturated fatty acids.

Butyl esters had higher calorific value than methyl esters indicating dependence of calorific value on chain length; the higher the carbon content the higher the calorific value.

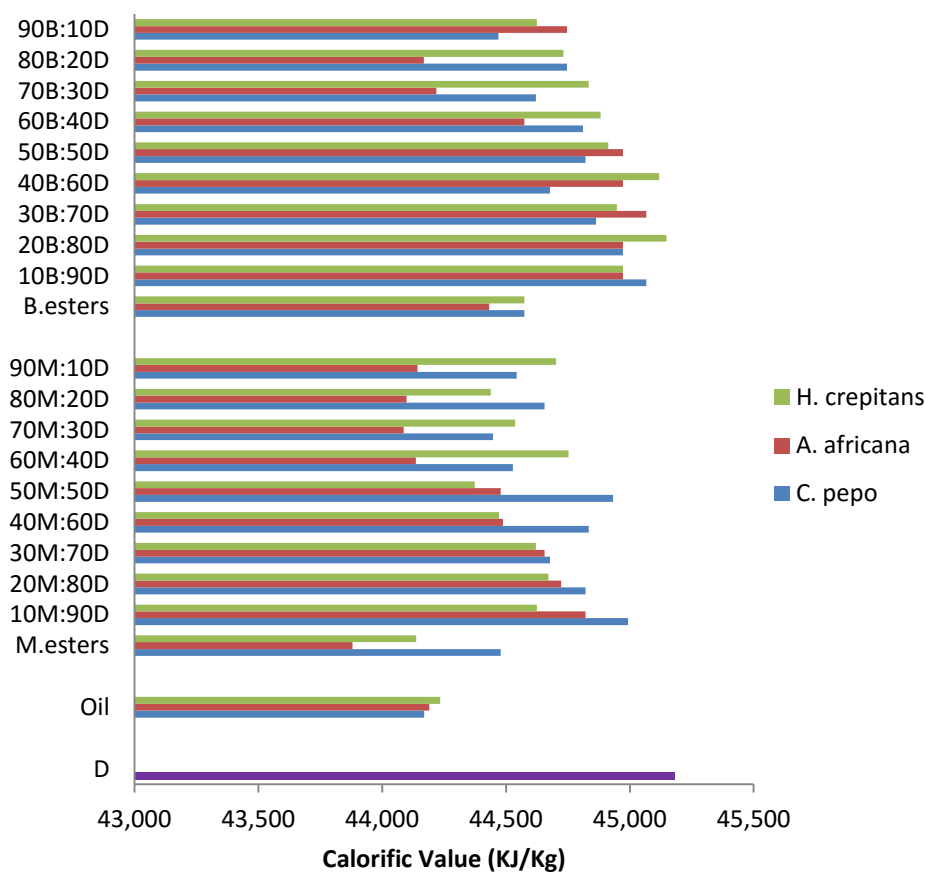


Fig.4.98: Calorific Value of the Various Seed Oils and their Derivatives

4.4.5. Variation of Pour Point

Cold-flow properties; cloud point (CP), pour point (PP) and cold-filter plugging point (CFPP) are interrelated. They indicate the lowest temperature at which a fuel will lose its normal flow and tend to solidify or form crystals, which can have a detrimental effect on fuel supply system. Pour point measures the lowest temperature at which the fuel can be pumped (Lee *et al.*, 1995). If ambient temperature drops lower than the pour point the fuel eventually stops flowing, congeals in the fuel tanks and fuel supply tubes. From our results, *H. crepitans* samples had the best (lowest) pour point among the samples analysed and compared very well with petroleum diesel (Fig.4.99). The results equally revealed that *C. pepo* and *A. africana* might not be right feedstock for countries with a very cold weather (below 5 °C) without pour point improver; most of the samples congealed below 5 °C. Unfortunately, dilution with petroleum diesel did not effectively improve the pour point of both feedstocks. Nevertheless, cold flow properties will not be a strong factor in the use of the feedstocks in tropical countries such as Nigeria where ambient temperature is always above 20 °C. Cold flow properties become very important for countries with very low ambient temperature.

The variations in the pour points of the three feedstocks can be accounted for by differences in chain lengths of the molecules. Literatures show that the longer the carbon chains in the biodiesel the higher the pour point (Wu *et al.*, 2005; Ramos *et al.*, 2009). *A. africana* had the highest average chain length followed by *C. pepo*, and the pour point increased in the same order.

Butyl esters of the feedstocks appeared to have a better pour point than methyl esters. The results are in conformity with the reports of Knothe (2005) that higher alcohol has advantage of producing a biodiesel with reduced cloud and pour points.

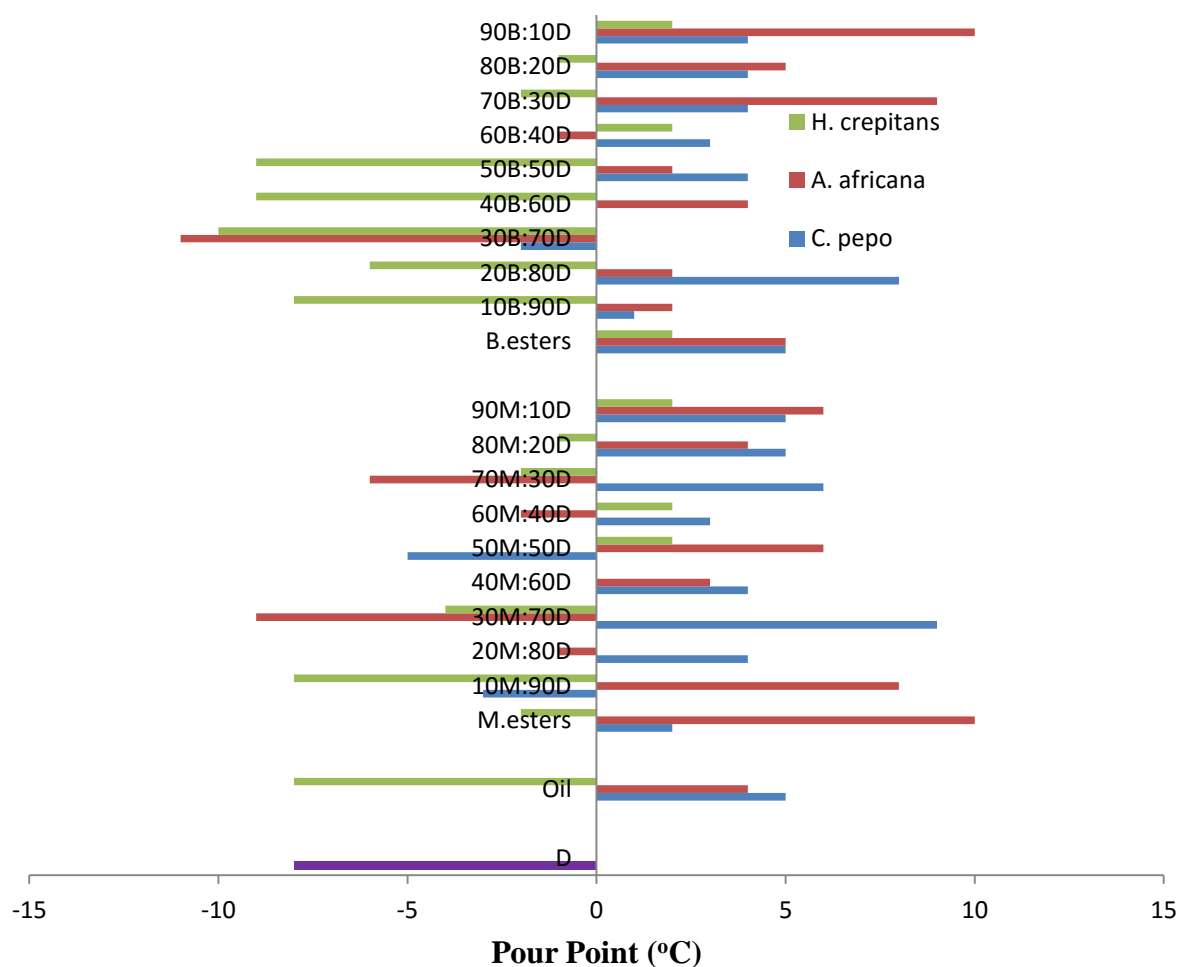


Fig.4.99: Pour Point of the Various Seed Oils and their Derivatives

4.7. Correlations of Fuel Properties of the Methyl- and Butyl esters from the Various Seed Oils

Pearson Correlation was used to evaluate the relationship between the structural features of the fatty acids and the biodiesel properties. The correlation coefficients are presented in Table 4.29. There were strong correlations between density and both average chain length and degree of unsaturation; increase in these parameters increased density due to corresponding increase in %C. The observation conformed to the reports of previous investigators (Blangino *et al.*, 2008; Giakoumis, 2013). *A. africana* had the highest chain length and degree of unsaturation followed by *C. pepo* and the density increased in that order in both methyl- and butyl esters. Strong inverse correlations were equally found

between density and: viscosity (at 40 °C), calorific value, %SFAs, %O and %H; density decreased with increase in these parameters.

Pour point correlated very well with average chain length, $r = 0.99$ (methyl esters) and $r = 0.67$ (butyl esters), showing that the longer the carbon chains in the biodiesel, the higher the pour point. Similar observation has also been made by other researchers (Wu *et al.*, 2005; Ramos *et al.*, 2009). Increase in %C and density also increased the pour point. %MUFAs was shown to favoured pour point while %PUFAs and degree of unsaturated had weak correlations with pour point.

Table 4.29 also indicated that viscosity strongly correlated with %SFAs; increased in %SFAs increased viscosity. *C. pepo* had the highest %SFAs (62.43 %) followed by *H. crepitans* (54.33 %) and the viscosity increased in the same order. Average chain length and degree of unsaturation however showed weak correlations with viscosity. It was equally observed that as temperature was increased, the correlation between viscosity and average chain length tend to appreciate: 40 °C ($r = 0.38$ and 0.60), 70 °C ($r = 0.83$ and 0.77) and 100 °C ($r = 0.79$ and 0.40), suggesting that collapsing of intermolecular attractions between the fuel molecules by the effect of heat allowed chain length to show a stronger effect on the viscosity of the samples.

The Pearson correlation results confirmed the interdependence of calorific value, average chain length, %C, viscosity (at 40 °C), %SFAs and cetane number. Increase in these parameters favoured calorific value while increase in degree of unsaturation and %PUFAs decreased calorific value. It was equally observed that as temperature was increased, the correlations between calorific value and viscosity reversed. This might be due to decrease in the viscosity of the samples which strongly correlated with calorific value.

Finally, strong inverse correlation between cetane number and %PUFAs, degree of unsaturation, average chain length, %C and IV, indicated that increase in these parameters decreased cetane number. In the other hand, increase in %SFAs, %H and %O favoured cetane number.

Table 4.29: Pearson Correlation Coefficients of the Fuel Properties of the Methyl esters and Butyl esters of *C. pepo*, *A. africana* and *H. crepitans* Oils

	FP	PP	Density	Cal. value	CN	Visc. (40 °C)	Visc. (70 °C)	Visc. (100°C)	% SFA	% MUFAs	% PUFAs	Unsat.	Chain. L	% C	% O	% H	IV
FP	1																
PP	-0.75 (-0.98)	1															
Density	0.15 (-0.65)	0.53 (0.50)	1														
Cal. value	-0.08 (0.65)	-0.59 (-0.50)	-0.99 (-0.98)	1													
CN	0.67	-0.99	-0.63	0.69	1												
Visc. (40 °C)	-0.42 (0.60)	-0.26 (-0.44)	-0.96 (-0.99)	0.93 (0.99)	0.39	1											
Visc. (70 °C)	-0.14 (-0.27)	0.76 (0.08)	0.95 (0.90)	-0.97 (-0.90)	-0.83	-0.83	1										
Visc. (100 °C)	-0.08 (0.80)	0.72 (-0.67)	0.97 (-0.97)	-0.98 (0.97)	-0.79	-0.86 (0.96)	0.99 (-0.79)	1									
% SFAs	0.25 (0.43)	-0.82 (-0.25)	-0.91 (-0.96)	0.94 (0.96)	0.89	0.77 (0.98)	-0.99 (-0.98)	-0.98 (0.88)	1								
% MUFAs	0.99 (0.98)	-0.73 (-0.99)	0.18 (-0.47)	-0.11 (0.47)	0.64	-0.45 (0.40)	-0.11 (-0.04)	-0.05 (0.64)	0.21 (0.21)	1							
% PUFAs	-0.92 (-0.98)	0.35 (0.52)	0.25 (0.80)	-0.32 (-0.80)	-0.91	0.02 (-0.75)	0.52 (0.47)	0.47 (-0.91)	-0.61 (-0.61)	-0.90 (-0.90)	1						
Unsat.	-0.69 (-0.82)	0.39 (0.49)	0.61 (0.97)	-0.66 (-0.97)	-0.99	-0.36 (-0.95)	0.82 (0.77)	0.78 (-0.99)	-0.87 (-0.87)	-0.67 (-0.67)	0.92 (0.92)	1					
Chain. L	-0.67 (-0.80)	0.99 (0.67)	0.63 (0.97)	0.68 (0.97)	-0.99	0.38 (0.60)	0.83 (0.79)	0.79 (0.40)	-0.88 (-0.88)	-0.64 (-0.64)	0.91 (0.91)	0.99 (0.96)	1				
% C	-0.64 (0.77)	0.98 (0.64)	0.66 (0.98)	0.71 (0.98)	-0.99	-0.42 (-0.97)	0.85 (0.81)	0.81 (-0.99)	-0.90 (-0.90)	-0.61 (-0.61)	0.89 (0.89)	0.97 (0.99)	0.99 (0.99)	1			
% O	0.54 (0.65)	-0.96 (-0.54)	-0.75 (-0.99)	0.79 (0.42)	0.98	0.53 (0.99)	-0.91 (-0.88)	-0.88 (0.98)	0.95 (0.95)	0.51 (0.51)	-0.83 (-0.83)	-0.98 (-0.99)	-0.98 (-0.98)	-0.99 (-0.99)	1		
% H	0.71 (0.83)	-0.99 (-0.71)	-0.59 (-0.96)	0.65 (0.96)	0.99	0.346 (0.947)	-0.80 (-0.76)	-0.76 (0.99)	0.86 (0.86)	0.68 (0.68)	-0.92 (-0.92)	-0.95 (-0.95)	-0.99 (-0.99)	-0.99 (-0.99)	0.97 (0.97)	1	
IV	-0.89 (-0.96)	0.97 (0.88)	0.32 (0.84)	-0.38 (-0.84)	-0.93	-0.041 (-0.802)	0.58 (0.53)	0.53 (-0.94)	-0.66 (-0.66)	-0.87 (-0.87)	0.99 (0.99)	0.95 (0.80)	0.93 (0.93)	0.92 (0.92)	-0.86 (-0.86)	-0.95 (-0.95)	1

Values in parentheses are for butyl esters, Unsat. = Degree of unsaturation, PP = pour point, FP = flash point, chain. L = Average chain length

4.8. Bond Structure/Stability Relationship of the Various Seed Oils and their Derivatives

Bond structures of the vegetable oil esters and petroleum diesel would suggest why there is similarity in their fuel properties. Stability of the bonds at various temperatures would also give an insight into the thermal stability of the fuel molecules. Biodiesel from certain feedstocks have the tendency to polymerize or undergo rapid oxidative deterioration at high temperature condition, resulting in formation of resinous substances with attendant poor atomization and various engine malfunctions during the use (Schumacher and Tabitha, 1997; Graboski and McCormick, 1998; Srivastava and Prasad, 2000). Therefore, thermal stability is an important parameter to be considered in the choice of feedstock for biodiesel production.

FTIR spectroscopy monitoring of various changes in the bond structures of lipid molecules under thermal stress gives insight into various changes in the fuel sample and hence useful for assessing the thermal stability (Li *et al.*, 2000; Yildiz *et al.*, 2001). This method provides quicker, less tedious and environmentally benign technique for assessing lipid stability.

In this study, FTIR was used to compare the bond structures/stability of the biofuel samples with that of petroleum diesel at: room temperature (28 °C), 100, 150, 200, 250 and 300 °C. The spectra peaks and the corresponding bond structures are shown in (Table 4.30-4.47).

Table 4.30: FTIR Bond Structure Comparison for *C. pepo* Seed Oil, Methyl esters, Butyl esters and Petrodiesel (cm⁻¹) at 28 °C

Diesel	<i>C. pepo</i> Oil	<i>C. pepo</i> M. esters	<i>C. pepo</i> B. esters	M. esters/Diesel Blends					Description
				10:90	20:80	30:70	50:50	90:10	
absent	3854.87	absent	absent	absent	3377.47	absent	absent	absent	O-H stretch for alcohols and carboxylic acids.
2929.97 2352.27	2929.00	2929.00	2929.97	2929.97	2929.97	2929.00	2929.97	2929.00	C-H stretch for alkanes, alkenes and aromatics
absent	1738.89	1741.78	1735.03	1742.74	1743.71	1742.74	1741.78	1742.74	C=O stretch for esters, carboxylic acids, aldehydes, and ketones.
1457.27	1450.52	1449.55	1452.45	1456.30	1454.38	1453.41	1452.45	1451.48	C=C stretch for alkenes and aromatics.
absent	absent	absent	absent	1371.43	1369.50	1363.72	1363.72	1359.86	C-H bending for alkane. N-O stretch for nitro groups.
1138.04	1164.08	1171.79	1175.65	1171.79	1153.47	1174.69	1175.65	1173.72 1027.13	C-O stretch for esters, carboxylic acid and ethers
790.84	714.65	714.65	716.58	731.05	717.54	720.44	870.89 721.4	716.58	C-H deformation for alkenes, alkanes and aromatics
419.53	450.39	448.46	434.96	448.46	433.03	439.78	436.89	430.14	C-H deformation for alkyl groups.

M.esters = methyl esters**B.esters = butyl esters**

Table 4.31: FTIR Bond Structure Comparison for *C. pepo* Seed Oil, Methyl esters, Butyl esters and Petrodiesel (cm⁻¹) at 100 °C

Diesel	<i>C. pepo</i> Oil	<i>C. pepo</i> M.esters	<i>C. pepo</i> B.esters	M.esters/Diesel Blends					Description
				10:90	20:80	30:70	50:50	90:10	
absent	3461.38	3450.77	3451.97	3450.54	3450.30	3593.52	3854.88 3739.44	3451.77	O-H stretch for alcohols and carboxylic acids.
2931.9	2932.86 2871.14	2929.97	2929.99	2931.94	2936.84	2929.94	2929.90 2422.12 2277.94 1834.32	2931.99	C-H stretch for alkanes, alkenes and aromatics
absent	1735.99	1738.89	1738.89	1742.94	1741.93	1742.74	1742.80	1742.84	C=O stretch for esters, carboxylic acids, aldehydes, and ketones.
1458.23	1448.59	1449.55	1449.58	1458.33	1454.78	1449.55	1454.37	1448.30	C=C stretch for alkenes and aromatics.
1371.43	absent	1358.90	absent	1371.43	1366.69	1371.44	1366.69	1378.93	C-H bending for alkane. N-O stretch for nitro groups.
1129.36	1168.90	1170.83	1171.58	1129.56	1154.97	1154.41	1154.51	absent	C-O stretch for esters, carboxylic acid and ethers
absent	719.47	894.04 718.51	894.04 718.51	718.52	723.83	absent	723.34	718.72	C-H deformation for alkenes, alkanes and aromatics
443.64	441.71	439.56	439.47	443.61	442.71	absent	441.98	437.47	C-H deformation for alkyl groups.

Table 4.32: FTIR Bond Structure Comparison for *C. pepo* Seed Oil, Methyl esters, Butyl esters and Petrodiesel (cm⁻¹) at 150 °C

Diesel	<i>C. pepo</i>	<i>C. pepo</i>	<i>C. pepo</i>	M.esters/Diesel Blends					Description
	Oil	M.esters	B.esters	10:90	20:80	30:70	50:50	90:10	
absent	3496.09	3444.98	3448.84	absent	3744.11 3569.30	3447.87	3854.87 3744.92 3569.39	3855.73 3552.77	O-H stretch for alcohols and carboxylic acids.
2932.86	2931.90 2872.10	2930.93 2870.17 2346.48	2930.93 2294.40 2106.34	2933.66	2929.47	2929.97 2929.97 2423.64	2929.97 2414.96 2289.58 1831.47	2929.87 2419.81	C-H stretch for alkanes, alkenes and aromatics
absent	1736.96	1736.96	1732.13	1744.40	1741.72	1741.70	1741.78	1743.71	C=O stretch for esters, carboxylic acids, aldehydes, and ketones.
1458.23	1448.59	1447.62	1452.45	1459.33	1455.34	1612.54 1454.38	1660.77 1536.35 1455.34	1542.16 1454.00	C=C stretch for alkenes and aromatics.
1371.43	1363.72 1238.34	1356.97	1355.04	1374.44	absent	1364.68	1368.54	1367.60	C-H bending for alkane. N-O stretch for nitro groups.
absent	1168.90	1176.62 1003.02	1166.97	1145.67	1162.11	1147.68	1166.01	1162.05	C-O stretch for esters, carboxylic acid and ethers
absent	719.47	868.96 719.47	724.29 611.45	absent	723.43	723.33 608.56	890.18 718.51	717.52	C-H deformation for alkenes, alkanes and aromatics
438.82 386.74	453.29	443.64	434.96	438.12	437.81	436.89	448.46	447.51	C-H deformation for alkyl groups.

Table 4.33: FTIR Bond Structure Comparison for *C. pepo* Seed Oil, Methyl esters, Butyl esters and Petrodiesel (cm⁻¹) at 200 °C

Diesel	<i>C. pepo</i> Oil	<i>C. pepo</i> M. esters	<i>C. pepo</i> B. esters	M.esters/Diesel Blends					Description
				10:90	20:80	30:70	50:50	90:10	
3511.53	3469.09	3512.49	3855.83 3740.10 3462.34	3512.50 3532.71	3852.81 3744.93 3532.94	3854.87 3744.92 3532.74	3449.87	3448.89	O-H stretch for alcohols and carboxylic acids.
2932.86	2929.97 2868.24 2344.55	2930.93 2868.24 2351.3	2931.90 2419.78 2271.26	2932.86	2929.07	2929.97 2056.19	2938.73 2107.30	2933.53	C-H stretch for alkanes, alkenes and aromatics
1725.38	1735.99	1739.85	1735.13 1545.03	1735.88	1743.94	1742.74 1658.84 1540.21	1743.75	1743.79	C=O stretch for esters, carboxylic acids, aldehydes, and ketones.
1448.59	1447.62	1448.59	1454.38	1448.59	1456.94	1455.34	1452.44	1453.49	C=C stretch for alkenes and aromatics.
1367.58	1363.72	1361.79	1364.68	1368.18	absent	1370.47	1367.63	1367.62	C-H bending for alkane. N-O stretch for nitro groups.
1177.58 1008.80	1161.19	1174.69	1174.69	absent	1160.12	1160.22	1171.68	1122.69	C-O stretch for esters, carboxylic acid and ethers
728.15	719.47	720.44	722.37	728.10	720.54	880.12 720.23	723.93 612.45	724.32	C-H deformation for alkenes, alkanes and aromatics
429.18	442.68	439.78	439.34	absent	452.30	450.39	462.99	absent	C-H deformation for alkyl groups.

Table 4.34: FTIR Bond Structure Comparison for *C. pepo* Seed Oil, Methyl esters, Butyl esters and Petrodiesel (cm⁻¹) at 250 °C

Diesel	<i>C. pepo</i> Oil	<i>C. pepo</i> M.esters	<i>C. pepo</i> B.esters	M.esters/Diesel Blends					Description
				10:90	20:80	30:70	50:50	90:10	
absent	3476.81	3497.06	3854.87 3739.13 3528.89	3768.67	3768.21	3768.07 3392.97	3854.37 3632.18	3498.26	O-H stretch for alcohols and carboxylic acids.
2931.90	2929.97 2866.32	2929.97 2866.32 2351.30	2931.9 2419.78 2276.08 1825.68	2931.95	2931.93	2929.97	2929.00	2929.97	C-H stretch for alkanes, alkenes and aromatics
1744.67 1600.97	1736.96	1739.85	1733.1 1540.21	1744.87 1661.43 1535.69	1744.00	1743.71 1624.12	1743.78	1738.84	C=O stretch for esters, carboxylic acids, aldehydes, and ketones.
1459.2	1449.55	1448.59	1455.34	1459.25	1458.28	1454.38	1457.37	1448.59	C=C stretch for alkenes and aromatics.
1371.43	1364.68	1356.97	1367.58	absent	absent	1365.65	1369.54	1358.47	C-H bending for alkane. N-O stretch for nitro groups.
absent	1166.97	1175.65 1013.63	1173.72	1166.43	1167.85	1149.61	absent	1175.65	C-O stretch for esters, carboxylic acid and ethers
735.87	718.51	874.75 717.54	722.37	736.89	736.12	724.29 605.67	716.67	873.05 716.54	C-H deformation for alkenes, alkanes and aromatics
443.64	436.89 387.70	443.64	423.39	443.44	absent	447.50	429.19	absent	C-H deformation for alkyl groups.

Table 4.35: FTIR Bond Structure Comparison for *C. pepo* Seed Oil, Methyl esters, Butyl esters and Petrodiesel (cm⁻¹) at 300 °C

Diesel	<i>C. pepo</i> Oil	<i>C. pepo</i> M.esters	<i>C. pepo</i> B.esters	M.esters/Diesel Blends					Description
				10:90	20:80	30:70	50:50	90:10	
absent	3471.98	3471.98	3853.90 3738.17 3462.34	3472.28	absent	3855.83 3739.13 3476.81	3447.80	3471.91	O-H stretch for alcohols and carboxylic acids.
2931.9 2246.18	2925.15 2857.64 2360.95	2930.93 2351.30	2931.90 2422.67 2103.44 1824.72	2932.93	2931.74	2929.97 2416.89 2279.19	2928.46 2284.96	2932.93	C-H stretch for alkanes, alkenes and aromatics
1749.49 1604.83	1743.71 1648.23	1739.85	1734.06 1540.21	1749.42 1606.82	1742.69 1604.03	1740.81 1658.84 1537.32	1744.70 1655.04	1739.88	C=O stretch for esters, carboxylic acids, aldehydes, and ketones.
1454.38	1455.34	absent	1455.34	1454.18	1455.32	1456.35	1455.30	absent	C=C stretch for alkenes and aromatics.
1371.43	1371.43	1358.90	1368.54	1371.43	1371.43	1369.50	1367.62	1356.98	C-H bending for alkane. N-O stretch for nitro groups.
1135.15	1160.22 1106.21	1171.79	1166.97	1135.05	absent	1166.01	1128.40	1171.79	C-O stretch for esters, carboxylic acid and ethers
731.05	721.4 606.63	884.39 718.51	723.33	732.15	731.35	721.40	726.02	883.36 718.54	C-H deformation for alkenes, alkanes and aromatics
442.68 398.31	445.57	426.28	461.00	absent	451.84	425.32	451.32	426.38	C-H deformation for alkyl groups.

Table 4.36: FTIR Bond Structure Comparison for *A. africana* Seed Oil, Methyl esters, Butyl esters and Petrodiesel (cm⁻¹) at 28 °C

Diesel	A. <i>africana</i> Oil	A. <i>africana</i> M.esters	A. <i>africana</i> B.esters	M.esters/Diesel Blends					Description
				10:90	20:80	30:70	50:50	90:10	
absent	absent	3443.05	3424.73	absent	absent	absent	3447.80	3437.26	O-H stretch for alcohols and carboxylic acids.
2929.97 2352.27	2928.04	2932.86 2872.1	2932.86	2929.97	2930.93	2930.93	2928.46 2284.96	2931.90	C-H stretch for alkanes, alkenes and aromatics
absent	1736.96	1738.89	1731.17	1736.96	1736.96	1736.96	1744.70 1655.04	1739.85	C=O stretch for esters, carboxylic acids, aldehydes, and ketones.
1457.27	1445.70	1447.62	1451.48	1455.34	1457.27	1456.03	1455.30	1450.52	C=C stretch for alkenes and aromatics.
absent	absent	1360.82	absent	1373.36	1373.36	absent	1367.62	1359.86	C-H bending for alkane. N-O stretch for nitro groups.
1138.04	1158.29	1166.97	1179.51	1173.72	1174.69	1171.79	1128.40	1166.97	C-O stretch for esters, carboxylic acid and ethers
790.84	716.58	721.40	724.29	724.29	absent	absent	726.02	722.37	C-H deformation for alkenes, alkanes and aromatics
419.53	426.28	435.93	447.50	447.50	444.61	419.53	451.32	436.89	C-H deformation for alkyl groups.

Table 4.37: FTIR Bond Structure Comparison for *A. africana* Seed Oil, Methyl esters, Butyl esters and Petrodiesel (cm⁻¹) at 100 °C

Diesel	A. <i>africana</i> Oil	A. <i>africana</i> M.esters	A. <i>africana</i> B.esters	M.esters/Diesel Blends					Description
				10:90	20:80	30:70	50:50	90:10	
absent	3441.12	3436.30	3437.35	3399.65	3398.95	3398.55	3433.41	3436.3	O-H stretch for alcohols and carboxylic acids.
2931.90	2929.97 2211.46	2931.90 2869.21	2931.98 2869.25	2931.90 2348.41	2932.99 2348.41	2932.52	2930.93 2350.34	2869.27	C-H stretch for alkanes, alkenes and aromatics
absent	1734.06	1739.85	1739.72	1739.85	1739.25	1735.25	1739.85	1739.80	C=O stretch for esters, carboxylic acids, aldehydes, and ketones.
1458.23	1446.66	1448.59	1449.99	1454.38	1457.98	1457.58	1454.38	1448.58	C=C stretch for alkenes and aromatics.
1371.43	1366.61	1361.79	1363.68	1371.43	1371.49	1371.18	1367.58	1361.49	C-H bending for alkane. N-O stretch for nitro groups.
1129.36	1152.51	1166.01	1167.81	1150.58	1151.58	1151.51	1166.97	1166.81	C-O stretch for esters, carboxylic acid and ethers
absent	724.29	719.47	719.75	absent	725.25	724.05	725.26	719.46	C-H deformation for alkenes, alkanes and aromatics
443.64	442.68	439.78	439.88	442.94 422.42	443.64 422.42	443.66	429.18	439.78	C-H deformation for alkyl groups.

Table 4.38: FTIR Bond Structure Comparison for *A. africana* Seed Oil, Methyl esters, Butyl esters and Petrodiesel (cm⁻¹) at 150 °C

Diesel	A. <i>africana</i> Oil	A. <i>africana</i> M.esters	A. <i>africana</i> B.esters	M.esters/Diesel Blends					Description
				10:90	20:80	30:70	50:50	90:10	
absent	3464.27	3461.38	3435.34	3397.76	3396.76	3397.86	3461.38	3461.48	O-H stretch for alcohols and carboxylic acids.
2932.86	2932.86 2208.57	2931.90	2933.83 2869.21 2355.16 2212.43 2107.37	2933.82	2932.86 2351.30	2933.12	2931.90 2349.38	2931.99	C-H stretch for alkanes, alkenes and aromatics
absent	1735.03	1740.81	1732.13 1728.28 1650.16	1738.88	1738.89 1601.93	1739.18	1739.85	1740.83	C=O stretch for esters, carboxylic acids, aldehydes, and ketones.
1458.23	1449.55	1448.59	1450.52	1456.74	1455.34	1456.84	1451.48	1448.49	C=C stretch for alkenes and aromatics.
1371.43	1363.72	1357.93	1365.65	absent	1370.47	1374.82	1364.68	1359.93	C-H bending for alkane. N-O stretch for nitro groups.
absent	1166.97	1164.08	1117.79	1163.22	1166.97	1163.82	1166.97	1164.01	C-O stretch for esters, carboxylic acid and ethers
absent	724.29	721.40	726.22 613.38	733.87	732.97	734.17	722.43	absent	C-H deformation for alkenes, alkanes and aromatics
438.82 386.74	438.82	440.75	462.93	absent	438.82	absent	432.78	441.75	C-H deformation for alkyl groups.

Table 4.39: FTIR Bond Structure Comparison for *A. africana* Seed Oil, Methyl esters, Butyl esters and Petrodiesel (cm⁻¹) at 200 °C

Diesel	A. <i>africana</i> Oil	A. <i>africana</i> M.esters	A. <i>africana</i> B.esters	M.esters/Diesel Blends					Description
				10:90	20:80	30:70	50:50	90:10	
3511.53	3477.77	3477.77	3461.38	3512.51	absent	absent	3475.84	3476.74	O-H stretch for alcohols and carboxylic acids.
2932.86	2931.90 2931.90 2209.53	2933.83 2870.17 2043.65	2934.79 2874.03	2922.85	2929.97	2928.69	2930.93 2350.34 2209.53	2930.93 2352.32 2200.50	C-H stretch for alkanes, alkenes and aromatics
1725.38	1734.06	1739.85	1729.24	1725.08	1743.41	1747.49	1740.81	1740.81	C=O stretch for esters, carboxylic acids, aldehydes, and ketones.
1448.59	1447.60	1448.59	1451.48	1448.99	1455.34	1455.34	1453.41	1452.49	C=C stretch for alkenes and aromatics.
1367.58	1362.75	1359.86	1365.65	absent	1369.50	1370.15	1364.68	1362.18	C-H bending for alkane. N-O stretch for nitro groups.
1177.58 1008.80	1165.04	1166.01 1166.01	1172.76	1178.52	1150.58	1160.57	1160.22	1163.92	C-O stretch for esters, carboxylic acid and ethers
728.15	725.26	720.44	726.22	728.58	726.26	725.36	726.22	726.22	C-H deformation for alkenes, alkanes and aromatics
429.18	422.42	419.53 395.42	424.35	absent	447.50	447.56 395.40	449.43	absent	C-H deformation for alkyl groups.

Table 4.40: FTIR Bond Structure Comparison for *A. africana* Seed Oil, Methyl esters, Butyl esters and Petrodiesel (cm⁻¹) at 250 °C

Diesel	A. <i>africana</i> Oil	A. <i>africana</i> M.esters	A. <i>africana</i> B.esters	M.esters/Diesel Blends					Description
				10:90	20:80	30:70	50:50	90:10	
absent	3472.95	3480.66	3854.87 3739.13 3510.56	3517.26		3518.28	3517.88	absent	O-H stretch for alcohols and carboxylic acids.
2931.90	2929.97 2217.25	2934.79 2869.21	2933.83 2418.82 1821.83	2931.94	2931.90	2933.83 2873.07	2934.23 2875.27	2934.69 2869.21	C-H stretch for alkanes, alkenes and aromatics
1744.67 1600.97	1735.99	1739.85	1732.13 1543.10	1747.66	1746.60	1739.85	1739.31	1738.25	C=O stretch for esters, carboxylic acids, aldehydes, and ketones.
1459.20	1447.62	1447.60	1455.34	1453.43	1453.41	1604.83 1451.48	1451.98	1446.64	C=C stretch for alkenes and aromatics.
1371.43	1360.82	1359.86	1363.72	1367.58	1367.58	1363.72	1362.72	1358.84	C-H bending for alkane. N-O stretch for nitro groups.
absent	1147.68	1165.04	1176.62	1165.19	1163.11	1165.04	1166.34	1166.84	C-O stretch for esters, carboxylic acid and ethers
735.87	725.26	722.37	726.22	absent	723.33	727.19	728.29	722.39	C-H deformation for alkenes, alkanes and aromatics
443.64	452.32	439.78	429.18	429.23	429.18	436.89	435.79	438.28	C-H deformation for alkyl groups.

Table 4.41: FTIR Bond Structure Comparison for *A. africana* Seed Oil, Methyl esters, Butyl esters and Petrodiesel (cm⁻¹) at 300 °C

Diesel	A. <i>africana</i> Oil	A. <i>africana</i> M.esters	A. <i>africana</i> B.esters	M.esters/Diesel Blends					Description
				10:90	20:80	30:70	50:50	90:10	
absent	3471.98	3519.24	3868.37 3464.27	3793.38	3792.18 3390.97	3793.43	3497.06	absent	O-H stretch for alcohols and carboxylic acids.
2931.9 2246.18	2930.93 2281.87 2107.37	2932.86	2932.86	2932.99 2247.28	2929.97 2742.87 2357.09 2125.63	2932.93 2246.18	2934.79 2874.03	2934.69 2869.21	C-H stretch for alkanes, alkenes and aromatics
1749.49 1604.83	1735.99	1740.81	1732.13 1547.93	1748.45 1614.13	1739.85 1612.54	1748.14	1739.85	1737.15	C=O stretch for esters, carboxylic acids, aldehydes, and ketones.
1454.38	1448.59	1448.59	1454.38	1455.18	1454.38	1454.34	1451.48	1446.04	C=C stretch for alkenes and aromatics.
1371.43	1361.79	1359.86	1364.68	1371.43	1367.58	1372.13	1364.68	1358.80	C-H bending for alkane. N-O stretch for nitro groups.
1135.15	1156.36	1166.01	1172.76	1136.85	1155.40	1135.39	1166.97	1166.04	C-O stretch for esters, carboxylic acid and ethers
731.05	725.26 600.85	894.04 720.44	725.26	731.05	727.44	731.05	729.12	722.35	C-H deformation for alkenes, alkanes and aromatics
442.68 398.31	454.25	430.14	424.35	442.68 398.31	442.98	442.76 397.33	436.89	438.85	C-H deformation for alkyl groups.

Table 4.42: FTIR Bond Structure Comparison for *H. crepitans* Seed Oil, Methyl esters, Butyl esters and Petrodiesel (cm⁻¹) at 28 °C

Diesel	<i>H. crepitans</i> Oil	<i>H. crepitans</i> M.esters	<i>H. crepitans</i> B.esters	M.esters/Diesel Blends					Description
				10:90	20:80	30:70	50:50	90:10	
Absent	3459.45	3470.06	absent	absent	absent	absent	absent	absent	O-H stretch for alcohols and carboxylic acids.
2929.97 2352.27	2929.97	2929.00 2042.68	2931.90	2930.93	2929.97	2929.97	2929.00	2929.00	C-H stretch for alkanes, alkenes and aromatics
Absent	1735.03	1743.71	1732.13	1745.64	1744.67	1745.64	1739.85	1743.71	C=O stretch for esters, carboxylic acids, aldehydes, and ketones.
1457.27	1448.59	1448.59	1453.41	1457.27	1455.34	1455.34	1451.48	1451.48	C=C stretch for alkenes and aromatics.
Absent	1368.54	1355.04	1178.55	1371.43	1371.43	1369.50	absent	1362.75	C-H bending for alkane. N-O stretch for nitro groups.
1138.04	1167.94	1155.4	absent	1166.01	1166.01	1165.04	1169.87	1169.87	C-O stretch for esters, carboxylic acid and ethers
790.84	717.54	882.46 716.58	718.51	723.33	absent	719.47	712.72	717.54	C-H deformation for alkenes, alkanes and aromatics
419.53	443.64	431.10	442.68	429.18	447.5	435.93	433.03	445.57	C-H deformation for alkyl groups.

Table 4.43: FTIR Bond Structure Comparison for *H. crepitans* Seed Oil, Methyl esters, Butyl esters and Petrodiesel (cm⁻¹) at 100 °C

Diesel	<i>H. crepitans</i> Oil	<i>H. crepitans</i> M.esters	<i>H. crepitans</i> B.esters	M.esters/Diesel Blends					Description
				10:90	20:80	30:70	50:50	90:10	
absent	3457.52	3854.35	3454.62	3456.99	3446.91	3446.99	2928.37	3854.99	O-H stretch for alcohols and carboxylic acids.
2931.90	2929.97 2362.88	2929.48	2935.76 2875.00	2931.90 2348.40	2932.86 2875.96 2348.41	2932.86 2876.06	1740.67	2929.62	C-H stretch for alkanes, alkenes and aromatics
absent	1735.03	1742.85	1725.38	1744.66	1744.67 1635.69	1754.65	1453.98	1743.70 1543.28	C=O stretch for esters, carboxylic acids, aldehydes, and ketones.
1458.23	1449.55	1450.59	1449.43	1458.33	1454.38	1453.98	1366.81	1454.56	C=C stretch for alkenes and aromatics.
1371.43	1369.50	1356.37	1365.65	1370.13	1370.47	1371.48	1167.04	1356.87	C-H bending for alkane. N-O stretch for nitro groups.
1129.36	1167.94	1162.22	1176.62	1128.66	1129.36	1128.32	absent	1162.52	C-O stretch for esters, carboxylic acid and ethers
absent	718.51	absent	730.08	absent	884.39 720.44	721.34	719.44	717.55	C-H deformation for alkenes, alkanes and aromatics
443.64	425.32	447.56	446.54	443.66	462.93	463.43	448.43	446.50	C-H deformation for alkyl groups.

Table 4.44: FTIR Bond Structure Comparison for *H. crepitans* Seed Oil, Methyl esters, Butyl esters and Petrodiesel (cm⁻¹) at 150 °C

Diesel	<i>H. crepitans</i> Oil	<i>H. crepitans</i> M.esters	<i>H. crepitans</i> B.esters	M.esters/Diesel Blends					Description
				10:90	20:80	30:70	50:50	90:10	
4332.26	4337.09	4337.19	3463.30	4331.30	4331.3	absent	4335.16	absent	O-H stretch for alcohols and carboxylic acids.
absent	3456.55	3853.95	2936.72 2872.10	3853.98	3853.9 3738.17 3420.87	absent	3855.83 3742.99	3853.99	C-H stretch for alkanes, alkenes and aromatics
2932.86	2929.00 1832.44	2929.00	1725.38	2928.99 2421.70	2929.97 2420.74 2274.15 2107.3 1833.4	2291.26 2040.76 1835.33	2929.97 2418.82 2271.26 2040.76 1835.33	2929.72	C=O stretch for esters, carboxylic acids, aldehydes, and ketones.
absent	1735.99	1742.75 1661.07 1542.28	1450.52	1743.81	1743.71 1655.94	1743.75	1743.71 1656.91 1541.18	1742.75 1542.26	C=C stretch for alkenes and aromatics.
1458.23	1447.62	1450.56	1366.61	1455.33	1455.34	1455.33	1454.38	1453.56	C-H bending for alkane. N-O stretch for nitro groups.
1371.43	1370.47	1356.17	1178.55 1093.67	1358.50	1368.54	1368.50	1366.61	1356.87	C-O stretch for esters, carboxylic acid and ethers
absent	1161.19	1162.22	729.12	1138.14	1138.04	absent	1162.15	1162.02	C-H deformation for alkenes, alkanes and aromatics
absent	718.51	absent	430.14	726.26	725.26 607.60	726.29	718.51	718.55	C-H deformation for alkyl groups.

Table 4.45: FTIR Bond Structure Comparison for *H. crepitans* Seed Oil, Methyl esters, Butyl esters and Petrodiesel (cm⁻¹) at 200 °C

Diesel	<i>H. crepitans</i> Oil	<i>H. crepitans</i> M.esters	<i>H. crepitans</i> B.esters	M.esters/Diesel Blends					Description
				10:90	20:80	30:70	50:50	90:10	
3511.53	3862.58 3746.85 3465.23 3343.71 3190.37	3853.90 3739.13 3477.77	3457.52	absent	3740.10 3433.41	3740.15	3856.80 3462.34	3853.95	O-H stretch for alcohols and carboxylic acids.
2932.86	2928.04 2693.68 2278.01 2185.42 2035.93 1848.83	2929.00 2419.78 2101.51	2934.79 2871.14	2932.86	2929.97 2106.34	2928.83 2267.67 2106.80	2929.97 2417.85 2267.49 2106.34 1836.29	2929.00	C-H stretch for alkanes, alkenes and aromatics
1725.38	1733.10 1561.43	1742.74 1660.77 1540.21	1726.35	1735.38	1741.78 1659.8	1742.76 1658.89	1743.71 1655.94	1743.24 1660.88 1540.61	C=O stretch for esters, carboxylic acids, aldehydes, and ketones.
1448.59	1446.66	1450.52	1450.52	1449.19	1456.30	1456.34	1454.38	1454.58	C=C stretch for alkenes and aromatics.
1367.58	1363.72	1356	1366.61	1362.68	1371.43	1372.83	1362.75	1356.83	C-H bending for alkane. N-O stretch for nitro groups.
1177.58 1008.80	1166.97	1160.22	1178.55 1095.60	1177.88	1122.61	1123.67	1144.79	1166.52	C-O stretch for esters, carboxylic acid and ethers
728.15	716.58	717.54		728.15	732.97 601.81	733.87	721.40 611.45	717.24	C-H deformation for alkenes, alkanes and aromatics
429.18	428.21	446.54		absent	453.29	454.22	441.71	446.54	C-H deformation for alkyl groups.

Table 4.46: FTIR Bond Structure Comparison for *H. crepitans* Seed Oil, Methyl esters, Butyl esters and Petrodiesel (cm⁻¹) at 250 °C

Diesel	<i>H. crepitans</i> Oil	<i>H. crepitans</i> M.esters	<i>H. crepitans</i> B.esters	M.esters/Diesel Blends					Description
				10:90	20:80	30:70	50:50	90:10	
absent	3474.88	3470.06	3401.58	absent	3856.80 3401.58	3866.80	3462.34	3470.06	O-H stretch for alcohols and carboxylic acids.
2931.90	2930.93 2870.17 2353.23	2930.93 2865.35 2349.38 2035.93	2931.90 2278.97	2932.94	2929.97	2929.87	2929.97 1838.22	2930.91	C-H stretch for alkanes, alkenes and aromatics
1744.67 1600.97	1734.06	1742.74	absent	1745.68	1744.67	1746.62	1744.67 1654.01	1743.64	C=O stretch for esters, carboxylic acids, aldehydes, and ketones.
1459.20	1528.64 1448.59	1523.82 1449.55	1608.69 1455.34	1459.29	1456.3	1456.36	1454.38	1448.05	C=C stretch for alkenes and aromatics.
1371.43	1365.65	1365.65	1373.36	absent	1370.47	1371.49	1364.68	1364.15	C-H bending for alkane. N-O stretch for nitro groups.
absent	1168.90	1159.26	1149.61	1167.61	1152.51	1155.52	1166.01	1154.20	C-O stretch for esters, carboxylic acid and ethers
735.87	717.54	892.11 712.72	732.01	735.81	881.50 724.29	absent 723.49	719.47	896.21 713.71	C-H deformation for alkenes, alkanes and aromatics
443.64	440.75	461.97	461.00	443.64	442.68	442.78	421.46	461.94	C-H deformation for alkyl groups.

Table 4.47: FTIR Bond Structure Comparison for *H. crepitans* Seed Oil, Methyl esters, Butyl esters and Petrodiesel (cm⁻¹) at 300 °C

Diesel	<i>H. crepitans</i> Oil	<i>H. crepitans</i> M.esters	<i>H. crepitans</i> B.esters	M.esters/Diesel Blends					Description
				10:90	20:80	30:70	50:50	90:10	
absent	3750.71 3471.98	3856.80 3740.10 3468.13	3445.94	3761.35	3761.32 3417.98	3855.63	3400.62	3853.45	O-H stretch for alcohols and carboxylic acids.
2931.90 2246.18	2928.04 2694.65 2280.90 2038.83	2929.97 2420.74 2271.26 2103.44 1835.33	2933.83 2185.42	2932.96 2247.35	2929.00 2746.73 2281.87	2929.99 2746.54 2342.61	2929.00 2746.73 2342.62 2110.19 1857.51	2929.48	C-H stretch for alkanes, alkenes and aromatics
1749.49 1604.83 1454.38	1847.87 1734.06 1445.70	1742.11 1639.53 1450.02	1730.21 1453.41	1743.71 1638.58 1450.52	1743.79 1656.54 1455.32	1743.28 1748.19 1454.51	1748.19 1608.89 1455.88	1742.46 1451.42	C=O stretch for esters, carboxylic acids, aldehydes, and ketones. C=C stretch for alkenes and aromatics.
1371.43	1358.90	1356.97	1362.75	1376.94	1368.54	1358.13	1357.93	1357.80	C-H bending for alkane. N-O stretch for nitro groups.
1135.15	1166.01	1157.33	1177.58	1136.95	1156.36	1145.29	1143.83	1167.51	C-O stretch for esters, carboxylic acid and ethers
731.05	717.54	719.47 601.81	727.19	731.85	720.44	718.37	719.47	716.23	C-H deformation for alkenes, alkanes and aromatics
442.68 398.31	430.14	453.29	424.35	443.60 399.34	453.29	449.03	449.43	absent	C-H deformation for alkyl groups.

The FTIR data show that the spectra of the seed oils, methyl esters, butyl esters and esters/diesel blends were very close to that of petroleum diesel. This could be why they have similar fuel properties. Little differences however observed include: the absorption bands at interval of 3200- 3600 cm^{-1} (O-H stretch vibration of alcohol, carboxylic acids and hydroperoxide) and peak around 1731 cm^{-1} (C=O stretch of esters, carboxylic acids, aldehydes or ketones). They were initially absent in petroleum diesel but appeared at about 200 °C (Table 4.30-4.39) due to thermal oxidation of the fuel. O-H bands in the oils, methyl- and butyl esters were due to some free fatty acids, alcohols and hydroperoxides present in the samples.

The peaks around 1456 cm^{-1} were due to C=C stretch while 1363 cm^{-1} were due to C-H bending of alkane. Both bonds were present in all the samples. C-O stretch for esters, carboxylic acid and ethers were observed around 1166 cm^{-1} . Bands between 675-730 cm^{-1} were due to C-H bending out-of-plane of carbon-carbon double bonds (*cis*-RCH=CHR). This band can equally be very useful in determining C=C absorption (Morrison and Boyd, 2011).

4.6.1. Effect of Temperature on the Bond Stability

Bond deformations commenced in some of *C. pepo* and *H. crepitans* samples at about 100 °C with OH (3593 cm^{-1}), C-H (2929 cm^{-1}) and C=O (1742 cm^{-1}), showing more deformations (Table 4.31). Deformation of C=C (1456 cm^{-1}) started around 150 °C (Table 4.32). The bond deformation was characterized by multiple bands showing within the regions. In *A. africana*, C-H and C=O deformations became pronounced as from 150 °C, (Table 4.32).

Thermal degradation of a fuel is normally accompanied by formation of oxidative products. Concentration of the characteristic bonds of these products can give indication of the stability of the fuel. Therefore, thermal-stress resistant ability of the oils, methyl esters, butyl esters and esters/diesel blends was further examined by following the relative changes in the peak intensities around 3441 cm^{-1} (O-H) and 1740 cm^{-1} (C=O) due to formation of oxidative products such as hydroperoxides, aldehydes, ketones and carboxylic acids, and peak intensity around 1457 cm^{-1} due to carbon-carbon double bonds (C=C). Increase in C=O and OH intensities would signify thermal oxidation of the fuel while polymerization (e.g. Diels-Alder reaction) as well as cleavage of C=C during thermal oxidation would be signified by decrease in C=C intensity. Intensity of a band in a spectrum is proportional to the concentration of the respective functional group according to Beer-Lambert's law (Yildiz *et al.*, 2001; Chiniwalla *et al.*, 2003; Hamed *et al.*, 2006).

The FTIR analysis was measured in transmittance, increase in percentage transmittance indicated decrease in absorbance and hence a decrease in concentration. To have a direct relationship between intensity and concentration, the %Transmittance were converted to absorbance using a logarithmic relationship: $A = 2 - \log_{10} \%T$.

Changes in peak intensities of the functional group are presented in Figs.4.100-4.108. C=O intensity remained fairly stable up to $300\text{ }^{\circ}\text{C}$, indicating that the fuel samples were thermally stable up to $300\text{ }^{\circ}\text{C}$ towards formation of carbonyl compounds except butyl esters of *A. africana*. C=O peak intensity of butyl esters of *A. africana* showed a pronounced decrease starting from $200\text{ }^{\circ}\text{C}$, indicating consumption of the bond.

The peak intensities of petroleum diesel indicated that it did not originally contain C=O bonds but as temperature approached 200 °C, thermal oxidation commenced, yielding carbonyl compounds such as carboxylic acid, ketone and aldehydes.

Bands around 3441 cm⁻¹ were majorly due to OH of hydroperoxide. *A. africana* samples were shown to contain the highest concentration of hydroperoxides among the samples analyzed (Figs.4.103- 4.105). This was due to high degree of unsaturation of the samples which was equally confirmed by the peak intensities of C=C (Figs. 4.19-4.21). The rise and fall observed in the intensity of the hydroperoxides was due to differences in the rate of formation and decomposition of the hydroperoxides at different temperatures. Lipid oxidation involves the continuous formation of hydroperoxides as primary oxidation products that may break down to a variety of volatile, nonvolatile, and polymeric secondary oxidation products (Li *et al.*, 2000; Dobarganes and Velasco, 2002; Shahidi and Zhong, 2005).

Changes in the peak intensities of C=C, C=O and OH indicate that the bonds were still stable up 300 °C for all the samples since they were not permanently consumed. The exception was butyl ester of *A. africana*. The bond structures of butyl esters of *A. africana* showed a remarkable instability at temperature above 200 °C and might not be recommended for long term use in engines operating above 200 °C. The observed instability of the bond structures of *A. africana* butyl esters may be attributed to the synergic effect of high degree of unsaturation and long chain length of the fuel molecules.

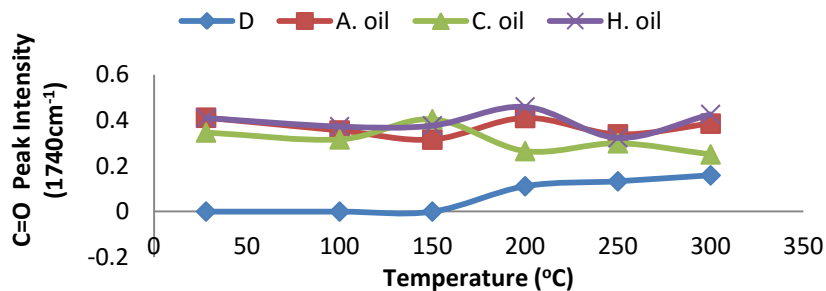


Fig. 4.100: Changes in C=O peak intensities of the oils

D = diesel, A = *Afzelia africana*, C = *Cucurbita pepo*, H = *Hura crepitans*

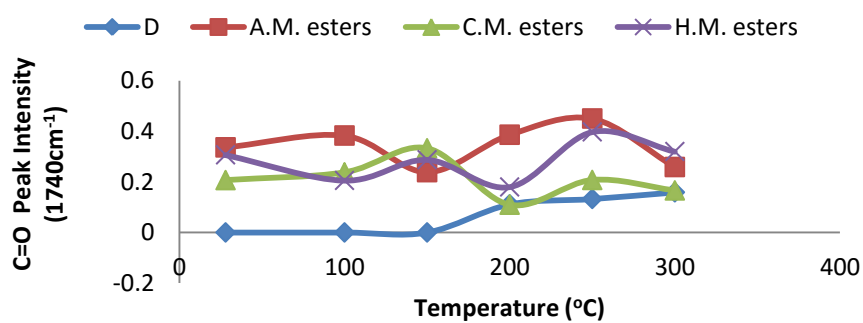


Fig. 4.101: Changes in C=O peak intensities of the methyl esters

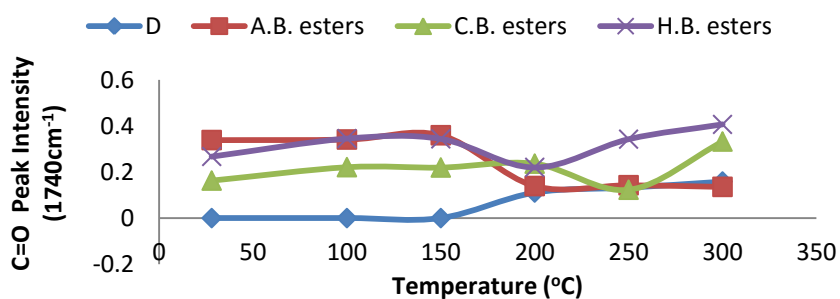


Fig. 4.102: Changes in C=O peak intensities of the butyl esters

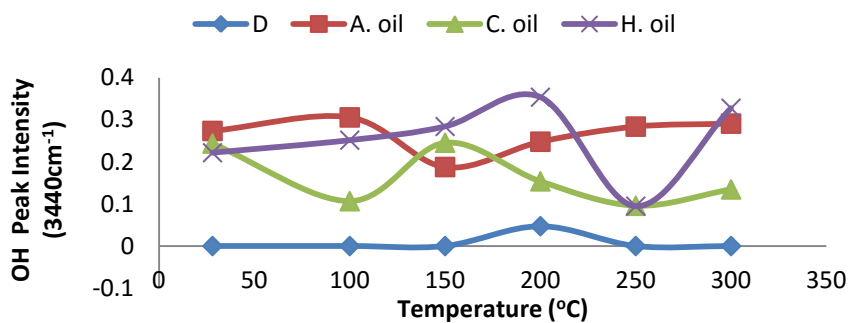


Fig. 4.103: Changes in HO (hydroperoxides) peak intensities of the oils

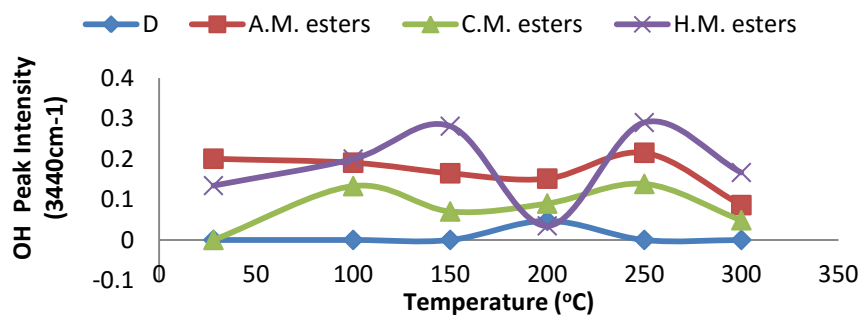


Fig. 4.104: Changes in HO (hydroperoxides) peak intensities of the methyl esters

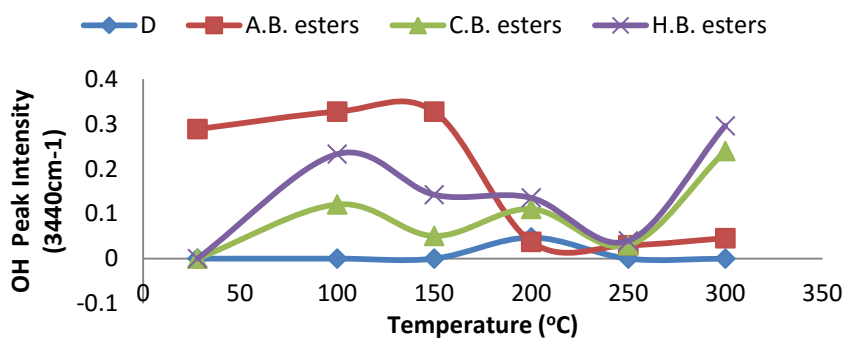


Fig. 4.105: Changes in HO (hydroperoxide) peak intensities of the butyl esters

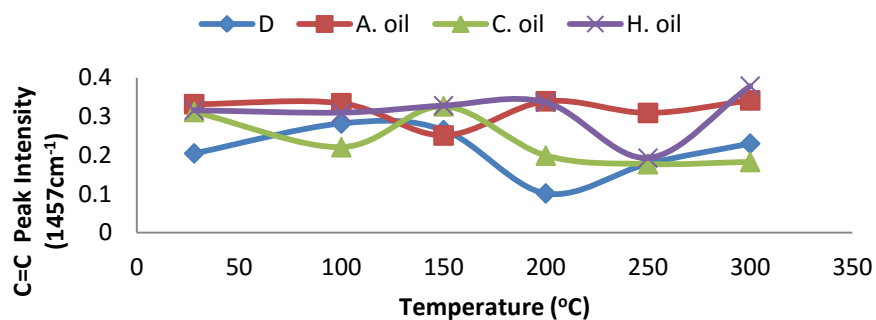


Fig. 4.106: Changes in C=C peak intensities of the oils

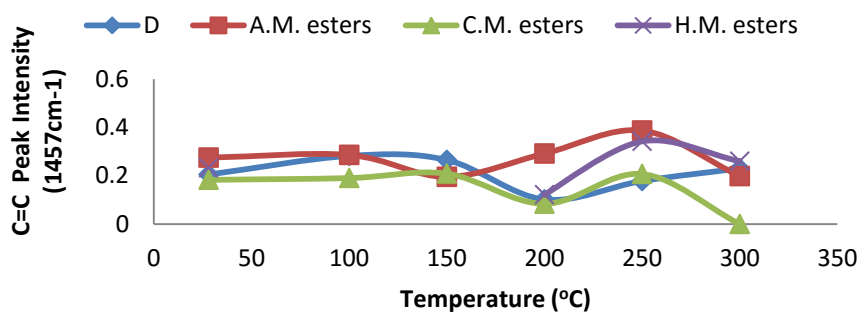


Fig. 4.107: Changes in C=C peak intensities of the methyl esters

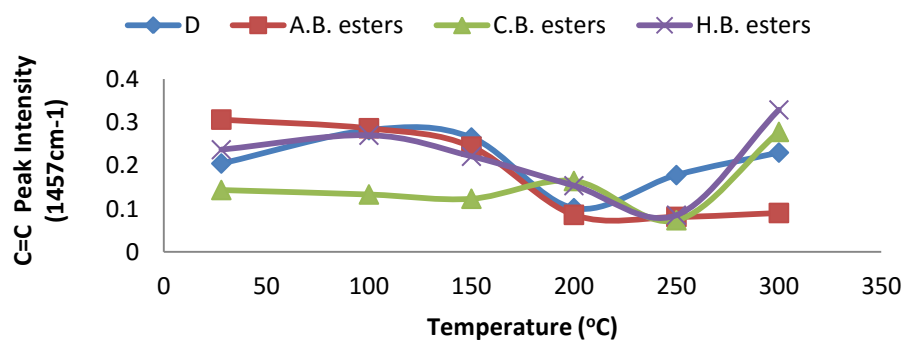


Fig. 4.108: Changes in C=C peak intensities of the butyl esters

4.9. Metal Composition of the Seed Oils their Derivative

The results of heavy metal composition of the oils, methyl esters and butyl esters of the feedstocks are shown in Table 4.48. The heavy metals were in trace amounts in all the samples and were below that of petroleum diesel. This indicated that none of the fuel samples would constitute a corrosion problem in the injector and piston chambers of diesel engines.

Table 4.48: Metal Composition (mg/g) of the Fuel Samples

Metals	Diesel	<i>Cucurbita</i> Oil	<i>Afzelia</i> Oil	<i>Hura</i> Oil	CME	CBE	AME	ABE	HME	HBE
As	2.02	1.20	0.82	1.90	0.71	0.81	0.60	0.64	0.74	0.84
Sn	0.89	0.62	0.41	0.58	0.33	0.43	0.17	0.11	0.36	0.35
Cu	0.40	1.90	1.01	0.50	1.12	0.70	0.49	0.52	0.92	0.31
Zn	1.73	0.89	1.20	0.43	0.80	1.32	0.72	0.79	0.11	0.54
Pb	0.55	0.42	0.10	0.76	0.32	0.32	0.09	0.10	0.76	0.76
Ag	1.94	1.23	0.78	1.24	2.00	1.09	0.95	0.75	0.88	0.98
Bi	2.16	0.43	1.03	0.99	0.33	0.32	0.76	0.76	0.54	0.64
Hg	0.89	0.67	1.21	0.75	0.23	0.67	0.58	0.54	0.67	0.47
Cd	1.23	0.49	1.15	0.68	0.33	0.33	0.90	0.91	0.43	0.23

CME, AME and HME are *Cucurbita pepo*, *Afzelia africana* and *Hura crepitans* methyl esters respectively, while CBE, ABE and HBE are the butyl esters.

CHAPTER FIVE

CONCLUSION AND RECOMMENDATION

5.1. Conclusion

C. pepo, *H. crepitans* and *A. africana* plants are among the oil crops in Nigeria that have remained underutilized despite their abundance. The suitability of the seed oils for biodiesel production was evaluated in this work through a wide range of investigations, and the results can be summarized as follows:

The percentage oil yields of the seeds: 42.43 % (*C. pepo*), 21.80 % (*A. africana*) and 39.87 % (*H. crepitans*) were quite promising for commercial biodiesel production.

The acid values, 26.32, 23.52 and 52.08 mg KOH/g for *C. pepo*, *A. africana* and *H. crepitans* respectively were very high, indicating that the vegetable oils could not be processed into biodiesel using conventional base-catalyzed transesterification method hence, acid catalysed process was necessitated.

Form the fatty acid analysis, linolenic acid content of *A. africana* seed oil (36.32 %) was high compared to the European Standard for biodiesel (EN 14103), suggesting poor oxidative stability of the oil; the oil would need antioxidant in case of long storage. *H. crepitans* contained high percentage of oleic acid (45.67 %) which has been identified as an ideal fatty acid for biodiesel feedstock.

Biowaste derived solid acid catalysts prepared from seed cake/shell of the plant seeds were effective for biodiesel synthesis and had advantage of easy

separation and being reused. The catalysts however required above 3 h for a similar % conversion as H₂SO₄.

FTIR analysis of the catalysts showed that 60 min. of partial carbonization (at 500 °C) was most favourable for formation of polyaromatic-rich structure needed for attachment of –SO₃H group. The surface morphology also indicated that carbonization time between 30 and 60min. was most favourable for attaining large pore sizes on the catalysts. TGA results showed that the solid acid catalysts were thermally stable up to 230 °C after which sulfonic acid groups started dissociating from the carbon structures.

Temperatures between 50 to 60 °C, 3 % catalyst (concentrated H₂SO₄) and stirring rate of 200 rpm were shown to be optimal for the methyl esters synthesis from the oils while that of butyl esters, higher temperature (between 70 °C and 80 °C) and stirring rate between (300 rpm to 400 rpm) were indicated to be optimum.

Results of fuel properties of biodiesels from the three oil crops indicated that they were suitable for biodiesel production. *H. crepitans* made the best fuel among the three oil crops in terms of cetane number, cold-flow properties and flash point. *C. pepo* and *A. africana* samples however might not be suitable for countries with a very cold weather (below 5 °C); most of the biodiesel derived from the two oils congealed below 5 °C. Dilution with petroleum diesel however did not improve their pour point.

Butyl esters of the oils were better biodiesels than the methyl esters in terms of kinematic viscosity and heating value. According to ASTM specification for biodiesel, the maximum recommendable methyl esters/diesel blends from the feedstocks are: 40:60 (*H. crepitans*), 30:70 (*C. pepo*) and 30:70 (*A.*

africana) in order to meet up with the kinematic viscosity upper limit. For butyl esters/diesel blends, as much as 80:20 blend met ASTM specification for kinematic viscosity.

Strong correlations were established between density and both average chain length and degree of unsaturation. Strong inverse correlations were equally found between density and: viscosity (at 40 °C), calorific value, %SFAs, %O and %H; density decreased with increase in these parameters. Pour point correlated with average chain length, showing that the longer the carbon chains in the biodiesel the higher the pour point.

FTIR analysis of the bond structures/stability of the samples showed that bond structures of the methyl esters, butyl esters and their diesel blends were similar to that of petrodiesel. This suggested why they have similar fuel properties. The FTIR analysis also indicated that the bonds were thermally stable up to 300 °C; though deformation of some bonds: OH (3593 cm^{-1}), C-H (2929 cm^{-1}), C=O (1742 cm^{-1}) and C=C (1456 cm^{-1}) in some samples started between 100 and 150 °C, the concentrations of the bonds remains fairly stable up to 300 °C indicating their stability.

The metal composition of the fuel samples was found to be in trace amounts in all the samples. This indicated that none of the fuel samples would constitute a corrosion problem in the injector and piston chambers of diesel engines.

5.2. Contribution to Knowledge

1. This work has provided detailed information on the fuel properties of methyl esters from *C. pepo*, *A. africana* and *H. crepitans* seed oils which were lacking before. Such information include cetane number, kinematic viscosity at various temperatures, pour point, flash point and their correlations with the structural features of the fuel molecules.
2. This work has also reported for the first time, the fuel properties of butyl esters from the three seed oils.
3. This work has provided foundational information on the preparation and characterization of efficient biowaste-derived solid acid catalysts from *A. africana* and *H. crepitans* seed shell/cake and their application in biodiesel synthesis.
4. From this work, it was showed that a locally constructed carbonizer could be an alternative for partial carbonization of biomass for catalyst preparation instead of nitrogen-flow apparatus which is rarely available in Nigeria.
5. It has been indicated from this study that *C. pepo* and *A. africana* seed oils might not be a suitable feedstock for biodiesel in countries with cold weather (below 11 °C) without cold-flow property improver.

5.3. Recommendation

- i. Research should be carried out on other local sustainable feedstock for their utilization for biodiesel production. This will provide reliable information on their performance and hence, facilitate optimal biodiesel blending.
- ii. Further research should be carried out on finding a better method of separating residual butanol after butyl esters synthesis from vegetable oils.
- iii. More work is also needed to improve on the catalytic activity of biowaste-derived solid acid catalysts to compete favourably with their homogeneous counterparts in terms of reaction rate and %conversion.

Reference

Aam, K.K., (2002): Research into Biodiesel Kinetics and Catalyst Development; Department of Chemical Engineering, University of Queensland. (<http://www.cheque.uq.edu.au/ugrad /chee4001 /CHEE400102/Adamkhanthesis.pdf>). Retrieved, 14-10-2014.

Abdulkadir, M. N., Amoo, I. A., and Adesina, A. O., (2013): Chemical Composition of Hura Crepitans Seeds and Antimicrobial Activities of its Oil; International Journal of Science and Research, 2(3): 2319-7064.

Abigor, R., D., Uadia, P.O., Foglia, T.A., Hass, M.J., Jones, K.C., Okpefa, E., Obibuzor, J.U., and Bafor, M.E., (2000): Lipase-catalysed Production of Biodiesel Fuel from Some Nigeria Lauric Oils, Biochemical Society Transactions, 28(6): 976-981.

Abiney, L.C., Soraia, C.G. N., and da Silva, M, J., (2008): Esterification of Oleic Acid for Biodiesel Production Catalyzed by SnCl₂: A Kinetic Investigation; Energies, 1: 79-92.

ACREVO, (2000): Advanced Combustion Research for Energy from Vegetable Oils (<http://www.nf-2000.org/>). Retrieved, 17-10-2014.

Addison, K., (2013): The TDI-SVO Controversy (http://journeytoforever.org/biodiesel_TDI.html) Retrieved, 15-10-2014.

Agarwal, A.K., (2007): Biofuels (Alcohols and Biodiesel) Applications as Fuels in Internal Combustion Engines. Progress in Energy Combustion Science, 32: 233–71.

Agarwal, A.K., and Das, L.M., (2001): Biodiesel Development and Characterization for Use as a Fuel in Compression Ignition Engines, Trans ASME Journal of Engineering for Gas Turbine and Power, 123: 440-447.

Ajiwe, V.I.E, Nsionu, C.A., and Eukora, E.A.O., (2006a): Possible Biofuels from Broad Leave Pumpkin (*Curcubita pepo*) Seed Oil; Proceedings of the NASEF' 06 International Conference, Awka, Solar Energy Society of Nigeria, pp. 178-182.

Ajiwe, V.I.E., Ajibola, V.O., and Martins, C.M.A.O., (2001): *Prosopis Africana* (Mesquite) Oil, its Methyl ester and Ester/diesel Blends as Possible Diesel Fuels; *Journal of Science, Engineering and Technology* 8(4): 3674-3689.

Ajiwe, V.I.E., and Obika, A.E., (2000): African Pear Seed: Potential for Alternative Source of Diesel Oil; *Energy and Fuels*, 14(1): 112-116.

Ajiwe, V.I.E., Mbonu, S.O., and Enukorah, E.A.O., (2006b): Biofuel from *Irvingia gabonensis* Seed Oil and its Methyl esters, Proceedings of the NASEF'06 International Conference, Awka, Solar Energy Society of Nigeria, pp. 247-252.

Akintayo ET (2004): Characteristics and Composition of *Parkia bioglobbosa* and *Jatropha curcas* Oils and Cakes. *Bioresource Technology*; 92: 307-310.

Alamu, O.J., Waheed, M.A., and Jekayinfa, S.O., (2007): Alkali-catalysed Laboratory Production and Testing of Biodiesel from Nigerian Palm Kernel Oil; *Agricultural Engineering International: the CIGR eJournal Manuscript Number EE 07 009*. Vol. IX.

Albuquerque, M.C.G., Machado, Y.L., Torres, A.E.B., Azevedo, C.S., Cavalcante Jr, C.L., and Firmiano, L.R., (2009): Properties of Biodiesel Oils Formulated Using Different Biomass Sources and their Blends, *Renewable Energy*; 34: 857–9.

Alípio, C. C., Luiz, K.C., Carlos, E.F., Longo, E., José, R. Z., and Geraldo, N., (2009): Production of Biodiesel by Esterification of Palmitic Acid over Mesoporous Aluminosilicate Al-MCM-41, *Fuel*, 88: 461–468.

Altıparmak, D., Keskin, A., and Koca, A., (2007): Alternative Fuel Properties of Tall Oil Fatty Acid Methyl Ester-diesel Fuel Blends, *Bioresource Technology*, 98 (2): 241-246.

Anderson, J.A., Beaton, A., Galadima, A., and Wells, R.P.K., (2009): Role of Barium Dispersion in BaO/Al₂O₃ Catalysts for Transesterification; *Catalysis Letters*, 131: 213-218.

Arora, R., Kapoor, V., and Toor, A. P., (2014): Esterification of Free Fatty Acids in Waste Oil Using a Carbon-based Solid Acid Catalyst, 2nd International Conference on

Emerging Trends in Engineering and Technology (ICETET'2014), May 30-31, 2014 London (UK). pp. 1-10.

Aruah, C. B., Uguru, M. I., and Oyiga, B. C., (2011): Nutritional Valuation of Some Nigerian Pumpkins (*Cucurbita spp.*), Fruit, Vegetable and Cereal Science and Biotechnology, Global Science Books, 5(Special Issue 2): 64-71.

Ashley, D. K., (2011): Two-step Biodiesel Production Using Supercritical Methanol and Ethanol; Ph.D Thesis, Chemical and Biochemical Engineering, University of Iowa, pp. 1-9.

ASTM, (2009a): D7467: Specification for Diesel Fuel Oil, Biodiesel Blend (B6 to B20). ASTM International, West Conshohocken, PA.

ASTM, (2009b): Standard Specification for Biodiesel Fuel (B100) Blend Stock for Distillate Fuels; West Conshohocken, PA; American Society for Testing and Materials. In: Annual Book of ASTM Standards, Philadelphia, pp. 1131-1136.

Atkins, P.W., (1992): The Elements of Physical Chemistry-chemical Kinetics, Oxford University Press; pp. 237-266.

Ataya, F., Dube, M.A., and Ternan, M., (2007): Acid-Catalysed Transesterification of Canola Oil to Biodiesel under Single- and Two-Phase Reaction Conditions, Energy & Fuels, 21, 2450-2459.

Azil, I., (2007): Biofuel Demand: Opportunities for Rural Development in Africa (Nigeria Case-Study); A Paper Presented at the 2nd European Forum on Sustainable Development, Berlin, Germany. Pp. 1-6.

Batts, B. D., and Fathoni, A. Z., (1991): A Literature Review on Fuel Stability Studies with Particular Emphasis on Diesel Oil; Energy Fuels, 5(1): 2-21.

Bennett, J.A., Wilson, K., and Lee, A.F., (2016): Catalytic Application of Waste Derived Materials, Journal of Material Chemistry A, 4,3617-3637.

Berrios, M., Siles, J., Martí'n, M.A., and Martí'n, A., (2007): A Kinetic Study of the Esterification of Free Fatty Acids (FFA) in Sunflower Oil, Fuel, 86: 2383–2388.

Blangino, E., Riveros, A.F., and Romano, S.D., (2008): Numerical Expressions for Viscosity, Surface Tension and Density of Biodiesel: Analysis and Experimental Validation. *Physics and Chemistry of Liquids*, 46: 527–547.

Boerrigter, H. (2002): ‘Green’ Diesel Production with Fischer-Tropsch Synthesis, a Paper Presented at the Biomass Meeting Bio-energy Platform.

Canoira, L., Alca´ntara, R., Jesus Garcí’a-Martí’nez, M., and Carrasco, J., (2006): Biodiesel from Jojoba Oil-wax: Transesterification with Methanol and Properties as a Fuel. *Biomass Bioenergy*, 6(30): 76–81.

Caterpillar, Inc., (2001): Caterpillar Position on the Use of Biodiesel Fuel; Information Released Memo PMP01-01, pp. 1-2.

Cetinkaya, M., Ulusay, Y., and Karaosmanoglu, F., (2005): Engine and Winter Road Test Performance of Used Cooking Oil Originated Biodiesel, *Energy Covers Manage*, 46: 1279-1291.

Chen, G., and Fang, B.S., (2011): Preparation of Solid Acid Catalyst from Glucose–starch Mixture for Biodiesel Production. *Bioresource Technology*, 102: 2635-2640.

Chevron, (2007): Diesel Fuels Technical Review, Chevron Products Company 6001 Bollinger Canyon Road San Ramon, CA 94583. Pp. 1-20.

Chiniwalla, P., Bai, Y., Elce, E., Shick, R., McDougall, C.W., Allen, S.A.B., and Kohl, P.A., (2003): Crosslinking and Decomposition Reactions of Epoxide Functionalized Polynorborene. Part I., FTIR and Thermogravimetric Analysis; *Journal of Applied Polymer Science*, 89: 568–577.

Christie W.W (2003): *Lipid Analysis*, 3rd Ed, The Oily Press, U.K; Pp. 1-30.

Christie, W.W., (1993): Preparation of Ester Derivatives of Fatty Acids for Chromatographic Analysis; *Advances in Lipid Methodology*, 2: 69-111.

Darnoko, D., and Cheryan, M., (2000): Kinetics of Palm Oil Transesterification in a Batch Reactor, *Journal of the American Oil Chemists’ Society*, 77(12): 1263-1267.

Davis, U.C., (2010): ChemWiki, University of California, Powered by Mindtouch Core 2010. (http://chemwiki.ucdavis.edu/Physical_Chemistry/Kinetics/Rate_Laws/The_Rate_Law). Retrieved, 9th June, 2013.

Dawodu, F.A., Akpomie, G.K., and Ogbu, I.C., (2012): Isotherm Modeling on the Equilibrium Sorption of Cadmium (II) from Solution by Agbani Clay; *International Journal of Multidisciplinary Sciences and Engineering*, 3 (9): 9-14.

Delahaut, K.A., and Newenhouse, A.C., (2006): *Growing Pumpkin and other Vine Crops in Wisconsin: A guide for Fresh-market Growers (A3688)*. University of Wisconsin-Extension Publication, p. 22.

Dhanasekaran, K., and Dharmendirakumar, M. D., (2012): A Kinetic Study of Biodiesel in Waste Cooking Oil; *African Journal of Biotechnology*, 11(41): 9797-9804.

Diesel Power Products (2011): *The Different Types of Diesel Fuel: D1, D2, and D4*, (<http://blog.dieselpowerproducts.com/the-different-types-of-diesel-fuel>). Retrieved, 12th May, 2014.

Dobarganes, M. C., and Velasco, J., (2002): Analysis of Lipid Hydroperoxides, *European Journal of Lipid Science and Technology*, 104: 420–428.

Duke, J.A., and Ayensu, E.S., (1985): *Medicinal Plants of China*. Reference Publications, Inc., Pp. 218-219.

Dunn, J.G., (2002): *Characterization of Materials: Thermogravimetric Analysis*. Second Ed., John Wiley & Sons, Inc. p. 1-145.

ECN, (2009): *Biofuels Training Manual*, Energy Commission of Nigeria, Abuja. pp. 1-49.

Ejikeme, P. M., Anyaogu, I. D., Ejikeme, C. L., Nwafor, N. P., Egbuonu, C. A., Ukogu C. K., and Ibemesi, J. A., (2010): Catalysis in Biodiesel Production by Transesterification Processes-An Insight; *E-Journal of Chemistry*, 7(4), 1120-1132.

Ejikeme, P. M., Obasi, L. N., and Egbuonu, A. C. C., (2010): Physico-chemical and Toxicological Studies on *Afzelia africana* Seed and Oil; African Journal of Biotechnology, 9 (13): 1959-1963.

Elinge, C. M., Muhammad, A., Atiku, F. A., Itodo, A. U., Peni, I. J., Sanni, O. M., and Mbongo, A. N., (2012): Proximate, Mineral and Anti-nutrient Composition of Pumpkin (*Cucurbita pepo L.*) Seeds Extract, International Journal of Plant Research, 2(5): 146-150.

Elliott, M. A., George, J. N., and Fred G. R., (1955): The Composition of Exhaust Gases from Diesel, Gasoline and Propane Powered Motor Coaches; APCA Meeting, Paper No. 55-19, Detroit, Mich.

Emil, A., Zahira, Y., Siti, K.K, Manal, I., and Jumat, S., (2009): Characteristic and Composition of *Jatropha Curcas* Oil Seed from Malaysia and its Potential as Biodiesel Feedstock, European Journal of Scientific Research; 29(3): 396-403.

Emrani, J and Shahbazi A., (2012): A Single Bio-based Catalyst for Bio-fuel and Biodiesel; Journal of Biotechnology and Biomaterial, 2(1): 1-7.

EPA, (2002): Clean Alternative Fuel- biodiesel, Fact Sheet, Environmental Protection Agency Document No. EPA 420-F-00-032.

Foster, D., Scofield, E. H., and Dallenbach, K. M., (1950): An Olfactorium, American Journal of Physiology, 63: 431.

Freedman, B., and Pryde, E. H. (1982): Fatty Esters from Vegetable Oils for Use as a Diesel Fuel. In Vegetable Oils Fuels: Proc. of the Intl. Conf. on Plant and Vegetable Oils as Fuels, St.Joseph, Mich.: ASAE, pp. 117–122.

Freedman, B., Butterfield, R., O., and Pryde, E. H., (1986): Transesterification Kinetics of Soybean Oil. Journal of American Oil Chemists' Society, 63: 1375–1380.

Freedman, B., Pryde, E.H., and Mounts, T.L., (1984): Variables Affecting the Yield of Fatty Esters from Transesterified Vegetable Oils, Journal of the American Oil Chemists' Society, T61T (10): 1638-1643.

FSSAI (2012): Manual of Methods of Analysis of Food (Oils and Fats); Food Safety and Standard Authority of India, Ministry of Health and Family Welfare, Government of India, New Delhi ([http://www.fssai.gov.in/Portals/0/Pdf/15Manuals/OILS%20AND%](http://www.fssai.gov.in/Portals/0/Pdf/15Manuals/OILS%20AND%20)). Retrieved, 23-01-15.

GAIN Report (2005): Brazil Biofuels Annual- Ethanol and Biodiesel; Global Agricultural Information Information Network; GAIN Report Number: BR 15006. (<http://www.gain.fas.usda.gov/Biofuels%20Annual>). Retrieved 11-03-16.

Galadima, A., and Garba, Z.N., (2009): Catalytic Synthesis of Ethyl Ester from Some Common Oils; Science World Journal, 4(4): 1-4.

Galadima, A., Garba, Z.N., and Ibrahim, B.M., (2008): Homogeneous and Heterogeneous Transesterification of Groundnut Oil for Synthesizing Methyl Biodiesel; International Journal of Pure and Applied Sciences, 2(3): 138-144.

Gerard, J., and Louppe, D., (2011): *Afzelia Africana* Sm.ex pers, Record from PROTA4U; (<http://www.prota4u.org/protav8.asp?>). Retrieved, January 20th, 2013.

Giakoumis, E.G., (2013): A Statistical Investigation of Biodiesel Physical and Chemical Properties, and Their Correlation with the Degree of Unsaturation; Renewable Energy, 50: 858-878.

Giakoumis, E.G., Rakopoulos, C.D., Dimaratos, A.M., and Rakopoulos, D.C., (2012): Exhaust Emissions of Diesel Engines Operating under Transient Conditions with Biodiesel Fuel Blends, Progress in Energy Combustion Science, 38(5): 691- 715.

Good Energy (2013): Welcome to BioDiesel Filling Station, Good Energy (<http://www.biodieselfillingstations.co.uk/>) Retrieved, 15-10-2014.

Gouveia, L., and Oliveira, A.C. (2009): Microalgae as a Raw Material for Biofuels 507 Production. J. Ind. Microbiol. Biotechnology, 36, 269–274

Graboski, M.S., and McCormick, R.L., (1998): Combustion of Fat and Vegetable Oil Derived Fuels in Diesel Engines; Progress in Energy and Combustion Science, 24: 125–64.

Graeve, M., and Janssen, D., (2009): Improved Separation and Quantification of Neutral and Polar Lipid Classes by HPLC-ELSD Using a Monolithic Silica Phase: Application to Exceptional Marine Lipids, *Journal of Chromatography B*, 877: 1815-1819.

Gunstone, F.D., (2004): Rapeseed and Canola Production, Processing, Properties and Uses. Oxford EN: Blackwell Publishing. pp. 1-6.

Gutnikov, G., (1995): Fatty Acid Profiles of Lipid Samples, *Journal of Chromatography B*, 671: 71-89.

Hamed, S.F. and Allam, M A., (2006): Application of FTIR Spectroscopy in the Determination of Antioxidant Efficiency in Sunflower Oil; *Journal of Applied Sciences Research*, 2(1): 27-33.

Hannu, J., (2007): Fuel Property Testing: Ignition Quality, Ecopoint Inc. Revision (http://www.dieselnet.com/login.php?url=/tech/fuel_diesel_ignition.php); Retrieved on March 20th, 2013.

Hara, M., Yoshida, T., and Takagaki, A., (2004): A Carbon Material as a Strong Protonic Acid. *Angewandte Chemie International Edition*, 43: 2955-2958.

Huang, Y.B. and Fu, Y., (2013): Hydrolysis of Cellulose to Glucose by Solid Acid Catalysts; *Green Chemistry*, 15: 1095–1111.

Hutchings, A., Scott, A. H., Lewis, G. and Cunningham, A., (1996): Zulu Medicinal: An Inventory, University of Natal Press, Pietermaritzburg. pp. 1-5.

IEA, (2011): "IEA Says Biofuels can Displace 27% of Transportation Fuels by 2050 Washington". (<https://www.iea.org/topics/renewables/subtopics/bioenergy/>). Retrieved 2014-01-12.

Igwenyi, I. O., Offor, C. E., Aja, P. M., Aloh, G. S., Orji, O. U. and Ugwu, O. O., (2011): Potentials of *Afzelia africana* Vegetable Oil in Biodiesel Production; *Progress in Renewable Energies*, 1: 8-14.

Immer, J. G., Kelly, M. J., and Lamb, H. H., (2009): Catalytic Reaction Pathways in Liquid-phase Deoxygenation of C18 Free Fatty Acids. *Applied Catalysis A: General*, 375, 134-139

Itodo, A.U., Itodo, H.U., and Gafar, M.K., (2010): Estimation of Specific Surface Area using Langmuir Isotherm Method, *Journal of Applied Science and Environmental Management*, 14(4): 141-145.

Jahirul, M.I., Brown, R.J., Senadeera, W., O'Hara, I.M., Ristovski, Z.D., (2013): The Use of Artificial Neural Networks for Identifying Sustainable Biodiesel Feedstocks. *Energies*, 6: 3764-3806.

Jaichandar, S., and Annamalia, K., (2011): The Status of Biodiesel as an Alternative Fuel for Diesel Engine- An Overview, *Journal of Sustainable Energy and Environment*, (2): 71-75.

Johnson, O.C., and Kummerow, F.A., (1995): Chemical Changes which Take Place in Edible Oil During Thermal Oxidation; *Journal of American Oil Chemists' Society*; 34: 407-409.

Judy, A.L., Kyoung, S.R., Claudia, K., Axel, F., Nicole, D.B., York, N., Maria-Magdalena, T., Christoph, F., Oliver, B., Jürgen, K and Karl-Heinz, M., (2011): Hydrothermal Carbonization of Biomass Residuals: A Comparative Review of the Chemistry, Processes and Applications of Wet and Dry Pyrolysis; *Biofuels*, 2(1): 89–124.

Kaewta, S., (2008): Biodiesel Production from High Free Fatty Acid Content Feedstocks, A Dissertation Presented to the Graduate School of Clemson University. Paper 207, pp. 1-30.

Kaluzny, M.A., Duncan, L.A., Merritt, M.V., and Epps, D.E., (1985): Rapid Separation of Lipid Classes in High Yield and Purity Using Bonded Phase Columns. *Journal of Lipid Research*, 26 (1): 135–40.

Kaplan, C., Arslan, R., and Surmen, A., (2006): Performance Characteristic of Sunflower Methyl Ester as Biodiesel, *Energy Sources Part A*, 28: 751-755.

Karmakar, A., Karmakar, S., and Mukherjee, S., (2010): Properties of Various Plants and Animals Feedstocks for Biodiesel Production. *Bioresource Technology*, 101: 7201–7210

Addison, K., (2001): Handmade Projects (http://journeytoforever.org/keith_cv.htm). Retrieved, 29-01-2015.

Khan, S.A., RashmiHussain, M.Z., Prasad, S., and Banerjee, U.C., (2009): Prospects of Biodiesel Production from Microalgae in India; *Renewable Sustainable Energy Review*, 139: 2361–2372

Kiss, A.A., Dimian, A.C. and Rothenberg, G., (2008): Biodiesel by Catalytic Reactive Distillation Powered by Metal Oxides, *Energy and Fuels*, 22: 298.

Knothe, G., (2005): Dependence of Biodiesel Fuel Properties on the Structure of Fatty Acid Alkyl Esters. *Fuel Process Technology*, 86: 1059–1070

Knothe, G., (2007): Some Aspects of Biodiesel Oxidative Stability; *Fuel Process Technology*; 88: 669–77.

Knothe, G., (2008): Designer Biodiesel Optimizing Fatty Ester Composition to Improve Fuel Properties. *Energy and Fuels*, 22: 1358–1364.

Knothe, G., and Steidley, K.R., (2005): Kinematic Viscosity of Biodiesel Fuel Components and Related Compounds; Influence of Compound Structure and Comparison to Petrodiesel Fuel Components; *Fuel*, 84: 1059–65.

Knothe, G., (2001): Historical Perspectives on Vegetable Oil-Based Diesel Fuels, *Inform*, 12(1): 1103-1107.

Knothe, G., Dunn, R.O., and Bagby, M.O., (1997): Biodiesel: the Use of Vegetable Oils and Their Derivatives as Alternatives Diesel Fuels. In: *ACS Symposium Series No.666: Fuels and Chemicals from Biomass*, Washington DC, USA, pp. 172-208.

Kopia, G., (2004): Effect of Reducing Coconut Viscosity on Engine Performance, PNG University of Technology, Lae, Papua New Guinea., pp. 1 – 6.

Kreft, S. and Kreft, M., (2007): Physicochemical and Physiological Basis of Dichromatic Colour, *Naturwissenschaften*, 94: 935-939.

Kumar, V., and Kumar, J., (2008): Kinetics of *Jatropha Curcas* Transesterification in Batch Reactor, *Proceedings of the World Congress on Engineering and Computer Science*, WCECS 2008, October 22 - 24, San Francisco, USA, pp.1-4.

Labeckas, G., and Slavinskas, S., (2006): The Effect of Rapeseed Oil Methyl Ester on Direct Injection Diesel Engine Performance and Exhaust Emissions; *Energy Conversion and Management*, 47: 1954–1967.

Lapuerta, M., Armas, O., and Rodríguez-Fernández, J., (2008): Effect of Biodiesel Fuels on Diesel Engine Emissions, *Progress in Energy and Combustion Science*, 34 (2): 198-223.

Lee, A. F., Bennet, J.A., Manayil, J.C., and Wilson K., (2014): Heterogeneous Catalysis for Sustainable Biodiesel Production via Esterification and Transesterification: Review Article; *Chemical Society Reviews*, 43: 7887-7916.

Lee, Duckhee (2013): Preparation of a Sulfonated Carbonaceous Material from Lignosulfonate and Its Usefulness as an Esterification Catalyst; *Molecules* 2013, 18, 8168-8180.

Lee, I., Johnso, L.A., and Hammond, E.G., (1995): Use of Branched-chain Esters to Reduce the Crystallization Temperature of Biodiesel. *Journal of the American Oil Chemists' Society*, 72: 1155–1160.

Li, H., van de Voort, F.R., Ismail, A.A., and Cox, R., (2000): Determination of Peroxide Value by Fourier Transform Near-Infrared Spectroscopy; *Journal of American Oil Chemist's Society*, 77: 137-142.

Lidstrom, P., Tierney, J.P., Wathey, B., and Westman, J., (2001): Microwave Assisted Organic Synthesis – A Review; *Tetrahedron* 57: 9225–9283.

Lin, Y.C., Lee, W.J., Wu, T.S., and Wang, C.T., (2006): Comparison of PAH and Regulated Harmful Matter Emissions from Biodiesel Blends and Paraffinic Fuel Blends on Engine Accumulated Mileage Test, *Fuel*, 85: 2516-2523.

Linnell, R. H, and Scott, W. E., (1962): Diesel Exhaust Composition and Odour Studies; *Journal of the Air Pollution Control Association*, 12(11): 510-515.

Liping, X. (2010): Evaluation of Extraction Methods for Recovery of Fatty Acids from Marine Products, Master Thesis of EMQAL Project, University of Bergen, pp. 8-30.

Liu, T., Li, Z., Wei, L., Shi, C. and Wang, Y., (2013): Preparation and Characterization of Biomass Carbon-based Solid Acid Catalyst for the Esterification of Oleic Acid with Methanol, *Bioresource Technology*, 133: 618–621.

Lotero, E., Liu, Y., Lopez, D. E., Suwannakarn, K., Bruce, D. A., and Goodwin, J. G., (2005): Synthesis of Biodiesel via Acid Catalysis. *Industrial and Engineering Chemistry Research*, 44(14): 5353-5363.

Ma, F.R. and Hanna, M.A., (1999): Biodiesel Production: A Review; *Bioresource Technology*, 70: 1.

Makkar, H., Maes, J., De Greyt, W., and Becker, K., (2009): Removal and Degradation of Phorbol Esters during Pre-treatment and Transesterification of *Jatropha Curcas* Oil; *Journal of the American Oil Chemists'*, 86: 173–81.

Malavolta, M., Bocci, F., Boselli, E., and Frega, N.G., (2004): Normal Phase Liquid Chromatography-electrospray Ionization Tandem Mass Spectrometry Analysis of Phospholipid Molecular Species in Blood Mononuclear Cells: Application to Cystic Fibrosis. *Journal of Chromatography. B, Analytical Technologies in the Biomedical and Life Sciences*, 810 (2): 173–86.

Mariod, A., Klupsch, S., Hussein, I.H. and Ondruschka, B., (2006): Synthesis of Alkyl Esters from three Unconventional Sudanese Oils for their Use as Biodiesel; *Energy and Fuels*, 20: 2249–52.

Miguel Carriquiry (2007): U.S Biodiesel Production: Recent Development and Prospects, Center for Agricultural and Rural Development (CARD) IOWA, State University, Spring, 13 (2), 1 (<http://www.caed.iastate.edu/iowa.ag-review/spring-07/article4.aspx>). Retrieved 11-03-16.

Mittelbach, M., and Trathnig, B., (1990): Kinetics of Alkaline Catalyzed Methanolysis of Sunflower Oil, *Fat Science and Technology*, 92(4): 145-148.

Mohammad, I. J., Mohammad G. R., Ashfaque, A. C., and Nanjappa, A., (2012): Biofuels Production through Biomass Pyrolysis —A Technological Review, *Energies*, 5: 4952-5001.

Moreau, R.A., (2006): The Analysis of Lipids via HPLC with a Charged Aerosol Detector, *Lipids*, 41: 727-734.

Moser, B.R., (2009): Biodiesel Production, Properties, and Feedstocks. In *Vitro Cellular and Developmental Biology – Plant*; 45: 229–2266.

Morrison, R.T., and Boyd, R.N., (2011): *Organic Chemistry*; Dorling Kindersley (India) Pvt. Ltd, 7th Ed. P 812.

Muhammad, D. S., and Satriana, S., (2009): Esterification of Free Fatty Acid in Crude Palm Oil Off Grade; *JurnalRekayasa Kimia danLingkungan*, 7(2): 70-74.

Murari, M. R., (2007): Charcoal-adsorption, Water- Washing and Air-Dilution System to Reduce Diesel Emissions with Special Emphasis on Odour Reduction, *Energy Resource Technology*, 129: 338-347.

Murari, M.R., (2011): Performance and Emissions of a Diesel Engine Fueled by Diesel-biodiesel Blends with Special Attention to Exhaust Odour, *Canadian Journal on Mechanical Sciences and Engineering*, 2 (1): 1-10.

Nakagaki, M. and Nakayama, F., (1997): Class Separation of Bile Lipids by Thin-layer Chromatography; *Journal of Chromatography A*, 177 (2): 343-348.

Nakamura, T., Bratton, D.L., and Murphy, R.C., (1997): Analysis of Epoxyeicosatrienoic and Monohydroxyeicosatetraenoic Acids Esterified to Phospholipids in Human Red Blood Cells by Electrospray Tandem Mass Spectrometry. *Journal of Mass Spectrometry* 32 (8): 888–96.

Nakajima, K., Hara, M., Hayashi, S., (2007): Environmentally Benign Production of Chemicals and Energy using a Carbon-based Strong Solid Acid. *Journal of American Ceramics Society*; 90: 3725–3734.

NNPC, (2007): Official Gazette of the Nigerian Biofuels Policy and Incentives: Renewable Energy; Nigeria National Petroleum Corporation. (<http://www.nnpcred.com/images/policy.pdf>). Retrieved, 08 July 2015.

Noureddini, D. Zhu., (1997): Kinetics of Transesterification of Soybean Oil, *Journal of American Oil Chemists' Society*, 74 (11): 1457–1463.

Novaczek, I., (2000): Canada's Fossil Fuel Dependency; Elements. (<http://www.elements.nb.ca/theme/fuels/irene/novaczek.htm>). Retrieved 2013-01-12.

Okeola, O.F., Odebunmi, E.O., and Ameen, O.M., (2012): Comparison of Sorption Capacity and Surface Area of Activated Carbon Prepared From *Jatropha curcas* Fruit Pericarp and Seed Coat, *Bulleten of Chemical Society of Ethiopia*, 26(2): 171-180.

Oloyede, F.M., (2012): Growth, Yield and Antioxidant Profile of Pumpkin (*Cucurbita pepo L.*) Leafy Vegetable as Affected by NPK Compound Fertilizer, *Journal of Soil Science and Plant Nutrition*, 12 (3): 379-387.

Oniemola, P. K., and Sanusi, G., (2007): The Nigerian Bio-fuel Policy and Incentives: A Need to Follow the Brazilian Pathway, *International Association for Energy Economics*. (<https://www.iaee.org/en/publications/newsletterdl.aspx?id=88>). Retrieved on 30th June, 2013.

Oyeleke, G.O., Olayiwola, O.A. and Latona, D.F., (2012): Chemical Examination of Sandbox (*Hura Crepitans*) Seed: Proximate, Elemental and Fatty Acid Profile; *Journal of Applied Chemistry (IOSRJAC)*, 1(2): 10-13.

Pandey, K.K., and Pitman, A.J., (2003): FTIR Studies of the Changes in Wood Following Decay by Brown-rot and White-rot Fungi, *International Biodeterioration and Biodegradation*, 52: 151–160.

Park, J., Kim, D., Wang, Z., Lu, P., Park, S., and Lee, J., (2008): Production and Characterization of Biodiesel from Tung Oil; *Applied Biochemistry and Biotechnology*, 148: 109–17.

Pasias, S., Barakos, N., Alexopoulos, C., and Papayannakos, N., (2006): Heterogeneously Catalyzed Esterification of FFAs in Vegetable Oils, *Chemical Engineering and Technology*, 29 (11): 1365–1371.

Perreux, L., and Loupy, A., (2001): A Tentative Rationalization of Microwave Effects in Organic Synthesis According to the Reaction Medium, and Mechanistic Considerations. *Tetrahedron* 57: 9199–9223.

Ramakrishnan, K., Kudchadker, A.P. and Sathish, K.K., (2010): Microwave Assisted Transesterification of Rice Bran Oil; *Journal of Engineering Research and Studies*, 1: 165-170.

Ramos, M.J., Fernandez, C.M., Casas, A., Rodriguez, L., and Perez, A., (2009): Influence of Fatty Acid Composition of Raw Materials on Biodiesel Properties. *Bioresource Technology*, 100: 261–8.

Rathore, V. and Madras, G., (2007): Synthesis of Biodiesel from Edible and Non-edible Oils in Supercritical Alcohols and Enzymatic Synthesis in Supercritical Carbon dioxide. *Fuel*, 86(17-18): 2650-2659.

Razon, F.L., (2009): Alternative Crops for Biodiesel Feedstock, *CAB Review: Perspectives in Agriculture, Veterinary Science, Nutrition and Natural Resources*, 4 (56): 1-9.

Refaat, A.A. (2009): Correlation between the Chemical Structure of Biodiesel and its Physical Properties; *International Journal of Environmental Science and Technology*, 6(4): 677-694

Royal Society, (2008): Sustainable Biofuels: Prospects and Challenges, Policy Document, the Royal Society, London, pp. 1-90.

Ruiz-Gutierrez, V., and Perez-Camino, M.C. (2000): Update on Solid-phase Extraction for the Analysis of Lipid Classes and Related Compounds; *Journal of Chromatography A*, 885, 321-341.

Russo, P. A., Antunes, M. M., Neves, P., Wiper, P. V., Fazio, E., Neri, F., Barreca, F., Mafra, L., Pillinger, M., Pinna, N., and Valente, A. A., (2014): Solid Acids with SO₃H Groups and Tunable Surface Properties: Versatile Catalysts for Biomass Conversion, *Journal of Material Chemistry A*, 2: 11813-11824.

Rutherford, D.W., Wershaw, R L., and Cox, L.G., (2005): Changes in Composition and Porosity Occurring During the Thermal Degradation of Wood and Wood Components, U.S. Geological Survey, Scientific Investigations Report 2004-5292, pp. 1- 88.

Santamarina, J. C., Klein, K. A., Wang, Y.H., and Prencke, E., (2002): Specific Surface: Determination and Relevance, *Canadian Geotechnical Journal*, 39: 233-241.

Schinas, P., Karavalakis, G., Davaris, A., C., Anastopoulos, G., Karonis, D., Zannikos, F., Stournas. S., and Lois, E., (2009): Pumpkin (*Cucurbita pepo L.*) Seed Oil as an Alternative Feedstock for the Production of Biodiesel in Greece, *Biomass and Bioenergy*, 33: 44-49.

Schumacher, L.G., and Tabitha, M., (1997): Lessons Learnt While Fuelling with Biodiesel in: *Proceedings of Commercialization of Biodiesel: Producing a Quality Fuel*. Biose (ID): 187-208.

Schumacher, L.G., Borgelt, S.C., Hires, W.G., Fosseen, D., and Goetz, W., (1994): Fuelling Diesel Engines with Blends of Methyl Ester Soybean Oil and Diesel Fuel. (http://web.missouri.edu/~schumacher1/Fueling_Diesel_Engines_with_Blends_of_Methyl_Ester_Soybean_Oil.pdf). Retrieved, 24th March, 2014.

Seppane-Laakso, T., and Oresic, M., (2009): How to Study Lipidomes, *Journal of Molecular Endocrinology*, 42(3): 185-190.

Serdari, A., Fragioudakis, K., Teas, C., Zannikos, F., Stournas, S., and Lois, E., (1999): Effect of Biodiesel Addition to Diesel Fuel on Engine Performance and Emissions, *Journal of Propulsion and Power*, 15 (2): 224–231.

Shahidi, F., and Zhong, Y., (2005): *Lipid Oxidation: Measurement Methods*; Bailey's Industrial Oil and Fat Products, John Wiley & Sons, Inc., Canada, pp. 355-378.

Shresther, D.S., Van, G. and Thompson, J., (2008): Effectiveness of Cold Flow Additives on Various Biodiesels, Diesel and their Blends. *Transactions of the ASASE*, 51 (4): 1365-1370.

Siriporn, L., Chalermchai, J., Rattikan, T., and Siriporn, T., (2010): Ultrasonic on Transesterification Reaction for Biodiesel Production; 7th Biomass Asia Workshop, Jakarta, Indonesia, pp.1-5.

Sivanesan, S., (2009): Kinetic Study of the Esterification of Free Fatty Acids in Non-edible *Pongamia pinnata* Oil Using Acid Catalyst; *Indian Journal of Science and Technology*, 2 (12): 20-24.

Sonntag, N.O.V., (1979): Composition and Characteristics of Individual Fats and Oils. In: Swern D, Ed. *Bailey's Industrial Oil and Fat Products*, Vol. 1, 4th Ed. John Wiley and Sons, Inc., New York; p. 459.

Srivastava, A., and Prasad, R., (2000): Triglycerides-based Diesel Fuels; *Renewable and Sustainable Energy Reviews*, 4: 111.

Statista (2016): The World's biggest Biodiesel Producers in 2015, by Country (in Billion Liters); The Statistics Portal, (<https://www.statista.com/statistics/271472/biodiesel-production-in-selected-countries/>). Retrieved 11-03-16.

Swain, M. D., and Tom, B., (1977): Explosive Seed Dispersal in *Hura crepitans* L. (Euphorbiaceae); *New Phytologist*, 78: 695–708.

Thiago, P., (2008): Historical Background of Biodiesel, What About Brazil, Biodiesel, Energy. (<http://www.whataboutbrazil.com/historical-background-ofbiodiesel/>). Retrieved on 30th August, 2013.

Thiruvengadaravi, K.V., Nandagopal, J., Sathya, S.B.V., Dinesh. K.S., Vijayalakshmi, P. and Sivanesan, S., (2009): Kinetic Study of the Esterification of Free Fatty Acids in Non-edible Pongamiapinnata Oil Using Acid Catalyst; Indian Journal of Science and Technology, 2 (12): 20-24.

Tierney, J.P., and Lidstrom, P., (2005): Microwave Assisted Organic Synthesis. CRC Press, Oxford, UK. pp. 1-5.

Tong, D., Hu, C., Jiang, K., and Li, Y., (2011): Cetane Number Prediction of Biodiesel from the Composition of the Fatty Acid Methyl Esters; Journal of American Oil Chemists' Society, 88: 415–423

Tony, C., (2011): Western Australian Renewable Fuels Association, Inc. (<http://www.shortcircuit.com.au/warfa/warfa.htm>). Retrieved, 9th June, 2013.

Tsunemoto, H., Ishitani, H., and Kudo, R., (1996): Evaluation of Exhaust Odour in a Direct Injection Diesel Engine, Transactions of the Japan Society of Mechanical Engineers. B, 62 (604): 254–260.

Tyson, K.S., (2001): Biodiesel Handling and Use Guidelines, National Renewable Energy Laboratory, Golden (CO), Report No. NREL/TP-580-30004.

Ulf. S., Ricardo, S., and Rogério, M., (1998): Transesterification of Vegetable Oils: A Review. Journal of Brazilian Chemical Sociece, 9(1): 199-210.

US-EIA, (2005): 'What Are Greenhouse Gases?' US Department of Energy. (<http://www.eia.gov/oiaf/1605/ggccebro/chapter1.html>). Retrieved 2007-09-09.

US-EPA, (2002): A Comprehensive Analysis of Biodiesel Impacts on Exhaust Emissions, Assessment and Standards Division (Office of Transportation and Air Quality of the US Environmental Protection Agency), EPA420-P-02-001.

Usoro, E.U., Suyamsothy, E.G.A. and Sanny, G.A., (1982): Manual of Chemical Methods of Food Analysis, Bencox International Ltd., Sydney, pp. 1-35.

VOA News, (2007): Nigerian Expert: Biofuels as Alternative Fuel May Not Be Best Choice, July 04 (<http://www.voanews.com/english/news/a-13-2007-07-04-voa46-66781517.html>). Retrieved 09- 09- 2011.

Volkman, J.K., Everitt, D.A. and Allen, D.I., (1986): Some Analysis of Lipid Classes in Marine Organisms, Sediments and Seawater Using Thin-layer Chromatography-flame Ionization Detection, *Journal of Chromatography A*, 356: 147-162.

Wang, L., Dong, X., Jiang, H., Li, G., and Zhang, M., (2014): Preparation of a Novel Carbon-based Solid Acid from Cassava Stillage Residue and its Use for the Esterification of free Fatty Acids in Waste Cooking Oil. *Bioresource Technology*, 158: 392–395.

Warabi, Y., Kusdiana, D. and Saka, S., (2004): Reactivity of Triglycerides and Fatty Acids of Rape Seed Oil in Supercritical Alcohols. *Bioresource Technology*, 91(3): 283-287.

Wexler, H., (1964): Polymerization of Drying Oils. *Chemical Review*; 64: 591-611.

Wilhelm, R., and Hermann, M. B., (2005): Esters, Organic, *Ullmann's Encyclopedia of Industrial Chemistry*, Wiley-VCH, Weinheim, pp. 2-20.

Wu, M., Wu, G., Han, L., and Wang, J., (2005): Low-temperature Fluidity of Bio-diesel Fuel Prepared from Edible Vegetable Oil. *Petrol, Process, Petrochem*, 36: 57–60.

Yan, S., Lu, H., and Liang, B., (2008): Supported CaO Catalysts Used in the Transesterification of Rapeseed Oil for the Purpose of Biodiesel Production; *Energy and Fuels*, 22: 646-651.

Yildiz, G., Wehling, R.L., and Cuppett, S.L., (2001): Method for Determining Oxidation of Vegetable Oils by Near-Infrared Spectroscopy. *Journal of American Oil Chemists' Society*, 78 (5): 495–502.

Ziejewski, M., Kaufman, K.R., Schwab, A.W., and Pryde, E.H., (1984): Diesel Engine Evaluation of a Nonionic Sunflower Oil-aqueous Ethanol Microemulsion; *Journal of American Oil Chemists' Society*, 6: 1620.

Zong, M.H., Duan, Z.Q., Lou, W.Y., Smith, T.J., and Wu, H., (2007): Preparation of a Sugar Catalyst and its Use for Highly Efficient Production of Biodiesel. *Green Chemistry*, 7: 434-437.

Appendix 1

Table 3.27: Relationship between Gross Calorific Value and Specific Gravity of Fuel (Shell International Ltd)

Specific gravity	Gross Calorific Value (Specific Energy)		
	Cal/g	Cal/cm ³	KJ/Kg
0.80	11,050	8,840	46,287
0.81	11,010	8,920	46,101
0.82	10,970	8,990	45,915
0.83	19,920	9,060	45,729
0.84	10,870	9,130	45,520
0.85	10,830	9,200	45,334
0.86	10,780	9,270	45,124
0.87	10,730	9,340	44,938
0.88	10,690	9,410	44,752
0.89	10,640	9,470	44,543
0.90	10,590	9,540	44,357
0.91	10,540	9,590	44,147
0.92	10,400	9,660	43,938
0.93	10,440	9,710	43,729
0.94	10,390	9,770	43,519
0.95	10,340	9,830	43,310
0.96	10,290	9,880	43,101
0.97	10,240	9,940	42,891
0.98	10,190	9,990	42,682
0.99	10,140	10,040	42,475
1.00	10,090	10,090	42,263

Appendix 2

Kinetics of esterification of *Cucurbita pepo*, *Azelia africana* and *Hura crepitans* base oils using H_2SO_4 catalyst

Table 4.49: methyl esterification of the Cucurbita base Oil at 40°C using H_2SO_4 catalyst

Time (min.)	[A] (mgKOH/g)	ln[A]	1/[A]
0	126.26	4.838	0.00792
10	98.00	4.585	0.0102
20	52.00	3.950	0.019
30	8.30	2.116	0.120
40	6.10	1.808	0.164
50	3.50	1.253	0.286

[A]: Acid value of the base oil at a time, t.

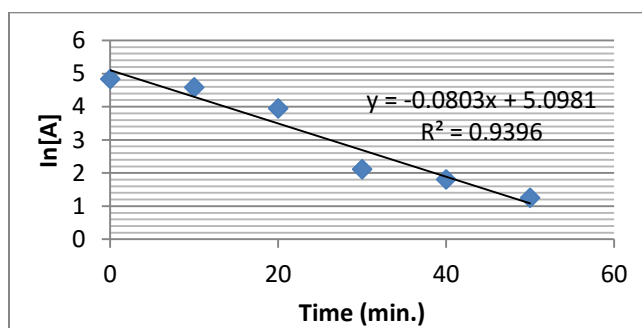


Fig.4.23: Verification of first order behavior for methyl esterification of the Cucurbita pepo base oil 40°C using H_2SO_4 catalyst

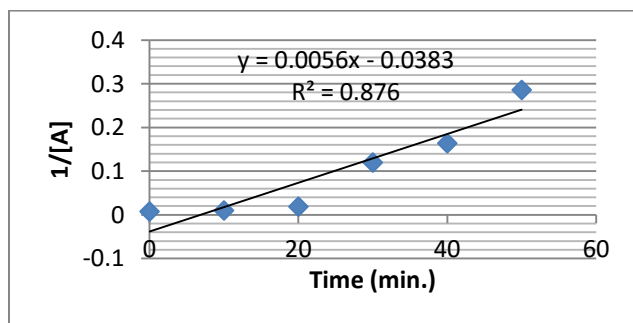
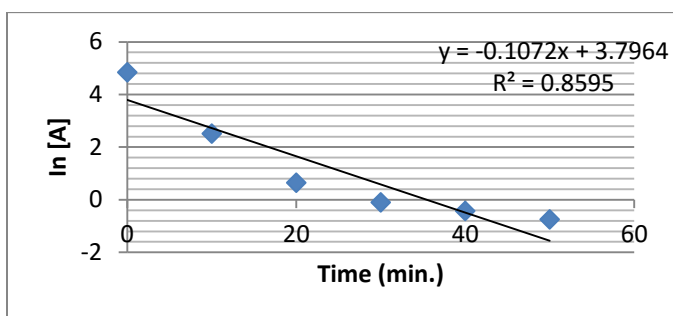
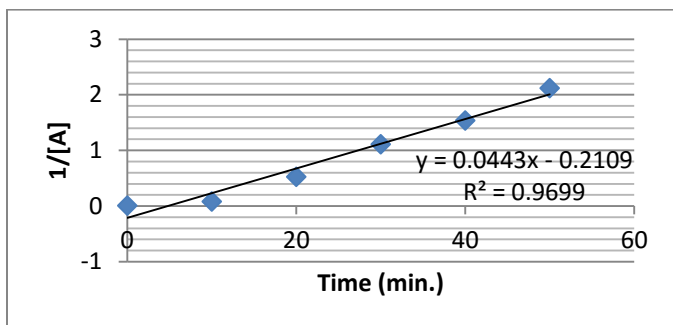


Fig.4.24: Verification of second order behaviour for methyl esterification of the Cucurbita pepo base oil at 40°C using H_2SO_4 catalyst

Table 4.50: methyl esterification of the Cucurbita pepo base oil at 50°C using H₂SO₄ catalyst

Time	[A] (mgKOH/g)	ln[A]	1/[A]
0	126.26	4.838	0.00792
10	12.30	2.509	0.0813
20	1.90	0.642	0.526
30	0.90	-0.105	1.111
40	0.65	-0.431	1.538
50	0.47	-0.755	2.128

Fig.4.25: Verification of first order behaviour for methyl esterification of the Cucurbita pepo base oil at 50°C using H₂SO₄ catalystFig.4.26: Verification of second order behaviour for methyl esterification of the Cucurbita pepo base oil at 50°C using H₂SO₄ catalystTable 4.51: methyl esterification of the Cucurbita base oil at 60°C using H₂SO₄ catalyst

Time (min.)	[A] (mgKOH/g)	ln[A]	1/[A]
0	126.26	4.838	0.00793
10	4.60	1.526	0.217
20	0.56	-0.579	1.786
30	0.50	-0.693	2.000
40	0.50	-0.693	2.000
50	0.34	-1.609	5.000

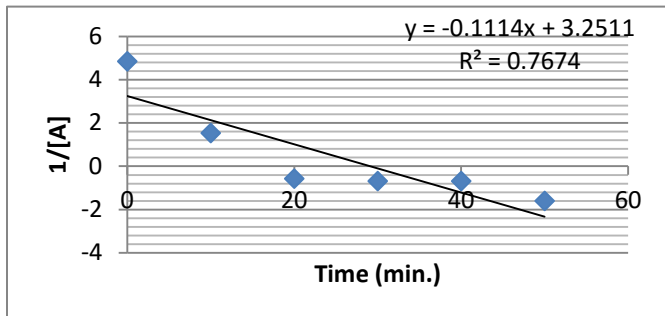


Fig.4.27: Verification of first order behaviour for methyl esterification of the Cucurbita pepo base oil at 60°C using H₂SO₄ catalyst

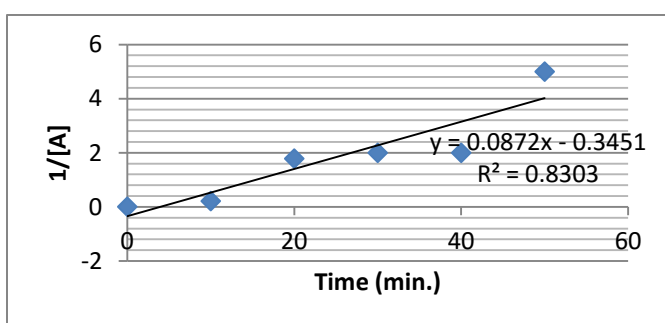


Fig.4.28: Verification of second order behaviour for methyl esterification of the Cucurbita pepo base oil at 60°C using H₂SO₄ catalyst

Table 4.52: methyl esterification of the Cucurbita base oil at 70°C using H₂SO₄ catalyst

Time (min.)	[A] (mgKOH/g)	ln[A]	1/[A]
0	126.260	4.838	0.00793
10	1.110	0.104	0.900
20	0.840	-0.174	1.190
30	0.485	-0.724	2.062
40	0.345	-1.064	2.899
50	0.200	-1.609	5.000

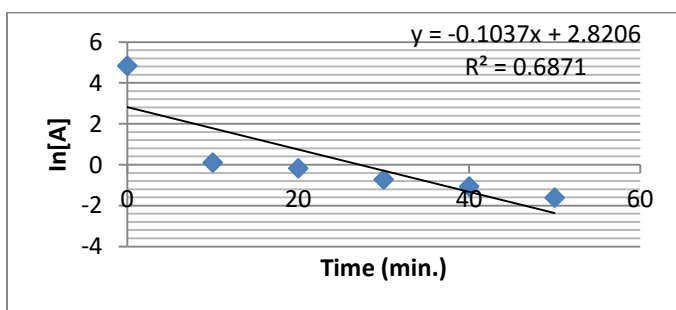


Fig.4.29: Verification of first order behaviour for methyl esterification of the Cucurbita pepo base oil at 70°C using H₂SO₄ catalyst

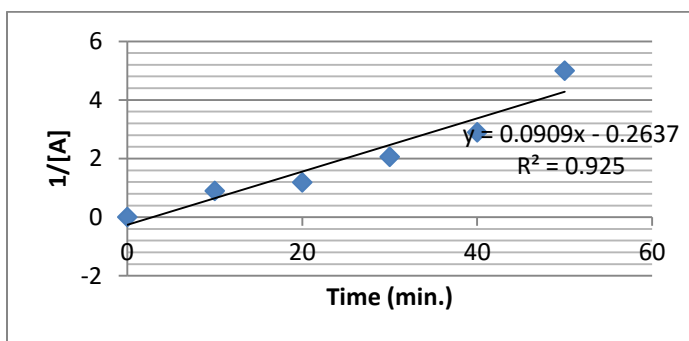


Fig.4.30: Verification of second order behaviour for methyl esterification of the Cucurbita pepo base oil at 70°C using H₂SO₄ catalyst

Table 4.53: Determination of activation energy for the second order methyl esterification of the Cucurbita pepo base oil

Temp. (°C)	Temp. (K)	k	1/T	Ink
40	313	0.0056	0.00319	-5.185
50	323	0.044	0.00309	-3.123
60	333	0.087	0.00300	-2.442
70	343	0.090	0.00292	-2.408

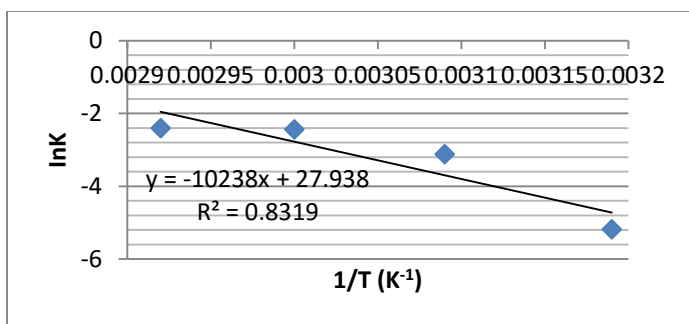


Fig4.31: Determination of Activation Energy for methyl esterification of the *Cucurbita pepo* base oil

$$\text{Slope} = -E_a/R$$

$$-10238 = -E_a/R$$

$$R = 8.314\text{J/K.mol}$$

$$E_a = -(-10238\text{K}) (8.314\text{J/Kmol})$$

$$E_a = 85.12\text{KJ/mol.}$$

Table 4.54: methyl esterification of the Afzelia africana base oil at 40°C using H₂SO₄ catalyst

Time (min.)	[A] (mgKOH/g)	ln[A]	1/[A]
0	122.00	4.804	0.008
10	70.00	4.248	0.0143
20	40.00	3.689	0.025
30	18.10	2.896	0.055
40	6.70	1.902	0.149
50	6.20	1.825	0.161

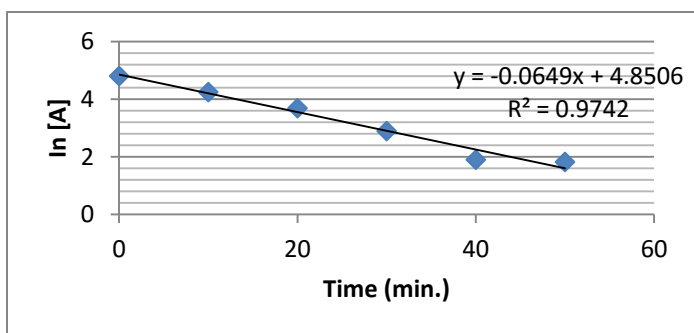
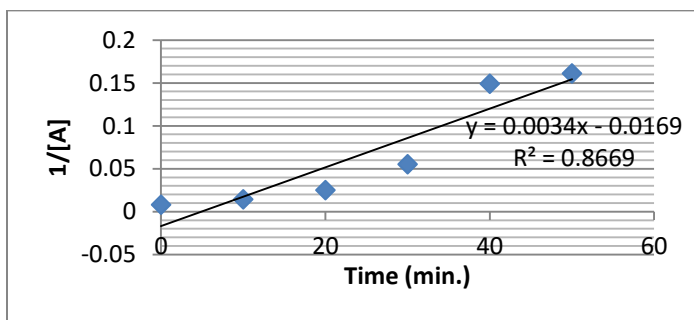
Fig.4.32: Verification of first order behaviour for methyl esterification of the Afzelia africana base oil at 40°C using H₂SO₄ catalystFig.4.33: Verification of second order behaviour for methyl esterification of the Afzelia africana base oil at 40°C using H₂SO₄ catalyst

Table 4.55: methyl esterification of the Afzelia africana base oil at 50°C

Time (min.)	[A] (mgKOH/g)	ln[A]	1/[A]
0	122.00	4.804	0.00819
10	9.20	2.219	0.109
20	2.10	0.742	0.476
30	1.310	0.270	0.763
40	0.90	-0.105	1.111
50	0.43	-0.844	2.326

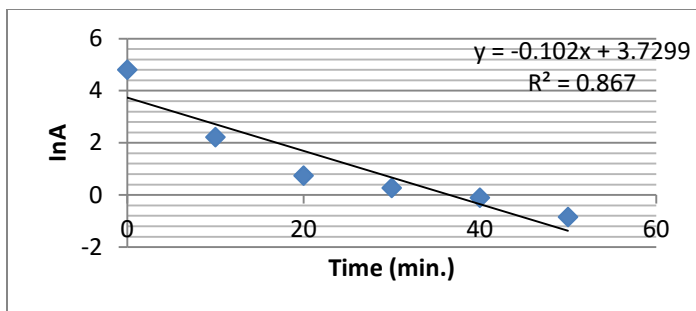


Fig.4.34: Verification of first order behaviour for methyl esterification of the Afzelia africana base oil at 50°C using H₂SO₄ catalyst

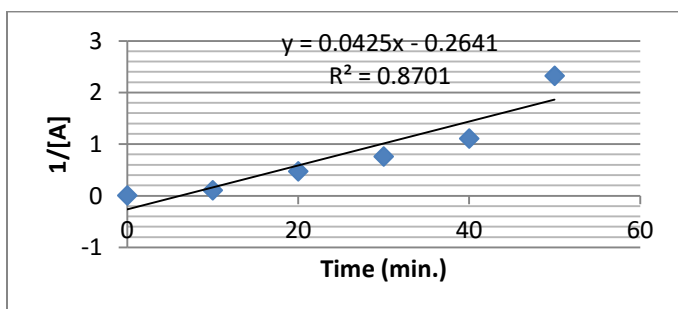


Fig.4.35: Verification of second order behaviour for methyl esterification of the Afzelia africana base oil at 50°C using H₂SO₄ catalyst

Table 4.56: methyl esterification of the Afzelia africana base oil at 60°C using H₂SO₄ catalyst

Time (min.)	[A] (mgKOH/g)	ln[A]	1/[A]
0	122.00	4.804	0.00819
10	2.80	1.029	0.357
20	1.12	0.113	0.893
30	0.89	-0.117	1.124
40	0.30	-1.204	3.333
50	0.29	-1.238	3.448

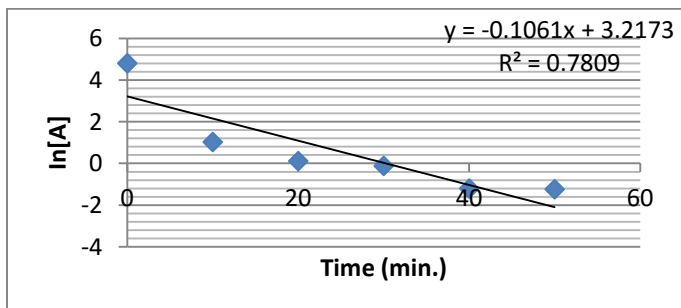


Fig.4.36: Verification of first order behaviour for methyl esterification of the Afzelia africana base oil at 60°C using H₂SO₄ catalyst

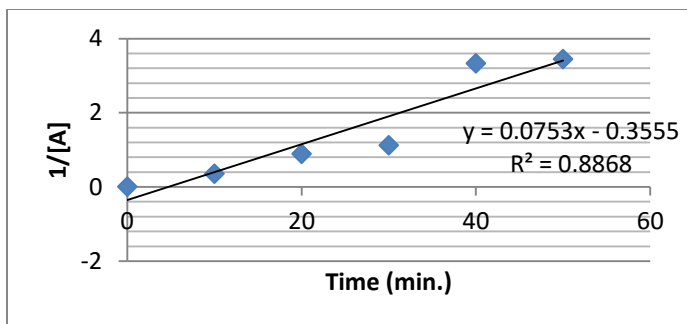


Fig.4.37: Verification of second order behaviour for methyl esterification of the Afzelia africana base oil at 60°C using H₂SO₄ catalyst

Table 4.57: methyl esterification of the Afzelia africana base oil at 70°C using H₂SO₄ catalyst

Time (min.)	[A] (mgKOH/g)	ln[A]	1/[A]
0	122.00	4.804	0.00819
10	4.10	1.410	0.243
20	0.40	-0.916	2.500
30	0.38	-0.967	2.632
40	0.25	-1.386	4.000
50	0.25	-1.386	4.000

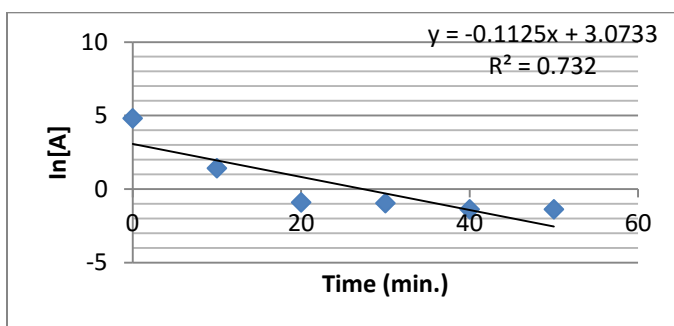


Fig.4.38: Verification of first order behaviour for methyl esterification of the Afzelia africana base oil at 70°C using H₂SO₄ catalyst

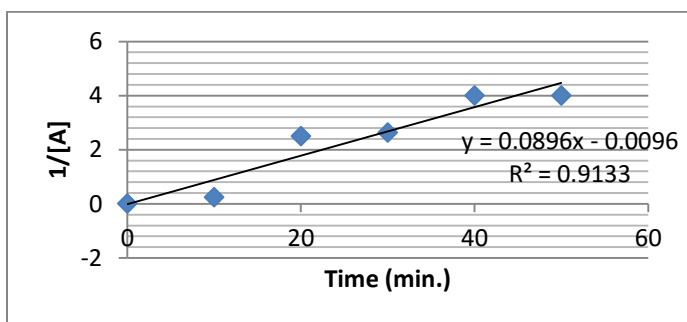


Fig.4.39: Verification of second order behaviour for methyl esterification of the Afzelia africana base oil at 70°C using H₂SO₄ catalyst

Table 4.58: Determination of activation energy for the second order methyl esterification of the *Afzelia africana* base oil

Temp. (°C)	Temp. (K)	k	1/T	lnk
40	313	0.0034	0.00319	-5.68
50	323	0.044	0.00309	-3.12
60	333	0.087	0.00300	-2.44
70	343	0.09	0.00292	-2.41

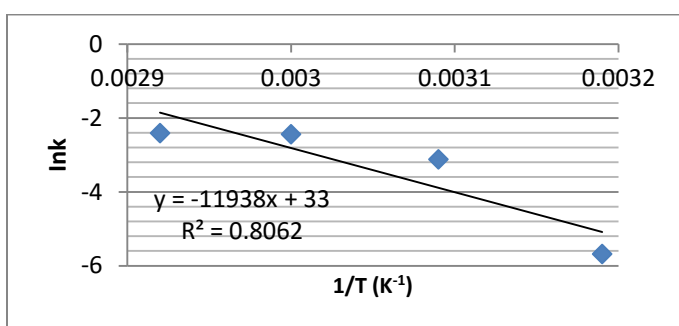


Fig4.40: Determination of Activation Energy for Methyl esterification of the *Afzelia africana* base oil

$$\begin{aligned} \text{Slope} &= -E_a/R \\ -11938 &= -E_a/R \\ R &= 8.314\text{J/K.mol} \\ E_a &= -(-11938\text{K})(8.314\text{J/K.mol}) \\ E_a &= 99.25\text{KJ/mol.} \end{aligned}$$

Table 4.59: methyl esterification of the *Hura crepitans* base oil at 40°C using H₂SO₄ catalyst

Time (min.)	[A] (mgKOH/g)	ln[A]	1/[A]
0	86.24	4.457	0.0116
10	70.00	4.248	0.0143
20	47.00	3.850	0.0213
30	30.00	3.402	0.0333
40	19.20	2.955	0.0520
50	2.60	0.955	0.3850

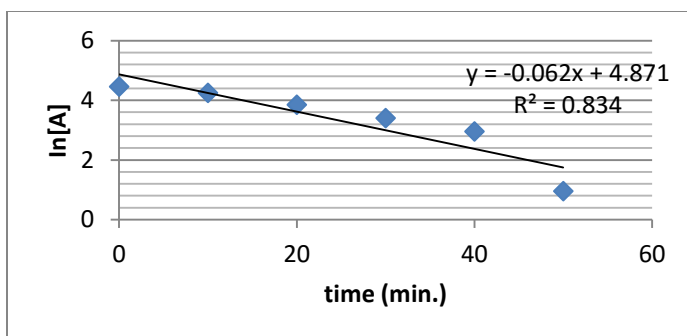


Fig.4.41: Verification of first order behaviour for methyl esterification of the Hura crepitans base oil at 40°C using H₂SO₄ catalyst

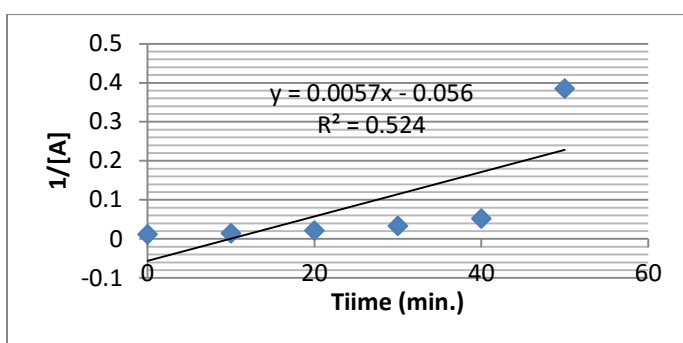


Fig.4.42: Verification of second order behaviour for methyl esterification of the Hura crepitans base oil at 40°C using H₂SO₄ catalyst

Table 4.60: methyl esterification of the Hura crepitans base oil at 50°C using H₂SO₄ catalyst

Time (min.)	[A] (mgKOH/g)	ln[A]	1/[A]
0	86.24	4.457	0.0116
10	18.90	2.939	0.0529
20	3.20	1.163	0.3123
30	1.60	0.470	0.6250
40	0.90	-0.105	1.1110
50	0.90	-0.105	1.1110

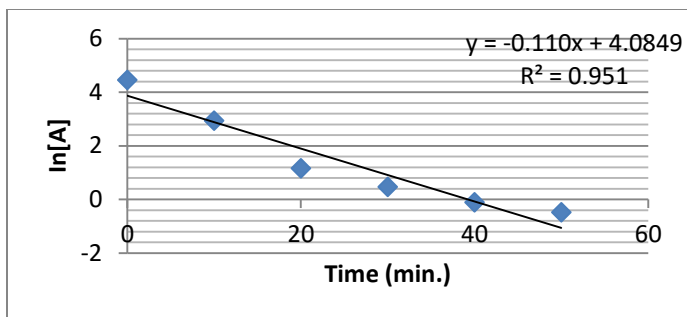


Fig.4.43: Verification of first order behaviour for methyl esterification of the Hura crepitans base oil at 50°C using H₂SO₄ catalyst

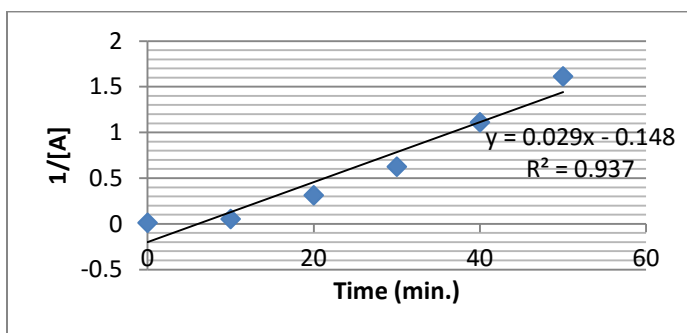


Fig.4.44: Verification of second order behaviour for methyl esterification of the Hura crepitans base oil at 50°C using H₂SO₄ catalyst

Table 4.61: methyl esterification of the Hura crepitans base oil at 60°C using H₂SO₄ catalyst

Time (min.)	[A] (mgKOH/g)	ln[A]	1/[A]
0	86.24	4.457	0.0116
10	4.90	1.589	0.204
20	0.80	-0.223	1.250
30	0.53	-0.635	1.887
40	0.40	-0.916	2.500
50	0.37	-0.994	2.700

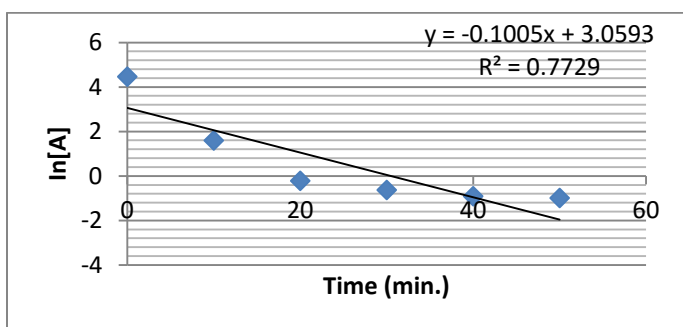


Fig.4.45: Verification of first order behaviour for methyl esterification of the Hura crepitans base oil at 60°C using H₂SO₄ catalyst

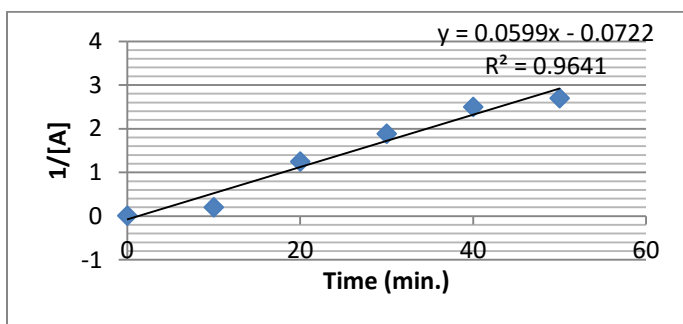


Fig.4.46: Verification of second order behaviour for methyl esterification of the Hura crepitans base oil at 60°C using H₂SO₄ catalyst

Table 4.62: methyl esterification of the Hura crepitans base oil at 70°C using H₂SO₄ catalyst

Time (min.)	[A] (mgKOH/g)	ln[A]	1/[A]
0	86.24	4.457	0.0116
10	1.34	0.293	0.746
20	1.11	0.104	0.900
30	0.50	-0.693	2.000
40	0.48	-0.734	2.083
50	0.30	-1.204	3.333

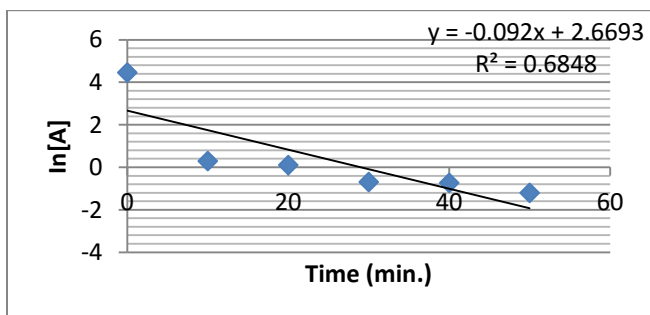


Fig.4.47: Verification of first order behaviour for methyl esterification of the Hura crepitans base oil at 70°C using H₂SO₄ catalyst

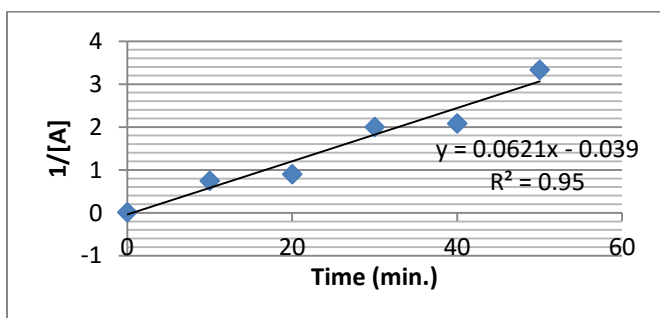


Fig.4.55: Verification of second order behaviour for methyl esterification of the Hura crepitans base oil at 70°C using H₂SO₄ catalyst

Table 4.48: Determination of activation energy for the second order methyl esterification of the *Hura crepitans* base oil

Temp. (°C)	Temp. (K)	k	1/T	lnk
40	313	0.0057	0.00319	-5.167
50	323	0.029	0.00309	-3.540
60	333	0.059	0.00300	-2.830
70	343	0.062	0.00292	-2.781

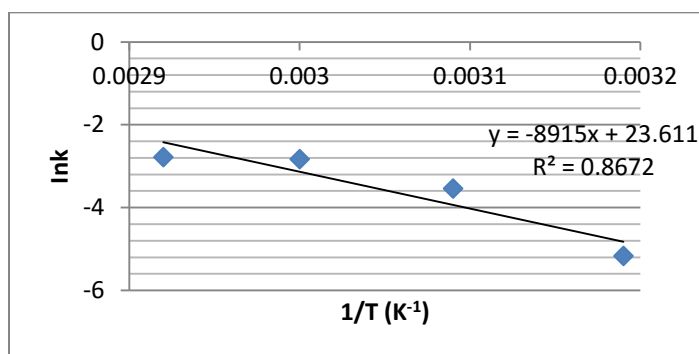


Fig4.49: Determination of Activation Energy for Methyl esterification of the *Hura crepitans* base oil

$$\begin{aligned} \text{Slope} &= -E_a/R \\ -8915 &= -E_a/R \\ R &= 8.314\text{J/K.mol} \\ E_a &= -(-8915\text{K}) (8.314\text{J/K.mol}) \\ E_a &= 74.12\text{KJ/mol.} \end{aligned}$$

Table 4.64: butyl esterification of the Cucurbita pepo base oil at 40°C using H₂SO₄ catalyst

Time (min.)	[A] (mgKOH/g)	ln[A]	1/[A]
0	86.94	4.465	0.0115
10	79.50	4.376	0.0126
20	64.00	4.159	0.0156
30	60.01	4.094	0.0167
40	51.00	3.932	0.0196
50	45.20	3.811	0.0221

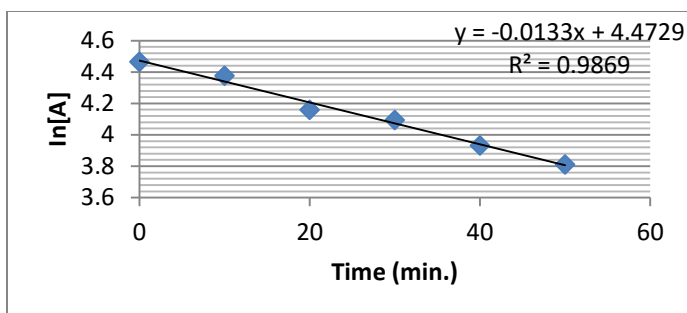


Fig.4.50: Verification of first order behaviour for butyl esterification of the Cucurbita pepo base oil at 40°C using H₂SO₄ catalyst

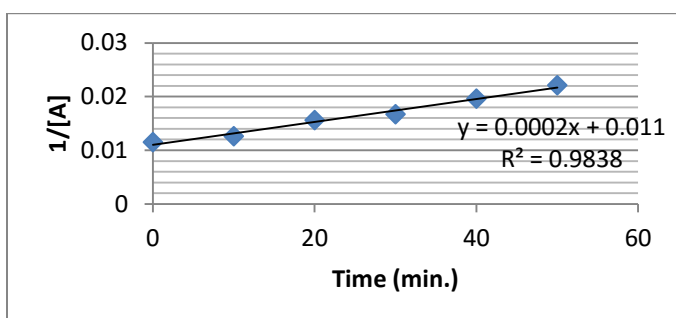


Fig.4.51: Verification of second order behaviour for butyl esterification of the Cucurbita pepo base oil at 40°C using H₂SO₄ catalyst

Table 4.65: butyl esterification of the Cucurbita pepo base oil at 50°C using H₂SO₄ catalyst

Time	[A] (mgKOH/g)	ln[A]	1/[A]
0	86.94	4.465	0.0115
10	66.30	4.194	0.0150
20	59.30	4.080	0.0168
30	33.90	3.520	0.0295
40	26.10	3.262	0.0383
50	24.60	3.202	0.0407

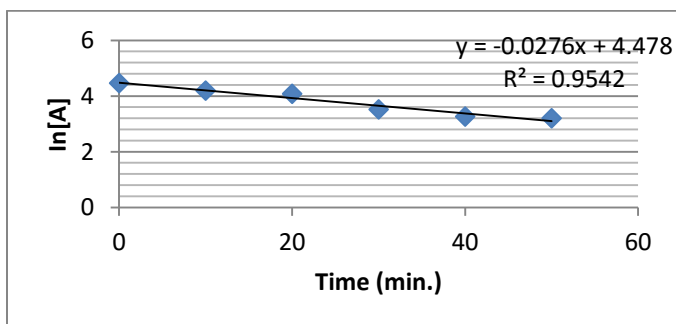


Fig.4.52: Verification of first order behaviour for butyl esterification of the Cucurbita pepo base oil at 50°C using H₂SO₄ catalyst

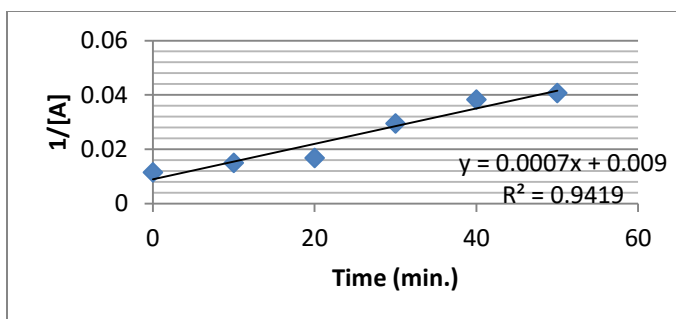


Fig.4.53: Verification of second order behaviour for butyl esterification of the Cucurbita pepo base oil at 50°C using H₂SO₄ catalyst

Table 4.66: butyl esterification of the Cucurbita pepo base oil at 60°C using H₂SO₄ catalyst

Time (min.)	[A] (mgKOH/g)	ln[A]	1/[A]
0	86.94	4.465	0.0115
10	42.56	3.751	0.0235
20	28.50	3.349	0.0350
30	20.10	3.000	0.0498
40	10.50	2.351	0.0952
50	10.00	2.303	0.1000

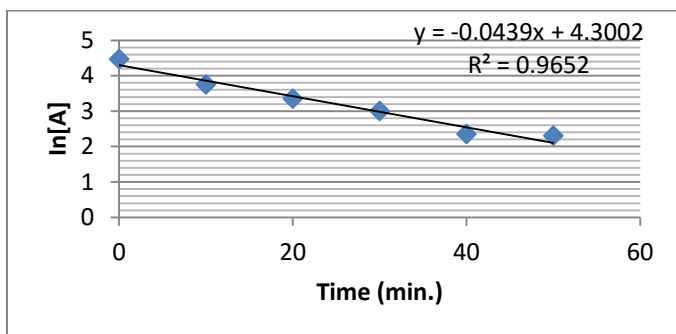


Fig.4.54: Verification of first order behaviour for butyl esterification of the Cucurbita pepo base oil at 60°C using H₂SO₄ catalyst

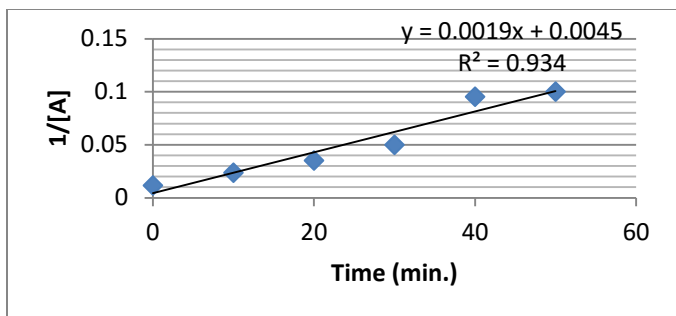


Fig.4.55: Verification of second order behaviour for butyl esterification of the Cucurbita pepo base oil at 60°C using H₂SO₄ catalyst

Table 4.67: butyl esterification of the Cucurbita pepo base oil at 70°C using H₂SO₄ catalyst

Time (min.)	[A] (mgKOH/g)	ln[A]	1/[A]
0	86.94	4.465	0.0115
10	39.20	3.669	0.0255
20	28.80	3.360	0.0347
30	13.55	2.606	0.0738
40	12.88	2.556	0.0776
50	7.90	2.067	0.1260

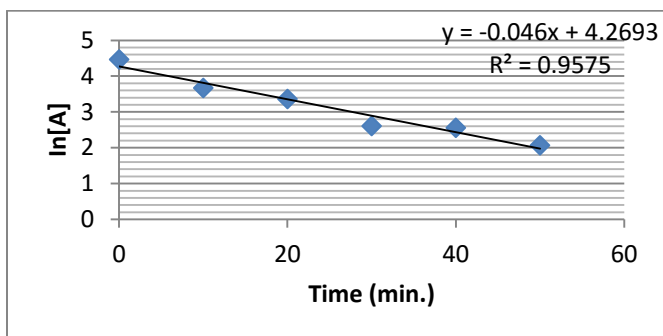
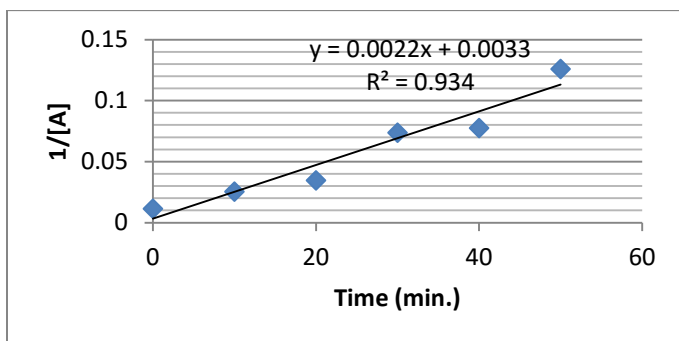
Fig.4.56: Verification of first order behaviour for butyl esterification of the Cucurbita pepo base oil at 70°C using H₂SO₄ catalystFig.4.57: Verification of second order behaviour for butyl esterification of the Cucurbita pepo base oil at 70°C using H₂SO₄ catalyst

Table 4.68: Determination of activation energy for the first order butyl esterification of the Cucurbita pepo base oil

Temp. (°C)	Temp. (K)	k	1/T	lnk
40	313	0.0133	0.00319	-4.319
50	323	0.027	0.00309	-3.612
60	333	0.043	0.00300	-3.147
70	343	0.046	0.00292	-3.079

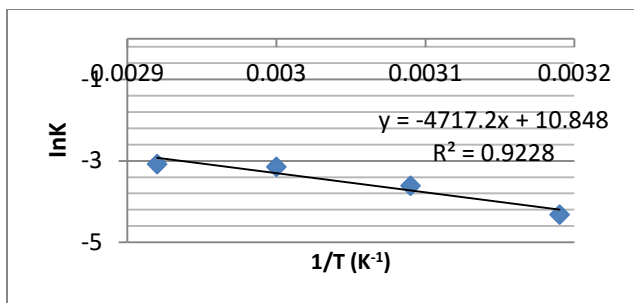


Fig4.58: Determination of Activation Energy for Butyl esterification of the *Cucurbita pepo* base oil

$$\text{Slope} = -E_a/R$$

$$-4717.2 = -E_a/R$$

$$R = 8.314\text{J/K.mol}$$

$$E_a = (-4717.2\text{K}) (8.314\text{J/K.mol})$$

$$E_a = 39.19\text{KJ/mol.}$$

Table 4.69: butyl esterification of the *Afzelia africana* base oil at 40°C using H₂SO₄ catalyst

Time (min.)	[A] (mgKOH/g)	ln[A]	1/[A]
0	122.0	4.804	0.00819
10	108.0	4.682	0.00926
20	102.0	4.625	0.00980
30	100.4	4.609	0.00996
40	100.8	4.613	0.00992
50	82.7	4.415	0.01210

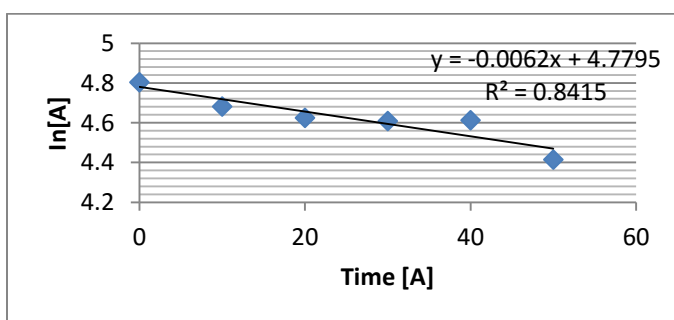


Fig.4.59: Verification of first order behaviour for butyl esterification of the *Afzelia africana* base oil at 40°C using H₂SO₄ catalyst

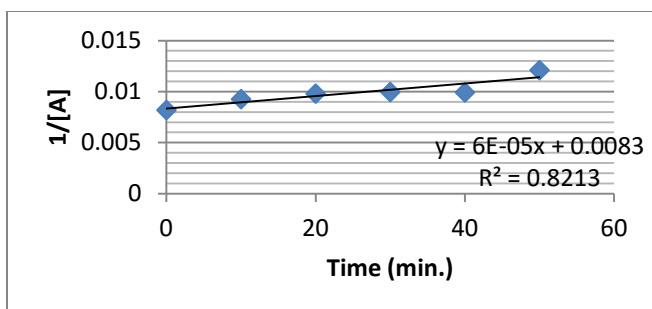


Fig.4.60: Verification of second order behaviour for butyl esterification of the Afzelia africana base oil at 40°C using H₂SO₄ catalyst

Table 4.70: butyl esterification of the Afzelia africana base oil at 50°C using H₂SO₄ catalyst

Time (min.)	[A] (mgKOH/g)	ln[A]	1/[A]
0	122.00	4.804	0.00819
10	92.20	4.523	0.0108
20	52.30	3.956	0.0191
30	38.30	3.645	0.0261
40	35.84	3.579	0.0279
50	23.40	3.153	0.0427

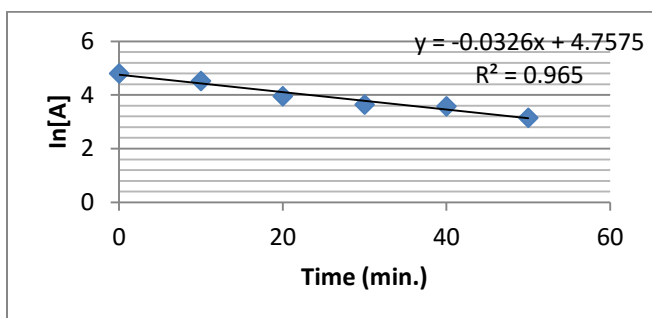


Fig.4.61: Verification of first order behaviour for butyl esterification of the Afzelia africana base oil at 50°C using H₂SO₄ catalyst

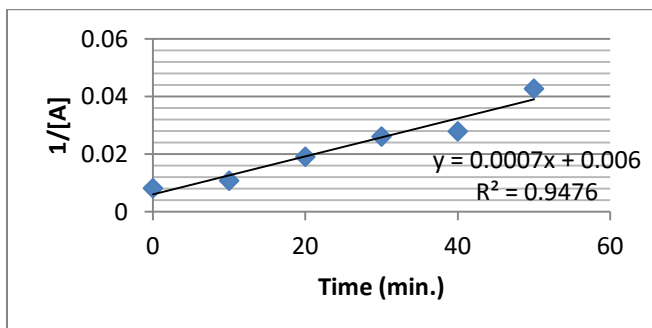
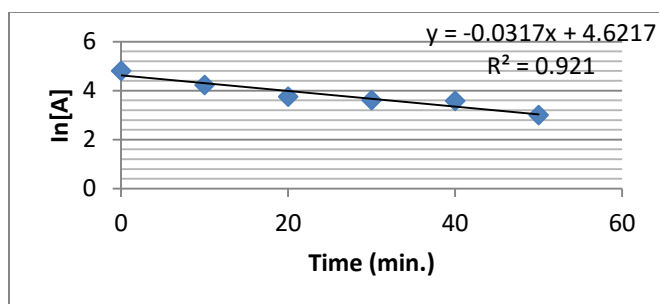
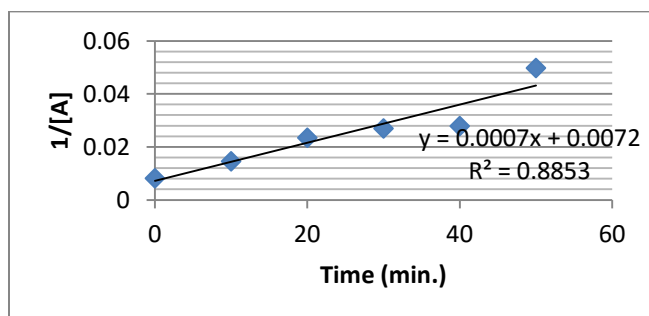


Fig.4.62: Verification of second order behaviour for butyl esterification of the Afzelia africana base oil at 50°C using H₂SO₄ catalyst

Table 4.71: butyl esterification of the Afzelia africana base oil at 60°C using H₂SO₄ catalyst

Time (min.)	[A] (mgKOH/g)	ln[A]	1/[A]
0	122.00	4.804	0.00819
10	68.54	4.227	0.0146
20	42.56	3.751	0.0235
30	36.90	3.610	0.0270
40	35.84	3.579	0.0279
50	20.09	3.000	0.0498

Fig.4.63: Verification of first order behaviour for butyl esterification of the Afzelia africana base oil at 60°C using H₂SO₄ catalystFig.4.64: Verification of second order behaviour for butyl esterification of the Afzelia africana base oil at 60°C using H₂SO₄ catalystTable 4.72: butyl esterification of the Afzelia africana base oil at 70°C using H₂SO₄ catalyst

Time (min.)	[A] (mgKOH/g)	ln[A]	1/[A]
0	122.00	4.804	0.00819
10	40.44	3.699	0.0247
20	20.53	3.022	0.0487
30	18.10	2.896	0.0552
40	9.80	2.282	0.1020
50	5.60	1.723	0.1790

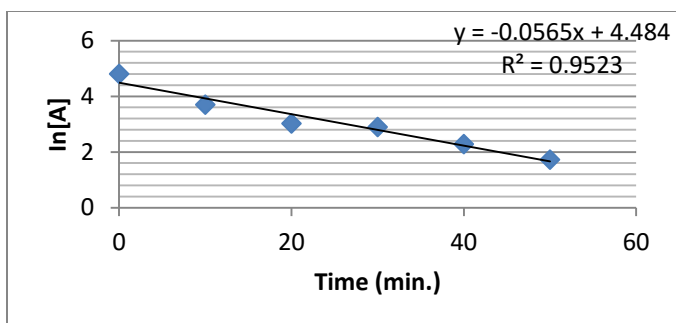


Fig.4.65: Verification of first order behaviour for butyl esterification of the *Afzelia africana* base oil at 70°C using H₂SO₄ catalyst

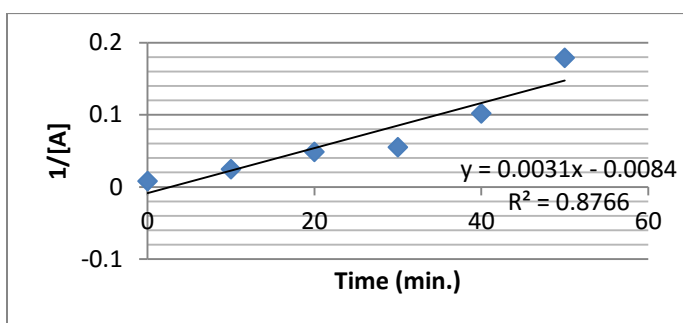


Fig.4.66: Verification of second order behaviour for butyl esterification of the *Afzelia africana* base oil at 70°C using H₂SO₄ catalyst

Table 4.73: Determination of activation energy for the first order butyl esterification of the *Afzelia africana* base oil

Temp. (°C)	Temp. (K)	k	1/T	lnk
40	313	0.0062	0.00319	-5.748
50	323	0.030	0.00309	-3.772
60	333	0.030	0.00300	-3.506
70	343	0.055	0.00292	-3.101

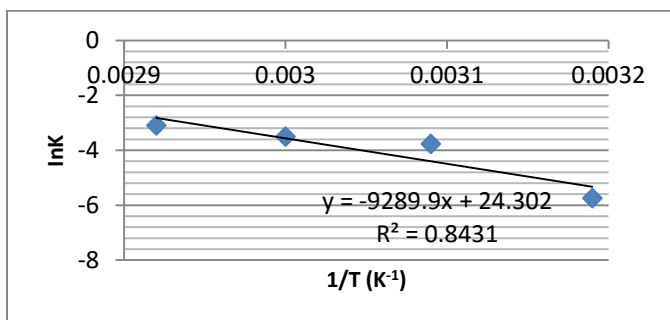


Fig.4.67: Determination of Activation Energy for Butyl esterification of the *Afzelia africana* base oil

$$\begin{aligned} \text{Slope} &= -E_a/R \\ -9289.9 &= -E_a/R \\ R &= 8.314\text{J/K.mol} \\ E_a &= (-9289.9\text{K}) (8.314\text{J/K.mol}) \\ E_a &= 77.24\text{KJ/mol.} \end{aligned}$$

Table 4.74: butyl esterification of the Hura crepitans base oil at 40°C using H₂SO₄ catalyst

Time (min.)	[A] (mgKOH/g)	ln[A]	1/[A]
0	86.94	4.465	0.0115
10	80.10	4.383	0.0125
20	73.00	4.290	0.0137
30	66.90	4.203	0.0149
40	60.40	4.100	0.0165
50	42.60	3.752	0.0235

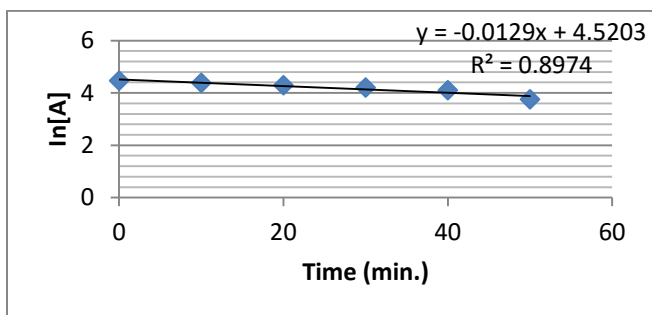
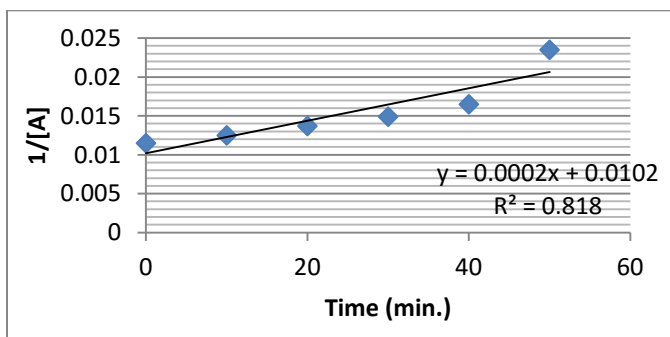
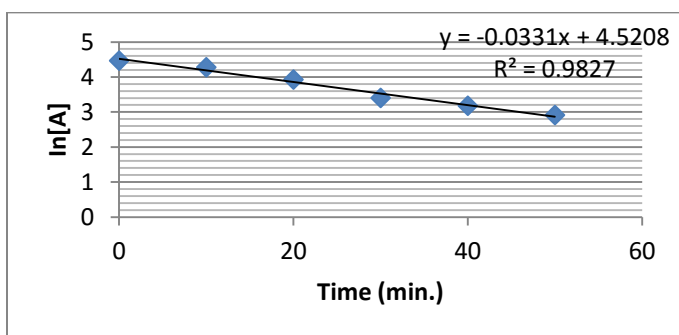
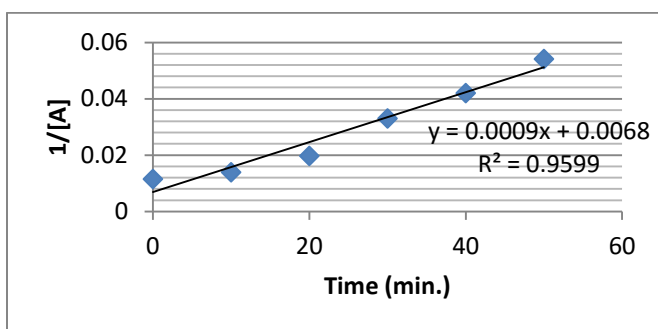
Fig.4.68: Verification of first order behaviour for butyl esterification of the Hura crepitans base oil at 40°C using H₂SO₄ catalystFig.4.69: Verification of second order behaviour for butyl esterification of the Hura crepitans base oil at 40°C using H₂SO₄ catalyst

Table 4.75: butyl esterification of the Hura crepitans base oil at 50°C using H₂SO₄ catalyst

Time (min.)	[A] (mgKOH/g)	ln[A]	1/[A]
0	86.94	4.465	0.0115
10	72.00	4.277	0.0139
20	50.70	3.926	0.0197
30	30.00	3.401	0.0330
40	24.00	3.178	0.0420
50	18.50	2.912	0.0541

Fig.4.70: Verification of first order behaviour for butyl esterification of the Hura crepitans base oil at 50°C using H₂SO₄ catalystFig.4.71: Verification of second order behaviour for butyl esterification of the Hura crepitans base oil at 50°C using H₂SO₄ catalystTable 4.76: butyl esterification of the Hura crepitans base oil at 60°C using H₂SO₄ catalyst

Time (min.)	[A] (mgKOH/g)	ln[A]	1/[A]
0	86.940	4.465	0.0115
10	60.46	4.102	0.0165
20	36.100	3.586	0.0277
30	35.900	3.581	0.0279
40	18.174	2.900	0.0550
50	16.440	2.800	0.0608

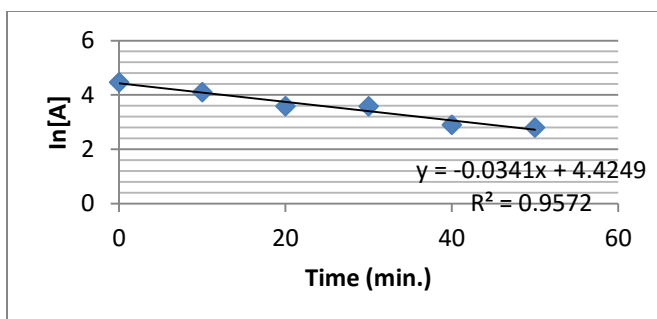


Fig.4.72: Verification of first order behaviour for butyl esterification of the Hura crepitans base oil at 60°C using H₂SO₄ catalyst

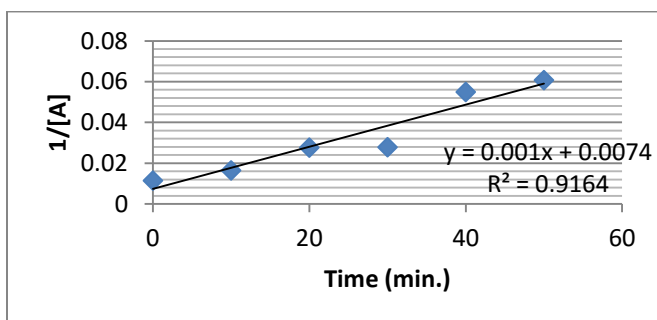


Fig.4.73: Verification of second order behaviour for butyl esterification of the Hura crepitans base oil at 60°C using H₂SO₄ catalyst

Table 4.77: butyl esterification of the Hura crepitans base oil at 70°C using H₂SO₄ catalyst

Time (min.)	[A] (mgKOH/g)	ln[A]	1/[A]
0	86.94	4.465	0.0115
10	28.57	3.352	0.035
20	8.10	2.092	0.123
30	6.20	1.825	0.161
40	0.56	-0.579	1.786
50	0.52	-0.654	1.923

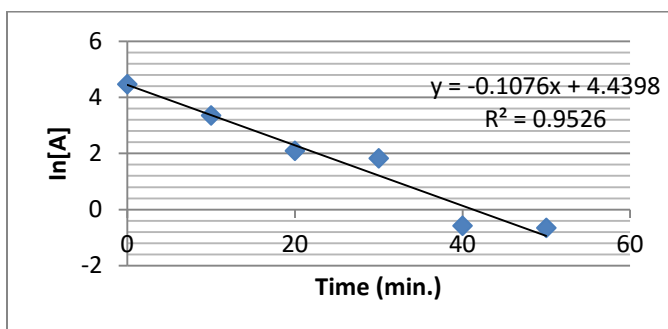


Fig.4.74: Verification of first order behaviour for butyl esterification of the Hura crepitans base oil at 70°C using H₂SO₄ catalyst

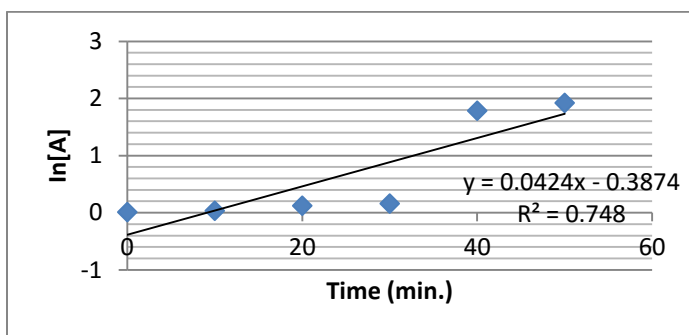


Fig.4.75: Verification of second order behaviour for butyl esterification of the *Hura crepitans* base oil at 70°C using H₂SO₄ catalyst

Table 4.78: Determination of activation energy for the first order butyl esterification of the *Hura crepitans* base oil

Temp. (°C)	Temp. (K)	k	1/T	lnk
40	313	0.0129	0.00319	-4.351
50	323	0.033	0.00309	-3.411
60	333	0.035	0.00300	-3.352
70	343	0.095	0.00292	-2.354

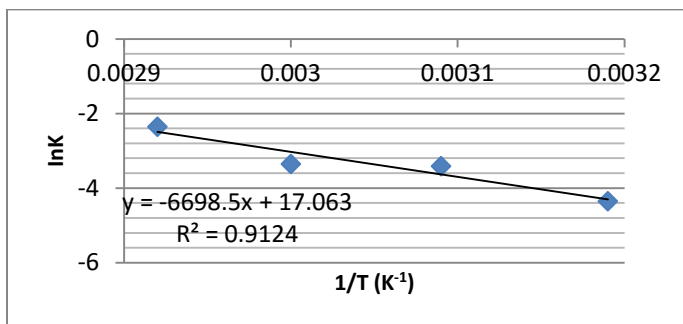


Fig.4.85: Determination of Activation Energy for Butyl esterification of the *Hura crepitans* base oil

$$\begin{aligned} \text{Slope} &= -E_a/R \\ -6698.5 &= -E_a/R \\ R &= 8.314\text{J/K.mol} \\ E_a &= (-6698.5) (8.314\text{J/K.mol}) \\ E_a &= 55.69\text{KJ/mol.} \end{aligned}$$

Kinetics of esterification of *Cucurbita pepo*, *Azzeria africana* and *Hura crepitans* base oils using 60Hu-SO₃H catalyst

Table 4.79: methyl esterification of the Hura crepitans base oil at 50°C using 60Hu-SO₃H catalyst

Time (min.)	[A] (mgKOH/g)	ln[A]	1/[A]
0	131.57	4.879	0.0076
10	95.04	4.585	0.0102
15	31.95	3.464	0.0313
25	29.85	3.396	0.0335
35	16.18	2.784	0.0618
55	9.302	2.23	0.1075

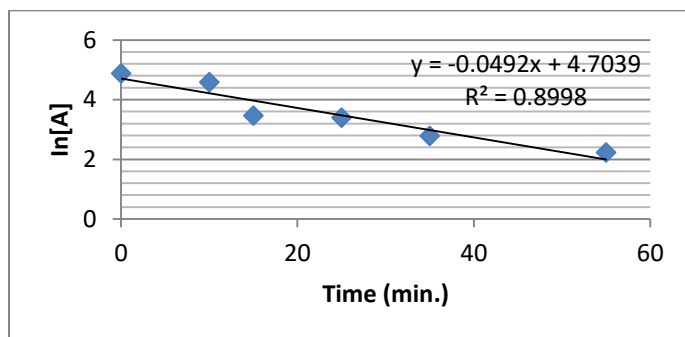


Fig.4.76: Verification of first order behaviour for methyl esterification of the Hura crepitans base oil at 50°C using 60Hu-SO₃H catalyst

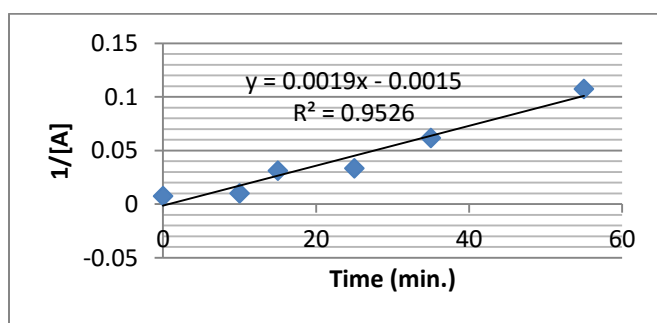
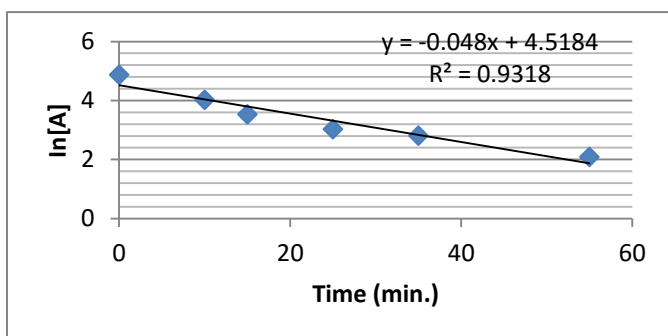
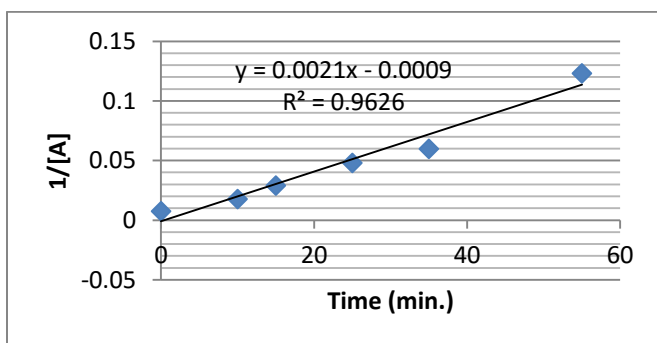


Fig.4.77: Verification of second order behaviour for methyl esterification of the Hura crepitans base oil at 50°C using 60Hu-SO₃H catalyst

Table 4.80: methyl esterification of the Hura crepitans base oil at 60°C using 60Hu-SO₃H catalyst

Time (min.)	[A] (mgKOH/g)	ln[A]	1/[A]
0	131.57	4.879	0.0076
10	56.18	4.029	0.0178
15	34.36	3.537	0.0291
25	20.79	3.034	0.0481
35	14.04	2.642	0.0712
55	12.66	2.538	0.0790

Fig.4.78: Verification of first order behaviour for methyl esterification of the Hura crepitans base oil at 60°C using SO₃H-Hu-60 catalystFig.4.79: Verification of second order behaviour for methyl esterification of the Hura crepitans base oil at 60°C using 60Hu-SO₃H catalystTable 4.81: methyl esterification of the Hura crepitans base oil at 70°C using 60Hu-SO₃H catalyst

Time (min.)	[A] (mgKOH/g)	ln[A]	1/[A]
0	131.57	4.879	0.0076
10	49.26	3.897	0.0203
15	47.39	3.858	0.0211
25	12.59	2.533	0.0794
35	11.66	2.456	0.0858
55	10.20	2.322	0.0980

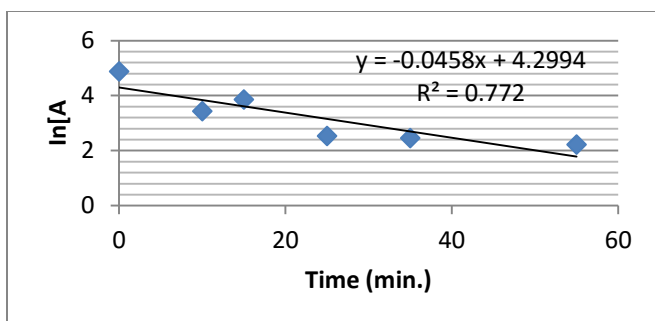


Fig.4.80: Verification of first order behaviour for methyl esterification of the Hura crepitans base oil at 70°C using 60Hu-SO₃H catalyst

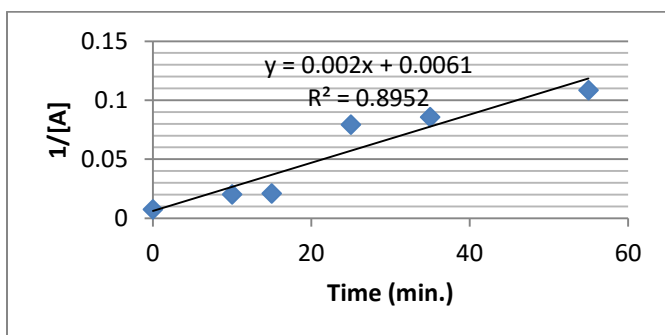


Fig.4.81: Verification of second order behaviour for methyl esterification of the Hura crepitans base oil at 70°C using 60Hu-SO₃H catalyst

Table 4.82: methyl esterification of the Hura crepitans base oil at 80°C using 60Hu-SO₃H catalyst

Time (min.)	[A] (mgKOH/g)	ln[A]	1/[A]
0	131.57	4.879	0.0076
10	27.93	3.329	0.0358
15	19.57	2.974	0.0511
25	16.64	2.812	0.0601
35	9.27	2.227	0.1079
55	5.21	1.651	0.1921

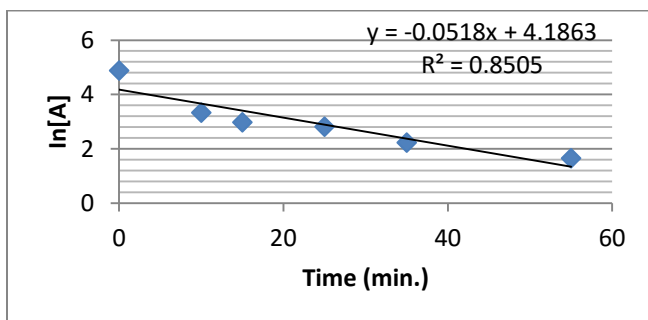


Fig.4.82 Verification of first order behaviour for methyl esterification of the Hura crepitans base oil at 80°C using 60Hu-SO₃H catalyst

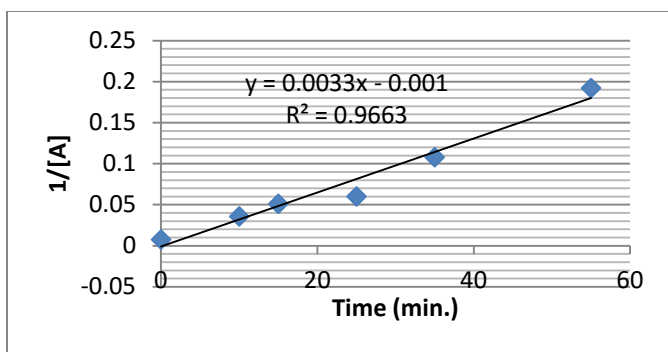


Fig.4.83: Verification of second order behaviour for methyl esterification of the Hura crepitans base oil at 80°C using 60Hu-SO₃H catalyst

Table 4.83: Determination of activation energy for the first order butyl esterification of the *Afzelia africana* base oil

Temp. (°C)	Temp. (K)	k	1/T	Ink
50	323	0.0019	0.00309	-6.266
60	333	0.0021	0.00300	-6.166
70	343	0.0020	0.00292	-6.215
80	353	0.0033	0.00283	-5.714

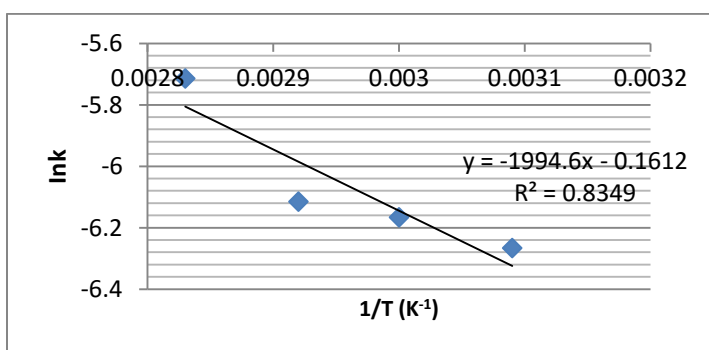
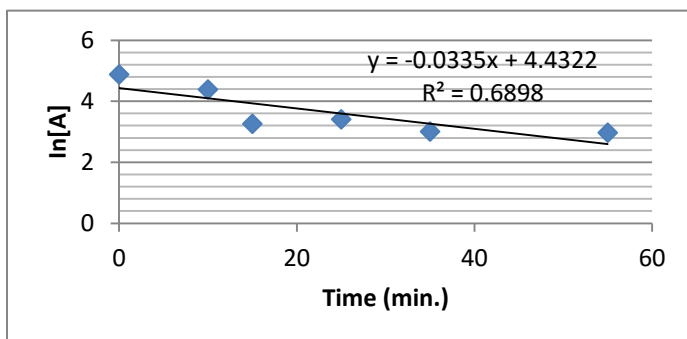
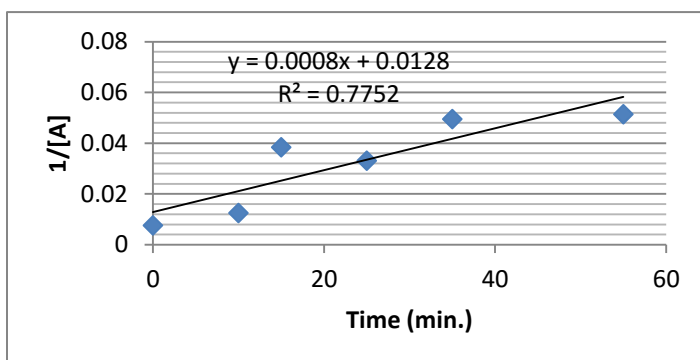


Fig4.84: Determination of Activation Energy for Methyl esterification of the *Afzelia africana* base oil using 60Hu-SO₃H

$$\begin{aligned} \text{Slope} &= -E_a/R \\ -1994.6 &= -E_a/R \\ R &= 8.314 \text{ J/K.mol} \\ E_a &= -(-1994.60) (8.314 \text{ J/K.mol}) \\ E_a &= 16.58 \text{ KJ/mol.} \end{aligned}$$

Table 4.84: butyl esterification of the Hura crepitans base oil at 50°C using 60Hu-SO₃H catalyst

Time (min.)	[A] (mgKOH/g)	ln[A]	1/[A]
0	131.49	4.879	0.0076
10	80.00	4.385	0.0125
15	26.04	3.26	0.0384
25	30.21	3.408	0.0331
35	21.56	3.007	0.0495
55	19.45	2.968	0.0514

Fig.4.85: Verification of first order behaviour for butyl esterification of the Hura crepitans base oil at 50°C using 60Hu-SO₃H catalystFig.4.86: Verification of second order behaviour for butyl esterification of the Hura crepitans base oil at 50°C using 60Hu-SO₃H catalystTable 4.85: butyl esterification of the Hura crepitans base oil at 60°C using 60Hu-SO₃H catalyst

Time (min.)	[A] (mgKOH/g)	ln[A]	1/[A]
0	131.49	4.879	0.0076
10	60.97	3.929	0.0164
15	30.21	3.409	0.0331
25	20.79	3.034	0.0481
35	36.36	3.591	0.0275
55	15.11	2.715	0.0662

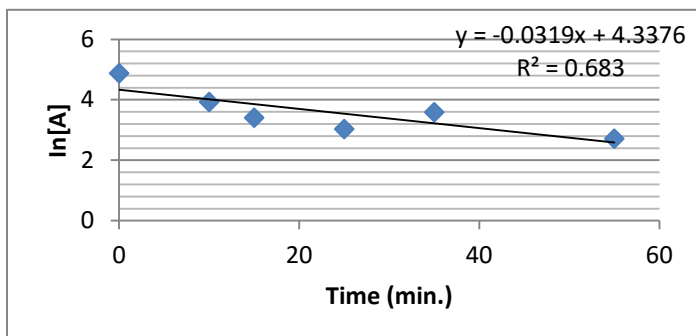


Fig.4.87: Verification of first order behaviour for butyl esterification of the Hura crepitans base oil at 60°C using 60Hu-SO₃H catalyst

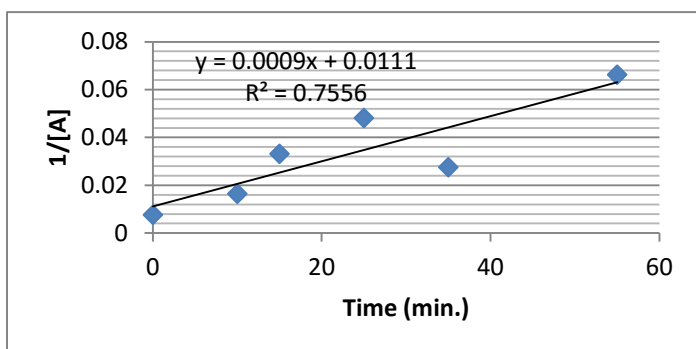


Fig.4.88: Verification of second order behaviour for butyl esterification of the Hura crepitans base oil at 60°C using 60Hu-SO₃H catalyst

Table 4.86: butyl esterification of the Hura crepitans base oil at 70°C using 60Hu-SO₃H catalyst

Time (min.)	[A] (mgKOH/g)	ln[A]	1/[A]
0	131.49	4.879	0.0076
10	31.95	3.463	0.0313
15	25.13	3.225	0.0398
25	24.88	3.215	0.0402
35	10.01	2.303	0.0999
55	8.55	2.146	0.117

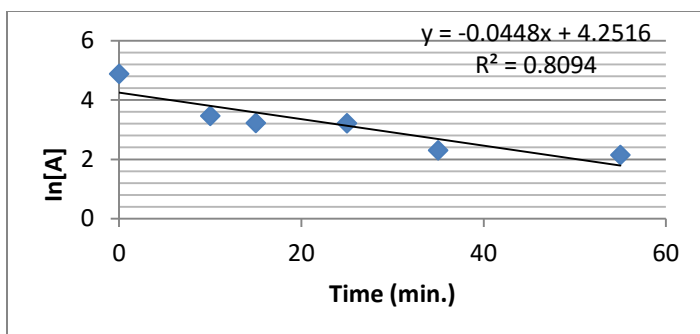


Fig.4.89: Verification of first order behaviour for butyl esterification of the Hura crepitans base at 70°C using 60Hu-SO₃H catalyst

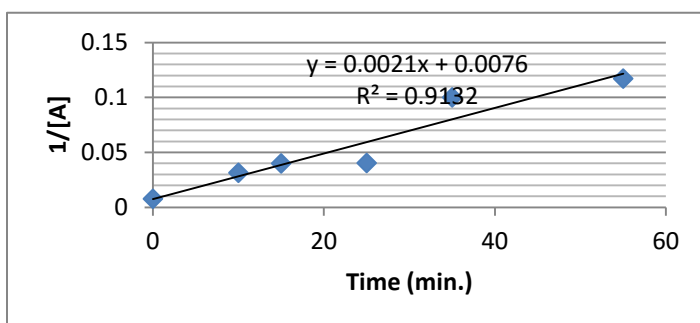


Fig.4.90: Verification of second order behaviour for butyl esterification of the Hura crepitans base oil at 70°C using 60Hu-SO₃H catalyst

Table 4.87: butyl esterification of the Hura crepitans base oil at 80°C using 60Hu-SO₃H catalyst

Time (min.)	[A] (mgKOH/g)	ln[A]	1/[A]
0	131.49	4.879	0.0076
10	40.13	3.692	0.0249
15	22.69	3.122	0.0440
25	10.65	2.366	0.0938
35	9.09	2.208	0.1099
55	12.84	2.697	0.0779

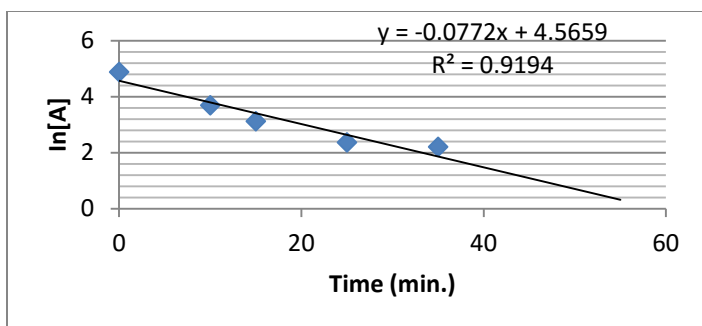


Fig.4.91: Verification of first order behaviour for butyl esterification of the Hura crepitans base oil at 80°C using 60Hu-SO₃H catalyst

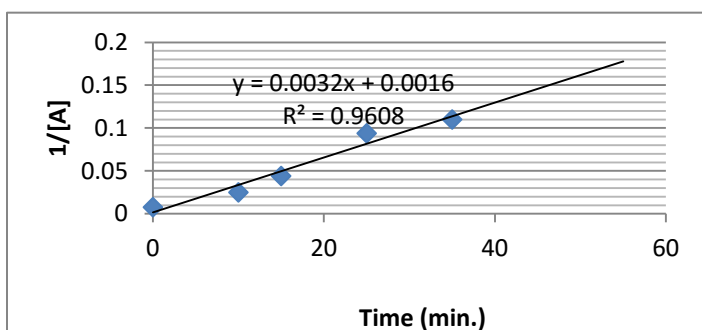


Fig.4.92: Verification of second order behaviour for butyl esterification of the Hura crepitans base oil at 80°C using 60Hu-SO₃H catalyst

Table 4.88: Determination of activation energy for the second order butyl esterification of the Hura crepitans base oil

Temp. (°C)	Temp. (K)	k	1/T	lnk
50	323	0.0019	0.00309	-7.131
60	333	0.0021	0.00300	-7.013
70	343	0.0020	0.00292	-6.166
80	353	0.0033	0.00283	-5.745

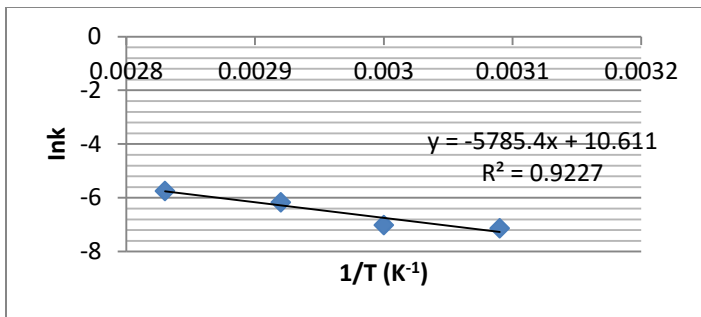


Fig.4.93: Determination of Activation Energy for butyl esterification of the *Afzelia africana* base oil using 60Hu-SO₃H

$$\text{Slope} = -E_a/R$$

$$-5785.4 = -E_a/R$$

$$R = 8.314 \text{ J/K.mol}$$

$$E_a = -(-5785.4) (8.314 \text{ J/K.mol})$$

$$E_a = 48.09 \text{ KJ/mol.}$$